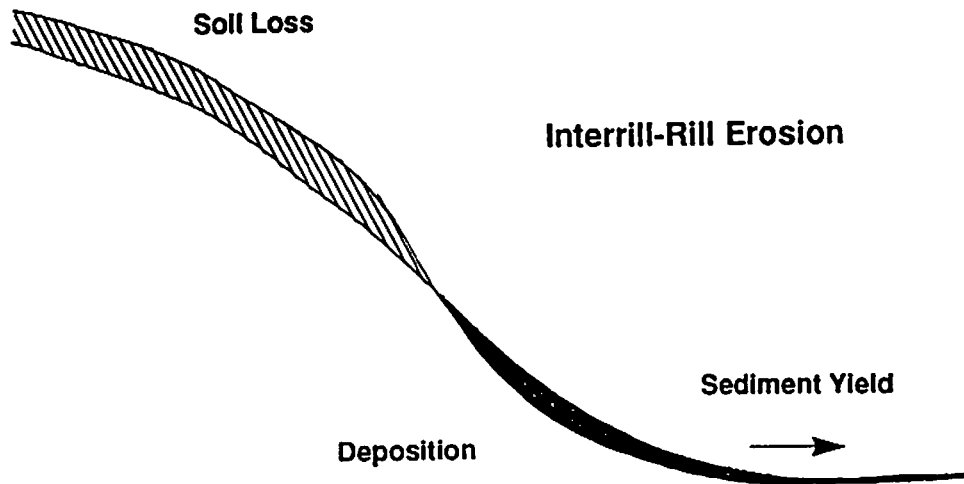


USDA - Water Erosion Prediction Project:

HILLSLOPE PROFILE VERSION



**USDA - WATER EROSION PREDICTION PROJECT:
HILLSLOPE PROFILE MODEL DOCUMENTATION**

August, 1989

L. J. Lane
and
M. A. Nearing
(Editors)

NSERL Report No. 2
USDA-ARS National Soil Erosion Research Laboratory
West Lafayette, Indiana 47907

ABSTRACT

The objective of the Water Erosion Prediction Project is to develop new generation prediction technology for use by the USDA-Soil Conservation Service, USDA-Forest Service, USDI-Bureau of Land Management, and other organizations involved in soil and water conservation and environmental planning and assessment. This improved erosion prediction technology is based on modern hydrologic and erosion science, process oriented, and computer implemented. The technology includes three versions: a hillslope profile version, a watershed version, and a grid version. This document is a detailed description of the hillslope profile version of the technology.

The hillslope profile erosion model is a continuous simulation computer model which predicts soil loss and deposition on a hillslope. It includes a climate component which uses a stochastic generator to provide daily weather information, an infiltration component which is based on the Green-Ampt infiltration equation, a surface runoff component which is based on the kinematic wave equations, a daily water balance component, a plant growth and residue decay component, and a rill-interrill erosion component. The profile erosion model computes spatial and temporal distributions of soil loss and deposition. It provides explicit estimates of when and where on the hillslope erosion is occurring so that conservation measures can be designed to most effectively control soil loss and sediment yield.

The hillslope profile erosion model is based on the best available science for predicting soil erosion on hillslopes. The relationships in the model are based on sound scientific theory and the parameters in the model were derived from a broad base of experimental data. The model runs on standard computer hardware and is easily used, applicable to a broad range of conditions, robust, and valid.

TABLE OF CONTENTS

	Page
WEPP HILLSLOPE PROFILE EROSION MODEL USER SUMMARY	S.1
L. J. Lane, M. A. Nearing, J. J. Stone, and A. D. Nicks	
CHAPTER 1. Overview of WEPP Hillslope Profile Erosion Model.....	1.1
A. D. Nicks, V. L. Lopes, M. A. Nearing, and L. J. Lane	
CHAPTER 2. Weather Generator	2.1
A. D. Nicks and L. J. Lane	
CHAPTER 3. Snowmelt and Frozen Soil	3.1
R. A. Young, G. R. Benoit, and C. A. Onstad	
CHAPTER 4. Infiltration	4.1
W. J. Rawls, J. J. Stone, and D. L. Brakensick	
CHAPTER 5. Surface Runoff.....	5.1
M. Hernandez, L. J. Lane, and J. J. Stone	
CHAPTER 6. Soil Component.....	6.1
E. E. Alberts, J. M. Laflen, W. J. Rawls, J. R. Simanton and M. A. Nearing	
CHAPTER 7. Water Balance and Percolation.....	7.1
M. R. Savabi, A. D. Nicks, J. R. Williams, and W. J. Rawls	
CHAPTER 8. Plant Growth Component	8.1
E. E. Alberts, M. A. Weltz, and F. Ghidry	
CHAPTER 9. Hydraulics of Overland Flow	9.1
J. E. Gilley, S. C. Finkner, M. A. Nearing, and L. J. Lane	
CHAPTER 10. Erosion Component	10.1
G. R. Foster, L. J. Lane, M. A. Nearing, S. C. Finkner, and D. C. Flanagan	
CHAPTER 11. Parameter Identification from Plot Data	11.1
M. A. Nearing, M. A. Weltz, S. C. Finkner, J. J. Stone, and L. T. West	
CHAPTER 12. Irrigation Component.....	12.1
G. Kottwitz and J. E. Gilley	
CHAPTER 13. Implications of the WEPP Hillslope Model for Soil Conservation Planning	13.1
P. B. Hairsine, G. A. Weesies, and M. A. Nearing	
CHAPTER 14. WEPP Model Sensitivity Analysis	14.1
M. A. Nearing, L. D. Ascough, and H. M. L. Chaves	
APPENDIX A. Computer Code Description	A.1
V. L. Lopes, E. Perry, J. J. Stone, J. C. Ascough, and J. Ferris	
APPENDIX B. Status of Computer Code as of August, 1989.....	B.1
M. A. Nearing	

WEPP HILLSLOPE PROFILE EROSION MODEL USER SUMMARY

L.J. Lane, M.A. Nearing, J.J. Stone, and A.D. Nicks

S.1 Introduction

The objective of the Water Erosion Prediction Project is: "To develop new generation water erosion prediction technology for use by the USDA-Soil Conservation Service, USDA-Forest Service, and USDI-Bureau of Land Management, and other organizations involved in soil and water conservation and environmental planning and assessment" (Foster, 1987).

The USDA - Water Erosion Prediction Project (WEPP) hillslope profile model is a major step towards meeting that objective. The model represents erosion prediction technology based on fundamentals of infiltration theory, hydrology, soil physics, plant science, hydraulics, and erosion mechanics. The model provides several major advantages over existing erosion prediction technology, including: 1) capabilities for estimating spatial and temporal distributions of soil loss; net soil loss for an entire hillslope or for each point on a slope profile can be estimated on a daily, monthly, or average annual basis, and 2) since the model is process-based it can be applied on a broad range of conditions that may not be practical or economical to field test. Processes considered in the model include climate, snowmelt, sprinkler irrigation, soil evaporation, plant transpiration, percolation, infiltration, surface runoff, rill hydraulics, plant growth, residue decomposition, and sediment generation, transport, and deposition on interrill and rill areas. The model is intended to accommodate spatial and temporal variability in topography, surface roughness, soil properties, crops, and land use conditions on hillslopes.

S.2 Model Description

S.2.1 Model Summary

The WEPP profile version erosion model is intended to be executed primarily as a continuous simulation model, although it can be run on a single-storm basis. By continuous simulation it is meant that the model "mimics" the processes which are important to erosion prediction as a function of time, and as affected by management decisions and climatic environment. Surface residue, for example, plays an important role in the amount of soil lost during a given rainfall event. The WEPP erosion model uses a plant growth model to estimate the amount of crop residue present on the soil surface for each day through the year. A certain amount of residue is generated by leaf drop during senescence and by harvesting, and the model will adjust surface cover as a function of those processes. A pass of a given tillage implement will bury a percentage of residue. The model predicts this also. The user does not need to specify the amount of residue cover as a function of time.

The important aspect to the user is that the model inputs are in terms that the user understands: planting dates, tillage dates, harvest dates, yields, implement types, etc... More technical information will be provided by various sources. Climate information, for instance, can be generated by the CLIGEN model, which is a stochastic weather generator. Crop specific information, such as growth parameters, will be provided by ARS and SCS technical experts to the user of the model. Soils information that the model requires will also be available from SCS

soil characterization data and soil survey information. Topographic information required is compatible with current methods of measuring slope profiles in the field.

The time step for most calculations in the model is daily. Soil parameters, residue amounts, crop growth, soil water content, surface roughness, and essentially all other adjustments to model parameters are made on the daily time step.

The output of the continuous simulation model represents time-integrated estimates of erosion. In nature, as well as in the model predictions, a large percentage of erosion occurs due to a small percentage of rainfall events. The model simulates some number of years of erosion and sums the total soil loss over those years for each point on the hillslope to obtain average annual values of erosion. The model calculates both detachment and deposition. It predicts where deposition begins and/or ends on a hillslope, which may vary from storm to storm. Certain points on the hillslope may experience detachment during some rainfall events and deposition during other events. The output of the continuous simulation model represents an average over all of the erosion events.

The model output includes two sections, one for onsite effects of erosion and one for offsite effects. These two sections are clearly delineated in the output. The onsite effects of erosion section includes the time integrated (average annual) soil loss over the areas on the hillslope of net soil loss. This term is the one that is most analogous to USLE estimates. It is the soil loss estimate which is most closely tied to onsite loss of productivity. The section for onsite effects also includes estimates of average deposition over the areas on the hillslope of net deposition. Lastly, it provides a table of soil loss at each of a minimum of 100 points down the slope. The second section of the output is for offsite effects of erosion. It includes estimates of sediment loads leaving the profile. This is the sediment which is a potential problem in terms of delivery of sediment to waterways, as well as the offsite delivery of agricultural pollutants which may be bound to soil particles. This section also includes sediment particle size information. Since agricultural pollutants are preferentially bound to certain size classes of sediment, this information can have significance in assessing offsite pollution problems.

The output options also include the potential for obtaining monthly or daily (storm-by-storm) estimates of onsite and offsite effects of erosion. The output as a whole provides a potentially powerful tool for conservation planning. The model estimates where and when soil loss problems are occurring on a given hillslope for a given management option. It also provides an inexpensive and fast method for evaluating conservation methods.

The model may also be executed in the single-storm mode. In that case, all the parameters used to drive the hydrology and erosion components of the model must be input by the user, including soil properties for the day of the rainfall event, crop canopy, surface residue, days since last disturbance, surface random roughness, oriented roughness, etc... In the continuous simulation mode the influence of these user inputs, which represent the initial conditions for the simulation, is small since the model adjusts each of those variables internally. In the single storm mode those inputs have a major influence on the output. The single-storm option of the model requires a great deal more knowledge on the part of the user to interpret and use the output for planning, evaluation, and design for conservation purposes. The single-storm model helps in understanding and evaluating the factors that influence erosion on a hillslope; it is of

limited value in evaluating conservation systems wherein conditions change as a function of time through the year and from year to year.

S.2.2 Model components

The model can be subdivided into six conceptual components: climate generation, hydrology, plant growth, soils, irrigation, and erosion. A brief description of each major component is given below.

The climate generator is a model called CLIGEN and is run separately from the WEPP model. It generates rainfall amount, duration, maximum intensity, time to peak intensity, maximum and minimum temperature, and solar radiation for the on-site location. The generated data are written to a climate file which is read in by the WEPP model. Precipitation may be either in the form of rain or snow, depending on temperature. Redistribution of snow on the slope profile is calculated as function of wind speed and direction. Snowmelt and erosion due to snowmelt is calculated, also. Rainfall is disaggregated into a time-rainfall intensity format for use by the infiltration and erosion components.

The hydrology component calculates infiltration, the daily water balance including runoff, evapotranspiration, and deep percolation. Infiltration is calculated by the Green and Ampt infiltration equation. Runoff is calculated using the kinematic wave equations or by an approximation to the kinematic solution for a range of rainfall intensity distributions, hydraulic roughnesses, and infiltration parameter values. The water balance routines are a modification of the SWRRB water balance (Williams et al., 1985) and account for snow melt, percolation below the root zone, movement of water downwards between soil layers within the root zone, and both bare soil evaporation and plant transpiration. The crop growth component of the model calculates leaf area index for transpiration calculations.

The plant growth components calculate growth, senescence and decomposition of plant material. In the case of croplands, a particular crop or crops are grown as a function of growing degree days and soil moisture. The pattern of growth is controlled by crop specific parameters. After harvest, decomposition of the vegetative residue, if present, is simulated. In the case of rangelands, a plant community is simulated for a growing season. Grazing removes biomass at user defined intervals.

Many of the soil parameters which are used in the hydrology and erosion calculations change with time as a result of tillage operations, freezing and thawing, compaction, weathering, or history of precipitation. The soils component makes adjustments to soil properties on a daily time step. Examples of temporal varying factors include soil bulk density, saturated conductivity, surface roughness, and erodibility parameters.

The irrigation component accommodates solid set, sideroll, and handmove systems. Spatial variations in application rate and depth within the irrigation area are assumed negligible. If irrigation is available, the user can choose one of three scheduling options. One option determines irrigation dates and amounts based on available soil water depletion. A second scheduling option uses predetermined irrigation dates and amounts. The third scheduling option allows a combination of the first two options. An irrigation event is simulated as a rainfall event of uniform intensity.

The erosion component uses the steady state sediment continuity equation as a basis for the erosion computations. Soil detachment in the interrill areas is calculated from the rainfall intensity. Soil detachment in the rills occurs if the hydraulic shear stress is greater than critical shear and the flow is at less than transport capacity. Deposition occurs when the sediment load is greater than the capacity of the flow to transport it. The erosion component partitions the flow into rills and calculates a shear stress based on rill hydraulics. Adjustments to soil detachment are made to incorporate the effects of canopy cover, ground cover, and buried residue, each of which are calculated by the model in the plant growth, residue decomposition, and tillage portions of the model. Sediment size characteristics are calculated for the eroded sediment leaving the profile. The sediment sizes are a function of the original soil material and the preferential deposition of certain sized sediment along the profile.

S.2.3 Limits of Application

The erosion predictions from the WEPP profile model are applicable to "field-sized" areas or conservation treatment units. Although the size of a particular field to which the procedure applies will vary with complexity within a field, the maximum size "field" is about a section (640 acres) although an area as large as 2000 acres is needed for some rangeland applications. On some complex areas, the "field" may be much smaller than 640 acres. The model will not apply to areas having permanent channels such as classical gullies and stream channels.

The profile model is also not applicable to areas with channels which are farmed over and known as concentrated flow or "cropland ephemeral gullies." The watershed version of the WEPP technology specifically addresses areas with ephemeral gullies. The watershed version of the technology should be used also in rangeland and forestland applications for "fields" with large concentrated flow channels, and for estimating erosion in terrace channels or grassed waterways on cropland.

S.3 Input Data Files

Four input data files are required to execute the WEPP profile model: 1) a climate file, 2) a slope profile file, 3) a soil file, and 4) a management file. For the case of irrigation additional input files are required.

S.3.1 Climate File

The climate file for the continuous simulation option of the model is generated from CLIGEN for the location and the number of years of simulation desired. The number of years required will depend upon the reason for which the model is being used and the climate at the location of interest. Three years of simulation is normally adequate for comparing various management practices for making soil conservation decisions. More years will be required for climates which are semi-arid or arid. A greater number of years will be needed also if more accurate long-term predictions of soil loss are desired. The model will not run partial years of simulation.

Climate files for the single storm option must be built by the user, rather than generated by CLIGEN. Inputs for the single storm files are brief and are easily made.

Figure S.5.1 shows an example of a climate input file generated by CLIGEN. (Figures are located at the end of the User Summary.) Note that it includes the file structure for both the continuous and single storm simulation modes. Table S.3.1 has a description of the variables in Fig. S.5.1. The year column is not relevant to the execution of the model, except as a counter. Unless historical data is being used (generally the climate data is stochastically generated) the year does not correspond to historical weather records.

Table S.3.1. Climate input file description

Line 1: simulation mode (1-continuous, 2 - single storm)

Line 2: station i.d.

Line 3: beginning year and number of years simulated
(not relevant unless historical weather records are used)

Line 4: variable names

Line 5: variable dimensions

Line 6 (repeated for number of simulation days) :

- a) day of simulation - (day)
- b) month of simulation - (mon)
- c) year of simulation - (year)
- d) precipitation amount (mm) - (rain)
- e) duration of precipitation (hr) - (stmdur)
- f) ratio time to rainfall peak/rainfall duration - (timep)
- g) ratio maximum rainfall intensity/average rainfall intensity - (ip)
- h) maximum temperature (C) - (tmax)
- i) minimum temperature (C) - (tmin)
- j) solar radiation (lgy/day) - (rad)

 *** Note *** For single storm simulation, only lines 1 and 6 are used.

S.3.2 Slope File

The slope profile is described by slope length - steepness pairs starting at the upper end of the hillslope. Breakpoints for the end of input segments should be made at the locations on the hillslope where the most obvious changes in slope are. A typical "S" shaped profile, for instance, might best be described by three input segments: a relatively flat segment at the upper end of the hillslope, a steeper mid-segment, and a flatter end segment at the toe of the slope. Slope length does not end where deposition begins. The slope profile must be described to the end of the field, or to a concentrated flow channel, grass waterway, or terrace. The point where detachment ends and deposition begins is calculated by the model and given as output.

The slope input file always contains 6 lines (Table S.3.2). The first line gives the number of overland flow elements. An overland flow element is defined as a section of the hillslope which is homogeneous in terms of cropping, management, and soil properties. The user should be aware that each additional overland flow element increases the computational time of the computer model significantly. If soil properties, for example, are not greatly different down the

slope (i.e., if soils don't vary in texture classes) the improvement in erosion prediction on the hillslope may not be significant enough to warrant multiple overland flow elements for the soil texture variation downslope.

Table S.3.2. Slope input file description.

INPUT	Description
Line 1:	a) number of overland flow elements - (nelem)
Line 2:	a) aspect of field (degrees) - (aspect) b) width of field (m) - (fwidth)
Line 3:	a) flag for slope at top of field - (itop) 0 - slope equal to zero 1 - slope not equal to zero
Line 4:	a) Number of slope length pairs - (ninpts)
Line 5:	Pairs of: a) segment length (m) - (xdel(ninpts)) b) slope of the segment (fraction) - (xslp(ninpts))
Line 6:	a) lengths of overland flow elements (m) - (slplen(nelem))

The first line contains the number of overland flow elements. The second line contains the aspect of the field and the field width. Units of aspect are degrees from north (i.e., a hill facing east has aspect of 90 degrees). North should always be 360 degrees (not zero). This information is needed to calculate snow drift due to wind. Line 3 is the flag for the slope at the top of the profile. If the profile begins at a ridgetop, the slope at the top of the profile will be zero, and the flag in line 3 should be zero. If the slope is not zero at the top of the slope, line 3 should contain a "1". Line 4 is the number of slope segments which the user has measured in the field. Line 5 gives the lengths and average slope steepnesses of the segments which the user measures. There must be as many pairs of length/gradient inputs as are indicated in line 4. For example, if line four contains a 6, then line 5 must have 12 data elements in it. Line six contains the length(s) of the overland flow element(s). Line six must contain as many data elements as indicated in line 1. The sum of the lengths of the overland flow elements must equal the sum of the segment lengths. Also, input segments must NOT overlap overland flow elements. If 6 overland flow elements are given, the input file must have at least 6 input segments, even if the slopes on one or more of the segments are the same. An example of a slope input file is given in Fig. S.5.2.

S.3.3 Soil File

The soil profile can be represented by up to 10 layers. The second line of the soil file contains general information about the soil (i.e. name, textural class, number of soil layers). The remainder of the file contains information for each soil layer.

Figure S.5.3 shows an example of a soil file for the WEPP model. Table S.3.3 presents a description of the variables in Fig. S.5.3. Certain of the soil variables can either be user input or calculated by the program. These variables are denoted by a ** in Table S.3.3 (variables must be input as zero to have program calculate the values).

Table S.3.3. Soil input data file description

Line 1:

- a) number of overland flow elements

Line 2:

- a) soil name - (slid)
- b) soil texture - (texid)
- c) number of soil layers - (nsl)
- d) soil albedo - (salb)
- e) initial saturation - (sat)
- **f) baseline interrill detachment parameter ($\text{kg} \cdot \text{s} / \text{m}^{**4}$) - (ki)
- **g) baseline rill detachment parameter (s / m) - (kr)
- **h) baseline critical shear ($\text{N} / \text{m}^{**2}$) - (shcrit)

Line 3 (repeated for number of soil layers) :

- a) cumulative thickness of soil layer (mm) - (solthk)
(i.e., depth from surface to bottom of layer)
- **b) initial bulk density (gm / cc) - (bd)
- **c) initial saturated hydraulic conductivity (mm / hr) - (ssc)
- **d) field capacity (1/3-bar soil water content) (mm / mm) - (thetfc)
- **e) wilting point (15-bar soil water content) (mm / mm) - (thetdr)
- f) % of sand - (sand)
- g) % of clay - (clay)
- h) % of organic matter - (orgmat)
- i) cation exchange capacity - (cec)
- j) % of rock fragments - (rfg)

*** Note *** Lines 2 to number of soil layers are repeated for the number of overland flow elements.

S.3.4 Management File

The structure of the management file will depend on the land use. At present, croplands and rangelands are the two land uses supported by the WEPP profile version model. In the future, disturbed forest lands will be added.

S.3.4.1 Cropland Management Files

Figure S.5.4. shows an example of a management input file for a single element profile for two years, the first year alfalfa and the second year corn. Table S.3.4. has a description of the variables in Fig. S.5.4. Table S.3.5. shows the landuse and tillage codes used in the WEPP model.

The cropland management file is difficult to build without a file builder program. File builder programs are available to aid the process of building these input files. They contain crop specific growth and residue decay parameters, tillage parameters, and other information which

helps in building those files. Also, the file builder for the management files use as input information which the user generally has knowledge of and translates it into the format required by the WEPP model.

An important aspect of the WEPP model is that it contains no crop specific information internally. There are no parameters for corn, for example, internal to the WEPP model. All plant parameters are inserted via the input files. Thus, as the data bases for crops increase, the internal WEPP model code will not be affected. All crop information is contained in the management input files.

Table S.3.4. Management input data (cropland) file description

Line 1:

- a) number of overland flow elements - (nelem)

nelem corresponds to either the number of overland flow elements for strip cropping or the number different soil types down a hillslope

- b) number of crop types (ncrop)

ncrop is the number of different crop types grown during the simulation period. For example if the crops grown during the simulation are corn and wheat, ncrop = 2.

- c) sprinkler irrigation scheduling option - (irtype)
(0 - no irrigation, 1 - depletion level, 2 - fixed date, 3 - combination of 1 and 2)

Line 2:

- a) code for vegetation type (1-crop, 2-range, 3-forest) - (iplant))

Line 3:

- a) cropping system (1-annual, 2-perennial, 3-fallow) - (imngmt)

Line 4: The following are plant dependent parameters:

- a) carbon-nitrogen ratio of residue and roots - (cn)
- b) decomposition constant for flat residue - (aca)
- c) parameter for flat residue cover equation - (cf)
- d) decomposition constant for buried residue - (as)
- e) decomposition constant for roots - (ar)
- f) residue coefficient - (y7)
- g) maximum canopy height (m) - (hmax)
- h) growing degree days to emergence (C) - (crit)
- i) growing degree days at maturity (C) - (gddmax)
- j) parameter value for canopy height equation - (bb)
- k) maximum root depth (m) - (rdmax)
- l) root to shoot ratio - (rsr)
- m) fraction by which canopy cover decays after reaching senescence (0-1) - (decfct)
- n) fraction of growing season when leaf area index starts to decline (0-1) - (dlai)
- o) fraction of growing season to reach senescence (0-1) - (gssen)
- p) maximum leaf area index - (xmxlai)

- q) upper grain yield boundary (bu/ac) for which an adjustment to biomass is made - (y1)
- r) residue biomass (kg/ha) when grain yield is zero - (y2)
- s) change in residue mass per unit change in grain yield between grain yield limits (0 to y1) - (y3)
- t) pounds of grain per bushel of grain - (y4)
- u) pound/ac to kg/ha conversion - (y5)
- v) residue to grain yield ration - (y6)
- w) canopy cover coefficient - (b1)
- x) canopy cover coefficient - (b2)
- y) in-row plant spacing (m) - (pltsp)
- z) plant stem diameter at maturity (m) - (diam)
- aa) plant specific drought tolerance - (pltol)
- ab) base daily air temperature (C) - (btemp)
- bc) growth rate parameter - (grate)
- bd) number of days between beginning and end of leaf drop - (spriod)
- ae) portion of vegetative biomass partitioned into standing residue mass at harvest - (partcf)
- af) critical freezing temperature for a perennial crop (C) - (tmpmin)
- ag) maximum temperature that stops the growth of a perennial crop (C) - (tmpmax)
- ah) maximum root mass for a perennial crop (tons/acre) - (rtmmax)
- ai) standing to flat residue adjustment factor (wind, snow, etc) - (fact)
- aj) residue cover on ridges in spring (0-1) - (sprcov)
- ak) critical live biomass value below which grazing is not allowed / (kg/m**2) - (critvm)
- al) tillage intensity (30 values) - (mfo)

*** Note *** Lines 2, 3, and 4 are repeated for the number of crops required by the simulation. For example, if corn and wheat are being grown, then lines 2, 3, and 4 are input for corn, then for wheat.

Line 5:

- a) random roughness value after tillage (m) - (rro)
(30 values are currently given - one per tillage implement)

Line 6:

- a) ridge height value after tillage (m) - (rho)
(30 values, one per tillage implement)

Line 7:

- a) ridge interval (m) (rint)
(30 values, one per implement)

Line 8:

- a) mean tillage depth (m) - (tdmean)
(30 values, one per implement)

*** Note *** Lines 5, 6, 7 and 8 are implement dependent variables. Each variable has 30 values.

Line 9:

- a) number of tillage sequences - (nseq)

a tillage sequence is a set of tillage operations performed on one field or overland flow element during one calendar year.

Line 10:

- a) number of tillage operations for tillage sequence - (ntill)

Line 11:

- a) implement type (see table S.5.5. for implement codes) - (itill)
- b) day of tillage (Julian) - (mdate)
- c) tillage depth (m) - (tildep)
- d) tillage type - (tytil) (1-primary, 2-secondary).

Primary tillage is the operation which tills to the maximum depth.
Secondary tillages are all other tillage operations.

*** Note *** Lines 10 and 11 are repeated for the number of tillage sequences per simulation.

Line 12:

- a) planter row number - (nrplt)
- b) drill row number - (nrdril)
- c) cultivator row number - (nrkul)
- d) cultivator position - (cltpos)

Line 13:

- a) number of contour sets - (ncnt)

a contour set is the combination of length, slope, ridge height which is associated with one overland flow element or field.

Line 14: (line 14 exists only if $ncnt > 0$)

- a) contour slope (m/m) - (cntslp)
- b) contour row spacing (m) - (rowspc)
- c) contour row length (m) - (rowlen)
- d) contour ridge height (m) - (rdghgt)

*** Note *** Line 14 is repeated for the number of contour sets per simulation.

Line 15:

- a) an integer value to indicate if weed cover is important during the residue decomposition - (iweed)
0 - not important
1 - important

Line 16: Exists only if iweed is important

- a) julian data that weed cover becomes important - (jdwdst)
- b) julian data that weed cover becomes not important - (jdwdst)
- c) average weed cover during this period (0-1) - (wdcover)

Line 17:

- a) land use (1-agricultural, 2-rangeland, 3-forestland) - (landuse)

Line 18:

- a) initial canopy cover (0-1) - (cancov)
- b) initial interrill cover (0-1) - (inrcov)
- c) initial rill cover (0-1) - (rilcov)
- d) initial residue type (iresd)
- e) initial snow cover - (snoin)
- f) initial ridge roughness (m) - (rrinit)
- g) initial ridge height (m) - (rhinit)
- h) bulk density after last tillage (g/cc) - (bdtill)
- i) cumulative rainfall since last tillage (mm) - (rfcum)
- j) days since last tillage - (daydis)

***** Note ***** Lines 17 and 18 are repeated for the number of overland flow elements. They represent the initial conditions for each overland flow element for the simulation.

The initial conditions are the conditions which exists at the beginning of the simulation. Estimates of the initial conditions can be made by using long term average conditions which exist on January 1st.

Line 19:

- a) number of crops per year (nycrop)

nycrop is the number of crops grown during the current year for a field or overland flow element. For the case of continuous corn, nycrop=1. If two crops are grown in a year, then nycrop=2

Line 20:

- a) crop type - (itype)

itype refers to the current crop being grown on a field or overland flow element. The value for itype corresponds to the order that the crops are read in from lines 2 to 4. For example, if the crops being grown are corn and wheat and in lines 2 to 4 the first crop read in is corn and the second wheat, then corn will have a reference index of 1 and wheat will have a reference index of 2. So for any year when corn is being grown, itype will equal 1 and for any year when wheat is being grown, itype will equal 2.

- b) tillage sequence code - (tilseq)

tilseq refers to the tillage sequences read in on lines 10 and 11. The tillage sequences have reference indices in the order they are read in. For example, if a sequence of tillage dates for one year for conventional tillage are read in on lines 10 and 11, then conventional tillage will hve a reference index of 1 and notill an index of 2. So for any year when conventional tillage is done, tilseq=1 and for any year when notill is done, tilseq=2.

- c) contour set code - (conset)

conset refers to contour sets read in on lines 13 and 14. If ncnt = 0 conset must be 0.

d) weed cover set code - (wcode)

wcode refers to weed cover read in on lines 15 and 16.
If iweed = 0 wcode must be 0.

e) depth of secondary tillage layer (m) - (tillay (1))
f) depth of primary tillage layer (m) - (tillay (2))

The primary tillage layer is the depth of the deepest tillage operation.
The secondary tillage layer is the average depth of all secondary tillage operations. If there is no tillage, set tillay (1) = .1 and tillay (2) = .2

Line 21:

***** Management Inputs *****

Annual Crop Management Inputs

Line 21a:

- a) planting date (julian) - (jdplt)
- b) harvesting date (julian) - (jdharv)
- c) grain yield (bu/ac or lb/ac) - (yld)
- d) row width (m) - (rw)

Line 21b:

- a) residue management option - (resmgt)
 - 1) herbicide application
 - 2) burning
 - 3) silage
 - 4) shredding or cutting
 - 5) residue removal
 - 6) none

Line 21c:

If residue management option is 1:

- a) herbicide application date (julian) - (jdherb)

Option 2:

- a) residue burning date (julian) - (jdburn)
- b) fraction of standing residue burned (0-1) - (fbrnog)
- c) fraction of flat residue burned (0-1) - (fbrmag)

Option 3:

- a) silage date (julian) - (jdsilge)

Option 4:

- a) standing residue shredding or cutting date (julian) - (jdcut)
- b) fraction of standing residue shredded or cut (0-1) - (frcut)

Option 5:

- a) residue removal date (julian) - (jdmove)
- b) fraction of flat residue removed (0-1) - (frmove)

Option 6:

line 21c does not exist

Perennial Crop Management Inputs

Line 21a:

- a) flag for year of simulation - (ipmyr)
 - 1) first year of perennial growth
 - 2) otherwise

Line 21b:

- a) planting date (julian) - (jdplt)
does not exist if ipmyr = 2

Line 21c:

- a) row width (m) - (rw)

Line 21d:

- a) crop management option - (mgtopt)
 - 1) cutting
 - 2) grazing
 - 3) not harvested or grazed

Line 21e:

If mgtopt is option 1:

Line 21e1:

- a) number of cuttings (ncut)

Line 21e2:

- a) cutting date (julian) - (cutday)
- b) yield (tons/acre) - (yild)

Line 21e3:

- a) perennial growth stop date (julian) - (jdstop)
(if no stop date jdstop = 0)

*** Note *** Line 21e2 is repeated for the number of cuttings

If mgtopt is option 2:

Line 21e1:

- a) number of grazing cycles - (ncycle)

Line 21e2:

- a) date grazing begins (julian) - (gday)
- b) date grazing ends (julian) -(gend)
- c) number of animal units (animal)
- d) unit animal body weight (kg) - (bodywt)
- e) field size (m**2) - (area)
- f) digestibility - (digest)
- g) yield (tons/ac) - (yild)

Line 21e3:

- a) perennial crop growth stop date, if any (julian) - (jdstop)

*** Note *** Line 21e2 is repeated for the number of cycles

If mgtopt is option 3:

Line 21e1:

- a) approximate date to reach senescence (julian) - (jdharv)
- b) maximum above ground biomass produced (tons/acre) - (tothav)

Line 21e2:

- a) perennial crop growth stop date, if any (julian) -(jdstop)
(enter 0 if growth does not stop)

Fallow Crop Management Inputs

Line 21a:

- a) grain yield of previous crop
(bu/acre, lb/acre, or tons/acre) - (yld)
- b) row width of previous crop (m) - (rw)

Line 21b:

- a) residue management option - (resmngt)
 - 1) herbicide application
 - 2) burning
 - 3) silage
 - 4) shredding
 - 5) residue removal
 - 6) none

Line 21c:

if residue management option 1 chosen (see line 22b):

- a) herbicide application date (julian) - (jdherb)

If option 2:

- a) residue burning date (julian) - (jdburn)
- b) fraction of standing residue burned (0-1) - (fbrnog)
- c) fraction of flat residue burned (0-1) - (fbrmag)

If option 3:

- a) silage date (julian) - (jdsilge)

If option 4:

- a) standing residue shredding date (julian) - (jdcut)
- b) fraction of standing residue shredded (0-1) - (frcut)

If option 5:

- a) residue removal date (julian) - (jdmovr)
- b) fraction of flat residue removed (0-1) - (frcut)

If option 6: line 21c does not exist

***** Note ***** Lines 19 through 21 are repeated for the number of flow elements times the number of years of simulation. For example, if two overland flow elements are represented for three years, element one of year one is given first, then element two of year one. Year two for elements one and two would be given next, followed by the same order for year three. Within each element, year sequence, lines 20 and 21 are repeated for the number of crops on that element for that year.

Table S.3.5. Landuse and tillage codes (Aug. 1989).

Landuse	Code
Agriculture	1
Rangeland	2
Forest	3
Tillage	Code
Moldboard Plow	1
Straight Chisel	2
Twisted Chisel	3
Field Cultivation	4
Tandem Disk	5
Offset Disk	6
One Way Disk	7
Paraplow	8
Spike Tooth Harrow	9
Spring Tooth Harrow	10
Rotary Hoe	11
Bedder Ridge	12
V-Blade Sweep	13
Subsoiler	14
Rototiller	15
Roller Packer	16
Row Planter with Smooth Coulter	17
Row Planter with Fluted Coulter	18
Row Planter with Sweep	19
Rlister	20
Drill	21
Drill with Chain Drag	22
Row Cultivator with Finger Wheels	24
Rod Weeder	25
Rolling Cultivator	26
NH3 Applicator	27

* Data files currently available

S.3.4.2 Rangeland Management Files

Figure S.5.5 shows an example of a management for a single element profile for four years. Table S.3.6 has a description of the variables in Fig. S.5.5. As for the case of croplands, no community specific information is continued internal to the WEPP model. All plant community parameters are input via the rangeland management file.

Table S.3.6 Management input data file (rangeland) description

Line 1:	<ul style="list-style-type: none"> a) number of overland flow elements - (nelem) b) number of crops (ncrop)
Line 2:	<ul style="list-style-type: none"> a) code for vegetation type (1-crop, 2-range) - (iplant)
Line 3:	<ul style="list-style-type: none"> a) change in surface residue mass coefficient - (aca) b) change in root mass coefficient - (ar) c) parameter value for canopy height equation - (bbb)
Line 4:	<ul style="list-style-type: none"> a) carbon-nitrogen ratio of residue and roots - (cn) b) daily removal of surface organic residue by insects - (bugs) c) standing biomass where canopy cover is 100% - (cold) d) minimum temperature to initiate growth - (gtemp) e) minimum temperature to initiate senescence - (tempmn)
Line 5:	<ul style="list-style-type: none"> a) average height of shrubs - (shgt) b) average number of shrubs along a 100 m belt transect - (spop) c) average canopy diameter m for shrubs - (sdiam) d) projected plant area coefficient for shrubs - (scoeff) e) average height for grasses - (ghgt) f) average number of grasses along a 100 m belt transect - (gpop) g) average canopy diameter m for grasses - (gdiam) h) projected plant area coefficient for grasses - (gcoeff)
Line 6:	<ul style="list-style-type: none"> a) average height for trees - (thgt) b) average number of trees along a 100 m belt transect - (tpop) c) average canopy diameter m for trees - (tdiam) d) projected plant area coefficient for trees - (tcoeff) e) maximum herbaceous plant height (hmax)
Line 7:	<ul style="list-style-type: none"> a) day of peak standing crop, 1st peak - (pscday) b) frost free period - (ffp) c) fraction of first peak of growing season - (cf1) d) fraction of 2nd peak of growing season - (cf2) e) day on which peak occurs, 2nd growing season - (scday2) f) plant drought tolerance factor - (ptol) g) coefficient for leaf area index - (aleaf) h) maximum standing live biomass - (plive) i) minimum amount of live biomass - (rgcmin) j) flag for decomposition of standing dead biomass as a result of herbicide application - (woody) k) fraction of initial standing woody biomass - (wood)

Line 8:

- a) root biomass in top 10 cm - (root10)
- b) fraction of live and dead roots from maximum at start of year - (rootf)

*** Note *** Lines 2 through 9 are repeated for number of vegetation types per simulation.

Line 9:

- a) land use - (landuse)

Line 10:

- a) initial snow cover (snoin)

Line 11:

- a) initial residue mass on the ground (kg/m**2) - (rmogt)
- b) initial residue mass above the ground (kg/m**2) - (rmagt)
- c) rock and gravel surface cover (0-1) - (wcf)
- d) cryptogram surface cover (0-1) - (crypto)
- e) average rainfall during growing season (m) - (pptg)

Line 12:

- a) crop type - (itype)
- b) burning application date - (jfdate)
- c) herbicide application date - (ihdate)
- d) grazing flag (0-no grazing, 1-grazing) - (grazig)
- e) tillage sequence code - (null)
- f) secondary tillage layer (m) - (tillay(1))
- g) primary tillage layer (m) - (tillay(2))

If ihdate is not equal to zero then read in line 13.

Line 13:

- a) flag for soil activated herbicides - (active)
- b) fraction of change in evergreen biomass - (herb)
- c) fraction increase of foliage - (update)
- d) fraction change in above and below ground biomass - (regrow)
- e) fraction reduction in live biomass - (dleaf)

If jfdate is not equal to zero then read in line 14

Line 14:

- a) fraction of increase of forage - (alter)
- b) fraction of change in standing dead biomass - (burned)
- c) fraction change in potential above and below ground biomass - (change)
- d) fraction change in evergreen biomass - (hurt)
- e) fraction reduction in residue - (reduce)

If jgraz is not equal to zero then read in lines 15 to jgraz

Line 15:

- a) pasture area (m**2) - (area)
- b) fraction of forage available for consumption - (access)
- c) average amount of supplemental feed per day (kg/day) - (suppmt)
- d) number of animals grazing (animal units per year) - (animal)
- e) average body weight of an animal (kg) - (bodywt)
- f) number of grazing sequences per year - (jgraz)
- g) minimum digestibility of forage (digmin)
- h) maximum digestibility of forage (digmax)

Line 16 to jgraz:

- a) start of grazing period (Julian day) - (gday)
- b) end of grazing period (Julian day) - (gend)
- c) start of supplemental feeding day (Julian day) - (ssday)
- d) end of supplemental feeding day (Julian day) - (send)

S.3.5 Sprinkler Irrigation Scheduling File(s)

Zero, one, or two irrigation data files might be required to run the model, depending on the irrigation scheduling option specified in the management data file. Formats for the data files are discussed in the following sections.

S.3.5.1 Depletion Level Scheduling Data File

Figure S.5.6 is an example of the structure of a depletion level irrigation scheduling data file. The variables in Fig. S.5.6 are described in Table S.3.7. Line 1 contains variables used to determine whether the data file has the correct format. Line 2 contains variables that will not be changed during the simulation. The remaining lines define variables used to determine irrigation depths and durations, and the periods when irrigation events might occur for specific overland flow elements.

Table S.3.7. Depletion level irrigation scheduling data file description.

Line 1:

- a) flag indicating file is for depletion level irrigation scheduling (value compared to irtype)
- b) number of overland flow elements (value compared to nelem)

Line 2:

- a) minimum irrigation depth (m) - (irdmin)
- b) maximum irrigation depth (m) - (irdmax)

Line 3:

- a) flag identifying the overland flow element for which the remaining elements of the line apply - (depflg)
- b) application rate of the irrigation system (m/s) - (irate)
- c) ratio of application depth to amount of water needed to fill the soil profile to field capacity for the maximum rooting depth - (aprti)
- d) maximum value for the ratio of available soil water depletion to available water holding capacity (depletion ratio at which irrigation will occur) - (deplev)
- e) Julian date of the beginning of the period during which irrigation might occur - (irbeg)
- f) year of the beginning of the period during which irrigation might occur - (yrbeg)
- g) Julian date of the end of the period during which irrigation might occur - (irend)
- h) year of the end of the period during which irrigation might occur - (yrend)

***** Note ***** Line 3 is repeated as many time as is necessary to define all irrigation periods for all overland flow elements.

The repeated occurrences of line 3 must be carefully organized to simulate the desired irrigation periods. The minimum number of occurrences of line 3 is equivalent to the number of overland flow elements. These lines must be in order of increasing overland flow element number (see first five occurrences of line 3). The remaining lines must be in order based on the ending dates of the previous irrigation periods for the overland flow elements, with the following additional criteria:

1. If no additional irrigation periods are to occur for an overland flow element, no additional lines of data should appear for that element. Thus, in Fig. S.5.6, overland flow elements in 1 and 3 will not be irrigated after the 272nd day of the year labeled 81.
2. If two or more overland flow elements have the same ending date for their respective irrigation periods, subsequent lines of data must occur in order of increasing overland flow element number. Thus, the 6th and 7th occurrences of line 3 in Fig. S.5.6 are in order of increasing overland flow element number.

The additional criteria are not applicable for the last two occurrences of line 3 in Fig. S.5.6. Thus, these lines are in order based on the ending dates of the previous irrigation periods for the corresponding overland flow elements.

To prevent irrigation on an overland flow element, the first occurrence of information for that element should specify an irrigation period that begins after the end of the simulation period. This was done as an example in Fig. S.5.6 for overland flow element 5.

S.3.5.2 Fixed Date Scheduling File

Figure S.5.7. is an example of the structure of a fixed date irrigation scheduling data file. The variables in Fig. S.5.7. are described in Table S.3.8. Line 1 contains variables used to determine whether the data file has the correct format. The remaining lines define irrigation rates, amounts, and dates for specific overland flow elements.

Table S.3.8. Fixed date irrigation scheduling data file description.

Line 1:

- a) flag indicating file is for fixed date irrigation scheduling (value compared to irtype)
- b) number of overland flow elements (value compared to nelemt)

Line 2:

- a) flag identifying the overland flow element for which the remaining elements of the line apply - (fixflg)
 - b) application rate of the system (m/s) - (irrate)
 - c) irrigation depth (m) - (iramt)
 - d) Julian date of the irrigation event - (irday)
 - e) year of the irrigation event - (iryrt)
-

*** Note *** Line 2 is repeated as many times as is necessary to define all irrigation dates for all overland elements

The repeated occurrences for line 2 must be carefully organized to simulate the desired irrigation events. The minimum number of occurrences of line 2 is equivalent to the number of overland flow elements. These lines must be in order of increasing overland flow element number (see first five occurrences of line 2). The remaining lines must be in order based on the previous irrigation dates for the overland flow elements. This criteria is used to determine the order of the 6th and 7th occurrences of line 2 in Fig. S.5.7. The following criteria are used to handle two special cases that might occur.

1. If no additional irrigation events are to occur on an overland flow element, no additional lines of data should appear for that overland flow element.
2. If two or more overland flow elements have the same irrigation date, subsequent lines of data must occur in order of increasing overland flow element number. This criteria is used to determine the order of the last two lines of data in Fig. S.5.7.

To prevent irrigation on an overland flow element, the first occurrence of information for that element should specify an irrigation date that falls after the end of the simulation.

S.4 References

- Chu, S. T. 1978. Infiltration during unsteady rain. *Water Resource Res.* 14(3):461-466.
- Foster G. R. and L.J. Lane (compilers). 1987. User requirements: USDA-Water Erosion Prediction Project (WEPP). NSERL Report No. 1, USDA-ARS, W. Lafayette, IN., 43 p.
- Williams, J. R., Nicks, A. D., and Arnold, J. G. 1985. Simulator for water resources in rural basins. *ASCE Hydraulic J.* 3(6):970-986.

S.5 Figures

Figure S.5.1. Example climate input file.

1. Continuous simulation mode

```

1.          1
2.          Station: INDIANAPOLIS, INDIANA
3.          Beginning year: 01 Number of years simulated: 3
    
```

4.	day	mon	year	prcp (mm)	dur (hr)	tp	ip	tmax (C)	tmin (C)	rad (ly/day)
5.				1.77	1.92	.25	2.00	.45	-7.17	62.36
6.	1	1	01	.00	.00	.25	2.00	-4.63	-11.29	108.91
	2	1	01	11.12	.82	.25	2.00	-2.45	-10.92	168.35
	3	1	01	.00	.00	.25	2.00	11.56	-12.08	135.26
	4	1	01	.00	.00	.25	2.00	2.53	-2.28	117.69
	5	1	01	.00	.00	.25	2.00

2. Single storm simulation mode

```

1.      2
6.      3      1      01      11.12      .82      .25      2.00      -2.45      -10.92      168.35
    
```

*** Note *** Line numbers (2-5) are NOT included in the input file

Figure S.5.2. Example slope input data file

```

1.          1
2.      90  100.0
3.      0
4.      3
5.      20 .02 25 .10 30 .01
6.      75.
    
```

Figure S.5.3. Example soil data file

1.	1									
2.	'miami'	'siltloam'	4	0.5	0.5	0.0	0.0	0.0		
3.	252.0	1.35	2.40	0.40	0.27	40.0	33.0	2.39	10.	10.0
	500.0	1.35	2.40	0.40	0.27	40.0	33.0	2.39	10.	10.0
	780.0	1.35	2.40	0.40	0.27	40.0	30.0	2.39	10.	10.0
	1200.0	1.35	2.40	0.40	0.27	40.0	33.0	2.39	10.	10.0

Figure S.5.4. Example management data file for cropland

1.	1	2	0					
2.	1							
3.	1							
4.	62.0000	2.24000	4.00000	2.50000	2.50000	100.000	2.60000	60.0000
	750.000	3.00000	2.00000	0.250000	0.700000	0.800000	0.900000	3.00000
	100.000	3000.00	32.7200	56.0000	1.12000	1.00000	3.60000	
	1.31000	0.220000	5.10000e-02	0.	10.0000	2.58000	14	0.200000
	0.	9999.00	1.00000	0.990000	0.	0.		
	0.930	0.250	0.450	0.250	0.500			
	0.550	0.400	0.200	0.200	0.300			
	0.100	0.750	0.100	0.200	0.550			
	0.150	0.150	0.250	0.250	0.150			
	0.500	0.150	0.	0.	0.			
2.	1							
3.	2							
4.	80.0000	4.00000	5.00000	2.50000	2.50000	75.0000	0.800000	30.0000
	600.000	23.0000	2.00000	0.330000	0.700000	0.700000	0.850000	5.00000
	0.	0.	0.	0.	0.	0.	14.0000	
	0.260000	0.100000	1.00000e-03	0.	7.00000	2.58000	0	0.
	4.00000	9999.00	0.600000	0.990000	0.	0.100000		
	0.930	0.250	0.450	0.250	0.500			
	0.550	0.400	0.200	0.200	0.300			
	0.100	0.750	0.100	0.200	0.550			
	0.100	0.080	0.150	0.200	0.400			
	0.150	0.150	0.250	0.250	0.150			
	0.500	0.150	0.	0.	0.			
5.	0.043	0.023	0.026	0.015	0.026			
	0.038	0.026	0.010	0.015	0.018			
	0.012	0.025	0.015	0.015	0.015			
	0.010	0.010	0.012	0.013	0.025			
	0.012	0.009	0.015	0.015	0.010			
	0.015	0.013	0.	0.	0.			
6.	0.050	0.050	0.075	0.025	0.050			
	0.050	0.050	0.025	0.025	0.025			
	0.	0.150	0.075	0.075	0.			
	0.025	0.010	0.025	0.075	0.100			
	0.050	0.025	0.075	0.050	0.025			
	0.150	0.025	0.	0.	0.			
7.	0.360	0.100	0.100	0.150	0.230			
	0.230	0.230	0.360	0.050	0.100			
	0.	1.000	1.524	0.300	0.			
	0.075	1.000	1.000	1.000	1.000			
	1.000	1.000	1.000	1.000	0.125			
	1.000	0.300	0.	0.	0.			

Figure S.5.5. Management data file for rangeland for 4 years with no disturbance.

1.	1	1					
2.	2						
3.	5.890	2.100	1.300				
4.	35.000	0.00015	1.0000	15.000	2.0000		
5.	0.0000	0.0000	0.0000	0.0000			
	0.0000	60.0000	0.5000	0.7800			
6.	0.0000	0.0000	0.0000	0.0000	0.80		
7.	162.00	240.0000		1.0000	0.000		
	0.00	0.1500	6.0000	0.3960			
	0.0000	0.0000	0.00				
8.	0.80	0.66					
9.	2						
10.	0.0						
11.	0.0085	0.2100	0.0000	0.0000	0.20000		
12.	1	0	0	0	0	0.1	0.20
12.	1	0	0	0	0	0.1	0.20
12.	1	0	0	0	0	0.1	0.20
12.	1	0	0	0	0	0.1	0.20

Figure S.5.6. Example data file for depletion level irrigation scheduling.

1.	1	5					
2.	0.006	0.102					
3.	1	1.5e-6	0.7	0.40	120	81	272
	2	1.5e-6	0.7	0.40	120	82	170
	3	1.5e-6	0.7	0.40	120	81	272
	4	1.5e-6	0.7	0.40	120	82	170
	5	1.5e-6	0.7	0.40	1	83	2
	2	1.5e-6	0.8	0.30	171	82	222
	4	1.5e-6	0.8	0.30	171	82	220
	4	1.5e-6	0.7	0.40	221	82	272
	2	1.5e-6	0.7	0.40	225	82	272

Figure S.5.7. Fixed date irrigation scheduling data file

1.	2	5			
2.	1	1.5e-6	0.051	181	81
	2	1.5e-6	0.051	180	82
	3	1.5e-6	0.051	180	81
	4	1.5e-6	0.051	180	82
	5	1.5e-6	0.051	1	83
	3	1.5e-6	0.051	210	81
	1	1.5e-6	0.051	211	81
	2	2.0e-6	0.051	210	82
	4	2.0e-6	0.051	210	82

Chapter 1. OVERVIEW OF WEPP HILLSLOPE PROFILE EROSION MODEL

A. D. Nicks, V. L. Lopes, M. A. Nearing, and L. J. Lane

1.1 Introduction

The USDA - Water Erosion Prediction Project (WEPP) models represent a new erosion prediction technology based on fundamentals of stochastic weather generation, infiltration theory, hydrology, soil physics, plant science, hydraulics, and erosion mechanics. The hillslope or landscape profile version of the model discussed herein provides major advantages over existing erosion prediction technology. The most notable advantages include capabilities for estimating spatial and temporal distributions of soil loss (net soil loss for an entire hillslope or for each point on a slope profile can be estimated on a daily, monthly, or average annual basis), and since the model is process-based it can be extrapolated to a broad range of conditions that may not be practical or economical to field test.

Processes considered in the hillslope profile model include rill and interrill erosion, sediment transport and deposition, infiltration, soil consolidation, residue and canopy effects on soil detachment and infiltration, surface sealing, rill hydraulics, surface runoff, plant growth, residue decomposition, percolation, evaporation, transpiration, snowmelt, frozen soil effects on infiltration and erodibility, climate, tillage effects on soil properties, effects of soil random roughness, and contour effects including potential overtopping of contour ridges. The model accommodates the spatial and temporal variability in topography, surface roughness, soil properties, crops, and land use conditions on hillslopes.

In the following sections an overview of the WEPP profile or hillslope version is presented. This chapter briefly describes the model user requirements, the basic concepts involved in the development of the mathematical models, the model components, and the program design and development.

1.2 Model User Requirements

Expected users of the new generation of erosion prediction models include all current users of the Universal Soil Loss Equation (Wischmeier and Smith, 1978). Anticipated applications include conservation planning, project planning, and inventory and assessment. The WEPP overland flow profile version is to be applied to hillslopes without concentrated flow channels (the watershed and grid versions described in the User Requirements (Foster and Lane, 1987) will deal with erosion and deposition processes on a watershed scale). The length of the representative profile to which the WEPP hillslope version can be applied depends upon the topography and land use controlling stream channel density. The hillslope profile version computes interrill and rill erosion and deposition along selected landscape profiles. The procedure does not consider classical gully erosion. Also, the procedure is limited to areas where the hydrology is dominated by Horton overland flow (i.e., rainfall rates exceed infiltration capacity and subsurface flow is negligible). The new erosion prediction technology is designed to be operational on personal computers and operate quickly so that several management schemes can be evaluated in a relatively short period of time. Foster and Lane (1987) describes in detail the model user requirements outlined above and the land uses to which the erosion prediction technology is applicable.

1.3 Basic Concepts

The WEPP hillslope profile erosion model computes soil loss along a slope and sediment yield at the end of a hillslope. Interrill and rill erosion processes are considered. Interrill erosion is described as a process of soil detachment by raindrop impact and sediment delivery to rill flow areas. Sediment delivery rate to rill flow areas is assumed to be proportional to the square of rainfall intensity. Rill erosion is described as a function of the flow's ability to detach sediment, sediment transport capacity, and the existing sediment load in the flow.

Overland flow processes are conceptualized as a mixture of broad sheet flow occurring in interrill areas and concentrated flow in rill areas. Broad sheet flow on an idealized surface is assumed for

overland flow routing and hydrograph development. Overland flow routing procedures include both an analytical solution to the kinematic wave equations and regression equations derived from the kinematic approximation for a range of slope steepness and lengths, friction factors (surface roughness coefficients), soil textural classes, and rainfall distributions. Because the solution to the kinematic wave equations is restricted to an upper boundary condition of zero depth, the routing process for strip cropping (cascading planes) uses the concept of the equivalent plane as described in Chapter 5. Once the peak runoff rate and the duration of runoff have been determined from the overland flow routing, or by solving the regression equations to approximate the peak runoff and duration, steady state conditions are assumed at the peak runoff rate for erosion calculations. Runoff duration is calculated so as to maintain conservation of mass for total runoff volume.

The erosion equations are normalized to the discharge of water and flow shear stress at the end of a uniform slope and are then used to calculate sediment detachment, transport, and deposition at all points along the hillslope profile. Net detachment in a rill segment is considered to occur when hydraulic shear stress of flow exceeds the critical shear stress of the soil and when sediment load in the rill is less than sediment transport capacity. Net deposition in a rill segment occurs whenever the existing sediment load in the flow exceeds the sediment transport capacity.

1.4 Model Components

The WEPP hillslope model includes components for weather generation, frozen soils, snow accumulation and melt, irrigation, infiltration, overland flow hydraulics, water balance, plant growth, residue decomposition, soil disturbance by tillage, consolidation, and erosion and deposition. These components are briefly introduced in this chapter. They are discussed in detail in the following chapters. The model includes options for single storm, continuous storms, single crop, crop rotation, irrigation, contour farming, and strip cropping.

1.4.1 Weather Generation

The climate component (Nicks, 1985) generates mean daily precipitation, daily maximum and minimum temperature, mean daily solar radiation, and mean daily wind direction and speed. The number and distribution of precipitation events is generated using a two-state Markov chain model. Given the initial condition that the previous day was wet or dry, the model determines stochastically if precipitation occurs on the current day. A random number (0-1) is generated and compared with the appropriate wet-dry probability. If the random number is less than or equal to the wet-dry probability, precipitation occurs on that day. Random numbers greater than the wet-dry probability give no precipitation. When a precipitation event occurs, the amount of precipitation is determined from a skewed normal distribution function. The rainfall duration for individual events is generated from an exponential distribution using the monthly mean durations. The amount of daily precipitation is partitioned between rainfall and snowfall using daily air temperature. If the average daily air temperature is 0°C or below, the precipitation is considered snowfall. Daily maximum and minimum temperatures and solar radiation are generated from normal distribution functions.

A disaggregation model has been included in the climate component to generate time-rainfall intensity data or break point data from daily rainfall amounts. That is, given a rainfall amount and rainfall duration, the disaggregation model derives a rainfall intensity pattern with properties similar to those obtained from analysis of breakpoint data. The breakpoint rainfall data are required by the infiltration component to compute rainfall excess rates and thus runoff. The mathematical equations used in the climate component and storm disaggregation model are presented in Chapter 2.

1.4.2 Frozen Soils and Snow Accumulation and Melt

The snowmelt-frozen soil component is divided into three separate subcomponents that interact with each other on a daily basis. These subcomponents deal with soil frost, snowmelt, and snowdrift. The

soil frost subcomponent is based on heat flow theory. It assumes that heat flow in a frozen or unfrozen soil or soil-snow system is unidirectional and that the average 24-hour temperature of the system surface-air interface is approximated by average daily air temperature. This subcomponent predicts daily frost and thaw development for various combinations of snow, residue and tilled, and/or untilled soil. It is driven by daily inputs of maximum and minimum air temperature and snow depth. Snow and soil thermal conductivity and water flow components are considered as constants. The soil frost subcomponent outputs values for daily frost depth, thaw depth, number of freeze-thaw cycles, water accumulated in frozen soil, and infiltration capacity of the tilled layer (or top 20 centimeters of soil if the soil is untilled).

The snowmelt subcomponent is based on a generalized snowmelt equation developed by the U.S. Army Corps of Engineers (1956, 1960), as modified by Hendrick et al. (1971), to adapt it for use with readily available meteorological and environmental data. This equation was further modified by Young et al. (see Chapter 3) to make it compatible with a grid-based model. The snowmelt equation incorporates four major energy components of the snowmelt process: air temperature, solar radiation, vapor transfer, and precipitation. The following assumptions are made for snowmelt calculations: 1) any precipitation that occurs on a day when the maximum daily temperature is below 0°C is assumed to be snowfall; 2) no snowmelt occurs if the maximum daily temperature is below -2.8°C; 3) the snowpack does not melt until the density of the snow is greater than 0.35 g/cm³; 4) the surface soil temperature is 0°C during the melt period; 5) the albedo of melting snow is approximately 0.5; and 6) the maximum daily temperature is approximately 2.2 times the mean daily temperature.

The snowdrift subcomponent determines the distribution of snow along the profile by estimating the depth of snow on the ground on a daily basis. User inputs to the snowdrift subcomponent consist of the slope aspect in degrees north, the land slope, and the area of the hillslope. Calculations are based on surface roughness (obtained from the soil component), snow depth (obtained from the snowmelt subcomponent), amount of precipitation, minimum daily temperature, mean daily wind speed, and mean daily wind direction (all obtained from the weather generator component). The assumptions and mathematical formulations of the snowdrift model are presented in Chapter 3.

1.4.3 Irrigation

The irrigation component of the WEPP hillslope profile version accommodates a solid set sprinkler irrigation system. Four irrigation management schemes are currently available: 1) no irrigation, 2) irrigation based on available soil water depletion, 3) fixed schedule irrigation, and 4) a combination of the second and third options. The first option is the default option for irrigation in the WEPP overland flow profile version. For the second option, the decision on whether irrigation is necessary is determined by calculating the available soil water depletion for the entire soil profile and for the current root depth on a daily basis. For the fixed schedule option, the irrigation scheme is read in from a user-created data file. The fourth option is included primarily to allow a pre-planting irrigation. Parameters for depletion level and fixed schedule irrigation are read in from individual data files. The irrigation component is presented in Chapter 12.

1.4.4 Infiltration

The infiltration component of the hillslope model is based on the Green and Ampt equation, as modified by Mein and Larson (1973), with the ponding time calculation for an unsteady rainfall (Chu, 1978). The infiltration process is divided into two distinct stages: a stage in which the ground surface is ponded with water and a stage without surface ponding. During an unsteady rainfall the infiltration process may change from one stage to another and shift back to the original stage. Under a ponded surface the infiltration process is independent of the effect of the time distribution of rainfall. At this point the infiltration rate reaches its maximum capacity and is referred to as the infiltration capacity. At this stage rainfall excess is computed as the difference between rainfall rate and infiltration capacity.

Without surface ponding, all the rainfall infiltrates into the soil. The infiltration rate equals the rainfall intensity, which is less than the infiltration capacity, and rainfall excess is zero. The mathematical equations used in the infiltration component are presented in Chapter 4. The procedures for estimating the soil parameters that affect infiltration are presented in Chapters 4 and 6.

1.4.5 Overland Flow Hydraulics

Surface runoff is represented in two ways in the hillslope computer model. First, broad sheet flow is assumed for the overland flow routing and hydrograph development. Overland flow routing procedures include both an analytical solution to the kinematic wave equations and an approximate method. The approximate method uses two sets of regression equations, one for peak runoff rate and one for runoff duration. These regression equations were derived from the kinematic approximation for a range of slope gradients and lengths, friction factors (surface roughness coefficients), soil textural classes, and rainfall distributions. Because the solution to the kinematic wave equations is restricted to an upper boundary condition of zero depth, the routing process for strip cropping (cascading planes) uses the concept of the equivalent plane described in Chapter 5. Once the peak runoff rate and the duration of runoff have been determined from the overland flow routing, or by solving the regression equations to approximate the peak runoff rate and duration, steady state conditions are assumed at the peak runoff rate for rill erosion and transport calculations.

The proportion of the area in rills is represented by a rill density statistic (equivalent to a mean number of rills per unit area) and an estimated rill width. Representative rill cross sections are based on the channel calculations for equilibrium channel geometries similar to those used in the CREAMS model (Knisel, 1980) and width-discharge relationships derived from Laflen et al. (1987). Depth of flow, velocity, and shear stress in the rills are calculated assuming rectangular channel cross-sections. The erosion calculations are then made for a constant rate over a characteristic time to produce estimates of erosion for the entire runoff event. Details on the runoff calculation are given in Chapter 5.

1.4.6 Water Balance

The water balance and percolation component of the hillslope model is based on the water balance component of SWRRB (Simulator for Water Resources in Rural Basins) (Williams and Nicks, 1985), with some modifications for improving estimation of percolation and soil evaporation parameters. The water balance component maintains a continuous balance of the soil moisture within the root zone on a daily basis. Redistribution of water within the soil profile is accounted for by Ritchie evapotranspiration model (Ritchie, 1972) and by percolation from upper layers to lower layers based on a storage routing technique (Williams et al., 1984). The water balance component uses information generated by the weather generation component (daily precipitation, temperature, and solar radiation), infiltration component (infiltrated water volume), and plant growth component (daily leaf area index, root depth, and residue cover). Details on the mathematical equations used in the water balance component are given in Chapter 7.

1.4.7 Plant Growth

The plant growth component simulates plant growth for cropland and rangeland conditions. The purpose of this component is to simulate temporal changes in plant variables that influence the runoff and erosion processes. The cropland plant growth model will simulate the growth of any plant for which plant growth parameters are specified in the management input files. Crop growth variables computed in the cropland model include growing degree days, mass of vegetative dry matter, canopy cover and height, root growth, leaf area index, plant basal area, etc. The cropland plant growth model accommodates mono, double, rotation, and strip cropping practices.

The rangeland plant growth model estimates the initiation and growth of above and below-ground biomass for range plant communities by using a unimodal or a bimodal potential growth curve (Chapter

8). Range plant variables computed in the rangeland model include plant height, litter cover, foliar canopy cover, ground surface cover, exposed bare soil, and leaf area index.

1.4.8 Residue Decomposition

The residue decomposition component estimates decomposition of flat residue mass (residue mass in contact with the soil surface), standing material (residue mass standing above ground), submerged residue mass (residue mass that has been incorporated into the soil by a tillage operation), and root mass. Decomposition parameters must be specified in the management input file. The decomposition component partitions total residue mass at harvest into standing and flat components based upon harvesting and residue management techniques. The model also sets the initial stubble population at harvest equivalent to the plant population calculated in the plant growth component.

1.4.9 Soil Parameters

Soil parameters that influence hydrology and erosion are updated in the soil component, include: 1) random roughness, 2) oriented roughness, 3) bulk density, 4) wetting-front suction, 5) saturated hydraulic conductivity, 6) interrill erodibility, 7) rill erodibility, and 8) critical shear stress. Random roughness is most often associated with tillage of cropland soil, but any tillage or soil disturbing operation creates soil roughness. Random roughness decay following a tillage operation is predicted in the soil component from a relationship including a random roughness parameter and the cumulative rainfall since tillage. A random roughness parameter is assigned to a tillage implement based upon measured averages for an implement. Oriented roughness results when the soil is arranged in a regular way by a tillage implement. In the WEPP overland flow profile version, oriented roughness is the height of ridges left by tillage implements, which can vary by a factor of two or more depending upon implement type. Ridge decay following tillage is computed from a relationship including a ridge height parameter and the cumulative rainfall since tillage. A ridge height value is assigned to a tillage implement based on measured averages for an implement.

Bulk density reflects the total pore volume of the soil and is used to update several infiltration related variables, including wetting front suction and saturated hydraulic conductivity. Adjustments to bulk density are made due to tillage operations, soil water content, rainfall consolidation, weathering consolidation, wheel traffic compaction, and livestock compaction. The approach to account for the influence of tillage operations on soil bulk density is a classification scheme where each implement is assigned a tillage intensity value ranging from 0 to 1, which is similar to the approach used in EPIC (Williams et al., 1984). Adjustments to saturated hydraulic conductivity are made to account for soil susceptibility to sealing and crusting, macropore volume and soil cracks open to the surface, volume of coarse fragments, soil freezing, and soil canopy or residue cover.

The interrill erodibility parameter is a measure of the soil resistance to detachment by raindrop impact. Because the soil is disturbed for the cropland erodibility tests and not for rangeland tests (Lafren et al., 1987; Simanton et al., 1987), algorithms for adjusting the interrill erodibility parameter are different for cropland and undisturbed rangeland soils. Adjustments to the interrill erodibility parameter on croplands are made to account for root biomass, freezing and thawing, and wheel compaction. Adjustments to the interrill erodibility parameter on rangeland are made to account for rangeland tillage, root biomass, freezing and thawing, and livestock compaction. The rill erodibility parameter is a measure of the soil resistance to detachment by rill flow and is often defined as the increase in soil detachment per unit increase in shear stress of the flow. Critical shear stress is a threshold parameter defined as the value above which a rapid increase in soil detachment per unit increase in shear stress occurs. As for the interrill erodibility parameter, different adjustment relationships should be used for adjustments of the rill erodibility parameter and critical shear stress on cropland and rangeland soils. These adjusting equations include the effects of incorporated residue and roots, coarse fragments, and soil consolidation due to drying.

1.4.10 Erosion and Deposition

Soil erosion is represented in two ways in the WEPP overland flow profile version: 1) soil particle detachment by raindrop impact and transport by sheet flow on interrill areas (interrill delivery rate), and 2) soil particle detachment, transport and deposition by concentrated flow in rill areas (rill erosion). Calculations within the erosion routines are made on a per unit rill width basis and subsequently converted to a per unit field width basis.

Interrill delivery rate is modeled as proportional to the square of rainfall intensity. The mathematical function describing interrill delivery rate also includes parameters to account for the effects of ground cover, canopy cover, and soil erodibility on interrill detachment and transport (Lane et al., 1987). Detachment due to rainfall occurring during periods when infiltration capacity is greater than rainfall intensity is not considered to contribute to interrill detachment.

Rill erosion is modeled as the flow's capacity to detach soil, transport capacity, and the existing sediment load in the flow. Net soil detachment in rills occurs when hydraulic shear stress exceeds critical shear stress and when sediment load is less than sediment transport capacity (Lane et al., 1987). Net deposition occurs when sediment load is greater than sediment transport capacity. Sediment transport capacity and sediment load are calculated on a unit rill width basis. Sediment load is converted to a unit width basis at the end of the calculations. Sediment transport capacity is calculated as a function of x (distance downslope) using a simplified Yalin equation (Lane et al., 1987), and is modified for residue in rills.

Conditions at the end of a uniform slope through the endpoints of the given profile are used to normalize the erosion equations. Distance downslope is normalized to the total slope length. The slope at a point is normalized to the uniform slope. Shear stress is normalized to shear stress at the end of the uniform slope. Sediment load is normalized to transport capacity at the end of the uniform slope.

The erosion and deposition component has four dimensionless parameters: one for interrill erosion, two for rill erosion, and one for deposition. The normalized sediment continuity equation is solved analytically when net deposition occurs but it is numerically integrated when detachment occurs. A more complete description of the erosion and deposition component is given by Foster, et al. in Chapter 10.

1.5 Program Design and Development

The WEPP hillslope model has been developed and tested on VAX 11-780 computers running under VAX/VMS 4.3 and UNIX 4.3, on IBM/compatible personal computers running under MS-DOS environments, Prime 50 series and ATT 3B2 running UNIX V, 2.02.

The computer program has been developed in a modular fashion, integrating in a top-down design all the specialized modules (program units) which perform the basic computations. This modular structure has been designed to facilitate substitution of different components and/or subroutines as improved technology is developed. No restrictions have been imposed on the input data length, the only limitation being due to the storage capacity of the hardware support. The source code is written in ANSI FORTRAN 77 for efficiency and portability, especially among personal computers. Figure 1.5.1 shows the major calculation blocks and decision sequences in the current version of the computer program.

WEPP PROFILE MODEL

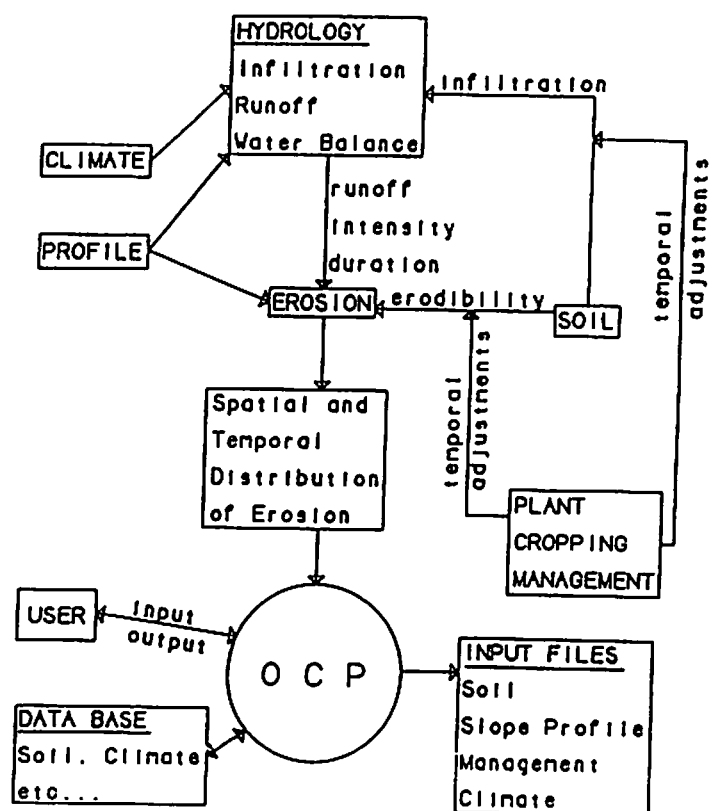


Fig. 1.5.1. Flow chart for WEPP computer model.

1.6 Summary

The USDA/WEPP profile computer model represents a new generation technology for estimating soil erosion caused by rainfall and overland flow on hillslopes and is a major improvement over existing erosion prediction technology. The model is based on fundamental hydrologic and erosion processes, including major components for climate, infiltration, water balance, crop growth and residue decomposition, surface runoff, and erosion. It calculates spatial and temporal distributions of soil loss. The model has been designed to meet the requirements of computational efficiency, flexibility and portability.

1.7 References

- Chu, S. T., 1978. Infiltration during an unsteady rain. *Water Resources Research*, 14(3):461-466.
- Foster G. R., and Lane, L.J. 1987. User requirements: USDA-Water Erosion Prediction Project (WEPP). NSERL Report No. 1, USDA-ARS, W. Lafayette, IN., 43p.
- Hendrick, R. L., Filgate, B. D., and Adams, W. M., 1971. Application of environmental analysis to watershed snowmelt. *J. Applied Meteorology*, 10:418-429.
- Knisel, W. G.(ed.), 1980. CREAMS: A field-scale model for chemicals, runoff and erosion from agricultural management systems. USDA Conservation Research Report No. 26, USDA-ARS, Washington, DC, 640p.

- Laffen, J. M., Thomas, A. W., and Welch, R. W., 1987. Cropland experiments for the WEPP project. ASAE Paper No. 87-2544.
- Lane, L. J., Foster, G. R., and Nicks, A. D., 1987. Use of fundamental erosion mechanics in erosion prediction. Paper presented 1987 Int. Winter Meeting of the Am. Soc. Agr. Engr., Chicago, IL, 10p.
- Mein, R. G., and Larson, C. L., 1973. Modeling infiltration during a steady rain. *Water Resources Research* 9(2):384-394.
- Nicks, A. D., 1985. Generation of climate data. In: D. G. DeCoursey (editor), *Proc. of the Natural Resources Modeling Symp.*, Pingree Park, CO, October 16-21, 1983, USDA-ARS, ARS-30.
- Ritchie, J. T., 1972. A model for predicting evaporation from a row crop with incomplete cover. *Water Res. Res.*, 8(5):1204-1213.
- Simanton, J. R., West, L. T., Weltz, M. A., and Wingate, G., D., 1987. Rangeland experiment for the WEPP project. ASAE Paper No. 87-2545.
- U. S. Army Corps of Engineers. 1960. *Runoff from snowmelt. Manual EM 1110-2-1406.* Gov. Printing Office.
- U. S. Army Corps of Engineers. 1956. *Snow hydrology: summary report of the snow investigations.* North Pacific Division.
- Williams, J. R., and Nicks, A. D., 1985. SWRRB, a simulator for water resources in rural basins: an overview. In: D. G. DeCoursey (editor), *Proc. of the Natural Resources Modeling Symp.*, Pingree Park, CO, October 16-21, 1983, USDA-ARS, ARS-30, pp. 17-22.
- Williams, J. R., Jones, C. A., and Dyke, P. T., 1984. A modeling approach to determining the relationship between erosion and soil productivity. *Trans. ASAE* 27(1):129-142.
- Wischmeier, W. H., and Smith, D. D., 1978. *Predicting rainfall erosion losses - a guide to conservation planning.* Agr. Handbook No. 537, U.S. Dept. of Agr., Washington, D.C., 58 pp.

Chapter 2. WEATHER GENERATOR

A.D. Nicks and L.J. Lane

2.1 Weather Generator and Equations

The weather generation methods used in the WEPP model are based on the generators used in the EPIC and SWRRB models (Williams, et al., 1984), and (Williams, et al., 1985). This selection was based on the following: 1) the generator has been well tested in many location across the United States (Nicks, 1985) (see Fig. 2.1.1), 2) the inputs for the model have been developed for nearly 200 stations, and 3) parameter estimation software and techniques are available. The methods used have been modified to include the additional requirements for intensity distributions. The following section describes the equations and algorithms for various components of the generator.



Fig. 2.1.1. Test locations for Weather Generator for EPIC and SWRRB models.

2.1.1 Precipitation Occurrence

The method used for generating the number and distribution of precipitation events is a two-state Markov chain. This method involves the calculation of two conditional probabilities: α , the probability of a wet day following a dry day, and β , the probability of a dry day following a wet day. The two-state Markov chain for the combination of conditional probabilities is

$$P(W|D) = \alpha \quad [2.1.1]$$

$$P(D|D) = 1 - \alpha \quad [2.1.2]$$

$$P(D | W) = \beta \quad [2.1.3]$$

$$P(W | W) = 1 - \beta \quad [2.1.4]$$

where $P(W | D)$, $P(D | D)$, $P(D | W)$, and $P(W | W)$ are the probabilities of a wet given a dry, dry given a dry, dry given a wet, and a wet given a previous wet day, respectively. Twelve monthly values of these probabilities are calculated and used to provide a transition from one season to another. Random sampling of the monthly distributions is then used to determine the occurrence of a wet or dry day.

2.1.2 Precipitation Amount

A skewed normal distribution is used to represent the daily precipitation amounts for each month. The form of this equation is

$$x = \frac{6}{g} \left\{ \left[\frac{g}{2} \left(\frac{X - \mu}{s} \right) + 1 \right]^{1/3} - 1 \right\} + \frac{g}{6} \quad [2.1.5]$$

where x is the standard normal variate, X is the raw variate, and μ , s , and g , are the mean, standard deviation, and skew coefficient of the raw variate, respectively. The mean standard deviation and skew coefficient of daily amounts are calculated for each month. Then, to generate a daily amount for each wet day occurrence, a random normal deviate is drawn and the raw variate, X (daily amount), is calculated using Eq. [2.1.5]. The precipitation amount is assumed to be snow if the generated average daily air temperature is at or below zero degrees Celsius ($^{\circ}\text{C}$).

2.1.3 Storm Duration

The method used to estimate the duration of generated precipitation events is that used in the SWRRB model (Arnold et al., 1987). It is assumed that the duration of storm events is exponentially related to mean monthly duration of events given by

$$D = \frac{4.607}{-2 \ln(1 - rl)} \quad [2.1.6]$$

where D is the event duration in hours and rl a dimensionless parameter from a gamma distribution of the half-hour monthly average precipitation amounts.

2.1.4 Peak Storm Intensity

The peak storm intensity is estimated by a method proposed by (Arnold and Williams, 1989) given as

$$r_p = -2P \ln(1 - rl) \quad [2.1.7]$$

where r_p is the peak storm intensity, P is the total storm amount and rl is as described previously.

Time from the beginning of the storm to the peak intensity is estimated by calculating the upper limit of storm duration by

$$D_u = 24.0 \left(1 - e^{\left(\frac{-0.3}{rl} \right)} \right) \quad [2.1.8]$$

and

$$D_p = 0.4 D_u \quad [2.1.9]$$

where D_u is the upper limit of storm duration varying from 0 to 24 h, and D_p is the time to peak intensity.

The rainfall depth-duration-frequency relationship produced by the weather generator is sensitive to the peak storm intensity, r_p , and the duration of the event, D . Equations [2.1.6] and [2.1.7] for the storm duration and peak storm intensity, respectively, are tentative and subject to modification as more historical precipitation data are analyzed. In addition, historical tabulations of rainfall depth-duration-frequency data for durations up to 24 h include multiple storms in the total daily rainfall. Further research is needed to analyze the national data base of hourly and breakpoint precipitation data to determine regional probability distributions for the number of storms per day, their duration, individual peak intensities, and the resulting influence on the apparent rainfall depth-duration-frequency relationships.

2.1.5 Air Temperature

The dependency of air temperature on a given day to the precipitation occurrence condition, is that for dry days following dry days, temperatures tend to be higher than normal and for wet days following wet days temperatures tend to be lower. Similar results are seen for wet following dry and dry following wet days (Nicks and Harp, 1980), (Richardson, 1981). The relationships used in the WEPP climate generator are

$$T_{max} = T_{mx} + (ST_{mx})(v)(B) \quad [2.1.10]$$

$$T_{min} = T_{mn} + (ST_{mn})(v)(B) \quad [2.1.11]$$

where T_{max} and T_{min} are generated maximum and minimum temperatures, T_{mx} and T_{mn} are the mean daily maximum and minimum temperatures for a given month, ST_{mx} and ST_{mn} are the standard deviation of maximum and minimum temperature for the month, v is a standard normal deviate, and B is a weighting function based on the wet-dry day probabilities. Values for B for a given month are

$$B(W|D) = 1 - \frac{P(W|D)}{PF} \quad [2.1.12]$$

$$B(W|W) = 1 - \frac{P(W|W)}{PF} \quad [2.1.13]$$

$$B(D|D) = \frac{P(D|D)}{PF} \quad [2.1.14]$$

$$B(D|W) = \frac{P(D|W)}{PF} \quad [2.1.15]$$

where $P(W|D)$ is the probability of wet day after a dry day and $P(W|W)$ is the probability of wet day following a wet day. PF is a probability factor based on the wet - dry day probabilities given by

$$PF = P(W|D)(1-P(W|D)) + P(W|W)(1-P(W|W)) \quad [2.1.16]$$

2.1.6 Solar Radiation

The generation of daily solar radiation is done in a similar manner as temperature using a normal distribution of daily values during a month. Daily generated solar radiation is given by

$$RA = (RAm) + (Ura)(x)(B) \quad [2.1.17]$$

where RA is the generated daily solar radiation, RAm is mean monthly solar radiation, Ura is the standard deviation for daily solar radiation and x is a standard normal variate. The generated solar radiation is constrained between a maximum value possible for the day of the year, $RAmax$, and a minimum value currently set at 5% of the maximum value. The maximum radiation possible is computed from the location of the station and the sun angle on the day to be generated. The standard deviation is estimated by

$$Ura = (RAmax) - \frac{(RAm)}{4} \quad [2.1.18]$$

2.1.7 Dew Point Temperature

Dew point temperatures are generated in the model by

$$Tdp = Tdpo + (STmn)(v)(B) \quad [2.1.19]$$

where Tdp is the generated daily dew point temperature, $Tdpo$ is the mean monthly dew point temperature, and v is a standard normal deviate.

2.1.8 Wind Speed and Direction

Wind speed and direction are required by the WEPP model in the calculation of snow accumulation and melt. The method used for these calculations is taken from the EPIC model subroutine WGEN (Richardson and Wright, 1984). A two-parameter gamma distribution is used to generate wind speed from the mean monthly observed speed. Wind direction is generated by sampling the cumulative distribution of wind direction constructed from the observed percent time during a month with wind blowing from the 16 cardinal directions.

2.1.9 Historical Data

Daily, hourly, and 15-minute data have been obtained from the National Weather Service, National Climatic Data Center. These data have been read and inventoried. There are approximately 7000 stations with record lengths of 25 years or more of either precipitation or precipitation and maximum and minimum temperature data. The distribution of these stations is shown in Fig. 2.1.2. As analyses of these data continue, selection of additional stations for parameterization will be made to allow the generation of weather inputs for the WEPP family of erosion models. A sub-set of approximately 1000 stations based on a grid 1- by 1- degree of longitude and latitude have been selected for parameterization. The distribution of these stations is shown in Fig. 2.1.3. Currently under investigation is the use of a Geographic Information System (GIS) to allow subsequent mapping of the parameter values.

Linking of the climatic data base developed under the WEPP with GIS would allow the user agencies more flexibility in the parameter selection than specific site values. It may also provide a partial solution to problems that have plagued the user of climatic data in remote areas of the western mountain areas of the United States. Current studies are investigating the possible use of GIS as a method to provide interpolation between the few high altitude climatic stations.

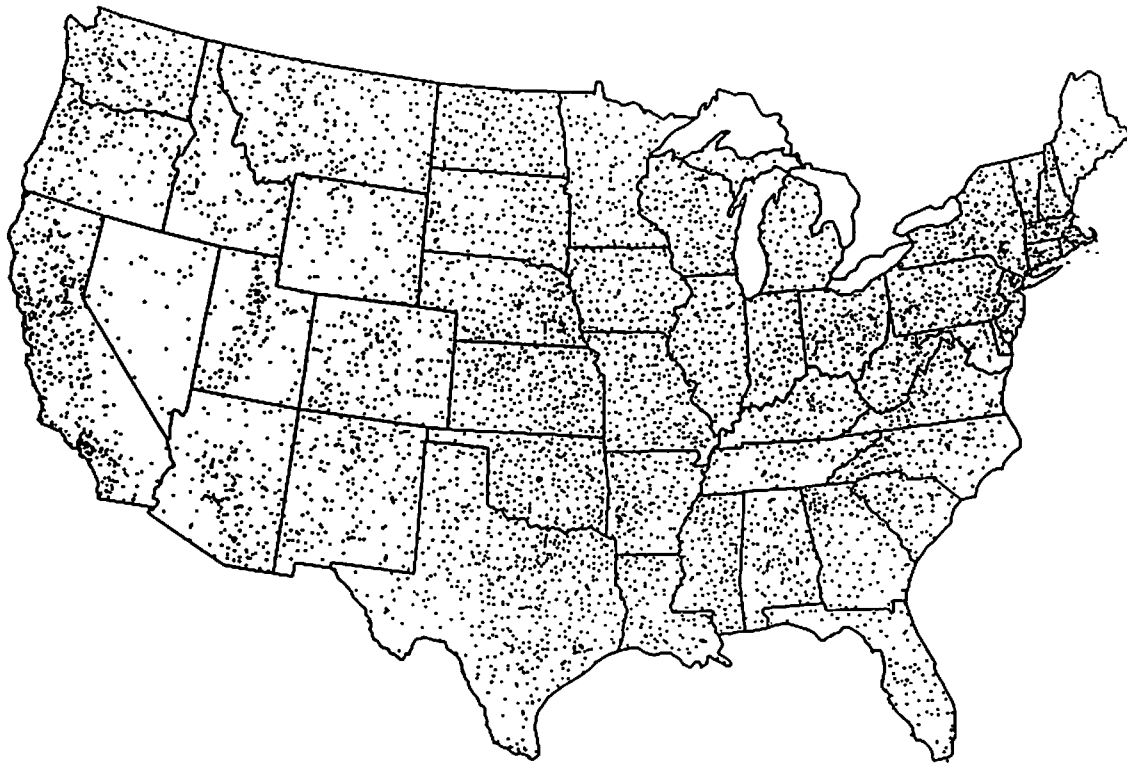


Fig. 2.1.2. Weather stations from National Climatic Data Center.

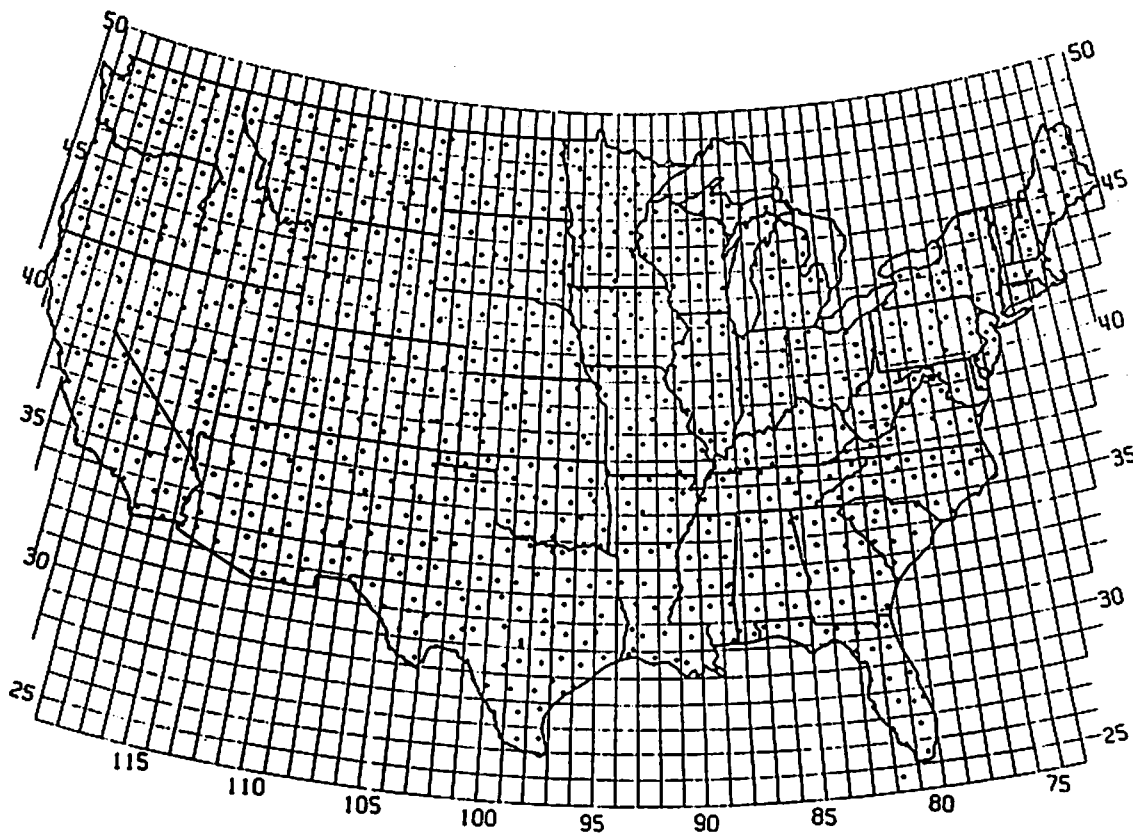


Fig. 2.1.3. Subset of 1000 weather stations selected for parameterization.

2.2 Storm Disaggregation for Rainfall Intensity Patterns

To apply the Green-Ampt infiltration equation in computing infiltration and thus runoff, rainfall input data must be in the form of breakpoint data. A file in breakpoint data form contains two columns with cumulative time from the beginning of the storm in the first column and average rainfall intensity over the time interval between successive times in the second column. The form is called breakpoint because the data result from numerical differentiation of the cumulative time vs. cumulative rainfall depth curve at the changes in slope or breakpoints.

Example calculations for a hypothetical storm are summarized in Table 2.2.1. Column 1 is the cumulative time (min) from the start of the rainfall storm and column 2 is the cumulative rainfall depth (mm) at the given times. Column 3 is the rainfall intensity ($mm\ h^{-1}$) calculated from columns 1 and 2 as follows. From time = 0 to time = 5 min, 2.0 mm of rain fell. Therefore, the average rainfall intensity ($mm\ h^{-1}$) from time 0 to 5 min is computed as

$$i = \left[\frac{2.0 - 0.0\ mm}{5.0 - 0.0\ min} \right] \frac{60\ min}{h} = 24.0\ \frac{mm}{h} \quad [2.2.1]$$

and the average rainfall intensity from time 5 to 7 min is computed as

$$i = \left[\frac{10.0 - 2.0\ mm}{7.0 - 5.0\ min} \right] \frac{60\ min}{h} = 240.0\ \frac{mm}{h} \quad [2.2.2]$$

Notice that a first value of intensity is listed at time zero. This means that from time zero until the first time (5 min in this case) the average rainfall intensity was $24.0\ mm\ h^{-1}$. The last intensity value in column 3 of Table 2.2.1 is zero. The storm ended at time = 30 min, so rainfall intensity from 30 min on is listed as zero. A similar convention (nonzero intensity value at time zero and zero intensity value at the last time given for the storm) is used throughout the WEPP computer programs.

Table 2.2.1. Example of rainfall intensity calculations using break-point data.

Time (min) (1)	Rainfall Depth (mm) (2)	Rainfall Intensity (mm/h) (3)	Normalized Time (4)	Normalized Intensity (5)
0.	0.0	24.0	0.0	0.60
5.	2.0	240.0	0.167	6.00
7.	10.0	80.0	0.233	2.00
10.	14.0	18.0	0.333	0.45
20.	17.0	18.0	0.667	0.45
30.	20.0	0.0	1.000	0.0

Again, columns 1 and 3 in Table 2.2.1 would be used as input data to the infiltration calculations while columns 1 and 2 would represent typical data from a recording rain gauge. Data shown in columns 4 and 5 of Table 2.2.1 will be discussed in section 2.2.1.

Development of data such as in Table 2.2.1 for a 10- to 20-year period at a particular location to use in calculating infiltration for WEPP would be very laborious. Disaggregation of total storm data into rainfall intensity patterns with properties similar to those obtained from analysis of observed breakpoint data could save a great deal of effort. That is, given a storm amount and storm duration, approximate intensity patterns which will yield similar infiltration, runoff, and erosion can be developed. The following sections provide a brief background and describe the method used in deriving approximate rainfall intensity data from data on storm amount and duration.

Schaake, et al. (1972) described a multivariate technique to generate rainfall for annual, seasonal, monthly, and daily events. The generation method involved the staged disaggregation of rainfall from annual to seasonal, seasonal to monthly, and finally monthly to daily values.

Franz (1974) developed a procedure to generate synthetic, hourly rainfall data within a storm and used empirically derived parameters to model hour to hour storm amounts with a multivariate normal distribution. An hour of zero rainfall was used to define the end of a storm period. Skees and Shenton (1974) noted that annual and monthly rainfall amounts had been successfully modeled as random variables with gamma, normal, and logarithmic normal distributions. For shorter intervals (weeks, days, hours), satisfactory distributions were more difficult to obtain.

Austin and Claborn (1974) derived a method to distribute the rainfall during storm events but assumed that no significant serial correlation existed between rainfall periods within the storm. A series of independent storm intensities were generated, then adjusted, to preserve the previously generated storm amount and duration. The procedure generated independent 4-minute intensities within the storm although analyses of observed data suggested the need for a serial correlation between 4-minute rainfall intensities.

Hershenhorn and Woolhiser (1987) reviewed previous rainfall disaggregation methods proposed by Betson, et al. (1980) and Srikanthan and McMahon (1985). Both methods were described as needing very large numbers of parameter estimates, and a procedure was proposed of a more parameter-efficient approach. Hershenhorn and Woolhiser (1987) disaggregated daily rainfall into one or more individual storms and then disaggregated the individual storms into rainfall intensity patterns. The disaggregated data included starting times of the events as well as the time-intensity data within each event.

Flanagan, et al. (1987) studied the influence of storm pattern (time to peak intensity and the maximum intensity) on runoff, erosion, and nutrient loss using a programmable rainfall simulator. Six rainfall patterns and three maximum intensities were used. Although the storm patterns were constant, triangular, and compound consisting of four straight line segments, all patterns could be described fairly well by a double exponential function. The double exponential function or distribution describes rainfall intensity as exponentially increasing with time until the peak intensity and then exponentially decreasing with time until the end of the storm.

The WEPP User Requirements (Foster and Lane, 1987) suggested that the maximum information required to represent a design storm consist of the following: (a) storm amount, (b) average intensity, (c) ratio of peak intensity to average intensity, and (d) time to peak intensity. Examination of appropriate functions to describe a rainfall intensity pattern given this information suggested consideration of a triangular distribution and a double exponential distribution. Because the area of a triangle is one half the product of the base (storm duration) and the height (maximum or peak intensity), the ratio of peak intensity to average intensity for a triangular distribution is fixed at exactly 2. Therefore, intensity patterns within a single storm are represented with the double exponential function.

2.2.1 Definition of Variables

If all times during the storm are normalized by the storm duration, D , and all intensity values are normalized by the average intensity, I_b , then the result is called a normalized intensity pattern and is shown in columns 4 and 5 in Table 2.2.1. The area under the normalized time-intensity curve is 1.0 and the normalized duration is also 1.0.

Let the normalized time be t and the normalized intensity be $i(t)$. The normalized time until the peak intensity, t_p , is calculated as the time to peak intensity over the storm duration. In the example in Table 2.2.1, the maximum rainfall intensity occurs from time = 5 to time = 7 min. Let the time to peak intensity be 6.0 min so that

$$t_p = \frac{D_p}{D} = \frac{6.0}{30.0} = 0.2 \quad [2.2.3]$$

is the normalized time to peak intensity, t_p . The normalized peak intensity is calculated as the peak intensity over the average intensity. In the example in Table 2.2.1, the maximum intensity is 240 mm h^{-1} and the average intensity is 40 mm h^{-1} (20 mm of rainfall over 0.5 hour). Therefore, the normalized peak intensity is

$$i_p = \frac{r_p}{i_b} = \frac{240.0}{40.0} = 6.0 \quad [2.2.4]$$

for the example data.

2.2.2 The Double Exponential Function for $i(t)$

A double exponential function fitted to the normalized intensity pattern is then

$$i(t) = \begin{cases} a e^{bt} & 0 \leq t \leq t_p \\ c e^{-dt} & t_p < t \leq 1.0 \end{cases} \quad [2.2.5]$$

which is an equation with four parameters (a, b, c, d) to be determined. If the area under the curve defined by Eq. [2.2.5] from 0.0 to t_p is assumed to be equal to t_p , then the area under the curve from t_p to 1.0 is $1.0 - t_p$. Using this assumption and the fact that $i(t=t_p) = i_p$, Eq. [2.2.5] can be rewritten as

$$i(t) = \begin{cases} i_p e^{b(t-t_p)} & 0 \leq t \leq t_p \\ i_p e^{d(t_p-t)} & t_p < t \leq 1.0 \end{cases} \quad [2.2.6]$$

which is now an equation with two parameters (b, d) to be determined.

If $I(t)$ is defined as the integral of $i(t)$, then

$$I(t_p) = \int_0^{t_p} i_p e^{b(t-t_p)} dt = t_p \quad [2.2.7]$$

and

$$I(1.0) = \int_{t_p}^{1.0} i_p e^{d(t_p-t)} dt = 1 - t_p. \quad [2.2.8]$$

Evaluation of these integrals results in two equations

$$i - e^{bt_p} = \frac{bt_p}{i_p} \quad [2.2.9]$$

and

$$i - e^{d(1-t_p)} = \frac{d(1-t_p)}{i_p} \quad [2.2.10]$$

which must be solved for b and d . With the above assumptions $i(0)$ is equal to $i(1.0)$ so that $d = b t_p / (1 - t_p)$. Now, Eq. [2.2.9] need only be solved for b for the entire solution. Newton's method can be used to solve for b . If b is restricted to values less than 60, then Newton's method can be used to solve for b with current microcomputers.

The integral $I(t)$ of Eq. [2.2.5] or [2.2.6] can be written as

$$i(t) = \begin{cases} \frac{a}{b} (e^{bt} - 1) & 0 \leq t \leq t_p \\ \frac{-c}{d} (e^{d(t_p-t)} - 1) & t_p < t \leq 1.0 \end{cases} \quad [2.2.11]$$

where, from above $a = i_p e^{-bt_p}$, $c = i_p e^{dt_p}$, and $0.0 \leq I(t) \leq 1.0$. Subdividing the interval $[0,1]$ into n equal subintervals and calling the right endpoint of these subintervals F_1, F_2, \dots, F_n , specific time values can be defined as T_1, T_2, \dots, T_{n+1} . These values of T_1, T_2, \dots are then defined by inverting the $I(t)$ function. Let Inverse $I(t)$ be the inverse of $I(t)$ and then

$$T_1 = \text{Inverse } I(0.0) = 0.0$$

$$T_2 = \text{Inverse } I(F_1)$$

$$T_3 = \text{Inverse } I(F_2)$$

$$T_4 = \text{Inverse } I(F_3)$$

.

.

$$T_{n+1} = \text{Inverse } I(F_n=1.0) = 1.0 \quad [2.2.12]$$

The average normalized intensity over the interval $[T_i, T_{i+1}]$ is then calculated as $I_i = (F_{i+1} - F_i) / (T_{i+1} - T_i)$. The result of these calculations is an array of ordered pairs $[T_i, I_i]$ which are normalized time-intensity values much like columns 4 and 5 in Table 2.2.1. However, because the values of F_i are on a regular subinterval, the time intervals $T_{i+1} - T_i$ vary inversely with $i(t)$. That is, when $i(t)$ is high, then $T_{i+1} - T_i$ is small and when $i(t)$ is low, $T_{i+1} - T_i$ is large.

The data in Table 2.2.1 indicate that the storm depth, P , is 20 mm, the storm duration, D , is 30 min, the normalized time to peak intensity, t_p , is 0.2, and the normalized peak intensity, i_p , is 6.0. Thus, for disaggregation purposes, the example storm is represented by four numbers: P, D, t_p, i_p . If n subintervals are used, then the disaggregated time intensity data are: $T_1, I_1, \dots, T_{n+1}, I_{n+1}$. To restore the original dimensions, multiply each T_i by D and each I_i by $(P 60.0/D)$. Example calculations for the example data from Table 2.2.1 are shown in Table 2.2.2.

Table 2.2.2 Example calculations for double exponential disaggregation of the storm shown in Table 2.2.1, with $n = 10$.

Dimensionless		Dimensioned		
Time T_i (1)	Intensity I_i (2)	Time (min) (3)	Intensity (mm/h) (4)	
0.0	0.565	0.0	22.6	
0.177	4.33	5.31	173.3	
0.200	5.62	6.00	224.7	
0.218	4.87	6.53	194.7	
0.238	4.12	7.15	164.7	
0.263	3.37	7.88	134.7	
0.292	2.62	8.77	104.6	
0.331	1.86	9.92	74.4	
0.384	1.10	11.5	43.8	
0.476	0.191	14.3	7.6	
1.00	0.0	30.0	0.0	

Notice that the peak intensity in Table 2.2.2 is 224.7 mm h^{-1} rather than exactly 240.0 mm h^{-1} . This is because the intensity is averaged over the interval from 6.0 to 6.53 min and the average intensity is always less than the instantaneous maximum.

Measured storm data for a ten year period at Chickasha, OK, are summarized in Table 2.2.3. Notice the high variability in the data (the standard deviation is about as large as the mean) for all the variables used to describe the storms.

Table 2.2.3. Summary of storm data with storm amounts greater than or equal to the threshold value. P_o . Chickasha, OK, Watershed R-5, 1966-1975.

Threshold P_o (mm)	Number of Storms	Precip. Mean	(mm) SD	Duration (h)		t_p		i_p	
				Mean	SD	Mean	SD	Mean	SD
0.0	612	10.7	14.2	2.45	2.78	0.43	0.30	4.8	5.5
2.54	425	15.0	15.2	3.29	2.92	.39	.32	6.1	5.9
6.35	278	20.8	16.0	4.01	3.21	.36	.29	6.8	5.7
12.7	177	27.3	16.9	4.49	3.53	.34	.28	7.7	6.4
25.4	71	41.6	18.7	5.34	4.01	.32	.28	7.8	3.4

2.2.3 Influence of Disaggregation on Computed Runoff

To determine the influence of the proposed disaggregation scheme on computed runoff, a comparison of how well runoff computed using measured rainfall intensity data compare with runoff computed using the rainfall intensity patterns obtained from the disaggregation. The following steps were taken to make the comparison: (a) select observed rainfall and runoff data from several small watersheds at various locations, (b) apply the Green-Ampt infiltration equation to the observed rainfall data and then adjust the Green-Ampt infiltration parameters (K_s , N_s) until the measured runoff volume is matched by the computed runoff volume, (c) route the overland flow on a single plane and adjust the hydraulic resistance parameter (Chezy C or friction factor) until the computed peak rate of runoff matches the measured peak rate or is as close to the measured peak as is possible, (d) apply the infiltration equation to the intensity pattern from the disaggregation and route the runoff on the plane using the K_s , N_s , and C values determined in b and c, and (e) compare the runoff volume and peak rates from step d with those obtained from steps b and c.

The selected watersheds are described in Table 2.2.4 and the observed data are summarized in Table 2.2.5. Notice that soils ranged from sandy loam to clay and that cover conditions ranged from near bare soil to complete cover by pasture grass.

Table 2.2.4. Selected storms for small watershed, watershed characteristics at time of storms.

Location	Watershed Area		Storm Date	Land Use & Management
	acres	(ha)		
Watkinsville, GA Watershed W-1 (Location 10) Sandy loam, approx. 63% Sa, 21% Si, 16% Cl	19.2	7.77	7/11/41	Bench terraces, broadcast cowpeas in rotation with cotton
			5/15/42	Cotton, 2-3" high, soil loose and without vegetative cover
			5/26/66	Terraces removed in 1957. Good, grazed coastal Bermuda grass, complete cover
Coshocton, OH Watershed 109 (Location 26) Muskingum silt loam	1.61	0.65	3/19/70	Dormant coastal Bermuda grass, just beginning spring growth, excellent cover
			7/7/69	Cover of 50-75%, 37" corn; 0-25%, 14" weeds, 75% density
Riesel, TX Watershed SW-17 (Location 42) 70% Houston Black clay 30% Heiden clay	2.89	1.21	22/22/71	Chopped corn stalks in field
			3/31/57	100% Bermuda grass pasture with burr-clover, weeds, dense growth
			8/12/66	100% Bermuda grass pasture 2-4" high, good cover, not grazed
			7/19/68	100% Bermuda grass pasture 10" high
			3/23/69	100% Bermuda grass pasture 6" high

Table 2.2.4. Selected storms for small watershed, watershed characteristics at time to storms. (Cont.)

Location	Watershed Area		Storm Date	Land Use & Management
	acres	(ha)		
Hastings, NE Watershed 3-H (Location 44) 75% of area is Holdrege silt loam & 25% is Holdrege silty clay loam (severely eroded)	3.77	1.53	7/3/59	Sorghum about 6" high and in good condition. Weeds beginning to grow. Last field operation 6/15/59
			5/21/65	No tillage during spring. Cover is weeds and wheat stubble.
Chickasha, OK (Location 69) Renfro, Grant, & Kingfisher silt loam	23.7	9.59	4/10/67	100% in virgin native grassland. Continuous grazing slightly in excess of optimum
			4/12/67	100% in virgin native grassland. Continuous grazing slightly in excess of optimum
			5/6/69	100% rangeland slightly overgrazed; however, range condition class good to excellent

Source of data: USDA-ARS 1963. Hydrologic data for experimental agricultural watersheds in the United States, 1956-9. USDA Misc. Publication No. 945, US Dept. of Agriculture, Agricultural Research Service, Washington, DC. Also subsequent Misc. Publications of the same title, through 1971.

The data summarized in Table 2.2.5 represent a wide range of storm sizes and patterns (i.e. P varying from 16 to 104 mm, D from 40 min to 1265 min, etc.). Individual storms selected for analysis were chosen to represent a wide range in durations, alternating periods of high and low intensity, and ranges in time to peak intensity, t_p , and peak intensity, i_p . Thus, the values of P , D , t_p , and i_p in Table 2.2.5 should provide a harsh test of the disaggregation method.

Table 2.2.5 Summary of selected events for five small watersheds, observed data.

Watershed	Date	P (mm)	D (min)	i_p	i_p	Q (mm)	Q_p (mm/h)	Antecedent	
								P (mm)	5-Day Q (mm)
Watkinsville, GA, W-1 (Location 10)	7/11/41	63.5	305	0.12	11.0	33.5	49.8	59.2	26.6
	5/15/42	50.5	71	.12	2.3	29.0	32.0	63.0	0.3
	5/26/66	88.6	633	.83	11.2	42.5	17.1	25.7	0.0
	3/19/70	69.1	1131	.42	9.7	19.9	7.2	41.9	0.1
Coshocton, OH W-109 (Location 26)	7/7/69	17.3	88	0.37	6.7	3.5	24.0	2.5	0.0
	22/22/71	20.6	1265	.11	6.0	10.9	3.7	8.9	0.0
Riesel, TX SW-17 (Location 42)	3/31/57	16.3	63	0.07	8.2	6.1	11.2	41.7	T
	8/12/66	104.2	382	.32	6.1	41.8	41.0	102.1	0.0
	7/19/68	39.1	40	.21	1.9	12.5	19.6	0.0	0.0
	3/23/69	25.1	180	.62	7.3	19.7	20.1	8.1	0.1
Hastings, NE 3-H (Location 44)	7/3/59	66.8	45	0.16	2.3	59.7	163.8	59.4	27.7
	5/21/65	85.4	98	.16	2.1	57.9	79.5	5.1	0.0
Chickasha, OK, R-5 (Location 69)	4/10/67	29.4	160	0.06	8.2	4.6	4.2	38.9	0.3
	4/12/67	64.1	519	.15	7.3	20.5	22.3	68.3	5.1
	5/6/69	43.7	380	.76	12.2	14.5e	17.9	54.4	0.5

Runoff data computed using the observed rainfall intensity patterns and computed using the approximate rainfall intensity patterns are summarized in Table 2.2.6. Notice the magnitude of the errors are less for runoff volume, Q , than for peak rate of runoff, Q_p .

An example of observed rainfall intensity data, the rainfall intensity pattern from the disaggregation, and the resulting runoff calculations is shown in Fig. 2.2.1. Notice that although the disaggregated intensity pattern does not fit the observed intensity pattern, the calculated runoff agrees quite well with measured runoff. This is not always the case, and significant errors can result from the disaggregation approximations (see Table 2.2.6). However, the overall goodness of fit of the runoff computed with the approximate intensity patterns to the runoff computed with the observed intensity patterns was significant (see Fig. 2.2.2). As shown in Fig. 2.2.2, using the disaggregated intensity patterns as input to the calibrated infiltration-runoff model explained some 90% of the variance in runoff computed using the observed rainfall intensity patterns.

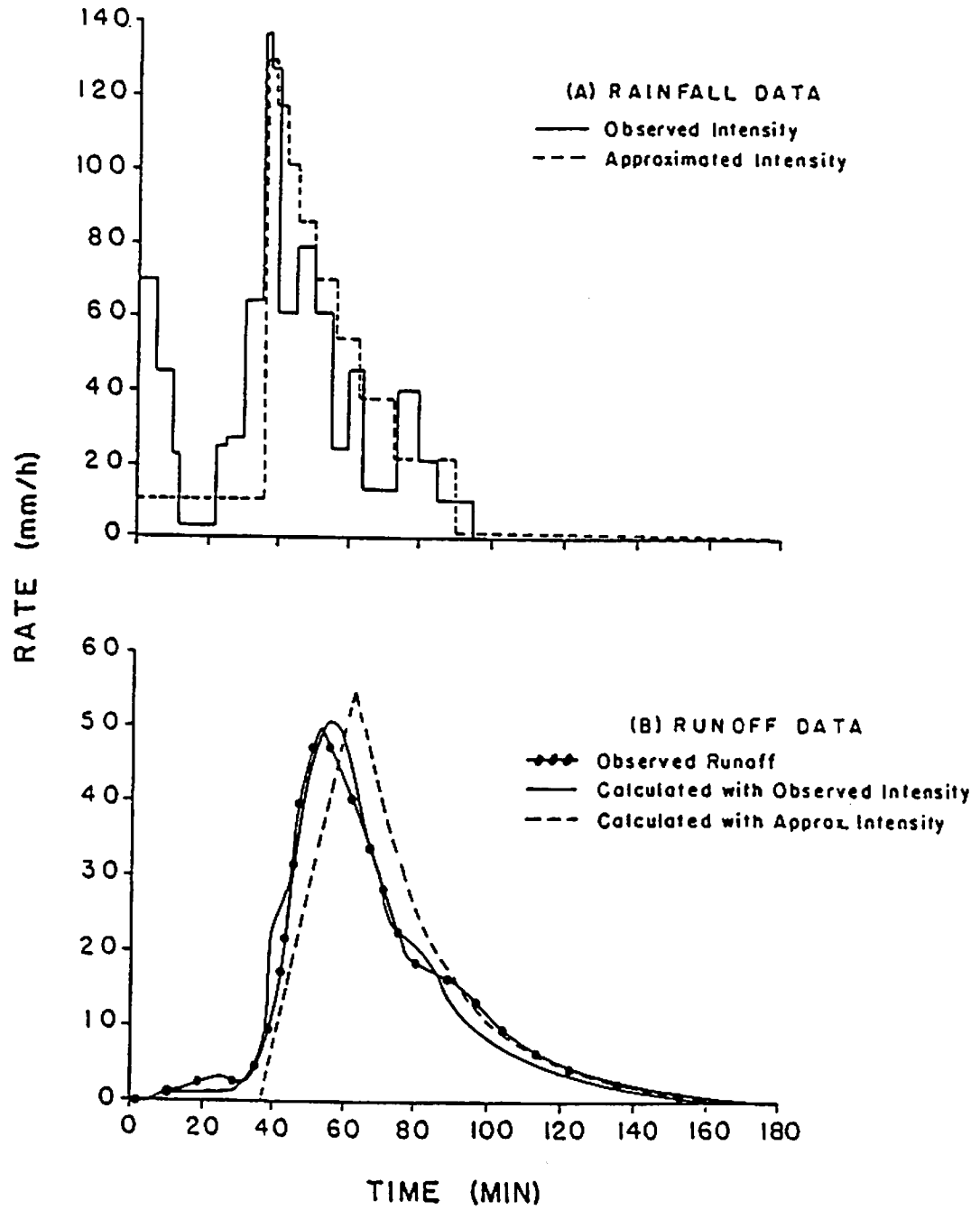


Figure 2.2.1. Rainfall and runoff data for storm of July 11, 1941 on Watershed W-1 at Watkinsville, GA.

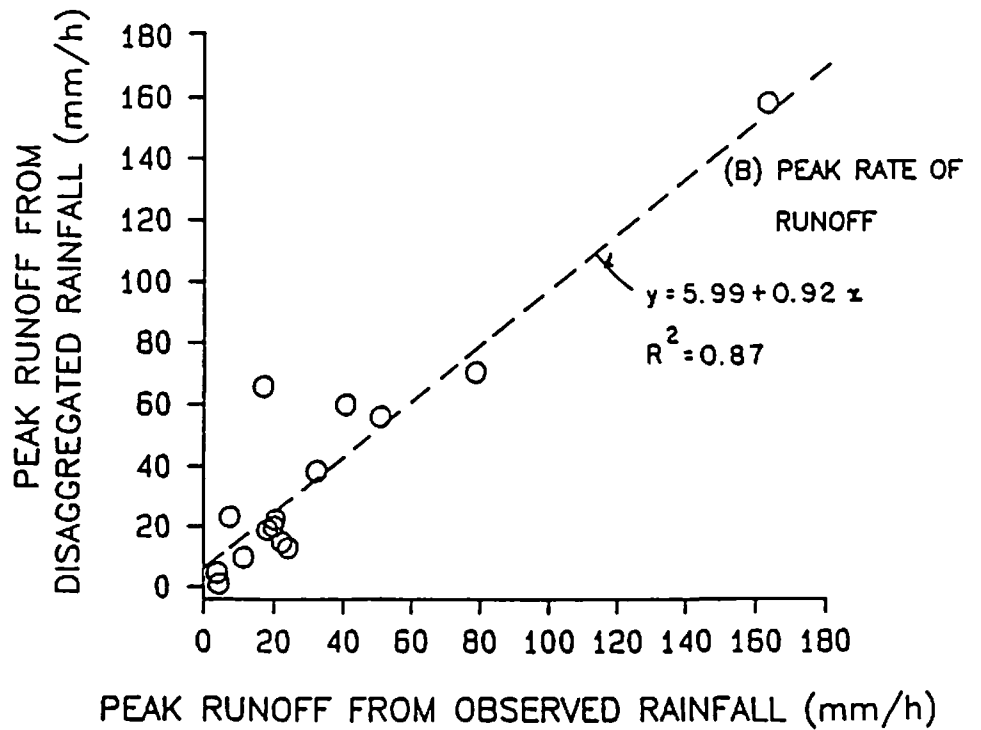
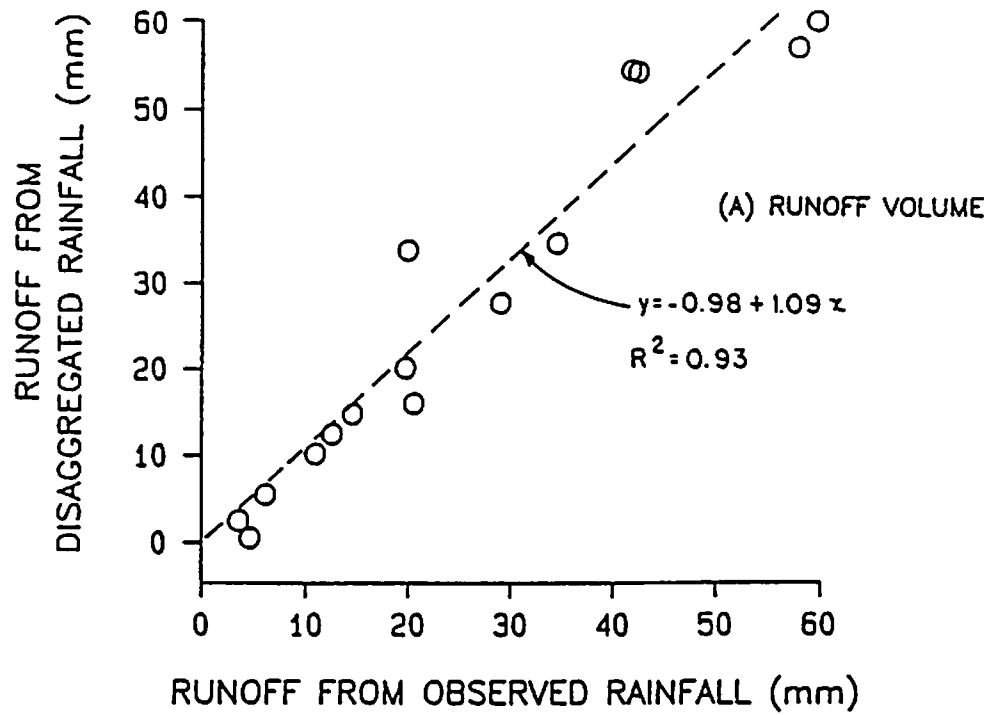


Figure 2.2.2. Relationships between runoff computed using observed and approximated rainfall intensity data.

Table 2.2.6. Summary of observed and computed runoff for selected events on five small watersheds.

Watershed & Date	Green-Ampt		Chezy C $m^{1/2}/s$	Observed Runoff		Computed Runoff			
	K_s (mm/h)	N_s (mm)		Q (mm)	Q_p (mm/h)	Measured Rain		Disag. Rain	
						Q	Q_p	Q	Q_p
Watkinsville, GA, W-1 L=350, S=.05									
7/11/41	7.20	22.0	5.0	33.5	49.8	34.5	50.8	34.2	55.0
5/15/42	7.20	18.7	4.7	29.0	32.0	29.0	32.2	27.3	37.4
5/26/66	6.72	7.5	4.1	42.5	17.1	42.5	16.8	53.8	64.8
3/19/70	4.78	7.2	3.9	19.9	7.2	19.9	7.2	33.4	22.2
Coshocton, OH, W-109 L= 97, S=.13									
7/7/69	8.17	29.1	8.7	3.5	24.0	3.5	24.0	2.2	11.8
2/22/71	0.40	7.1	2.1	10.9	3.7	10.9	3.7	9.9	3.7
Riesel, TX SW-17 L=119, S=.02									
3/31/57	2.57	59.2	5.5	6.1	11.2	6.1	11.2	5.2	8.8
8/12/66	9.64	17.5	2.3	41.8	41.0	41.8	40.7	54.0	58.8
7/19/68	16.06	21.1	3.3	12.5	19.6	12.5	19.8	12.2	18.9
3/23/69	0.65	6.6	1.9	19.7	20.1	19.7	20.3	19.8	21.2
Hastings, NE 3-H L=163, S=.05									
7/3/59	4.16	3.8	10.0	59.7	163.8	59.7	163.8	59.7	157.1
5/21/65	7.20	18.2	3.3	57.9	79.5	57.9	78.7	56.6	69.5
Chickasha, OK, R-5 L=390, S=.02									
4/10/67	11.72	42.0	10.3	4.6	4.2	4.6	4.2	0.2	0.1
4/12/67	11.72	11.9	5.8	20.5	22.3	20.5	22.2	15.7	13.8
5/6/69	11.72	20.8	7.9	14.5e	17.9	14.5	18.0	14.5	17.9

Note: All watersheds modeled as a single plane and infiltration parameters (K_s , N_s) selected to match observed runoff volume given the observed rainfall pattern. Chezy C values selected to match the observed peak rates given the observed rainfall.

Possible future improvements in the disaggregation procedure may involve the generation of multiple storm events on the same day. This modification will be undertaken if subsequent analyses of the type described above suggest it is essential to reproduce the probability distributions of runoff and sediment yield.

2.3 References

- Arnold, J. G., and Williams, J. R. 1989. Stochastic generation of internal storm structure. *Trans. ASAE* Vol. 32(1) pp. 161-166.
- Arnold, J. G., Williams, J. R., and Nicks, A. D. 1987. SWRRB, A simulator for water resources in rural basins. Volume I. Model Documentation. (in press). 71 pp.
- Austin, T. A., and Claborn, B. J. 1974. Statistical models of short-duration precipitation events. *Proc. of Symposium on Statistical Hydrology, Tucson, AZ, Aug. 31-Sept. 2, 1971. USDA-ARS, Misc. Pub. No. 1275, June 1974, pp. 356-365.*
- Betson, J. R., Bales, J., and Pratt, H. E. 1980. User's guide to TVA- HYSIM. U. S. EPA, EPA-600/7-80, pp. 40-44.
- Flanagan, D. C., Foster, G. R., and Moldenhauer, W. C. 1987. How storm patterns affect infiltration. *Proc. Intl. Conf. on Infiltration Development and Application, Jan. 6-9, 1987, Honolulu, HI, Univ. of Hawaii, Water Resources Research Center, pp. 444-456.*
- Foster, G. R., Lane, L.J. 1987. User requirements: USDA-Water erosion prediction project (WEPP). NSERL Report No. 1, Sept. 1, 1987. USDA-ARS National Soil Erosion Research Lab. Purdue Univ. 43 pp.
- Franz, D. D. 1974. Hourly rainfall generation for a network. *Proc. of Symposium on Statistical Hydrology, Tucson, AZ, Aug. 31-Sept. 2, 1971. USDA-ARS, Misc. Pub. No. 1275, June 1974, pp. 147-153.*
- Hershenthorn, J., and Woolhiser, D. A. 1987. Disaggregation of daily rainfall. *J. of Hydrology* 95:299-322.
- Nicks, A. D., and Harp, J. F. 1980. Stochastic generation of temperature and solar radiation data. *J. Hydrol.* 48:1-7.
- Nicks, A. D. 1985. Generation of climate data. *Proceeding of the Natural Resources Modeling Symposium. USDA-ASA ARS-30. pp. 297-300.*
- Richardson, C. W. 1981. Stochastic simulation of daily precipitation, temperature and solar radiation. *Water Resources Res.* 17(1):182-190.
- Richardson, C.W., and Wright, D.A. 1984. WGEN A model for generating daily weather variables. USDA-ARS ARS - 8. 80 pp.
- Schaake, J. C., Ganslaw, M. J., Fothergill, J. W., and Harbaugh, T. E. 1972. Multivariate rainfall generator for annual, seasonal, monthly, and daily events. *Proc. of the International Symposium on Mathematical Modelling Techniques in Water Resources Systems, Vol. 2, pp. 437-460, Environment Canada, Ottawa, Canada.*
- Skees, P. M., and Shenton, L. R. 1974. Comments on the statistical distribution of rainfall per period under various transformations. *Proc. of Symposium on Statistical Hydrology, Tucson, AZ, Aug. 31-Sept. 2, 1971. USDA-ARS, Misc. Pub. No. 1275, June 1974, pp. 172-196.*
- Srikanthan, R., and McMahon, T. A. 1985. Stochastic generation of rainfall and evaporation data. *Australian Water Resources Council Technical Paper No. 84, 301 p.*
- Williams, J. R., Jones, C. A., and Dyke, P. T. 1984. A modeling approach to determining the relationship between erosion and soil productivity. *Trans. ASAE* 27(1):129-144.

Williams, J. R., Nicks, A. D., and Arnold, J. G., 1985. Simulator for water resources in rural basins. ASCE Hydraulics J. 111(6):970-986.

2.3 List of Symbols

Symbols	Definitions	Units	Variable
a	parameter for the rising limb of the double exponential function	-	a
b	parameter for the falling limb of the double exponential function	-	b
B	weighting function based on the conditional probabilities	-	sum
c	parameter for the rising limb of the double exponential function	-	-
C	Chezy hydraulic resistance coefficient	$m^{1/2}/s$	chezyc
d	parameter for the falling limb of the double exponential function	-	-
D	duration of precipitation event	h	stmdur
D_p	time to peak storm intensity	h	timep
D_u	upper limit of storm intensity	h	r5u
F_i	i^{th} right endpoint of a subinterval on [0,1]	-	-
g	skew coefficient of daily precipitation in a month	-	rst(mo,3)
i	average rainfall intensity for a time interval	mm/h	avrnt
i_b	average rainfall intensity for a storm	mm/h	int
i_p	dimensionless ratio of peak to average rainfall intensity	-	ip
$i(t)$	dimensionless rainfall intensity	-	intd1
$I(t)$	integral of the dimensionless rainfall intensity	-	-
K_r	Green-Ampt equation parameter, hydraulic conductivity	mm/h	ks
L	length of overland flow plane	m	slplen
n	number of equal subintervals on [0,1]	-	-
N_s	Green-Ampt equation parameter, capillary potential	mm	sm
P	rainfall amount	mm	rain
P_o	threshold rainfall amount	mm	-
$P(D D)$	conditional probability of a dry day, D , following a dry day, D	-	prw(1,mo)
$P(D W)$	conditional probability of a dry day D following, a wet day, W	-	prw(2,mo)
$P(W D)$	conditional probability of a wet day, W , following a dry day, D	-	1 - prw (1, mo)
$P(W W)$	conditional probability of a wet day, W , following a wet day, W	-	1 - prw (2, mo)
PF	a probability factor based on wet-dry day probabilities	-	xx
Q	runoff volume	mm	runoff
Q_p	peak rate of runoff	mm/hr	peakro
RA	generated daily solar radiation	langley	rad
RAm	mean monthly solar radiation	langley	obsl

RA_{max}	maximum possible solar radiation for a day of the year	langley	rmx
r_l	dimensionless parameter in a gamma distribution	-	rl
r_p	storm peak intensity	mm/h	rsp
s	standard deviation of daily precipitation in a month	mm	rst (mo,2)
S	slope of overland flow plane	-	avgslp
ST_{mn}	standard deviation of minimum temperature for a month	°C	stdtm
ST_{mx}	standard deviation of maximum temperature for a month	°C	stdtx
t	dimensionless time	-	-
T_{dp}	daily mean dew point temperature	°C	tdp
T_{dpo}	monthly mean dew point temperature	°C	tdpo
T_i	inverse of $I(F_i)$	-	-
T_{max}	generated maximum daily temperature	°C	tmxg
T_{min}	generated minimum daily temperature	°C	tmxg
T_{mn}	mean daily minimum temperature for a given month	°C	obmn
T_{mx}	mean daily maximum temperature for a given month	°C	obmx
u	mean of daily precipitation in a month	mm	rst(1, mo)
U_{ra}	standard deviation of daily solar radiation for a month	langley	stdsl
v	standard normal deviate	-	v
x	standard normal variate	-	x
X	skewed normal random variable representing daily precipitation	-	X
α	conditional probability of a wet day following a dry day	-	-
β	conditional probability of a dry day following a wet day	-	-

Chapter 3. SNOWMELT AND FROZEN SOIL

R. A. Young, G. R. Benoit, and C. A. Onstad

Much of the world's cropland is subject to freezing at some time during each year. Freezing modifies the physical characteristics of a soil, changing its ability to transmit or retain water (Benoit and Bornstein, 1970; Benoit and Mostaghimi, 1985; Campbell et al., 1970; Loch and Kay, 1978), its structural stability (Benoit, 1973; Mostaghimi et al., 1988), and its erodibility (Bisal and Nielsen, 1967). The development of soil frost is the result of complex interactions of several primary factors, including soil characteristics, type of tillage and residue management, surface roughness, type of vegetative cover, duration and extent of freezing temperatures, and the extent and timing of snow cover. The freezing process itself modifies those soil physical properties that, along with temperature, determine the depth and duration of soil frost. The magnitude of soil changes that takes place as a result of soil freezing depends on freezing temperature, soil water content at freezing, initial size of soil aggregates, and the number of freeze-thaw cycles that take place over winter. As a result, tillage-residue management combined with over winter frost action determines a soil's erodibility during winter thaw periods and from spring snowmelt to planting (Benoit et al., 1986). The snowmelt-frozen soil subroutine is divided into three separate components which interact with each other on a daily basis. These components deal with soil frost, snowmelt, and snowdrift. The frost component estimates the extent of frost development and thawing over the winter period as well as changes in soil water content and infiltration capacity. The snowmelt component estimates the amount of snowmelt occurring and how much snowmelt water is available for runoff in the spring. The snowdrift component estimates the depth, density, and distribution of snow cover over a watershed. Interaction of the three components provides WEPP with the ability to predict the effect of soil frost and snowmelt on runoff and soil erosion.

3.1 Soil Frost

The soil frost subroutine is based on simple heat flow theory. It assumes that heat flow in a frozen or unfrozen soil or soil-snow system is unidirectional and that the average 24 hour temperature of the system surface-air interface is approximated by average daily air temperature. The subroutine predicts daily frost and thaw development for various combinations of snow, residue, and tilled and/or untilled soil and is driven only by daily inputs of maximum and minimum air temperature and snow depth. Snow and soil thermal conductivity and water flow components are considered as constants. The subroutine yields values for daily frost depth, thaw depth, number of freeze-thaw cycles, water accumulated in frozen soil, and infiltration capacity of the tilled layer or top 0.20 meters of soil if the soil is untilled.

The soil frost subroutine operates by a daily bookkeeping process that compares calories of heat lost or gained at the soil surface to heat flow from deeper unfrozen soil layers. Net calories of heat lost or gained are converted to centimeters of frozen or thawed soil. Unidirectional heat flow through the frozen soil or soil-residue-snow system is calculated from the relation:

$$Q_{sf} = \frac{K_{sf} T_{sf}}{Z_{sf}} \quad [3.1.1]$$

where Q_{sf} is the heat flux through the snow-residue-frozen soil system ($W m^{-2}$), K_{sf} is the average thermal conductivity through the combined snow residue-frozen soil depth thickness ($Wm^{-1} \circ C^{-1}$), T_{sf} is the temperature difference across the snow-residue-frozen soil thickness ($\circ C$), and Z_{sf} is the depth or thickness of the combined snow-residue-frozen soil layer (m).

Thus, heat flow through the snow-residue-frozen soil layer is the product of an average thermal conductivity for the layer and an average temperature gradient, with the gradient being the difference between average daily air temperature and the zero degree isotherm at the bottom of the frozen soil.

The basic assumption is made that the average temperature of the soil (snow) - air interface over a 24 hour period is equal to the average air temperature for the same period. The validity of this assumption varies with location as a function of those items such as emissivity, radiation, cloud cover, and wind. For this reason, the average daily surface temperature that drives the frost subroutine is computed by a surface energy balance routine that modifies average daily air temperature by a local accounting of wind speed, solar radiation, cloud cover, and atmospheric emissivity (Flersching, 1988).

The average thermal conductivity for a layered system can be shown to equal the harmonic mean for the layers in the system and is given by:

$$K_{\text{eff}} = \frac{Z_{\text{tot}}}{\sum_{i=1}^N \left(\frac{Z_i}{K_i} \right)} \quad [3.1.2]$$

where Z_i is the thickness of each layer (m), K_i is the thermal conductivity of each layer ($W m^{-1} \circ C^{-1}$) N is the number of layers, and $Z_{\text{tot}} = \sum_{i=1}^N Z_i$.

The soil frost subroutine is designed to handle a system with up to four layers - snow, residue, tilled soil, and untilled soil. In this case the average thermal conductivity equation becomes:

$$K_{\text{eff}} = \frac{(K_{\text{snow}} K_{\text{res}} K_{\text{fill}} K_{\text{fuit}})(S_{\text{nowd}} + R_{\text{esd}} + T_{\text{illd}} + U_{\text{illd}})}{K_{\text{snow}} K_{\text{res}} K_{\text{fill}} U_{\text{illd}} + K_{\text{snow}} K_{\text{res}} K_{\text{fuit}} T_{\text{illd}} + K_{\text{snow}} K_{\text{fill}} K_{\text{fuit}} R_{\text{esd}} + K_{\text{res}} K_{\text{fill}} K_{\text{fuit}} S_{\text{nowd}}} \quad [3.1.3]$$

where K_{snow} is the thermal conductivity of snow ($W m^{-1} \circ C^{-1}$), K_{res} is the thermal conductivity of residue ($W m^{-1} \circ C^{-1}$), K_{fill} is the thermal conductivity of frozen tilled soil ($W m^{-1} \circ C^{-1}$), K_{fuit} is the thermal conductivity of frozen untilled soil ($W m^{-1} \circ C^{-1}$), S_{nowd} is the snow depth (m), R_{esd} is the residue thickness (m), T_{illd} is the tilled soil depth (m), and U_{illd} is the untilled soil depth (m). With this approach, if any or all of the snow, residue or tilled depths are zero, the thermal conductivity reduces to the harmonic mean of the remaining layers.

Over any 24 hour period, Q_{eff} must be balanced by heat flow (Q_{uf}) from the unfrozen soil below the frozen layer. The frost subroutine defines Q_{uf} as the sum of heat transferred by the thermal conductivity properties of the soil matrix, the latent heat of fusion in freezing transferred water, and losses in heat content of the soil. That is:

$$Q_{\text{uf}} = K_{\text{uf}} \left[\frac{T_{\text{uf}}}{Z_{\text{uf}}} \right] + L K_w \left[\frac{P}{Z_{\text{uf}}} \right] + C_{\text{uf}} dT_{\text{uf}} Z_c \quad [3.1.4]$$

where Q_{uf} is the heat flow from unfrozen soil ($W m^{-2}$), K_{uf} is the thermal conductivity of unfrozen soil ($W m^{-1} \circ C^{-1}$), T_{uf} is the change in temperature from 0 degree isotherm to depth of stable temperature ($\circ C$), Z_{uf} is the depth of unfrozen soil to point of stable temperature (m), L is the latent heat of fusion ($W s m^{-3}$), K_w is the unsaturated hydraulic conductivity of soil ($m s^{-1}$), P is the change in total water potential (m), C_{uf} is the heat capacity of the unfrozen soil ($W m^{-3} \circ C^{-1}$), dT_{uf} is the change in temperature of a unit volume of soil in unit time ($\circ C$), and Z_c is the depth of unfrozen soil that supplies heat as a result of changes in soil temperature (m) (assume a constant value of 1 m).

In this equation, the soil temperature and water potential gradients are those that exist just below the 0 degree isotherm. As a practical convenience, the model assumes that heat flow through soil thermal conductivity and soil water movement are separate and discrete units of heat transfer.

The subroutine operates by iteratively balancing over each 24 hour period the heat lost through the snow-residue-frozen soil zone with heat flow through the unfrozen soil to the freezing front. Iteration is

on an hourly basis for each 24 hour period. During the balancing process, it is assumed that heat lost through the frozen zone is first balanced by heat flow in the unfrozen soil as a result of the soils temperature gradient and thermal conductivity. Additional heat loss is balanced by the heat of fusion released by freezing water that is held in place or migrates to the freezing front. Further heat loss is balanced by changes in soil heat content of the unfrozen soil, the magnitude of which is computed by difference.

3.2 Snowmelt

The snowmelt subroutine is based on a modification of a generalized basin snowmelt equation for melt in open areas developed by the U. S. Army Corp of Engineers (1956, 1960). This equation was modified by Hendrick et al. (1971) to adapt it for use with readily available meteorological and environmental data. The Hendrick equation was further modified to make it compatible for use as a subroutine within the WEPP computer program format.

The equation used in the subroutine in its modified form is:

$$M = \left[0.0606R(1 - 0.01F) - 0.84(1 - N_c)(1.0 - 0.01F) + 0.0268v_2(1 - 0.008F)(0.18T_x + 1.404T_d) + (T_x + T_m)(0.0225 + 0.248P_d) \right] (0.0254) \quad [3.2.1]$$

where M is the snowmelt (m), R is the estimated radiation on a sloping surface ($MJ m^{-2}$), F is the forest cover (%), T_x is the daily maximum temperature ($^{\circ}C$), N_c is the estimated cloud cover (dec %), v_2 is the mean daily wind speed measured at a height of 2 m ($m s^{-1}$), T_d is the mean daily dewpoint temperature ($^{\circ}C$), T_m is the daily minimum temperature ($^{\circ}C$), and P_d is the mean daily precipitation (m).

Since some snowmelt can occur in direct solar radiation to about $3^{\circ}C$ below freezing (Hendrick et al., 1971), the first term in the above equation is multiplied by the quantity $(0.36T_x + 1)$ whenever $-3^{\circ}C \leq T_x < 0^{\circ}C$. The values for T_x , T_m , v_2 , T_d , and P_d are obtained from the WEPP climate generator subroutine. The amount of cloud cover, N_c , is estimated from the relationship:

$$N_c = \frac{\left[1 - \frac{R_m}{R_c} \right]}{0.7} \quad [3.2.2]$$

where R_m is the mean measured daily solar radiation ($MJ m^{-2}$) and R_c is the potential clear sky radiation on a horizontal surface ($MJ m^{-2}$).

This equation is based on the fact that clouds reflect approximately 70% of solar radiation and transmit only 30% to the earth's surface (Sutton, 1953). Both R and R_c are calculated in a separate subroutine based on the slope inclination in radians (I), the slope facing direction in degrees from north (A), the calendar day (J), the measured radiation in $MJ m^{-2}$ (R_m), a solar constant (S_c) equal to $0.081 MJ m^{-2}$, and the latitude in degrees (L) (Swift and Luxmoore, 1973). This subroutine takes into account the effects of cloud cover and atmospheric transmissivity. The slope inclination, I , is calculated as:

$$I = \tan^{-1} \left[\frac{S}{100} \right] \quad [3.2.3]$$

where S is the land slope (%).

To run the snowmelt subroutine, the values of F , A , and S are input for each slope section, L is input for the entire slope, S_c is a constant value, and J is generated within the program.

Equation [3.2.1] deals with four major energy components of the snowmelt process - temperature, radiation, vapor transfer, and precipitation. When calculating snowmelt, the following assumptions are made: any precipitation that occurs on a day when the maximum daily temperature is $< 0^{\circ}\text{C}$ is assumed to be snowfall, no snowmelt will occur if the maximum daily temperature is $< -3^{\circ}\text{C}$, the snowpack will not melt until the density of the snowpack $\geq 350 \text{ kg m}^{-3}$, the surface soil temperature = 0°C during the melt period, and the temperature of a cloud base is approximately the same as the surface air temperature. The albedo of melting snow is approximately 0.5 (Sutton, 1953), and maximum daily temperature is approximately 2.2 times the mean daily temperature (Hendrick et al., 1971). Using Eq. [3.2.1], if the calculated value of snowmelt, M , is less than 0, then $M = 0$. If it is greater than the existing snow depth, D , from the preceding day, then $M = D$.

3.3 Snowdrift

The snowdrift subroutine determines the distribution of snow over the hillslope by estimating the depth of snow on the ground at the end of a day in any slope section, depending on the weather that day and the topography. Calculations are based on several initial assumptions:

- the density of fresh newfallen snow $\approx 100 \text{ kg m}^{-3}$,
- the density of a ripe snowpack must be $\geq 350 \text{ kg m}^{-3}$ before it begins to melt,
- the threshold wind velocity for moving falling snow $\approx 0.89 \text{ m s}^{-1}$ measured at a height of 2 m,
- the surface roughness of a uniform snow pack $\approx 0.0002 \text{ m}$, and
- the snow storage capacity of a tilled layer = the random roughness.

The amount of snow trapped and stored by standing vegetation is the storage capacity, S_t , and is a function of the height and the projected stem area, or basal density, of the vegetation, the surface roughness, and the amount of standing biomass. S_t is calculated as:

$$S_t = \epsilon H d_b \frac{R_t}{R_o} + z_o \quad [3.3.1]$$

where S_t is the storage capacity of snow (m), ϵ is the trapping efficiency (%), H is the height of standing vegetation (m), d_b is the basal density of standing vegetation (m/m), R_t is the standing residue mass after tillage (kg/ha), R_o is the standing residue mass before tillage (kg/ha), and z_o is the surface random roughness (m). The trapping efficiency, ϵ , reflects the effect of vegetative height and is calculated by:

$$\epsilon = (e^{-0.1H}) - 0.1 \quad [3.3.2]$$

The basal density of the standing vegetation, d_b , is a function of the mean stem diameter and the plant population and is calculated by:

$$d_b = \frac{d_s p_o^{1/2}}{25} \quad [3.3.3]$$

where d_s is the mean stem diameter of standing vegetation (m), and p_o is the plant population (plants/ha).

User inputs to the subroutine consist of the slope facing direction (A) in degrees from north, the land slope (S) in percent, and the length (L) and width (W) of the slope section in meters. The surface roughness (z_o) in m is obtained from the soil subroutine, and precipitation (P_d) in m , mean minimum daily temperature (T_{\min}) in $^{\circ}\text{C}$, mean daily wind speed (v_2) in m s^{-1} , and mean daily wind direction (W) in

degrees from north are all obtained from the climate generator subroutine. The height of standing residue (H) in m , mean stem diameter (d_s) in m , plant population (P_o) in plants/ha, and the standing residue mass before and after tillage (R_o and R_t) in kg/ha are all obtained from the plant subroutine.

The snowdrift subroutine works in two parts, first calculating the amount of scouring or drifting of newly falling snow occurring on a slope section, or plane, during the day, including any snow drifting into the section from an upwind section, and then calculating the amount of drifting or scouring of the existing snowpack. If the drift rate (D_r) calculated for an upwind section is negative, indicating that snow in that section is drifting out of the section (scouring), then the amount of snow scoured from that upwind section is added to the snow available for movement in the next downslope section. For falling snow, a threshold velocity of $0.89 m s^{-1}$ at a height of 2 m is assumed for the incipient blowing of snow. In order to route the blowing snow across the slope, certain assumptions must be made. An upwind slope section at the top of the hillslope must accumulate snow unless the wind is blowing in a direction directly perpendicular to the direction in which the slope faces. Snow drifting onto the upslope section from upwind is distributed onto successive downwind sections according to a decay function. A downwind slope section at the top of the hillslope must scour unless the wind is blowing directly perpendicular to the direction in which the slope faces. If the wind blows perpendicular to a slope section, then no scouring or drifting occurs and the net change in snow accumulation in that section due to wind is zero. It is also assumed that there is always a sufficient supply of snow available to satisfy a drifting requirement for a given slope section.

The friction velocity at the snow surface is calculated using a commonly used mathematical representation of the wind profile (Schlichting, 1979):

$$v_h = \left[\frac{v_o}{k} \right] \ln \left[\frac{h}{z_o} \right] \quad [3.3.4]$$

where v_h is the wind velocity measured at height h ($m s^{-1}$), v_o is the friction velocity at the snow surface ($m s^{-1}$), k is the von Karman's constant (assumed to be 0.4), h is the height above the surface (m), and z_o is the surface roughness (m).

After v_o is determined, if the value of v_o is $< 0.087 m s^{-1}$ (the friction velocity corresponding to a wind velocity of $.89 m/s$ measured at a height of 2 m), then no movement of falling snow will occur and the new snow depth will be equal to the snow depth from the preceding day plus the depth of new snowfall. If $v_o \geq 0.087 m s^{-1}$, falling snow will begin to drift and the transport capacity of the wind is calculated from an equation developed by Bagnold (1941) and modified by Iversen et al. (1975):

$$q_{sf} = c \left[\frac{d_a}{g} \right] \left[\frac{v_f}{v_{sf}} \right] (v_o^2)(v_o - v_{sf}) \quad [3.3.5]$$

where q_s is the transport rate of snow ($kg m^{-1} s^{-1}$), c is a proportionality constant ($= 100$), d_a is the density of air ($kg m^{-3}$), g is the acceleration of gravity ($m s^{-2}$), v_f is the settling velocity of a snow particle ($m s^{-1}$) (for falling snow assume $0.35 m s^{-1}$ for a $0.150 mm$ snow particle falling in still air) (Schmidt, 1982), v_{sf} is the threshold velocity for incipient motion of falling snow ($m s^{-1}$) (assume $0.087 m s^{-1}$), and v_o is the friction velocity at the snow surface ($m s^{-1}$).

The drift rate of falling snow is then determined from:

$$D_f = 86.4 \frac{q_{sf}}{d_f L_p} \quad [3.3.6]$$

where D_f is the drift rate of falling snow (m/day), d_f is the density of falling snow (kg/m^3) ($\approx 100 kg/m^3$), and L_p is the distance across a slope section parallel to the wind direction (m).

While the threshold velocity for incipient movement of snow varies with the nature of the snow surface (Radok, 1977), for a uniform surface of freshly fallen snow, the threshold friction velocity for movement of snow from the snowpack is approximately $0.25 m s^{-1}$ (Tabler and Schmidt, 1986) which is equivalent to a wind velocity of about $5.76 m s^{-1}$ at a height of 2 m. However, the threshold friction velocity for movement of snow from a snowpack is a function of the density of the snowpack and, thus, will increase with time since deposition (Schmidt, 1980). The threshold velocity for movement of snow from a snowpack, v_{thg} , in $m s^{-1}$ can be estimated from:

$$v_{thg} = \frac{-0.023 \sqrt{\frac{z_o}{3.2 \times 10^{-7}}}}{\left\{ 1 - \sin \left[\tan^{-1} \left[\frac{S}{100} \right] \right] \right\} \ln(0.001 d_g)} \quad [3.3.7]$$

where z_o is the surface roughness (m), S is the slope (%), and d_g is the density of the snowpack ($kg cm^{-3}$). If the calculated value of $v_o \geq v_{thg}$, then snow on the ground will begin to move. The transport capacity of the wind for moving ground snow is then calculated in a fashion similar to that for calculating the transport capacity of the wind for moving falling snow, as:

$$q_{sg} = c \left(\frac{d_a}{g} \right) \left[\frac{v_g}{v_{thg}} \right] (v_o^2)(v_o - v_{thg}) \quad [3.3.8]$$

where q_{sg} is the transport rate of ground snow ($kg m^{-1} s^{-1}$), and v_g is the settling velocity of a ground snow particle ($m s^{-1}$) (for ground snow assume $0.75 m s^{-1}$ for a $0.220 mm$ ice sphere falling in still air) (Schmidt, 1982), and v_{thg} is the threshold velocity for incipient motion of ground snow ($m s^{-1}$). The drift rate of ground snow is then calculated from:

$$D_g = \frac{8.64 q_{sg}}{d_g L_p} \quad [3.3.9]$$

where D_g is the drift rate of ground snow (m/day), and d_g is the density of the snowpack ($kg m^{-3}$).

The density of a snowpack on the ground is a function of several factors, including time and temperature. Daily changes in the density of the snowpack are calculated on the basis of the initial depth of the snowpack and how much snowmelt occurs each day. In the absence of snowmelt, changes in snowpack density are estimated daily from the relationship:

$$d_g = 0.522 - \left[\frac{20.5}{D} \right] (1 - e^{-0.0148D}) \quad [3.3.10]$$

where D is the existing snow depth (m). This relationship is based on 14 years of premelt snowdrift data (Tabler, 1985). If snowmelt occurs while the snowpack density is less than $350 kg m^{-3}$, the depth of the snowpack is reduced by the amount of the melt but the amount of melt water is added to the remaining snowpack, thus, increasing its density. Once the density of the snowpack equals or exceeds $350 kg m^{-3}$, any additional melt water will either infiltrate the ground or run off.

If D_g exceeds the existing snow depth, D , then D_g is set equal to D . The total drift rate, D_r , is the sum of the drift rates for falling snow and ground snow, or:

$$D_r = D_f + D_g \quad [3.3.11]$$

After the total drift rate is calculated based on the transport capacity of the wind to carry snow, the direction of the wind with respect to the direction the slope faces will determine whether the snow is drifting into the slope section or out of it. Maximum scouring will occur if the direction from which the wind is blowing is the same as the direction the slope is facing and maximum drifting will occur if the slope facing direction and the wind direction are exactly opposite each other. As previously stated, if the wind is blowing perpendicular to the slope, net scouring or drifting will be zero. Thus, to determine the net movement of blowing snow into or out of an area, the total drift rate D_r must be multiplied by a factor, s_c , to reflect either scouring or drifting:

$$s_c = 0.0111 |A - W| - 1.0 \quad [3.3.12]$$

where A is the slope azimuth (degrees from north), and W is the wind direction (degrees from north).

As the degree of slope inclination increases, the efficiency of the drifting process tends to decrease. This is accounted for by multiplying the net movement of blowing snow by an efficiency factor, i , based on land slope:

$$i = 1 - \sin \left[\tan^{-1} \left(\frac{S}{100} \right) \right] \quad [3.3.13]$$

If, due to wind angle and slope azimuth, the net movement of snow is positive, i.e. drifting into a slope section rather than out of it, the drifting snow will be distributed along the slope in a downwind direction. The amount of drifting snow falling on any slope section can be approximated by an exponential decay function:

$$D_p = 1 - \left[\frac{e^{-L_r}}{(1+10 L_r)} \right] \quad [3.3.14]$$

where D_p is the total percentage of available drifting snow falling on an upslope area (%) and L_r is the ratio of the length of the upslope area to the total slope length.

Not all of the moving snow will be deposited since some of it will evaporate. Net sublimation or evaporation losses can be an important consideration in climatic hydrological balances (Branton et al., 1972). The amount of evaporation is a function of air temperature, relative humidity, solar radiation, and particle diameter (Sturges and Tabler, 1981). An estimate of the amount of evaporation occurring can be obtained by considering the distance the snow is being blown along a slope and assuming that under average conditions, complete evaporation would occur after being blown a distance of about 3050 m (Tabler, 1975). Then:

$$D_r = D_r (e^{-0.00066 L_1}) \quad [3.3.15]$$

where L_1 is the distance across a slope section parallel to the wind direction (m). Evaporation losses are only calculated for those sections in which drifting is occurring. Evaporation losses of snow from areas that are scouring would be accounted for in their downwind areas and are neglected here.

3.4 References

- Bagnold, R.A. 1941. *The physics of blown sand and desert dunes*. Methuen, London. 256 pp.
- Benoit, G.R., S. Mostaghimi, R.A. Young, and M.J. Lindstrom. 1986. Tillage-residue effects on snow cover, soil water, temperature and frost. *Trans. ASAE* 29:473-479.
- Benoit, G.R., and S. Mostaghimi. 1985. Modeling soil frost depth under three tillage systems. *Trans. ASAE* 28:1499-1505.
- Benoit, G.R. 1973. Effect of freeze-thaw cycles in aggregate stability and hydraulic conductivity of three soil aggregate sizes. *Soil Science Society of America Proc.* 37:315.
- Benoit, G.R., and J. Bornstein. 1970. Freezing and thawing effects on drainage. *Soil Science Society of America Proc.* 34:551-557.
- Bisal, F., and K.F. Nielsen. 1967. Effect of frost action on the size of soil aggregates. *Soil Sci.* 104:268-272.
- Branton, C.I., L.D. Allen, and J.E. Newman. 1972. Some agricultural implication of winter sublimation gains and losses at Palmer, Alaska. *Agric. Meteorol.*, 10:301-310.
- Campbell, G.A., W.S. Ferguson, and F.G. Warder. 1970. Winter changes in soil nitrate and exchangeable ammonium. *Can. J. Soil Sci.* 50:151-162.
- Flerschinger, G.N. 1988. Simultaneous heat and water model of a snow-residue-soil system. PhD. Thesis. Washington State University. December. 138 pp.
- Hendrick, R.L., B.D. Filgate, and W.M. Adams. 1971. Application of environmental analysis to watershed snowmelt. *Jour. Applied Meteorology*, 10:418-429.
- Iversen, J., R. Greeley, B. White, and J. Pollack. 1975. Eolian erosion of the Martian surface, 1. Erosion rate similitude. *Icarus* 26:321-331.
- Loch, J.P.G., and B.D. Kay. 1978. Water redistribution in partially frozen, saturated silt under several temperature gradients and over burden loads. *Soil Science Society of America Proc.* 42:400-406.
- Mostaghimi S., R.A. Young, A.R. Wilts, and A.L. Kenimer. 1988. Effects of frost action on soil aggregate stability. *Trans. ASAE*, 31(2):435-439.
- Radok, U. 1977. Snow drift. *Jour. of Glaciology* 19 (81):123-139. Schlichting, H. 1979. *Boundary layer theory*. 7th ed. McGraw-Hill N.Y. 817 pp.
- Schlichting, H. 1979. *Boundary layer theory*. 7th ed. McGraw-Hill N.Y. 817 pp.
- Schmidt, R.A. 1982. Properties of blowing snow. *Reviews of Geophysics and Space Physics* 20 (1):39-44.
- Schmidt, R.A. 1980. Threshold wind-speeds and elastic impact in snow transport. *Jour. of Glaciology* 26 (94):453-467.
- Sturges, D.L., and R.D. Tabler. 1981. Management of blowing snow on sagebrush rangelands. *Jour. Soil and Water Cons.* 36 (5):287-292.
- Sutton, O.G. 1953. *Micrometeorology*. McGraw-Hill, N.Y. 333 pp.
- Swift, L.W., and R.J. Luxmoore. 1973. Computational algorithm for solar radiation on mountain slopes. Eastern Deciduous Forest Biome Memo Report #73-10.

Tabler, R.D., and R.A. Schmidt. 1986. Snow erosion, transport, and deposition in relation to agriculture. Proc. of Symp. Snow Management for Agriculture. Great Plains Agric. Council Pub. No. 120. pp. 11-58.

Tabler, R.D. 1985. Ablation rates of snow fence drifts at 2300-meters elevation in Wyoming. In: Western Snow Conference Proc. 53:1-12. Boulder, CO. April 16-18.

Tabler, R.D. 1975. Estimating the transport and evaporation of blowing snow. In: Snow Management of the Great Plains. Proc. of Symp. Great Plains Agric. Council Pub. No. 73. pp.85-104.

U. S. Army Corps of Engineers. 1960. Runoff from snowmelt. Manual EM 1110-2-1406. Govt. Printing Office.

U. S. Army Corps of Engineers. 1956. Snow hydrology: summary report of the snow investigations. North Pacific Division, Portland Division.

3.5 List of Symbols

Symbol	Definition	Unit	Variable
A	slope azimuth	deg from north	AZM
c	a proportionality constant	-	-
C_{uf}	heat capacity of the unfrozen soil	$W/m^3-^{\circ}C$	-
D	existing snow depth	m	SNODPY
D_f	drift rate of falling snow	m/day	DRIFTF
D_g	drift rate of ground snow	m/day	DRIFTG
D_p	total percentage of available drifting snow falling on an upslope area	%	PERD
D_r	total drift rate	m/day	DRIFT
d_a	density of air	kg/m^3	DENSA
d_b	basal density of standing residue	m/m	BASDEN
d_f	density of falling snow	kg/m^3	DENSF
d_g	density of ground snow	kg/m^3	DENSG
d_s	mean stem diameter of standing vegetation	m	DIAM
F	forest cover	%	FORCOV
g	acceleration of gravity	m/s^2	-
H	height of standing vegetation	m	HEIGHT
h	height above surface	m	-
I	slope inclination	radians	RADINC
i	efficiency factor based on slope inclination	%	-
j	calendar day	-	SDATE
k	Von Karman's constant (0.4)	-	-
K_{fill}	thermal conductivity of frozen tilled soil	$W/m-^{\circ}C$	KFTILL
K_{fuit}	thermal conductivity of frozen untilled soil	$W/m-^{\circ}C$	KFUTIL
K_i	thermal conductivity of any layer, i	$W/m-^{\circ}C$	-
K_{res}	thermal conductivity of residue	$W/m-^{\circ}C$	KRES
K_{snow}	thermal conductivity of snow	$W/m-^{\circ}C$	KSNOW
K_{sf}	average thermal conductivity of the snow-residue-frozen soil system	$W/m-^{\circ}C$	-
K_{uf}	thermal conductivity of unfrozen	$W/m-^{\circ}C$	
	a) tilled soil	-	KTILL
	b) untilled soil	-	KUTIL

K_w	unsaturated hydraulic conductivity of	m/s	
	a) tilled soil	-	KWTILL
	b) untilled soil	-	KWUTIL
L	latent heat of fusion	$W-s/m^3$	LATENT
L_1	distance across a slope section parallel to wind direction	m	LENGTH
L_p	distance across a slope section perpendicular to wind direction	m	WIDTH
L_r	ratio of length of the upslope section to the slope length		PERL
M	snowmelt	m	TMELT
N	number of layers	-	NSL
N_c	estimated cloud cover	dec %	CLDPCT
P	change in total water potential	m	-
P_d	mean daily precipitation	m	PRECIP
P_o	plant population	plants/ha	PPOP
Q_{srf}	heat flux through the snow-residue-frozen soil system	W/m^2	QOUT
Q_{sf}	heat flow from unfrozen soil	W/m^2	-
q_{sf}	transport rate of falling snow	kg/m-s	TRANF
q_{sg}	transport rate of ground snow	kg/m-s	TRANG
R	estimated radiation on a sloping surface	MJ/m^2	RCALSL
R_c	potential clear sky radiation on a horizontal surface	MJ/m^2	RPTH
R_{esd}	residue thickness	m	RESD
R_m	mean measured daily solar radiation	MJ/m^2	RMEAS
R_o	standing residue mass before tillage	kg/ha	RMASSO
R_t	standing residue mass after tillage	kg/ha	RMASST
S	land slope	%	SLOPE
S_c	solar constant (=0.081)	MJ/m^2	SOLCON
s_c	scour or drift factor	%	SCOURF
S_{snowd}	snow depth	m	SNOWD
S_t	storage capacity for snow	m	STOR
T_d	mean daily dewpoint temperature	°C	TDPT
T_{illd}	tilled soil depth	m	TILLD
T_m	daily minimum temperature	°C	TMIN
T_{srf}	temperature gradient across the snow-residue-frozen soil thickness	°C	DTEMP
T_{sf}	change in soil temperature from isotherm to depth of stable temperature	°C	TEMBOT
dT_{sf}	change in temperature of unit volume of soil in unit time	°C	-
T_x	daily maximum temperature	°C	TMAX
U_{illd}	untilled soil depth	m	UTILLD
v_f	settling velocity of a falling snow particle	m/s	-
v_g	settling velocity of a ground snow particle	m/s	-
v_h	wind velocity measured at height h	m/s	VWIND
v_{isf}	threshold velocity of incipient motion of falling snow	m/s	VTHF
v_{thg}	threshold velocity for incipient motion of ground snow	m/s	VTHG
v_o	friction velocity at the snow surface	m/s	VFRICT
v_2	mean daily wind speed measured at a height of 2 m	m/s	VWIND
W	wind direction	deg from north	WIND
z_c	depth of unfrozen soil that supplies heat as a result of changes in soil temperature	m	-

dZ_i	thickness of any layer, i, in the snow-residue-frozen soil system	m	-
z_o	surface random roughness	m	ROUGH
Z_{tot}	total thickness of the snow-residue-frozen soil system ($\sum dZ_i$)	m	-
dZ_{uf}	depth of unfrozen soil to point of stable temperature	m	BOTDP
ϵ	trapping efficiency	%	TRAPEF

Chapter 4. INFILTRATION

W. J. Rawls, J. J. Stone, and D. L. Brakensiek

4.1 Introduction

Infiltration is calculated using a solution of the Green and Ampt equation for unsteady rainfall as presented by Chu (1978). The original equation was derived from Darcy's law assuming infiltration from a ponded surface into a deep, homogeneous soil of uniform water content. The infiltrating water is also assumed to travel down the soil profile as "piston" flow with a sharp division between the wetted soil above the wetting front and the unwetted soil below (Skaggs and Khaleel, 1982).

Infiltration under steady rainfall is essentially a two stage process; infiltration before ponding and infiltration after ponding. Before ponding occurs, the infiltration rate is equal to the rainfall application rate. After ponding, the rate of infiltration begins to decrease until, if the time is long enough, the rate approaches a constant value or "final" infiltration rate. Mein and Larson (1973) modified the Green and Ampt equation to obtain the time to ponding for steady rainfall. Chu (1978) further modified the method to allow for alternating periods of drying and rewetting of the soil surface.

4.2 Rainfall Excess Calculations

4.2.1 Green and Ampt Equation

The form of the Green and Ampt equation (1911) for cumulative infiltration depth is

$$K_e t = F - N_e \ln \left[1 + \frac{F}{N_e} \right] \quad [4.2.1]$$

where K_e is the effective hydraulic conductivity (L/T), t is the time (T), F is the cumulative infiltration depth (L), N_e is the effective matric potential (L).

The effective matric potential, N_e is given by

$$N_e = (\eta_e - \Theta) \psi \quad [4.2.2]$$

where Θ is the soil water content (L/L), η_e is the effective porosity (L/L), ψ is the average wetting front capillary potential (L).

By differentiating Eq. [4.2.1], an expression for the infiltration rate, f (L/T), is obtained as

$$f = K_e \left[1 + \frac{N_e}{F} \right] \quad [4.2.3]$$

The infiltration rate before time to ponding is simply the rainfall intensity rate. After time to ponding, Eq. [4.2.1] is solved by Newton's method to obtain the cumulative infiltration that is then used in Eq. [4.2.3] to obtain the infiltration rate.

Time to ponding, t_p (T), that is the time when water begins to accumulate above the soil surface, is calculated as

$$t_p = \left[\frac{K_e N_e}{r_{i-1} - K_e} - R_{i-1} + V_{i-1} \right] \frac{1}{r_{i-1}} + t_{r_{i-1}} \quad [4.2.4]$$

where $i-1$ is the previous time interval, r is the rainfall intensity (L/T), R is the cumulative rainfall (L), V is the cumulative rainfall excess (L/T) and t_r is the rainfall time (T).

When ponding occurs within a given interval of rainfall intensity distribution (i.e., of the hctograph), it is noted that at the end of the interval, the rainfall intensity is greater than the infiltration rate or

$$r_{i-1} > f_{i-1} = K_e \left[1 - \frac{N_s}{F_i} \right] \quad [4.2.5]$$

and rearranging

$$F_i > \frac{K_e N_s}{r_{i-1} - K} \quad [4.2.6]$$

Chu (1978) used Eq. [4.2.6] to calculate a ponding indicator, C_u , as

$$C_u = R_i - V_i - \frac{K_e N_s}{r_{i-1} - K_e} \quad [4.2.7]$$

If C_u is positive, ponding occurs before the end of the interval, if it is negative, no ponding occurs. Similarly, he developed an indicator for the end of ponding C_p during an interval, assuming the surface was ponded at the beginning of the interval as

$$C_p = R_i - F_i - V_i \quad [4.2.8]$$

The rainfall excess rate, V , is calculated as

$$\begin{aligned} V_i &= 0 & \text{if } 0 < t < t_p \\ V_i &= r_i - f_i & \text{if } t > t_p \end{aligned} \quad [4.2.9]$$

and is used as input to the runoff component of the WEPP model.

4.2.2 Rainfall excess calculations for multiple overland flow elements

The preceding section describes how infiltration and rainfall excess are calculated on a single overland flow area or plane. Note that the rainfall excess is calculated first and then used as input to the overland flow routing routines. This simplified routing method was used to avoid a numerical solution to the kinematic wave equation. Although this simplification has the advantage of speeding up the computational time, it does not allow for any interaction between infiltration and runoff. Once rainfall ends, infiltration and rainfall excess ends. Under most situations, the approximation works well for a single element; however calculating infiltration and runoff on multiple element with different infiltration rates requires a modification of the method.

For those cases where soil properties or vegetation characteristics (strip cropping) vary downslope, the hillslope can be divided into multiple overland flow elements oriented along the contour of the hillslope to account for differences in infiltration, runoff, and/or erosion parameters. Because of these differences, the hydrologic response of each individual strip will be different from that of the strip immediately above and below. For example, there will be times when a strip will produce no rainfall excess for a given rainfall event while the strip above will produce rainfall excess for the same rainfall event.

The concept of the equivalent plane is used to route water on multiple elements in the WEPP hillslope model. Briefly this method assumes that a series of planes, each having different hydraulic

roughness values and slopes, can be represented by a single plane with an equivalent roughness and slope. The input rainfall excess is also for an equivalent plane.

Given the simplification of precalculating rainfall excess, there are four cases which can arise on any plane that has a plane above it. The first case occurs when runoff from the upper plane is zero. Infiltration and hydraulic routing are calculated as they would be for a single plane. The other three cases are

$$Q_{j-1} > 0, V_j > 0, Q_j > 0 \quad [4.2.10]$$

$$Q_{j-1} > 0, V_j = 0, Q_j > 0$$

$$Q_{j-1} > 0, V_j = 0, Q_j = 0$$

where j refers to the current plane being processed, $j-1$ refers to the plane immediately above the current plane, Q_j is the runoff volume (L) from the upper plane, V_j is the rainfall excess volume (L) for the current plane, and Q_j is the runoff volume (L) at the end of the current plane. The problem is to calculate which case will occur given a particular rainfall event, current soil moisture, soil hydraulic properties, and vegetation characteristics.

First, an average saturated conductivity, \bar{K}_s , and matric potential, \bar{N}_s , are calculated for the strips under consideration as

$$\bar{K}_s = \frac{1}{n-m+1} \sum_{j=m}^n K_{sj} \quad [4.2.11]$$

$$\bar{N}_s = \frac{1}{n-m+1} \sum_{j=m}^n N_{sj} \quad [4.2.12]$$

where K_{sj} and N_{sj} are the effective hydraulic conductivity and matric potential for the j th plane, m is the first plane above the current plane that has non zero runoff, and n is the current plane.

For example, consider a cascade of 10 planes and let the bottom most plane or the 10th plane be the plane being processed. If all the planes above have non-zero runoff, then the averages computed by Eq. [4.2.10] and [4.2.11] will be the average K_s and N_s for the ten planes. If, however a plane has had zero runoff, say, the third plane, then the average will be the average K_s and N_s for planes 4 through 10.

If the average saturated conductivity is less than the maximum rainfall intensity, then the rainfall excess on the plane is greater than zero or case 2 and the average saturated conductivity and matric potential is used with Eq. [4.1.1]. to calculate infiltration and rainfall excess.

If the event is case 3 or 4, a potential infiltration capacity, F_p (L), is calculated and compared to the volume of water, \hat{F} (L), entering the plane. The potential infiltration capacity is calculated by expanding the natural log term in Eq. [4.1.1] as

$$\bar{K}_s t = F - \bar{N}_s \ln \left[\frac{F}{N_s} - \frac{1}{2} \left(\frac{F}{N_s} \right)^2 + \frac{1}{3} \left(\frac{F}{N_s} \right)^3 - \dots \right] \quad [4.2.13]$$

If only the first two terms within the parenthesis are retained then Eq. [4.2.13] can be approximated as

$$F = \left[2\bar{K}_e \bar{N}_s \right]^{1/2} t^{1/2} \quad [4.2.14]$$

If t is assumed equal to the time during which water is present on the plane, then t can be thought of as the maximum infiltration opportunity time, t_m , and F_p can be thought of as a maximum potential infiltration capacity or

$$F_p = \left[2\bar{K}_e \bar{N}_s \right]^{1/2} t_m^{1/2} \quad [4.2.15]$$

The volume water entering the plane is simply the runoff volume, Q_{j-1} from the upper plane and the rainfall, R_j (L), on the current plane or

$$\hat{F} = Q_{j-1} + R_j \quad [4.2.16]$$

Case 3 and case 4, respectively, are defined as

$$\hat{F} - F_p > 0 ; Q_j > 0 \quad [4.2.17]$$

$$\hat{F} - F_p \leq 0 ; Q_j = 0$$

If the event is case 3, the runoff volume is estimated as

$$Q_j = \hat{F} - F_p \quad [4.2.18]$$

4.3 Estimation of Infiltration Parameters

The Green-Ampt parameters needed for application of the model are: 1) available porosity ($\eta_a - \Theta_i$), 2) wetting front capillary potential (Ψ), and 3) hydraulic conductivity (K_c). These parameters can be derived from measured hydraulic conductivity and water retention functions; however, an attractive alternative is to predict them from readily available soil properties such as texture, bulk density, organic matter, and clay mineralogy. In WEPP the average soil properties for the primary tillage zone for agricultural applications and the top 0.1 m of the soil for rangeland applications are used to predict the infiltration parameters. The methods used for predicting the parameters will be described in detail in the following sections.

4.3.1 Available Porosity

Available porosity is computed as the difference between the total porosity corrected for entrapped air (η_a) and the antecedent soil water (Θ_i). The derivation of total porosity is described in section 6.8.1. The antecedent soil water is computed from the water balance and plant growth modules (chapters 7 and 8).

4.3.2 Wetting Front Capillary Potential

The Green Ampt wetting front capillary potential parameter (Ψ) (m) can be estimated from the Brooks Corey method (1964) in the following manner (Rawls and Brakensiek, 1983):

$$\Psi = \frac{2 + 3\lambda}{1 + 3\lambda} \frac{\Psi_b}{2} \quad [4.3.1]$$

where λ is the Brooks Corey pore size index and Ψ_b is the Brooks Corey bubbling pressure. Rawls and Brakensiek (1983) related the Green-Ampt wetting front capillary potential parameter to soil properties in the following equation:

$$\Psi = .01 e^b \quad [4.3.2]$$

for

$$b = 6.531 - 7.33 \eta_c + 15.8 C_y^2 + 3.81 \eta_c^2 + 3.40 C_y S_D - 4.98 S_D \eta_c + 16.1 S_D^2 \eta_c^2 + 16.0 C_y^2 \eta_c^2 \\ - 14.0 S_D^2 C_y - 34.8 C_y^2 \eta_c - 8.0 S_D^2 \eta_c$$

where S_D is the decimal sand and C_y is the decimal clay.

4.3.3 Hydraulic Conductivity

Past research (Moore, 1981) has shown that the infiltration rate and amount are more sensitive to the hydraulic conductivity and available porosity than to the wetting front capillary potential. With the exception of management effects that alter the bulk density of the soil and change the porosity, management practices primarily influence the hydraulic conductivity parameter.

Management has major effects on ground canopy cover and thus hydraulic conductivity. These effects are incorporated using the proportions of the unit surface area composed of canopy and open space and by proportioning the canopy space and open space into the soil surface with or without ground cover.

The effective conductivity parameter, K_c ($m s^{-1}$) for the portion of unit area under canopy cover is estimated as

$$K_c = K_b C_f \left[\frac{B_c}{A_c} C_r + \eta_m \left(1 - \frac{B_c}{A_c} \right) \right] \quad [4.3.3]$$

where K_b is the base line soil saturated conductivity ($m s^{-1}$), C_f is the canopy correction factor, C_r is the crust reduction factor, B_c is the bare area under canopy, A_c is that canopy area, and η_m is the macro-porosity factor.

The effective conductivity parameter, K_o ($m s^{-1}$) for the portion of unit area outside the canopy is estimated as

$$K_o = K_b \left[\frac{B_o}{A_o} C_r + \eta_m \left(1 - \frac{B_o}{A_o} \right) \right] \quad [4.3.4]$$

where B_o is the bare area outside of canopy and A_o is the area outside of canopy.

Combining Eq. [4.3.3] and [4.3.4] for the total unit area consisting of canopy covered area and open area, an expression for the total effective conductivity, K_e is obtained as

$$K_e = A_c K_c + A_o K_o \quad [4.3.5]$$

or

$$K_e = K_b \left[C_f \left[\frac{B_c}{A_c} C_r + \eta_m \left(1 - \frac{B_c}{A_c} \right) \right] + \frac{B_o}{A_o} C_r + \eta_m \left(1 - \frac{B_o}{A_o} \right) \right] \quad [4.3.6]$$

The crust reduction factor (C_r) in the preceding equations was developed by Brakensiek and Rawls (1983) to reduce the saturated hydraulic conductivity for an established soil crust. The crust factor is

$$C_r = \frac{D_w}{\frac{D_w - C_t}{C_s} + \frac{C_t}{C_q}} \quad [4.3.7]$$

where C_r is the crust reduction factor, D_w is the average wetting front depth (m), C_t is the crust thickness (m) assumed to be 0.005m, C_s is the correction factor for partial saturation of the subcrust soil expressed as:

$$C_s = 0.74 + 0.19 S_D \quad [4.3.8]$$

and C_q is the crust factor expressed as:

$$C_q = 0.0099 + 7.21 C_t + 0.068 S_D^2 + 21.2 S_D^2 C_t + 315.1 S_D C_t^2 \quad [4.3.9]$$

The crust reduction factor varies linearly with accumulated rainfall since tillage in the following manner

$$C_{r_i} = 1 - \frac{(1 - C_{r_{i-1}})}{.1} R_c \quad R_c \leq .1 \quad [4.3.10]$$

$$C_{r_i} = C_{r_{i-1}} \quad R_c > .1$$

where $R_{c_{i-1}}$ is the accumulated rainfall since tillage (m).

The assumptions of Eq. [4.3.6] are: 1) all bare soil is crusted to a given degree; 2) soil under canopy (bare or covered) has a higher hydraulic conductivity than soil outside canopy; and 3) soil covered by aggregates, rocks, litter, residue, etc., normally has a higher conductivity than bare soil because of the increase in macroporosity due to biotic activity or the reduction of crust formation. Also surface rock on high sand soils for rangelands may decrease the conductivity. It is common on rangelands for the soil under canopy to have a higher hydraulic conductivity than bare soil not under canopy. In these situations hydraulic conductivity should be estimated separately for the two areas.

The crust factor, canopy factor, and macroporosity factor are the only parameters to be estimated in Eq. [4.3.6]. In the following sections estimators for these parameters are developed according to landuse.

4.3.3.1 Agricultural Landuse and Infiltration Parameters

Tillage, crops, and the addition of organic matter are primary agricultural practices that affect the infiltration process. Tillage primarily changes the bulk density of the soil and breaks up the surface soil crusts. Crops produce a canopy that protects the soil surface in addition to producing residue, which when left on the soil, provides additional soil surface protection. The addition of organic matter may reduce the bulk density of the soil and provide resistance to crusting.

Bulk density is a critical soil property for the infiltration model; therefore, the temporal changes of bulk density must be predicted for agricultural soils. Williams et al. (1984) presents a method for modeling the temporal nature of bulk density based on soil properties and rainfall. Williams et al. (1984) and Rawls and Brakensiek (1983) present methods for predicting the effect of tillage on bulk density according to soil texture and type of tillage. The addition of organic matter can be incorporated into the calculation of bulk density using the method presented by Rawls (1983).

The formation of soil crusts is also shown to be a major modifier of infiltration on agricultural lands (Moore, 1981). In the previous section the method for incorporating crusting into the hydraulic conductivity parameter for the one layer Green-Ampt infiltration model was presented. For crust

conductivity the thickness and average wetted depth need to be defined and since this is difficult to determine or model, the 0.005 m thickness reported by Sharma (1980) is recommended. Using infiltration data from Mannering (1967) for over 60 Midwest soils, developed the following equation to predict the average wetted depth D_w was developed:

$$D_w = 0.147 - 0.15 S_D^2 - .0003 C_y \rho_b \quad D_w > C_i \quad [4.3.11]$$

$$D_w = C_i \quad D_w \leq C_i$$

where ρ_b is the soil bulk density (kg/m^3).

The average wetted depth predicted varies from approximately 0.1 m for high silt soils to 0.01 m for high clay and high sand soils.

Procedures for describing the effect of agricultural canopy cover on the effective hydraulic conductivity are still under development. However, preliminary analysis has indicated that canopy cover over residue does not have a significant effect. Grass has no canopy effect because the area under it has a littered surface. The canopy factor in Eq. [4.3.6] for agricultural lands is:

$$C_f = 1 + \frac{A_c}{A_o + A_c} \quad [4.3.12]$$

The macroporosity factor, η_m , in Eq. [4.3.6] represents changes in infiltration potential of soil covered by rocks, litter or residue. Analysis of the 1987 WEPP agricultural data and data from the North Central Region (Jones, 1979) resulted in the following equation:

$$\eta_m = e^{[0.96 - 3.2 S_D - 4.0 C_y - .000032 \rho_b]} \quad [4.3.13]$$

η_e was arbitrarily limited to be greater than 0.4. Equation [4.3.13] indicates that clay with surface cover will yield a higher macroporosity value than a sand content > 50%, which produces a macroporosity factor < 1. This is indicative of a reduction in infiltration which shows that cover on highly porous soils retards the process because there is less uncovered area for water to infiltrate.

4.3.3.2 Rangeland Landuse and Infiltration Parameters

Rangelands differ from agricultural lands as they are seldom tilled and their management is normally not drastically changed from year to year; thus the soil surface properties have evolved over a period of time producing a stable environment. The primary rangeland management practices that affect the infiltration process are grazing systems which change the bulk density of the soil due to trampling and remove canopy cover. The following is a presentation of how to incorporate rangeland management practices into the factors used in Eq. [4.3.6]. The development and evaluation of the factors are given in detail by Rawls et al. (1989).

Since rangeland soil bulk density is normally changed by trampling and freeze-thaw cycles, a natural consolidation can be predicted using the procedure developed by Rawls (1983). From the experimental data of Warren (1985), the effect of trampling on soil bulk density can be estimated. At this time there are no means to describe the effect of freeze-thaw on bulk density.

Since rangeland soil surface has evolved from long term exposure to natural processes and land use practices, the soil crust is considered to be well established and it is assumed to be 0.01 m thick. The wetted depth, D_w , can be determined using Eq. [4.3.11].

The analysis of rangeland data has indicated that bush canopy, exclusive of grass canopy, has a significant effect on infiltration characteristics of bare, rock, and litter covered soil. The canopy factor in Eq. [4.3.6] for rangeland is calculated with Eq. [4.3.12].

The macroporosity factor η_m in Eq. [4.3.6] represents an increase or decrease in infiltration potential of the soil covered by residue, litter, or rocks. Rawls et al. (1989) developed the following equation relating η_m to soil properties:

$$\eta_m = e^{6.10 - 10.3 S_d - 3.7 C_y} \quad [4.3.14]$$

η_m is arbitrarily limited to greater than 0.4. As in the macroporosity correction factor for agricultural lands for high sand soils, rock surface cover may reduce the infiltration capacity.

4.4 Model Evaluation

The 1987 data obtained from the USDA Water Erosion Prediction Project (WEPP) (Lafren et al., 1987; Simanton et al., 1987; West et al., 1987) were used in evaluation of the infiltration model. These experiments had detailed soils, rainfall, runoff, and vegetation measurements on 21 range soils and 18 agricultural soils. A summary of the range of properties covered is presented in Table 4.4.1. The agricultural plots were freshly tilled; rangeland plots were either in natural condition or a bare condition where all canopy and surface material greater than 2 mm had been removed.

Table 4.4.1 Summary of 1987 WEPP Agricultural and Rangeland Plot Characteristics.

Landuse	Range of properties	
	Rangeland	Agricultural
Number soils	21	18
% Sand	8-84	3-84
% Clay	4-49	7-50
% Coarse Fragments	0-55	0-6
% Organic Matter	1-8	0.4-5.1
Bulk Density (g/cm ³)	1.17-1.62	0.67-1.45
Vegetation	Natural	Bare
% Bare (< 2 mm)	16-59	55-95
% Surface Cover	41-84	5-45
% Canopy	10-75	---
% Grass Canopy	0-39	---

The plots for agricultural soils were assumed to have 10% of the area covered with clods. Final infiltration rates shown in Fig. 4.4.1 are the end of the one-hour dry run. Figure 4.4.1 shows that the model consistently underpredicts because it assumes all bare ground to be crusted; whereas the plots actually were freshly tilled and the crust formed during the run. Also, since the actual amount of clods was not noted, more than 10% clod cover could also increase the measured infiltration. Since the variability (\pm one standard deviation) of the measured final infiltration rates ranged from 0.3 to 1.2 cm/hr, the model is considered to be performing adequately under such a transient condition.

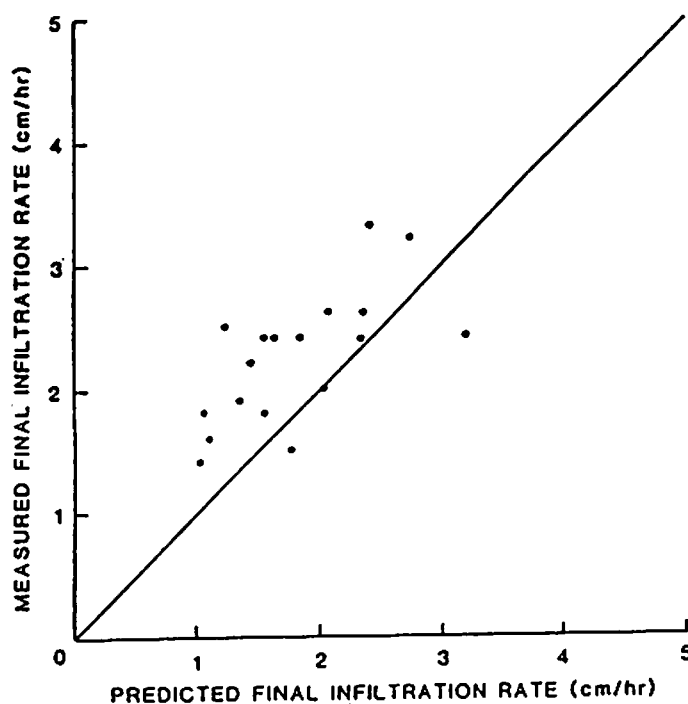


Figure 4.4.1. Comparison of predicted and measured final infiltration rates for agricultural plots.

The rangeland experiments provided data to test soils under natural vegetation and in a bare condition. Figure 4.4.2 shows the predicted and measured final infiltration rates for both conditions for the wet run. The results in Fig. 4.4.2 generally predict within \pm one standard deviation of the measured rates.

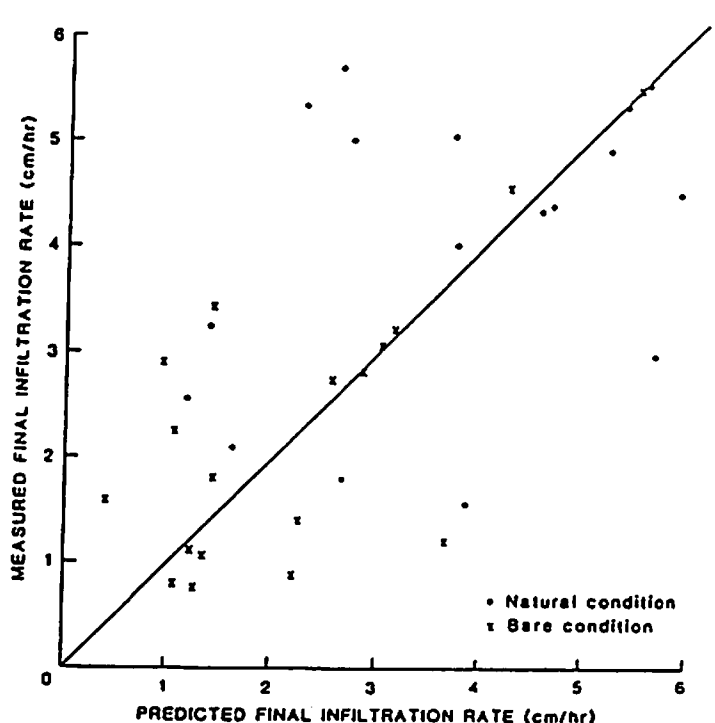


Figure 4.4.2. Comparison of predicted and measured final infiltration rates for rangeland plots.

4.5 References

- Brakensiek, D. L., and Rawls, W. J. 1983. Agricultural management effects on soil water processes. Part II. Green and Ampt parameters for crusting soils. *Trans. of the ASAE* 26(6):1753-1757.
- Brooks, R. H., and Corey, A. T. 1964. Hydraulic properties of porous media. Colorado State Univ. Hydrol. Paper No. 3, 27 pp.
- Chu, S. T. 1978. Infiltration during and unsteady rain. *Water Resour. Res.* 14(3):461-466.
- Green, W. H., and Ampt, G. A. 1911. Studies in soil physics. I. The flow of air and water through soils. *J. Agric. Science* 4:1-24.
- Jones, B.A., Jr. 1979. Water infiltration into representative soils of the North Central Region. Agricultural Experiment Station Bulletin 760, University of Illinois, Urbana, IL.
- Lafren, J.M., A. Thomas, and R. Welch. 1987. Cropland experiments for USDA Water Erosion Prediction Project. ASAE Paper 87-2544, St. Joseph, MI.
- Mannering, J.V. 1967. The relationship of some physical and chemical properties of soils to surface sealing. Unpub. PhD. Thesis, Purdue University, Lafayette, IN.
- Mein, R. G., and Larson, C. L. 1973. Modeling infiltration during a steady rain. *Water Resources Res.* 9(2):384-394.
- Moore, I.D. 1981. Effect of surface sealing on infiltration. *Trans. of the ASAE* 24(6):1546-1561.
- Rawls, W. J. 1983. Estimating soil bulk density from particle size analysis and organic matter content. *Soil Sci.* 135(2):123-125.

- Rawls, W. J., and Brakensiek, D. L. 1983. A procedure to predict Green and Ampt infiltration parameters. Proceedings of ASAE Conference on Advances in Infiltration, Chicago, IL, pp. 102-112.
- Rawls, W.J., D.L. Brakensiek, and R. Savabi. 1989. Infiltration parameters for rangeland soils. J. Rangeland Management. 42(2):139-142.
- Sharma, P.P. 1980. Hydraulic gradients and vertical infiltration through rain-formed quasi seals on a range of Minnesota soils. Unpublished M.S. Thesis, University of Minnesota, St. Paul, MN.
- Simanton, J.R., L.L. West, M.A. Wertz, and G.D. Wingate. 1987. Rangeland experiments for USDA Water Erosion Prediction Project. ASAE Paper 87-2545, St. Joseph, MI.
- Skaggs, R. W., and Khaleel, R. 1982. Infiltration, In Hydrologic modeling of small watersheds, C.T. Haan, Ed. ASAE Monograph 5, pp. 121-166.
- Warren, S.D. 1985. Hydrologic consequences of intensive rotation grazing. PhD. Dissertation, Dept. of Range Sciences, Texas A & M University, College Station, TX. pp. 112.
- West, L.T., E.E. Alberts, and C.S. Holzhey. 1987. Soil Measurements: USDA Water Erosion. ASAE Prediction Project Paper 87-2543, St. Joseph, MI.
- Williams, J.R., C.A. Jones, and P.T. Dyke. 1984. A modeling approach to determining the relationships between erosion and productivity. Trans. of the ASAE 27(1):129-144.

4.6 List of Symbols

Symbol	Definition	Units	Variable
A_c	canopy area	decimal	CANCOV
A_o	area outside of canopy	decimal	-
b	regression exponent for calculation	-	-
B_c	bare area under canopy	decimal	BAREU
B_o	bare area outside of canopy	decimal	BAREO
C_f	canopy factor	-	CF
C_p	indicator for end of ponding	m	CP
C_q	crust factor	-	BC
C_r	crust reduction factor	-	CRUST
C_s	crust correction factor	-	SC
C_t	crust thickness	m	TC
C_u	indicator for time to ponding	m	CU
C_y	clay amount	decimal	AVCLAY
D_w	wetting front depth	m	WETFRT
F	cumulative infiltration depth	m	FF
f	infiltration rate	m/s	F
F_p	potential infiltration depth	m	FPOT
F_j	depth of water entering the jth plane ($= Q_i - I + R$)	m	FHAT
i	index for time	-	I
j	index for overland flow plane	-	IPLANE
K_b	base line hydraulic conductivity	m/s	SSC
K_c	effective hydraulic conductivity under the canopy	m/s	KEC
K_e	effective hydraulic conductivity	m/s	EKE
\bar{K}_e	average effective hydraulic conductivity for multiple planes	m/s	AVEKS
K_o	effective hydraulic conductivity in open areas	m/s	KEO

m	last consecutive up hill plane with non zero runoff	-	-
n	current plane being processed	-	-
N_s	effective matric potential	m	AVENS
\bar{N}_s	average effective matric potential for multiple planes	m	AVENS
Q	runoff depth	m	RUNOFF
q	runoff rate	m/s	QPEAK
r	rainfall rate	m/s	R
R	cumulative rainfall depth for a single event	m	RR
R_c	cumulative rainfall depth between tillage operations	m	RFCUM
S_d	sand amount	decimal	AVSAND
t	time	s	T
t_m	infiltration opportunity time	s	TMAX
t_p	time to ponding	s	TP
t_r	rainfall elapsed time	s	TR
V	rainfall excess depth	m	RECUM
v	rainfall excess rate	m/s	RE
λ	Brooks Corey pore size index	-	LAMBDA
η_e	effective porosity	-	-
η_m	macro-porosity factor	m/m	AVPOR
ρ_b	bulk density of soil	kg/m**3	BD
Ψ	Green and Ampt wetting front capillary potential parameter	m	SF
Ψ_b	Brooks Corey bubbling pressure	-	PSIB
Θ	antecedent soil moisture	m/m	AVSAT
$1 - \frac{B_c}{A_c}$	ground cover under canopy	decimal	COVU
$1 - \frac{B_o}{A_o}$	ground cover outside of canopy	decimal	COVO

Chapter 5. SURFACE RUNOFF

M. Hernandez, L. J. Lane, and J. J. Stone

5.1 Overland Flow Routing and Hydrograph Development

Routing is a term used to describe modeling the movement of water over the land surface and implies the calculation of flow rates at positions along the hillslope. Horton (1945) described the process, and kinematic routing was subsequently used to model it (see Henderson and Wooding, 1964; Liggett and Woolhiser, 1967; Woolhiser and Liggett, 1967; and Eagleson, 1970).

A basic issue in modeling overland flow is how faithfully the actual land surface is represented in the model used to represent it. All land surfaces are more or less irregular. Realistic modeling of unsteady, nonuniform, and three dimensional flow processes on these natural surfaces remains beyond our ability. Two dimensional flow models have been developed but remain impractical for most applications. Therefore, most modeling efforts have been based on one-dimensional flow assumptions. Most models assume broad, uniform sheet flow as the basis for development of the flow equations. The assumption of broad, uniform sheet flow results in model parameter distortions with the degree of parameter distortion dependent on the irregularity of the overland flow surfaces (Lane and Woolhiser, 1977).

A standard assumption in deriving steady-state erosion equations (see Foster and Meyer, 1972) is that the overland flow surface is made up of areas of broad, uniform sheet flow dissected by areas of concentration flow in rills. On a larger scale, sheet flow and concentrated flow have been included in kinematic cascade models for unsteady flow routing on small watersheds (see Wooding, 1965 and Kibler and Woolhiser, 1970).

Overland flow is represented in two ways in the WEPP hillslope model. Broad, uniform sheet flow is assumed for the overland flow routing to develop the overland flow hydrograph. However, the equivalent hydraulic roughness factor is computed as an area weighted function of the hydraulic roughness in the rills and on the interrill areas. This hydrograph represents unsteady, nonuniform flow on an idealized surface. Once the unsteady flow calculations are made to get the runoff peak rate and the duration of runoff, quasi-steady state flow is assumed at the peak rate and is partitioned into broad sheet flow for interrill erosion calculations and concentrated flow for rill erosion calculations. The erosion calculations are then made for a constant rate over a characteristic time to produce estimates of erosion for the entire runoff event.

The kinematic wave equations for one-dimensional overland flow result when the momentum equation is approximated by assuming the land slope, S_o , is equal to the friction slope, S_f . The kinematic wave equations for runoff on a plane are

$$\frac{\partial h}{\partial t} + \frac{\partial q}{\partial x} = r - f = v \quad [5.1.1]$$

and

$$q = \alpha h^{3/2} \quad [5.1.2]$$

where h is the local depth of flow (m), t is the time (s), q is the discharge per unit width ($m^2 s^{-1}$), x is the distance down the plane (m), r is the rainfall intensity ($m s^{-1}$), f is the infiltration rate ($m s^{-1}$), v is the rainfall excess rate ($m s^{-1}$), and α is the depth-discharge coefficient ($m^{1/2} s^{-1}$). Equation [5.1.1] is the continuity equation, Eq. [5.1.2] is the simplified momentum equation, and the quantity $v = r - f$ is usually called rainfall excess. If $v = r - f$ in Eq. [5.1.1] is a constant, then Eq. [5.1.1] and [5.1.2] can be solved analytically by the method of characteristics (see Eagleson, 1970). Analytic solutions to these equations have been derived for the case where v is made up of a series of step functions in the typical rainfall

intensity hyetograph pattern, i.e., where intensity is constant within an arbitrary time interval but varies from interval to interval (i.e., Shirley, 1987). This development allows the WEPP hillslope model to compute the overland flow hydrograph for complex rainfall intensity patterns without resorting to finite difference methods with the resultant increase in computer time required for numerical solutions to Eq. [5.1.1] and [5.1.2].

5.2 Approximate Overland Flow Routing Method

The main effects of overland flow routing in the calculation of erosion rates in the hillslope model are the way peak discharge or peak rate of runoff is attenuated or reduced and the way the duration of runoff is extended or stretched during the routing process. Rainfall excess is produced when the rainfall intensity exceeds the infiltration rate, this rainfall excess can be characterized by the peak rate and the duration. The routing process (solving Eq. [5.1.1] and [5.1.2]) attenuates the rainfall excess pattern resulting in a peak rate of runoff less than or equal to the peak rate of rainfall excess. After the cessation of rainfall excess, the kinematic wave equations describe the process of water runoff from storage on the overland flow plane. Thus, the duration of runoff is longer than the duration of rainfall excess. If infiltration occurs after the end of rainfall, then the plane will become dry and the flow will reach zero after a finite time. However, in the WEPP model, rainfall excess is calculated first and then routed down an impervious plane. The flow then approaches zero asymptotically and the duration of runoff is infinite. The end of runoff is arbitrarily chosen to be that time when the runoff volume, obtained by integrating the hydrograph, is equal to 95% of the rainfall excess volume.

5.2.1 Derivation of Equations

The approximate method is based on the assumption that the routed overland flow hydrograph may be well approximated by the rainfall excess pattern. The method consists of a set of regression equations that will estimate peak runoff and duration of runoff based on plane characteristics and rainfall excess pattern.

Let the duration of rainfall excess, D_v , be defined as the time from the first time to ponding to the last time during the storm when rainfall rate is greater than the calculated infiltration capacity (the last time when $v > 0$). Let the volume of rainfall excess (equal to the volume of runoff) be V . Then, an average rainfall excess rate, σ , can be defined as

$$\sigma = \frac{V}{D_v} \quad [5.2.1]$$

where σ is the average rate of rainfall excess ($m s^{-1}$), V is the volume of rainfall excess (m), and D_v is the duration of rainfall excess (s). If the time to equilibrium, t_e , for runoff on a plane of length x is the time to steady-state runoff given an average rainfall excess rate, σ , for a long period, then the time to equilibrium is calculated as follows (Eagleson, 1970):

$$t_e = \left[\frac{x}{\alpha} \right]^{2/3} \left[\frac{1}{\sigma} \right]^{1/3} \quad [5.2.2]$$

where x is the length of the plane (m), t_e is the time to equilibrium (s), and the other variables are as described earlier.

It is now possible to define the dimensionless variables used to approximate the peak rate of runoff and the duration of runoff without doing the actual routing. Let the normalized time to equilibrium, t_e , be

$$t_e = \frac{t_e}{D_v} \quad [5.2.3]$$

and the normalized peak rate of runoff, q_{p^*} , be

$$q_{p^*} = \frac{q_p}{v_m} \quad [5.2.4]$$

where t_e is the normalized time to equilibrium, q_{p^*} is the normalized peak rate of runoff, q_p is the peak rate of runoff ($m s^{-1}$), and v_m is the peak rate of rainfall excess ($m s^{-1}$). Let the normalized duration of runoff, D_* , be

$$D_* = \frac{D_q}{D_v} \quad [5.2.5]$$

and let the normalized rainfall excess rate, V_* , be

$$V_* = \frac{v_m}{V} t_e \quad [5.2.6]$$

where D_q is the duration of runoff and D_v is the duration of rainfall excess.

Preliminary analyses suggested a relationship between q_{p^*} and t_e of the form

$$q_{p^*} = e^{-b_1 t_e^{b_2}} \quad [5.2.7]$$

and between D_* and v_* of the form

$$D_* = b_3 + b_4 v_*^{b_5} \quad [5.2.8]$$

where b_1 to b_5 are coefficients to be determined. Once the coefficients have been determined, the peak rate of flow and duration are obtained by solving Eq. [5.2.4] and [5.2.5] for q_p and D_q respectively.

5.2.2 Description of the Simulation Study

To determine the coefficients b_1 through b_5 in Eq. [5.2.7] and [5.2.8], Eq. [5.1.1] and [5.1.2] were solved for a range of rainfall intensities, soil textures, surface roughness, and slope lengths and gradients.

The method of representing rainfall events was described in Chapter 2. The rainfall intensities patterns selected are summarized in Table 5.2.1.

Table 5.2.1. Summary of selected storms for the simulation study.

Storm Type	No.	Depth (mm)	Duration (min)	tp	ip
Triangular	1	29.	30.	0.0	2.0
"	2	"	"	.25	"
"	3	"	"	.50	"
"	4	"	"	.75	"
"	5	"	"	1.0	"
Constant	6	"	"	1.0	1.0
Double Exp.	7	"	"	.10	4.0
Disaggregated	8	"	"	.25	"
(synthetic data)	9	"	"	.50	"
"	10	"	"	.75	"
"	11	"	"	.90	"
"	12	40.	90.	.30	1.5
"	13	"	"	"	5.0
"	14	"	"	"	7.0
"	15	"	"	.70	1.5
"	16	"	"	"	5.0
"	17	"	"	"	7.0
Double Exp.	18	64.	305.	.12	10.0
Disaggregated	19	51.	71.	.11	2.2
(observed data)	20	89.	633.	.82	10.1
"	21	69.	1131.	.42	9.1
"	22	17.	88.	.36	6.2
"	23	16.	63.	.07	7.5
"	24	39.	40.	.20	1.8
"	25	25.	180.	.62	6.6
"	26	67.	45.	.18	2.1
"	27	85.	98.	.18	1.9
"	28	29.	160.	.07	7.4
"	29	64.	519.	.14	6.5
"	30	44.	380.	.75	11.5

Note: "Triangular" refers to a triangular rainfall intensity pattern used for disaggregation, "Constant" refers to a constant intensity pattern, and "Double Exp." refers to the double exponential intensity pattern.

Soils data representative of 11 textural classes were selected as summarized in Table 5.2.2. The basis of the representative values for each of the textural classes was interpretation of data summarized by Rawls et al. (1982) as modified by Lane and Stone (1983).

Table 5.2.2. Summary of representative soils parameters, by textural class, used in the simulation study.

Textural Class j	Effective Porosity n (%)	Matric Potential Sf (mm)	Hydraulic Conductivity Ks (mm/h)	Rel. Sat. Se (%)
loamy sand	40.	63.	30.0	22.
sandy loam	41.	90.	11.0	22.
loam	43.	110.	6.5	22.
silt loam	49.	173.	3.4	22.
silt	42.	190.	2.5	22.
sandy clay loam	35.	214.	1.5	22.
clay loam	31.	210.	1.0	22.
silty clay loam	43.	253.	0.9	22.
sandy clay	32.	260.	0.6	22.
silty clay	42.	288.	0.5	22.
clay	39.	310.	0.4	22.

A number of overland flow planes were selected to produce a wide range of t_e , t_s , and D_e values given the information in Tables 5.2.1 and 5.2.2. Characteristics of these overland flow planes are listed in Table 5.2.3.

Table 5.2.3. Summary of the overland flow planes used in the simulation study.

Slope S (%)	Chezy C ($m^{1/2}/s$)	α ($m^{1/2}/s$)	Length x (m)
1	2.0	0.200	10.
"	5.0	.500	10.
"	10.0	1.000	10.
"	2.0	.200	50.
"	5.0	.500	50.
"	2.0	.200	75.
"	5.0	.500	100.
5	2.0	.447	10.
"	5.0	1.118	10.
"	10.0	2.236	10.
"	2.0	.447	50.
"	5.0	1.118	50.
"	2.0	.447	100.
"	5.0	1.118	100.

Table 5.2.3. Summary of the overland flow planes used in simulation study. (cont.)

Slope S (%)	Chezy C ($m^{1/2}/s$)	α ($m^{1/2}/s$)	Length x (m)
10	2.0	.632	1.
"	2.0	.632	10.
"	5.0	1.581	10.
"	10.0	3.162	10.
"	2.0	.632	50.
"	5.0	1.581	50.
"	2.0	.632	100.
"	5.0	1.581	100.

5.2.3 Results of the Simulation Study

A nonlinear least squares curve fitting program, based on the maximum neighborhood method of Marquardt (1963), was used to evaluate the coefficients b_1 and b_5 in Eq. [5.2.7] and [5.2.8].

The coefficients were evaluated for each soil texture and rainfall distribution using 22 different flow planes described in Table 5.2.3. Consequently, 330 values were obtained for each coefficient. The nonlinear least squares analysis on Eq. [5.2.7] and [5.2.8] indicates that values for the five coefficients vary as follow, Table 5.2.4.

Table 5.2.4. Extreme values for b_1 to b_5 .

coefficient	min	max
b_1	0.400	2.920
b_2	0.819	7.156
b_3	0.912	18.051
b_4	0.109	1.069
b_5	0.663	2.130

The t statistic was used to assess whether the coefficients were contributing significantly to the regression equation. According to the t test, b_2 is more significant than b_1 in Eq. [5.2.7]. Similarly, results show that b_5 is more significant than b_3 and b_4 in Eq. [5.2.8]. In order to check whether Eq. [5.2.7] and [5.2.8] can present a reasonable approximation to the data, the coefficient of determination between the observed and predicted values was calculated. Clearly, a mean value of 0.97 and 0.98 indicate an excellent fit to Eq. [5.2.7] and [5.2.8], respectively.

The next step in the simulation study was to obtain the coefficients b_1 to b_5 as a function of rainfall distribution and hydraulic conductivity. For this purpose, a linear model was proposed to represent the relation between b_i values and rainfall distribution and hydraulic conductivity. Such model has the following form,

$$b_i = c_0 + c_1 D_r + c_2 T + c_3 i_n + c_4 k_{sj} ; \text{ for } i=1, \dots, 5 \quad [5.2.9]$$

where b_i , coefficients in Eq. [5.2.7] and [5.2.8]; $c_0, c_1, c_2, c_3,$ and c_4 coefficients to be determined; D_r , duration of precipitation; T , the ratio of time to peak to duration of precipitation; i_n , the ratio of maximum

intensity to average intensity; k_{ij} , hydraulic conductivity; j , corresponds to soil classification index in Table 5.2.2.

The results from the multiple linear regression analysis show a poor relation between the b_i values and the described independent variables. That is, the coefficient of determination for the five cases are very low, as it can be seen in Table 5.2.5.

Table 5.2.5. Coefficient of determination for b_i .

coefficient	coefficient of determination
b_1	0.49
b_2	0.16
b_3	0.63
b_4	0.55
b_5	0.05

Due to the low values of the coefficient of determination, the coefficients b_1 , b_2 , and b_5 were determined using a mean value based only on soil texture and for all rainfall distributions, and Eq. [5.2.9] for b_3 and b_4 . Equation [5.2.9] was used to determine b_3 because the coefficient of determination was greater than 0.5. The computation of b_4 was performed without the variables D_r , T , and i_n because the regression analysis showed that such variables did not reduced the unexplained variance significantly. Consequently, b_4 was computed as follows,

$$b_4 = c_0 + c_4 k_{sj} \quad [5.2.10]$$

Three sets of eleven mean values were generated (Table 5.2.6).

Table 5.2.6. Coefficients as a function of soil texture.

Soil type	coefficient		
	b_1	b_2	b_5
loamy sand	0.730	1.161	1.521
sandy loam	0.747	1.341	1.502
loam	0.757	1.404	1.495
silt loam	0.754	1.410	1.517
silt	0.820	1.455	1.497
sand clay loam	0.910	1.506	1.524
clay loam	0.917	1.547	1.518
silty clay loam	0.890	1.507	1.507
sandy clay	0.996	1.524	1.538
silty clay	0.958	1.545	1.519
clay	1.031	1.518	1.531

Similarly, a mean value was computed for each coefficient for a given rainfall distribution and for all soil textures. Consequently, three sets of thirty mean values were produced (Table 5.2.7).

Table 5.2.7. Coefficients as a function of rainfall distribution.

Rainfall Distribution	coefficient		
	b_1	b_2	b_5
1	0.639	1.701	1.643
2	0.669	1.668	1.545
3	0.634	1.717	1.533
4	0.555	1.816	1.555
5	0.502	1.775	1.529
6	0.230	4.345	1.528
7	1.186	1.066	1.777
8	1.127	1.114	1.562
9	0.995	1.230	1.473
10	0.951	1.223	1.502
11	0.827	1.232	1.530
12	0.488	1.235	1.544
13	0.889	1.320	1.384
14	0.820	1.294	1.328
15	0.488	1.639	1.550
16	1.081	1.573	1.434
17	1.199	1.486	1.415
18	1.040	1.225	1.405
19	0.925	1.286	1.693
20	0.856	1.543	1.306
21	1.378	1.812	1.389
22	0.831	1.107	1.544
23	0.914	0.960	1.462
24	0.703	1.275	1.625
25	0.705	1.573	1.463
26	0.946	1.480	1.637
27	1.172	1.765	1.826
28	0.935	1.173	1.515
29	1.666	1.890	1.220
30	0.822	1.554	1.537

Further simplification was made to values of the coefficients in Tables 5.2.6 and 5.2.7. The criterion for such simplification was based only on soil texture. Table 5.2.8 shows the values of b_1 , b_2 and b_5 for different soil textures.

Table 5.2.8. Values of b_1 , b_2 and b_3 as a function of soil texture.

Soil type	coefficient		
	b_1	b_2	b_3
loamy sand	0.70	1.26	1.51
sandy loam			
loam			
silt loam			
silt			
sandy clay loam	1.07	1.64	
clay loam			
silty clay loam			
sandy clay			
silty clay			
clay			

In contrast, b_3 was determined using Eq. [5.2.9] for each soil texture. Thus a set of eleven equations were obtained to calculate b_3 . For instance, Table 5.2.9 shows the values of the coefficients in Eq. [5.2.9] for all soil textures.

Table 5.2.9. Coefficients to obtain b_3 as a function of D_r , T , and i_a .

Soil type	coefficient			
	c_0	c_1	c_2	c_3
loamy sand	-0.31	6.31	0.12	1.58
sandy loam	-0.48	6.73	0.12	1.45
loam	-0.56	4.41	0.12	1.38
silt loam	-0.53	1.34	0.13	1.30
silt	-0.52	3.17	0.11	1.13
sandy clay loam	-0.39	2.62	0.09	0.79
clay loam	-0.40	2.80	0.09	0.78
silty clay loam	-0.37	2.42	0.09	0.77
sandy clay	0.41	4.42	0.07	0.79
silty clay	-0.40	4.25	0.07	0.81
clay	-0.27	5.75	0.05	0.66

Similarly, b_4 can be determined as

$$b_4 = 0.47 + 5.55 \times 10^{-3} k_{ij} \quad [5.2.11]$$

Estimated peak runoff and runoff duration were determined with an average error of 7% and 12%, respectively. In the analysis it was noted that errors were greater in estimated peak runoff and duration of runoff for large values of time to equilibrium. In other words, for a given soil texture and any rainfall distribution, the larger the time to equilibrium the larger the error in the estimated values. Further, based on soil texture, rainfall distribution is more significant in sandy soils than in clay soils. That is, for rainfall distributions with large i_a values and low T values on sandy soils, the approximate method failed to determine accurately the peak runoff and duration of runoff. However, on clayed soils, results were obtained within 10% error.

Further analysis was carried out using the approximate method. Data from five small watersheds were used for the analysis. The following information was provided for each watershed: observed rainfall data and disaggregated rainfall data for 14 events, slope and length of the plane, ground and canopy cover, initial saturation and Chezy roughness coefficient. Results for the 14 events are shown in Tables 5.2.10 and 5.2.11.

Table 5.2.10. Comparison between Kinematic Routing and Approximate Method.

Rainfall	MEASURED RAIN				
	KINEMATIC ROUTING			APPROXIMATE METHOD	
	Volume Runoff mm	Peak Runoff mm/h	Duration Runoff min	Peak Runoff mm/h	Duration Runoff min
7/11/41	34.5	50.8	148.0	100.0	182.9
5/15/42	29.0	32.2	125.0	55.6	193.1
5/26/66	42.5	16.8	618.0	82.3	886.3
3/19/70	19.9	7.2	1215.0	29.3	2626.7
7/7/69	3.5	24.0	56.0	21.9	17.7
2/22/71	10.9	3.7	603.0	4.5	693.7
8/12/66	41.8	40.7	309.0	77.7	600.0
7/19/68	12.5	21.1	121.0	20.9	151.7
3/23/69	19.7	20.3	250.0	44.1	522.8
7/3/59	59.7	163.8	55.0	185.6	63.5
5/21/65	57.9	79.8	117.0	82.6	140.0
4/10/67	4.6	4.2	184.0	17.9	386.5
4/12/67	20.5	22.2	169.0	22.2	137.9
5/6/69	14.5	18.0	469.0	15.9	94.4

Table 5.2.11. Comparison between Kinematic Routing and Approximate Method.

Rainfall	DISAGGREGATED RAIN				
	KINEMATIC ROUTING			APPROXIMATE METHOD	
	Volume Runoff mm	Peak Runoff mm/h	Duration Runoff min	Peak Runoff mm/h	Duration Runoff min
7/11/41	34.5	55.2	125.0	67.7	208.9
5/15/42	27.3	37.4	114.0	43.5	127.2
5/26/66	53.8	64.8	576.0	59.4	445.9
3/19/70	33.4	22.2	626.0	22.2	613.2
7/7/69	2.2	11.8	61.0	12.6	38.3
2/22/71	9.9	3.7	481.0	3.9	971.9
8/12/66	54.0	59.0	231.0	60.3	217.5
7/19/68	12.2	20.3	99.0	24.4	96.7
3/23/69	19.8	21.2	231.0	30.5	399.8
7/3/59	59.7	157.1	49.0	157.1	51.7
5/21/65	56.6	69.5	113.0	68.7	113.8
4/10/67	0.2	0.1	478.0	0.0	518.5
4/12/67	15.7	13.8	246.0	14.8	278.8
5/6/69	14.5	17.9	382.0	19.1	271.1

Clearly, the approximate method failed to determine peak runoff and duration of runoff when observed rainfall data were used. In contrast, the approximate method provided fairly accurate values of peak runoff when disaggregated rainfall data were used. The average error involved in determining peak runoff was found to be 9% and duration of runoff was estimated with an average error of 15%.

The WEPP Model uses the steady-state sediment continuity equation as a basis for erosion computations. As a result, the peak runoff is considered to be the rate at steady-state conditions. However, under this assumption, the duration of runoff can not be used to compute total sediment load. That is, the steady state hydrograph with a maximum rate equal to peak runoff and duration of runoff produces a runoff volume greater than the rainfall excess volume. In order to match rainfall excess volume with runoff volume, an effective duration, D_e , is computed as follows,

$$D_e = \frac{V}{q_p} \quad [5.2.12]$$

5.3 Equivalent Plane

The WEPP model is capable of simulating contour strip cropping systems, multiple pastures, and mechanical treatments such as plowing, roller chopping, and chaining. The WEPP model used the concept of multiple plane to represent strip cropping systems, multiple pastures, and soil management treatments on a hillslope. A multiple plane can be divided up to ten different planes. That is, each plane may represent a strip crop, a pasture type, or a soil management treatment.

In the WEPP model there are two methods to route excess rainfall. One method is based on an analytical solution of the kinematic wave equations, and the other is an approximate overland flow routing method. The method based on the analytical solution requires zero runoff depth at the upper boundary of the plane. Consequently, this method will not be valid for routing planes in cascade. Likewise, the approximate overland flow routing method applies to a single plane. As a result, to use either method, a multiple plane system has to be transformed into a single equivalent plane. The equilibrium storage concept is used to transform a multiple plane system into a single uniform plane. Wu et al. (1978), developed a method to estimate depth-discharge coefficients for equivalent uniform planes. The method is based on computing a depth-discharge coefficient for the equivalent uniform plane by letting the average storage at equilibrium equate the accumulated storages of planes at equilibrium of the multiple plane.

Integrating the depth profile, at equilibrium, with respect to x , yields the total volume on the hillslope. Thus,

$$S_t = \frac{1}{L} \frac{m}{m+1} \left[\frac{v}{\alpha} \right]^{\frac{1}{m}} L \frac{m+1}{m} \quad [5.3.1]$$

$$\alpha = C S^{1/2} \quad [5.3.2]$$

where S_t is the average storage at equilibrium (m), L is the total length of the plane (m), m is the depth-discharge exponent, C is the Chezy coefficient ($m^{1/2} s^{-1}$), S is the average slope, and the other variables are as described earlier.

The method was tested on a two plane convex and concave cascades, a three plane convex and concave cascades and two complex cascades, Figs. 5.3.1, 5.3.2, and 5.3.3, respectively.

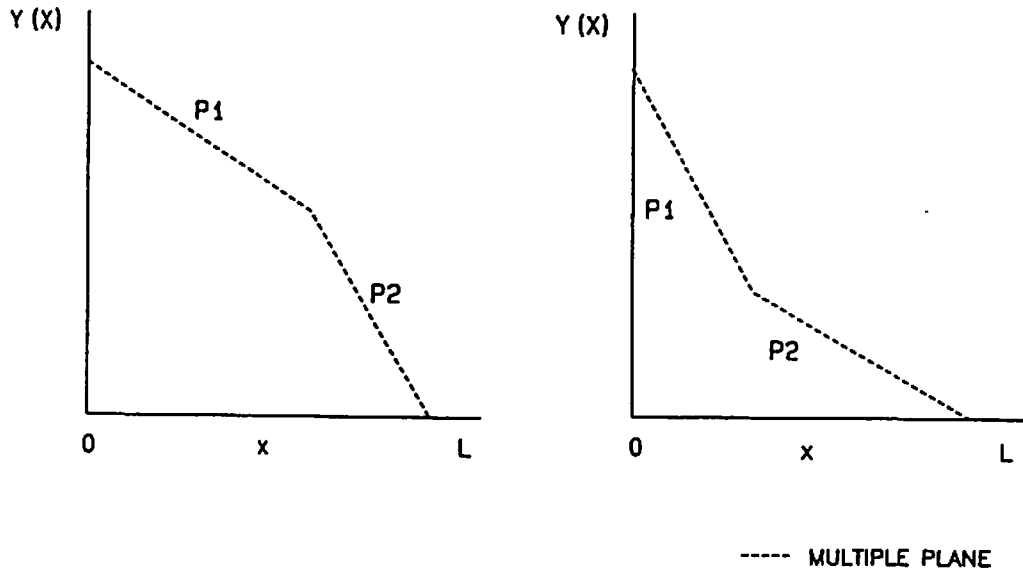


Figure 5.3.1. Two plane convex and concave cascades.

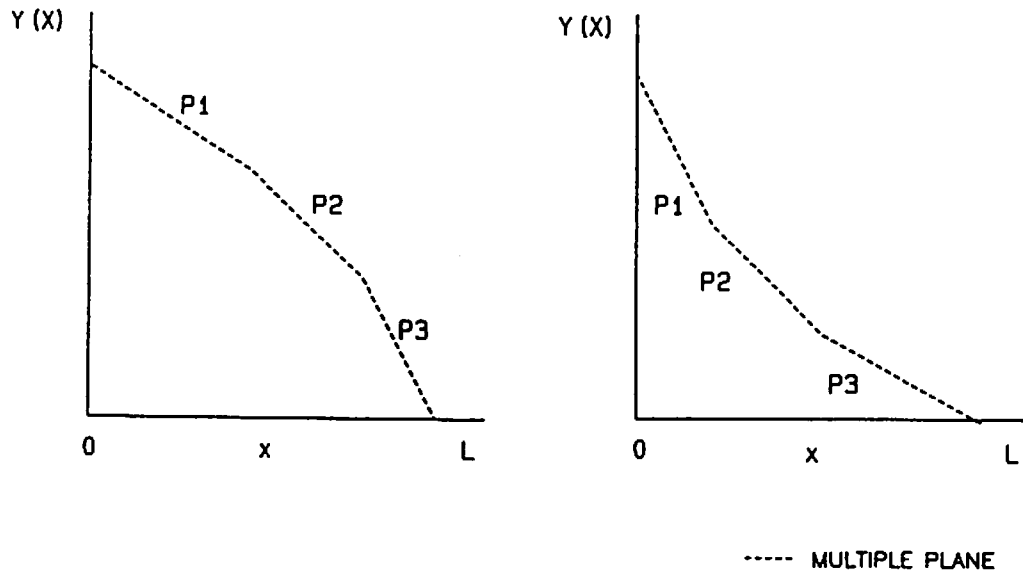


Figure 5.3.2. Three plane convex and concave cascades.

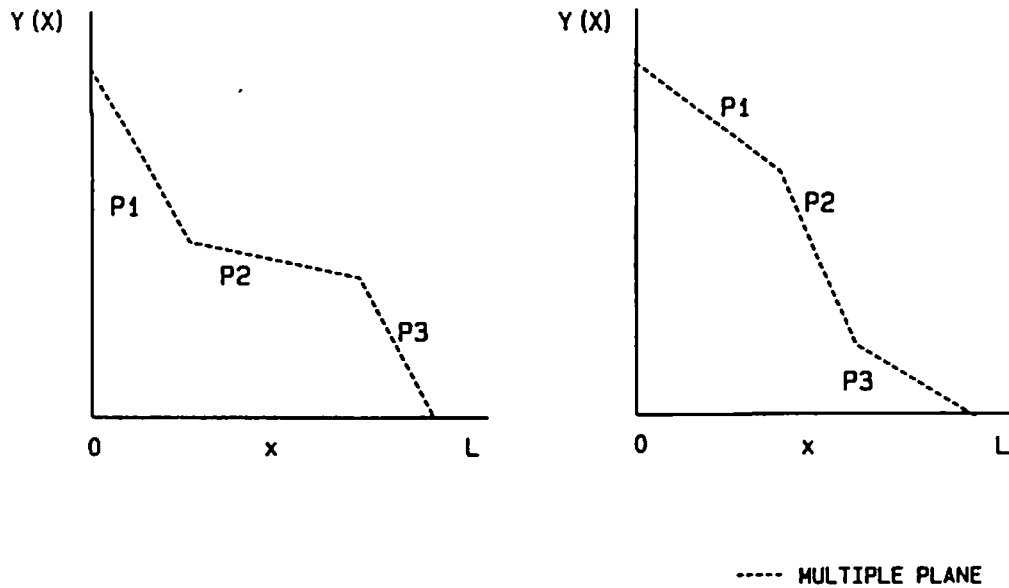


Figure 5.3.3. Three plane complex cascades.

Equations [5.3.1] and [5.3.2] were used to obtain the depth-discharge coefficient and the Chezy roughness coefficient for the equivalent planes. Parameters for each case are shown in Table 5.3.1.

Table 5.3.1. Multiple Plane Parameters.

Multiple Plane		Length (m)			Slope (%)			Chezy C. ($m^{1/2}/s$)		
		L1	L2	L3	S1	S2	S3	C1	C2	C3
Two Planes	Convex	100	100	-	6	12	-	10	5	-
	Concave	100	100	-	12	6	-	10	5	-
Three Planes	Convex	100	100	100	3	6	9	3	5	10
	Concave	100	100	100	12	6	3	3	5	5
Complex	Plane 1	100	100	100	12	6	12	10	5	10
Complex	Plane 2	100	100	100	6	12	6	10	5	10

Equation [5.3.1] takes the following form to obtain average storage at equilibrium for each plane,

$$S_i = \frac{P_1}{L} \left[\frac{v_i}{\alpha_i} \right]^{\frac{1}{m}} \left[x_{i+1}^{P_1} - x_i^{P_1} \right] \tag{5.3.3}$$

$$P_1 = \frac{m}{m+1}$$

$$P_2 = \frac{1}{P_1}$$

where S_i is the storage in plane i (m), $x_{(i+1)}$ is the distance from the upstream end of the multiple plane to the downstream end of the plane (m), and s_i is the distance from the upstream end of the multiple plane to the upstream end of the plane (m).

The estimates of parameters from the average storage are not sensitive to the difference in rainfall intensity. A uniform rainfall intensity of 60 mm/hr was used to estimate the overall value of α from the average storage at equilibrium. The average storage at equilibrium is calculated for each plane using Eq. [5.3.3], and the overall depth-discharge coefficient is computed as follows,

$$\alpha_e = L \left[P_1 \frac{v_i}{S_i} \right]^m \tag{5.3.4}$$

$$S_t = \Sigma S_i \tag{5.3.5}$$

Then, solving for the equivalent Chezy roughness coefficient in Eq. [5.3.2]

$$C_e = \frac{\alpha_e}{S^{1/2}} \tag{5.3.6}$$

Figures 5.3.4, 5.3.5, and 5.3.6 show the equivalent uniform plane for all cases. Table 5.3.2 presents values for the equivalent depth-discharge coefficients and Chezy roughness coefficients.

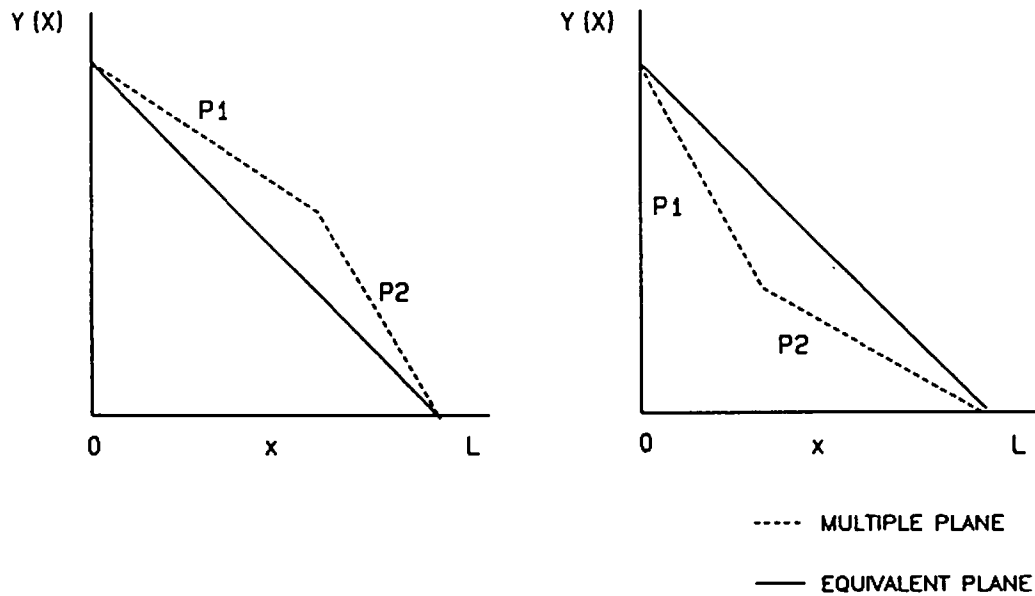


Figure 5.3.4. Two plane convex and concave cascades.

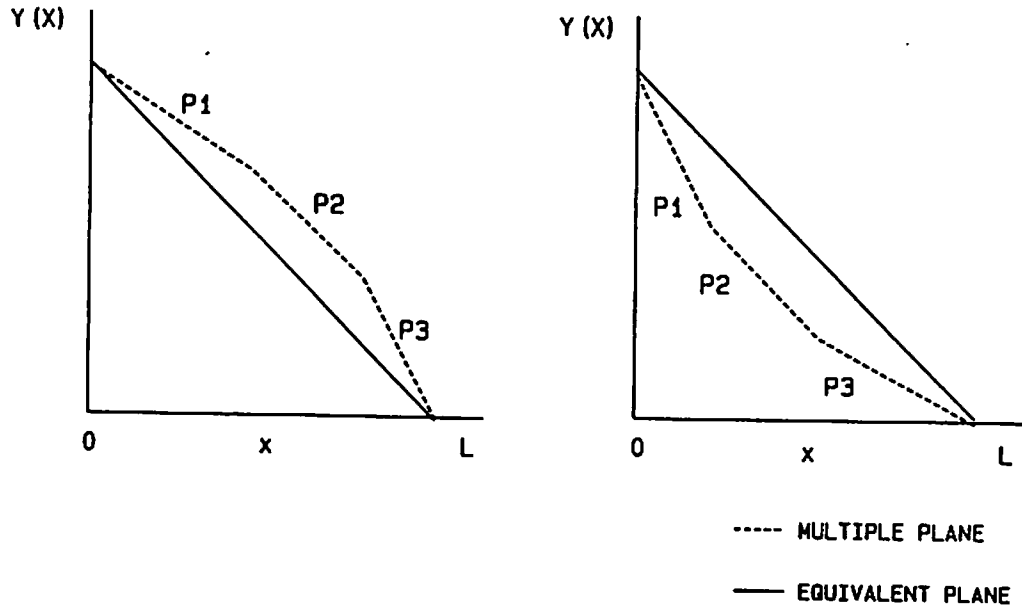


Figure 5.3.5. Three plane convex and concave cascades.

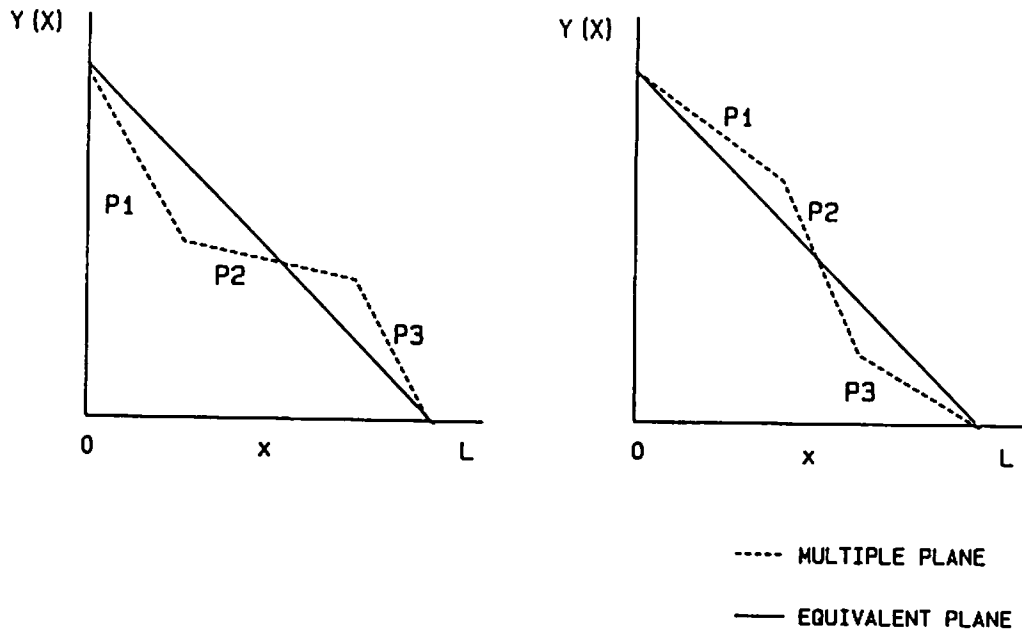


Figure 5.3.6. Three plane complex cascades.

Table 5.3.2. Overall α_e and C_e for equivalent uniform planes.

Multiple Plane		α_e	C_e
Two Planes	Convex	1.92	6.40
	Concave	1.58	5.27
Three Planes	Convex	1.24	5.07
	Concave	1.14	4.34
Complex	Plane 1	1.86	5.91
Complex	Plane 2	1.75	6.19

To evaluate the effectiveness of the equivalent plane approach in the development of the hydrograph, the overall α_e and C_e coefficients were used to generate equivalent runoff hydrographs for each equivalent uniform plane. These hydrographs were compared with hydrographs developed for the six multiple planes using a numerical solution of the kinematic wave equations. The results showed a good agreement between equivalent uniform and multiple plane peak rate of runoff and runoff volume, as shown in Table 5.3.3.

Table 5.3.3. Peak Rate of Runoff and Runoff Volume for equivalent uniform and multiple planes.

Multiple Plane		Peak Rate of Runoff		Runoff Volume	
		Equivalent	Multiple	Equivalent	Multiple
Two Planes	Convex	53.97	53.97	24.14	24.26
	Concave	53.89	53.91	23.57	23.98
Three Planes	Convex	52.99	48.62	20.35	20.22
	Concave	52.41	52.94	19.78	20.81
Complex	Plane 1	53.73	53.84	22.49	23.27
Complex	Plane 2	53.70	53.83	22.35	23.21

5.4 References

- Eagleson, P. S. 1970. *Dynamic Hydrology*. McGraw-Hill Book Co., New York, NY, 462 pp.
- Foster, G. R., and L. D. Meyer. 1972. A closed-form soil erosion equation for upland areas. In: H. W. Shen (Ed.), *Sedimentation: Symposium to Honor Professor H. A. Einstein*, Ft. Collins, CO, Ch. 12:12.1-12.19.
- Henderson, F. M., and R. A. Wooding. 1964. Overland flow and groundwater flow from a steady rainfall of finite duration. *J. Geophys. Res.* 69(8):1531-1540.
- Horton, R. E. 1945. Erosional development of streams and their drainage basins; Hydrophysical approach to quantitative morphology. *Bull. Geol. Soc. of Amer.* 56:275-370.
- Kibler, D. F., and D. A. Woolhiser. 1970. The kinematic cascade as a hydrologic model. *Hydrology Paper No. 39*, Colorado State Univ., Ft. Collins, CO, 27 pp.
- Lane, L. J., and J. J. Stone. 1983. Water balance calculations, water use efficiency, and aboveground net production. *Hydrology and Water Resources in Arizona and the Southwest* 13:27-34.
- Lane, L. J., and D. A. Woolhiser. 1977. Simplifications of watershed geometry affecting simulation of surface runoff. *J. Hydrol.* 35:173-190.

Liggett, J. A., and D. A. Woolhiser. 1967. The use of the shallow water equations in runoff computation. Proc. Third Annual Amer. Water Resources Conf., AWRA, San Francisco, CA, pp. 117-126.

Marquardt, D. W. 1963. An algorithm for least squares estimation of nonlinear parameters. J. Soc. Ind. Appl. Math. 11:431-441.

Rawls, W. J., D. L. Brakensiek, and K. E. Saxton. 1982. Estimation of soil water properties. Transactions of America Society of Agricultural Engineers Special Edition, Soil and Water 25:1316-1320.

Shirley, E. D. 1987. Program HDRIVER. Unpublished documentation for computer program. USDA-ARS, Tucson, AZ.

Wooding, R. A. 1965. A hydraulic model for the catchment-stream problem, 1. Kinematic wave theory. J. Hydrol. 3(3):245-267.

Woolhiser, D. A., and J.A. Liggett. 1967. Unsteady, one-dimensional flow over a plane--the rising hydrograph. Water Resources Res. 3(3):753- 771.

Wu, Yao-Huang, V. Yevjevich, and D.A. Woolhiser. 1978. Effects of surface roughness and its spatial distribution on runoff hydrographs. Colorado State University, Hydrology Paper No. 96.

5.5 List of Symbols

Symbol	Definition	Units	Variable
b_1	coefficient	-	b1
b_2	" "	-	b2
b_3	" "	-	b3
b_4	" "	-	b4
b_5	" "	-	b5
c_0	" "	-	c0
c_1	" "	-	c1
c_2	" "	-	c2
c_3	" "	-	c3
c_4	" "	-	c4
C_e	equivalent chezy coefficient	$m^{1/2}/s$	chezy
D_e	effective duration	s	effdm
D_q	duration of runoff	s	durrun
D_r	duration of precipitation	s	stmdur
D_v	duration of rainfall excess	s	durre
D_o	normalized duration of runoff	-	durstr
f	infiltration rate	m/s	f
h	local depth of flow	m	hdepth
i_n	ratio of maximum intensity to average intensity	-	ip
j	soil classification index	-	j
k_r	saturated hydraulic conductivity	m/s	ks
L	total length of plane	m	slplen

Symbol	Definition	Units	Variable
m	depth-discharge exponent	-	m
Q	volume of runoff	m	runoff
q	discharge per unit width	m^2/s	q
q_p^*	normalized peak rate of runoff	-	qpstar
q_p	peak rate of runoff	m/s	peakro
r	rainfall intensity rate	m/s	int
S	average slope	-	avgslp
S_i	average storage at equilibrium	m	sdst
T	ratio of time to peak to duration of precipitation	-	timep
t_e	time to equilibrium	s	teave
t_e^*	normalized time to equilibrium	-	testar
v	rainfall excess rate	m/s	re
V	rainfall excess volume	m	retot
v_m	peak rate of rainfall excess	m/s	remax
v_e^*	normalized rainfall excess rate	-	restar
x	distance down the plane	m	len
α_e	equivalent depth-discharge coef.	$m^{1/2}/s$	alpha
σ	average rainfall excess rate	m/s	avere

Chapter 6. SOIL COMPONENT

E. E. Alberts, J. M. Laflen, W. J. Rawls, J. R. Simanton and M. A. Nearing

6.1 Introduction and Objectives

Soil properties influence the basic water erosion processes of infiltration and surface runoff, soil detachment by raindrops and concentrated flow, and sediment transport. The purpose of this chapter is to provide the WEPP user with background information on the soil and soil-related variables currently predicted in the WEPP model.

6.2 Background

6.2.1 Hydrology Parameters

Four soil variables that influence the hydrology portion of the erosion process are predicted in this component, including: 1) random roughness, 2) ridge height, 3) bulk density, and 4) saturated hydraulic conductivity. Random roughness is most often associated with tillage of cropland soil, but any tillage or soil disturbing operation creates soil roughness. Ridge height, which is a form of oriented roughness, results when the soil is arranged in a regular way by a tillage implement and varies by a factor of two or more depending upon implement type. Depressional storage of rainfall and hydraulic resistance to overland flow are positively correlated with soil roughness. Soil roughness changes temporarily due to tillage, rainfall weathering, and freezing and thawing. Bulk density reflects the total pore volume of the soil and is used to predict several infiltration parameters, including wetting front suction (see Chapter 4 for details) and saturated hydraulic conductivity. Bulk density changes temporally due to tillage, wetting and drying, freezing and thawing, and wheel and livestock compaction. Adjustments to bulk density are needed to account for factors such as the volumes of entrapped air and coarse fragments in the soil.

6.2.2 Soil Detachment Parameters

Interrill erodibility (K_i) is a measure of sediment delivery rate to rills as a function of rainfall intensity. For cropland and rangeland soils, base K_i values were predicted from relationships developed from field experiments conducted in 1987 and 1988 (Laflen et al., 1987; Simanton et al., 1987). Base K_i values for cropland soils are measured when the soil is in a loose, unconsolidated condition typical of that found after primary and secondary tillage using conventional tillage practices. Base K_i values for rangeland are measured on undisturbed soils with all vegetation and coarse fragments removed. Base K_i values for cropland and rangeland soils need to be adjusted for factors that influence the resistance of the soil to detachment, such as live and dead root biomass, soil freezing and thawing, and mechanical and livestock compaction.

Rill erodibility (K_r) is a measure of soil susceptibility to detachment by concentrated flow, and is often defined as the increase in soil detachment per unit increase in shear stress of clear water flow. Critical shear stress (τ_c) is an important term in the rill detachment equation, and is the shear stress below which no soil detachment occurs. Critical shear stress (τ_c) is the shear intercept on a plot of detachment by clear water vs. shear stress in rills. Rate of detachment in rills may be influenced by a number of variables including soil disturbance by tillage, living root biomass, incorporated residue, coarse fragments, soil consolidation, freezing and thawing, and wheel and livestock compaction.

6.3 User and Climatic Inputs

The number of overland elements existing on the hillslope profile is specified by the user, with an overland flow element being defined as an area of uniform cropping, management and soil characteristics. Soil information at the mapping unit level is stored in a soil input file. If the hillslope segment begins on a ridge and ends in a alluvial valley, the location of each mapping unit can be specified and soil properties

of each read into the model from the soil input file. Mapping units on the hillslope profile are specified to better predict the effects of basic soil physical and chemical properties on infiltration and soil erodibility parameters.

Because tillage is one major process altering soil properties, the user must specify information on any tillage operation that occurs during the erosion simulation. Specific inputs include: 1) implement type, 2) tillage date, 3) tillage depth, and 4) tillage direction relative to the slope (see Chapter 8 for more information on tillage management and user input options).

After tillage, temporal changes in soil roughness, bulk density, and saturated hydraulic conductivity occur due to soil wetting and drying and freezing and thawing. Daily rainfall, max-min air temperatures, and soil water content are important variables in some equations that predict temporal soil properties.

6.4 Time Invariant Soil Properties

Time invariant soil properties are used to calculate baseline soil infiltration and erodibility parameters. Most baseline soil infiltration and erodibility parameters are calculated internal to the model using data read in from the soil input file (see User Summary for more information).

6.5 Random Roughness

Random roughness following a tillage operation is estimated based upon measured averages for an implement, which is similar to the approach used in EPIC (Williams et al., 1984). Table 6.5.1 shows the random roughness value assigned to each tillage implement in the current crop management input file.

Soil random roughness immediately after a tillage operation is predicted from:

$$R_{ri} = R_{ro} T_i + R_{r(t-1)} [1 - T_i] \quad [6.5.1]$$

where R_{ri} is the random roughness immediately after tillage, R_{ro} is the random roughness created by a tillage implement, T_i is the tillage intensity value associated with an implement, and $R_{r(t-1)}$ is the random roughness immediately prior to tillage. This approach accounts for the effect of prior random roughness on random roughness after tillage.

Random roughness decay with time after tillage is predicted from:

$$R_{r(t)} = R_{ri} e^{\alpha_{rr} R_c} \quad [6.5.2]$$

where $R_{r(t)}$ is the random roughness at time t (m), R_{ri} is the random roughness immediately after tillage (m), α_{rr} is a random roughness parameter, and R_c is the cumulative rainfall since tillage (m).

α_{rr} is predicted from:

$$\alpha_{rr} = 2.8 - 30 S_i \quad [6.5.3]$$

where S_i is the silt content of the soil (0-1). If $\alpha_{rr} \geq 0$, then α_{rr} is set to -0.1.

Table 6.5.1. Residue and soil parameters for original 27 WEPP tillage implements. †

Implement	Tillage Intensity‡		Other Tillage Parameters§			
	Corn	Soybeans	TDMEAN	RRo	RHo	RINT
	(0 to 1)		-----m-----			
1 Moldboard Plow	0.93	0.96	0.150	0.043	0.050	0.360
2 Chisel Plow, Straight	0.25	0.45	0.125	0.023	0.050	0.100
3 Chisel Plow, Twisted	0.45	0.65	0.125	0.026	0.075	0.100
4 Field Cultivator	0.25	0.35	0.100	0.015	0.025	0.150
5 Tandem Disk	0.50	0.65	0.100	0.026	0.050	0.230
6 Offset Disk	0.55	0.70	0.100	0.038	0.050	0.230
7 One-way Disk	0.40	0.50	0.100	0.026	0.050	0.230
8 Paraplow	0.20	0.25	0.150	0.010	0.025	0.360
9 Spike Tooth Harrow	0.20	0.25	0.025	0.015	0.025	0.050
10 Spring Tooth Harrow	0.30	0.45	0.050	0.018	0.025	0.100
11 Rotary Hoe	0.10	0.15	0.025	0.012	0.000	0.000
12 Bedder Ridge, Lister	0.75	0.80	0.150	0.025	0.150	1.000
13 V-Blade Sweep	0.10	0.15	0.075	0.015	0.075	1.524
14 Subsoiler	0.20	0.30	0.350	0.015	0.075	0.300
15 Rototiller	0.55	0.70	0.075	0.015	0.000	0.000
16 Roller Packer	0.10	0.10	0.000	0.010	0.025	0.075
17 Row Planter w/ Smooth Coulter	0.08	0.11	0.000	0.010	0.010	1.000
18 Row Planter w/ Fluted Coulter	0.15	0.18	0.000	0.012	0.025	1.000
19 Row Planter w/ Sweeps	0.20	0.30	0.000	0.013	0.075	1.000
20 Lister Planter	0.40	0.50	0.000	0.025	0.100	1.000
21 Drill	0.15	0.15	0.000	0.012	0.050	1.000
22 Drill w/ Chain Drag	0.15	0.15	0.000	0.009	0.025	1.000
23 Row Cultivator w/ Sweeps	0.25	0.30	0.000	0.015	0.075	1.000

Table 6.5.1. Residue and soil parameters for original 27 WEPP tillage implements. † (Continued)

Implement	Tillage Intensity‡		Other Tillage Parameters§			
	Corn	Soybeans	TDMEAN	RRo	RHo	RINT
	(0 to 1)		-----m-----			
24 Row Cultivator w/ Spider Wheels	0.25	0.30	0.000	0.015	0.050	1.000
25 Rod Weeder	0.15	0.20	0.000	0.010	0.025	0.125
26 Rolling Cultivator	0.50	0.55	0.000	0.015	0.150	1.000
27 NH ₃ Applicator	0.15	0.20	0.000	0.013	0.025	0.300

† List is being expanded to approximately 80 tillage implements.

‡ Tillage intensity values are used for altering soil and residue properties. Values for corn are used for all crops except those that have residue classified as fragile. WEPP crops that produce fragile residue include soybeans, peanuts, and potatoes.

§ TDMEAN's represent an average tillage depth and are used to adjust the fraction of residue cover remaining for certain primary and secondary tillage depths specified by the user (See Chapter 8 for more detail).

RRo and RHo are random roughness and ridge height parameters.

RINT represents the on-center ridge interval. If RINT = 1.0, then RINT is set to row width (RW) in the model.

6.6 Ridge Height

A ridge height value is assigned to a tillage implement based upon measured averages for an implement (see Table 6.5.1 for assigned ridge height values), which is similar to the approach used in EPIC (Williams et al., 1984).

Ridge height decay following tillage is predicted from:

$$R_{h(t)} = R_{ho} e^{-\alpha_{rh} R_c} \quad [6.6.1]$$

where $R_{h(t)}$ is the ridge height at time t (m), R_{ho} is the ridge height immediately after tillage (m), α_{rh} is a ridge height parameter, and R_c is the cumulative rainfall since tillage (m). α_{rh} is currently set equal to the random roughness parameter (α_{rr}).

Large ridges made by a rolling cultivator or a similar ridging implement do not decay as fast as smaller ridges made by a disk or chisel plow. Criteria used to identify a well-defined ridge furrow system is that ridge height after tillage is ≥ 0.1 m and the ridge interval is equal to the row spacing. For this condition, ridge height cannot decay below 0.1 m.

6.7 Bulk Density

6.7.1 Tillage Effects

Soil bulk density changes are used to predict changes in infiltration parameters. Bulk density after tillage is difficult to predict because of limited knowledge, particularly for point- and rolling-type implements, of how an implement interacts with a soil as influenced by tillage speed, tillage depth, and soil cohesion.

The approach chosen to account for the influence of tillage on soil bulk density is to use a classification scheme where each implement is assigned a tillage intensity value from 0 to 1, which is similar to the approach used in EPIC (Williams et al., 1984). The concept is based, in part, on measured effects of various tillage implements on residue cover.

Flat residue cover following a tillage operation is predicted from (Chapter 8):

$$C_{rf(t)} = C_{rf(t-1)} R_{mf} \quad [6.7.1]$$

where $C_{rf(t)}$ is the flat residue cover after tillage (0-1), $C_{rf(t-1)}$ is flat residue cover before tillage (0-1), and R_{mf} is the residue mixing factor (0-1).

The base R_{mf} value is predicted from:

$$R_{mf} = 1 - T_i. \quad [6.7.2]$$

The T_i variable, then, reflects the relative amount of soil disturbance caused by a tillage implement. A soil inverting implement, like a moldboard plow, disturbs the soil more than point- or rolling-type implements. Table 6.5.1 shows the tillage intensity value assigned to each tillage implement in the current crop management input file.

The equation used to predict soil bulk density after tillage is (Williams et al., 1984):

$$\rho_t = \rho_{(t-1)} - \left[\left(\rho_{(t-1)} - 0.667 \rho_c \right) T_i \right] \quad [6.7.3]$$

where ρ_t is the bulk density after tillage ($kg\ m^{-3}$), $\rho_{(t-1)}$ is the bulk density before tillage ($kg\ m^{-3}$), ρ_c is the consolidation soil bulk density at 0.033 MPa ($kg\ m^{-3}$), and T_i is the tillage intensity value (0-1).

Consolidated soil bulk density, ρ_c , is calculated by the model from the soil input data from the relationship:

$$\rho_c = \left[1.514 + 0.25 S_a - 13.0 S_a O_m - 6.0 C_l O_m - 0.48 C_l CEC_r \right] 10^3 \quad [6.7.4]$$

where ρ_c is the consolidated soil bulk density at 0.033 MPa ($kg\ m^{-3}$), S_a is the sand content (0-1), O_m is the organic matter content (0-1), C_l is the clay content (0-1), and CEC_r is the ratio of the cation exchange capacity of the clay (CEC_c) to the clay content of the soil.

The cation exchange capacity of the clay fraction of the soil is calculated from:

$$CEC_c = CEC - O_m \left[142 + 170 D_z \right] \quad [6.7.5]$$

where CEC is the cation exchange capacity of the soil ($cmol\ kg^{-1}$) and D_z is the average depth of the horizon of interest (m).

Soil properties for the average depth of all primary tillage implements used in one tillage sequence are initialized from the data in the soil input file. If the depth of primary tillage is less than the depth of the first soil horizon, one new soil layer is created. Another new soil layer is created if the average depth of all secondary tillage implements in the same tillage sequence is less than the average primary tillage depth. If the primary tillage depth is greater than the depth of the first soil horizon, soil properties of the tillage layer are depth-weighted averages of the soil properties of the soil horizons mixed by the tillage implement. Uniform mixing is assumed. All processes that influence soil bulk density are modeled within the primary and secondary tillage zones.

Three additional factors, including: 1) soil water content, 2) rainfall consolidation, and 3) weathering consolidation that influence temporal changes in soil bulk density are predicted.

6.7.2 Soil Water Content Effects

The influence of soil water content on bulk density changes is predicted from:

$$\rho_{(t)} = \rho_{(t-1)} + \Delta\rho_{wc} \left[\Theta_{(t)} - \Theta_{(t-1)} \right] \quad [6.7.6]$$

where $\rho_{(t)}$ is the bulk density ($kg\ m^{-3}$), $\rho_{(t-1)}$ is the bulk density of the previous day ($kg\ m^{-3}$), $\Delta\rho_{wc}$ is the parameter describing the change in bulk density with water content ($kg\ m^{-3}$), Θ_t is the water content ($m^3\ m^{-3}$), and $\Theta_{(t-1)}$ is the water content of the previous day ($m^3\ m^{-3}$).

The change in soil bulk density with soil water content ($\Delta\rho_{wc}$) is predicted from:

$$\Delta\rho_{wc} = \frac{\rho_d - \rho_c}{\Theta_r - \Theta_{fc}} \quad [6.7.7]$$

where ρ_d is the oven dry bulk density ($kg\ m^{-3}$), ρ_c is the consolidated bulk density at 0.033 MPa ($kg\ m^{-3}$), Θ_r is the residual water content ($m^3\ m^{-3}$), and Θ_{fc} is the water content of the consolidated soil at 0.033 MPa ($m^3\ m^{-3}$).

Oven dry bulk density is read into the model from the soil input file. If the value is zero, ρ_d is predicted from:

$$\rho_d = \left[-0.024 + 0.001 \rho_c + 1.55 C_l CEC_r + C_l^2 CEC_r^2 - 1.1 CEC_r^2 C_l - 1.4 O_m \right] 10^3. \quad [6.7.8]$$

The residual water content of the soil is predicted from (Baumer, personal communication):

$$\Theta_r = \left[0.000002 + 0.0001 O_m + 0.00025 C_l CEC_r^{0.45} \right] \rho_{(t)} \quad [6.7.9]$$

where Θ_r is the residual volumetric water content of the soil ($m^3\ m^{-3}$).

The gravimetric soil water content at 0.033 MPa ($kg\ water/kg\ of\ < 0.002\text{-m}\ soil\ material$) is read into the model from the soil input file and is converted to a volumetric basis by multiplying by the bulk density of the soil. If the value is zero, the volumetric water content is predicted from:

$$\Theta_{fc} = 0.2391 - 0.19 S_a + 2.1 O_m + 0.72 \Theta_d \quad [6.7.10]$$

where Θ_{fc} is the volumetric water content at 0.033 MPa ($m^3\ m^{-3}$).

The gravimetric soil water content at 1.5 MPa ($kg\ water/kg\ of\ < 0.002\text{-m}\ soil\ material$) is read into the model from the soil input file and is converted to a volumetric basis by multiplying by the bulk density of the soil. If the value is zero, the volumetric water content is predicted from:

$$\Theta_d = 0.0022 + 0.383 C_l - 0.5 C_l^2 S_a^2 + 0.265 C_l CEC_r^2 - \left[0.06 C_l^2 + 0.108 C_l \right] \left[\frac{\rho_{(t)}}{1000} \right]^2 \quad [6.7.11]$$

where Θ_d is the volumetric water content at 1.5 MPa ($m^3\ m^{-3}$).

6.7.3 Rainfall Consolidation

Rainfall on freshly tilled soil consolidates it and increases soil bulk density. Soil bulk density increases by rainfall are predicted from (Onstad et al., 1984):

$$\rho_{(t)} = \rho_t + \Delta\rho_{rf} \quad [6.7.12]$$

where $\rho_{(t)}$ is the bulk density after rainfall ($kg\ m^{-3}$), ρ_t is the bulk density after tillage ($kg\ m^{-3}$), and $\Delta\rho_{rf}$ is the bulk density increase due to consolidation by rainfall ($kg\ m^{-3}$).

The increase in soil bulk density from rainfall consolidation ($\Delta\rho_{rf}$) is calculated from:

$$\Delta\rho_{rf} = \Delta\rho_{mx} \frac{R_c}{0.01 + R_c} \quad [6.7.13]$$

where $\Delta\rho_{mx}$ is the maximum increase in soil bulk density with rainfall and R_c is the cumulative rainfall since tillage (m).

The maximum increase in soil bulk density with rainfall is predicted from:

$$\Delta\rho_{mx} = 1650 - 2900 C_l + 3000 C_l^2 - 0.92 \rho_t \quad [6.7.14]$$

The upper boundary for soil bulk density change with rainfall is reached after a freshly tilled soil receives 0.1 m of rainfall.

6.7.4 Weathering Consolidation

For most soils, 0.1 m of rainfall does not fully consolidate the soil. Consolidated soil bulk density (ρ_c) is assumed to be the upper boundary to which a soil naturally tends to consolidate.

The difference between the naturally consolidated bulk density and the bulk density after 0.1 m of rainfall is:

$$\Delta\rho_c = \rho_c - \rho_{(t)} \quad [6.7.15]$$

where $\Delta\rho_c$ is the difference in soil bulk density between a soil that is naturally consolidated and one that has received 0.1 m of rainfall. $\rho_{(t)}$ is soil bulk density on the day cumulative rainfall since tillage equals 0.1 m.

The adjustment for increasing bulk density due to weathering and longer-term soil consolidation is computed from:

$$\Delta\rho_{wt} = \Delta\rho_c F_{dc} \quad [6.7.16]$$

where $\Delta\rho_{wt}$ is the daily increase in soil bulk density after 0.1 m of rainfall ($kg\ m^{-3}$), and F_{dc} is the daily consolidation factor.

The daily bulk density consolidation factor is predicted from:

$$F_{dc} = 1 - e^{-\alpha_{bd}} \quad [6.7.17]$$

where α_{bd} is a bulk density parameter. α_{bd} is currently set to 0.005, which generally causes the soil to consolidate to its natural bulk density in about 200 days if no tillage occurs.

Soil bulk density changes following tillage are predicted from:

$$\rho(t) = \rho_t + \sum \rho_{wc} + \Delta \rho_{rf} \quad [6.7.18]$$

where $\sum \rho_{wc}$ is the cumulative bulk density change with water content from tillage until the soil receives 0.1 m of rainfall.

After the soil receives 0.1 m of rainfall, soil bulk density changes are predicted from:

$$\rho(t) = \rho_{(t-1)} + \Delta \rho_{wc} \left[\Theta_{(t)} - \Theta_{(t-1)} \right] + \Delta \rho_{wt} \quad [6.7.19]$$

where $(t-1)$ refers to the previous day.

6.8 Porosity

Total soil porosity (ϕ_t) is predicted from soil bulk density by:

$$\phi_t = 1 - \frac{\rho(t)}{2650} \quad [6.8.1]$$

where $\rho(t)$ is the bulk density at time t ($kg\ m^{-3}$).

The volume of entrapped air in the soil (F_a) is calculated from (Baumer, personal communication):

$$F_a = 1.0 - \frac{3.8 + 1.9 C_l^2 - 3.365 S_a + 12.6 CEC_r C_l + 100 O_m \left[\frac{S_a}{2} \right]^2}{100} \quad [6.8.2]$$

where the clay, sand, and organic matter contents of the soil are given as a fraction (0-1).

The correction for the volume of coarse fragments in the soil (F_{cf}) is predicted from (Brakensiek et al., 1986):

$$F_{cf} = 1 - V_{cf} \quad [6.8.3]$$

V_{cf} is the fraction of coarse fragments by volume (0-1) and is predicted from:

$$V_{cf} = \frac{M_{cf} \frac{\rho(t)}{1000}}{2.65 \left[1 - M_{cf} \right]} \quad [6.8.4]$$

where M_{cf} is the fraction of coarse fragments by weight (0-1).

The effective porosity of the soil (ϕ_e) is calculated from the total porosity determined from soil bulk density (< 2-mm material) and adjusted for the volumes of entrapped air and residual water. ϕ_e is computed from:

$$\phi_e = \left[\phi_t F_a \right] - \Theta_r \quad [6.8.5]$$

Soil porosity calculated in Eq. [6.8.1] and volumetric soil water contents at 0.020, 0.033, and 1.5 MPa are adjusted for the volumes of entrapped air (F_a) and coarse fragments (F_{cf}). These adjusted soil parameters are used in soil water storage computations (see Chapter 7).

6.9 Saturated Hydraulic Conductivity

The saturated hydraulic conductivity of the soil is predicted from:

$$K_s = \frac{\phi_c^3}{\left[1 - \phi_c F_a\right]^2 \left[\frac{0.001 \rho(t)}{\Theta_r}\right]^2 0.00020 C^2} \quad [6.9.1]$$

where K_s is the saturated hydraulic conductivity of the soil ($m s^{-1}$).

The parameter C is predicted from:

$$C = -0.17 + 18.1 C_1 - 69.0 S_a^2 C_1^2 - 41.0 S_a^2 S_i^2 + 1.18 S_a^2 \left[\frac{\rho(t)}{1000}\right]^2 + 6.9 C_1^2 \left[\frac{\rho(t)}{1000}\right]^2 + 49.0 S_a^2 C_1 - 85.0 S_i C_1^2 \quad [6.9.2]$$

where $\rho(t)$ is the bulk density of the soil at time t .

The saturated hydraulic conductivity of the soil (K_s) is adjusted for 1) weight of coarse fragments, 2) frozen soil, 3) crust, 4) macroporosity, and 5) soil cover. See Chapter 4 for information on crust, macroporosity, and soil cover adjustments.

6.9.1 Coarse Fragments in Soil

The saturated hydraulic conductivity adjustment for the weight of coarse fragments is predicted from:

$$K_s = K_s \left[1 - M_{cf}\right] \quad [6.9.3]$$

where M_{cf} is the fraction of coarse fragments in the soil by weight (0-1).

6.9.2 Frozen Soil

The saturated hydraulic conductivity adjustment for frozen soil (FS_a) is predicted from (Lee, 1983):

$$FS_a = 2 - 0.019 F_\Theta \quad [6.9.4]$$

F_Θ is predicted from:

$$F_\Theta = \frac{\Theta_f}{\Theta_{fc}} 100 \quad [6.9.5]$$

where Θ_f is the volumetric soil water content at freezing ($m^3 m^{-3}$). If $F_\Theta \geq 100$, then FS_a is set to 0.1.

If the average daily air temperature is $< 0^\circ C$, then:

$$K_s = K_s FS_a \quad [6.9.6]$$

6.10 Baseline Interrill Erodibility for Croplands

Data collected from a study of 36 cropland soils throughout the U.S. in 1987 and 1988 were analyzed to develop relationships between baseline interrill erodibility parameters and soil physical and chemical properties (Elliot et al., 1988). The interrill sediment delivery rate is (see Chapter 10 for more detail):

$$D_i = K_i I^2 \quad [6.10.1]$$

where D_i is the sediment delivery rate ($kg\ s^{-1}\ m^{-2}$), K_i is the interrill soil erodibility parameter ($kg\ s^{-1}\ m^{-4}$), and I is rainfall intensity ($m\ s^{-1}$).

The baseline K_i parameter for a soil in a seedbed condition is calculated from:

$$K_i = \left[-2.92 - 2.71 \left[\frac{C_{hwd}}{C_i} \right] - 0.51 M_g + 10.0 C_{hwd} + 4.19 \left[\frac{C_i}{F_e + A_i} \right]^{0.16} + 1.24 C_d \right] 10^6 \quad [6.10.2]$$

where K_i is the baseline interrill erodibility parameter for a cropland soil ($kg\ s^{-1}\ m^{-2}$), C_{hwd} is the fraction of water dispersible clay (0-1), C_i is the clay content (0-1), M_g is the magnesium content ($cmol\ kg^{-1}$), F_e and A_i are the iron and aluminum contents (0-1), and C_d is the electrical conductivity ($mmhos\ cm^{-1}$).

For soils with a clay fraction greater than 0.35, baseline K_i is predicted from:

$$K_i = \left[2.67 - 0.115 \ln \left[\left[(0.18 - A_g) 100 \right]^2 \right] \right] 10^6 \quad [6.10.3]$$

where A_g is the aggregate stability of the soil (fraction of 1- to 2-mm aggregates retained on a sieve with 0.5-mm openings after wet sieving).

6.11 Interrill Erodibility Adjustments for Cropland Soils

Effects of dead and live root biomass within the 0- to 0.15-m soil zone on interrill erodibility of a cropland soil are predicted separately. The effect of dead roots on interrill erodibility is predicted from (Alberts and Ghidry, unpublished data):

$$CK_{id} = 1.1 e^{-0.56 M_r} \quad [6.11.1]$$

where CK_{id} is the interrill erodibility adjustment for dead roots and M_r is dead root mass ($kg\ m^{-2}$) within the 0- to 0.15-m soil zone.

The effect of live roots on interrill erodibility is predicted from:

$$CK_{il} = 1.0 e^{-0.56 B_{r,1}} \quad [6.11.2]$$

where CK_{il} is the interrill erodibility adjustment for live roots and $B_{r,1}$ is live root biomass ($kg\ m^{-2}$) within the 0- to 0.15-m soil zone.

6.12 Baseline Interrill Erodibility for Rangeland Soil

Data collected from a study of 19 rangeland sites in 1987 and 1988 were analyzed to develop a relationship between interrill erodibility and soil physical and chemical properties (Simanton et al., 1987). Baseline K_i is predicted from:

$$K_i = \left[1709 - 1765 S_a - 645 S_i - 4557 O_m - 902 \Theta_{fc} \right] 10^3 \quad [6.12.1]$$

where K_i is the baseline interrill erodibility parameter for a rangeland soil ($kg\ s^{-1}\ m^{-4}$), S_a and S_i are the fractions of sand and silt (0-1), O_m is the fraction of organic matter (0-1), and Θ_{fc} is the volumetric water content of the soil at 0.033 MPa ($m^3\ m^{-3}$).

6.13 Baseline Rill Erodibility and Critical Shear for Cropland Soils

Data collected from a study of 36 soils throughout the U.S. in 1987 and 1988 were analyzed to develop relationships between rill erodibility and critical shear stress and soil physical and chemical properties (Elliot et al., 1988). For a detailed description of these parameters and their significance, see Chapter 10. Rill detachment capacity is predicted from:

$$D_r = K_r \left[\tau - \tau_c \right] \quad [6.13.1]$$

where D_r is the soil detachment capacity in a rill ($kg\ s^{-1}\ m^{-2}$), K_r is the rill soil erodibility parameter ($s\ m^{-1}$), τ is the shear stress of the flow (Pa), and τ_c is the critical shear stress of the flow necessary to initiate significant soil detachment (Pa).

The following equation is used to predict K_r :

$$K_r = \frac{196 + 0.015 \left[M - 3500 M^{0.2} \right] - \frac{32.7}{CEC^{0.4}} + 35.0 \left[1 + e^{(1-312 O_m)} \right] + \frac{0.16}{100 A_t S_{ar}^{0.75}} - 8 S_{ar}}{1000} \quad [6.13.2]$$

where K_r is the baseline rill erodibility parameter of a cropland soil ($s\ m^{-1}$), CEC is the cation exchange capacity ($cmol\ kg^{-1}$), and S_{ar} is the sodium adsorption ratio.

The textural parameter M is calculated from:

$$M = \left[S_i + S_{avf} \right] \left[1.0 - C_l \right] 10^2 \quad [6.13.3]$$

where S_{avf} is the fraction of very fine sand in the soil (0-1).

Baseline critical shear stress of a cropland soil is predicted from:

$$\tau_c = -2.85 - \frac{8.87}{(100 S_{avf} + 0.1)^{0.2}} - 16.0 C_c + 3.65 S_{ar} + 3.79 S_s^{0.2} + \frac{28.1}{100 S_a^{0.3}} \left[\frac{C_{lwd}}{C_l} \right]^{0.8} \quad [6.13.4]$$

where τ_c is the critical shear stress of the flow (Pa), and S_s is the specific surface of the soil (mg of ethylene glycol mono-ethyl ether adsorbed/g of soil).

For cropland soils with a clay fraction greater than 0.30, baseline τ_c is predicted from:

$$\tau_c = -0.5 - 284 \Theta_{(t)} \left[\Theta_{(t)} - 0.3 \right] \quad [6.13.5]$$

where $\Theta_{(t)}$ is the volumetric soil water content ($m^3\ m^{-3}$).

6.14 Rill Erodibility Adjustments for Croplands

6.14.1 Incorporated Residue

The following relationship is used to predict the effect of incorporated residue on K_r for a cropland soil (Brown and Foster, 1987; Alberts and Gantzer, 1988):

$$CK_{rm} = 1.1e^{-0.56 M_b} \quad [6.14.1]$$

where CK_{rm} is the rill erodibility adjustment for buried residue and M_b is the mass of buried residue ($kg\ m^{-2}$) within the 0- to 0.15-m soil zone.

6.14.2 Soil Consolidation

This routine estimates erodibility changes with time after tillage due to weathering and thixotropy. Details of the consolidation model, including equations for adjusting K_r and τ_c were described in detail by Nearing et al., 1988. The model calculates a relative increase in soil resistance due to drying and time, R' . The adjustment to K_r due to consolidation, CK_{rc} , is estimated by:

$$CK_{rc} = \frac{1}{R'} \quad [6.14.2]$$

where R' is the normalized rill erodibility adjustment due to consolidation.

The adjustment of τ_c , $C\tau_{cc}$, is predicted from:

$$C\tau_{cc} = 0.5 [R' + 1]. \quad [6.14.3]$$

6.15 Baseline Rill Erodibility and Critical Shear for Rangeland Soil

Data collected from a study of 19 rangeland soils in 1987 and 1988 were analyzed to develop relationships between rill erodibility and critical shear stress and soil physical and chemical properties. Baseline K_r is predicted from:

$$K_r = 0.0017 + 0.0024 C_l - .0088 O_m - 0.00088 \left[\frac{\rho_{(t)}}{1000} \right] - 0.00048 R_i \quad [6.15.1]$$

where K_r is the baseline rill erodibility parameter for a rangeland soil, C_l and O_m are fractions of clay and organic matter (0-1), $\rho_{(t)}$ is the soil bulk density ($kg\ m^{-3}$), and R_i is the total root biomass ($kg\ m^{-2}$) within the 0- to 0.10-m soil zone.

τ_c is predicted from:

$$\tau_c = 3.23 - 5.6 S_a - 24.4 O_m + 0.90 \left[\frac{\rho_{(t)}}{1000} \right] \quad [6.15.2]$$

where τ_c is the critical shear stress of the flow necessary to detach soil (Pa).

6.16 References

- Alberts, E.E., and C.J. Gantzer. 1988. Influence of incorporated residue and soil consolidation on rill soil erodibility. *Agronomy Abstracts*. p.270.
- Brakensiek, D.L., W.J. Rawls, and G.R. Stephenson. 1986. Determining the saturated hydraulic conductivity of soil containing rock fragments. *Soil Sci. Soc. Am. J.* 50(3):834-835.
- Brown, L.C., and G.R. Foster 1987. Rill erosion as affected by incorporated crop residue. *ASAE Paper No. 87-2069*.

Elliot, W.J., K.D. Kohl, and J.M. Laflen. 1988. Methods of collecting WEPP soil erodibility data. ASAE Paper No. MCR 88-138.

Laflen, J.M., A.W. Thomas, and R.W. Welch. 1987. Cropland Experiments for the WEPP project. ASAE Paper No. 87-2544.

Lee, H.W. 1983. Determination of infiltration characteristics of a frozen palouse silt from soil under simulated rainfall. PhD. Dissertation, University of Idaho, Moscow, Idaho.

Nearing, M.A., L.T. West, and L.C. Brown. 1988. A consolidation model for estimating changes in rill erodibility. Trans. ASAE 31(3):696-700.

Onstad, C.A., M.L. Wolf, C.L. Larson, and D.C. Slack. 1984. Tilled soil subsidence during repeated wetting. Trans. ASAE 27(3):733-736.

Simanton, J.R., L.T. West, M.A. Weltz, and G.D. Wingate. 1987. Rangeland experiment for the WEPP project. ASAE Paper No. 87-2545.

Williams, J.R., C.A. Jones, and P.T. Dyke. 1984. A modeling approach to determining the relationship between erosion and soil productivity. Trans. ASAE 27(1):129-142.

6.17 List of Symbols

Symbol	Definition	Unit	Variable
A_g	Wet aggregate stability parameter	Fraction	AS
A_l	Aluminum content	Fraction	AL
α_{bd}	Soil bulk density parameter	Fraction	BDE
α_{rh}	Ridge height parameter	Fraction	RHE
α_{rr}	Random roughness parameter	Fraction	RRE
$B_{r,1}$	Live root biomass in the 0- to 0.15-m soil zone	$kg\ m^{-2}$	RTM15
C	Saturated hydraulic conductivity parameter	Fraction	C1
C_c	Calcium carbonate content	Fraction	CACO3
C_d	Electrical conductivity	$mmhos\ cm^{-1}$	COND
C_l	Clay content	Fraction	CLAY
C_{hd}	Water-dispersible clay	Fraction	WDCLAY
C_f	Flat residue cover	Fraction	FLRCOV
CEC	Cation exchange capacity of the soil	$cmol\ kg^{-1}$	CEC
CEC_c	Cation exchange capacity of the clay	$cmol\ kg^{-1}$	CECC
CEC_r	Ratio of cation exchange capacity of the clay to the fraction of clay in the soil	$cmol\ kg^{-1}$	SOLCON
CK_{id}	Cropland interrill soil erodibility adjustment for dead root mass	Fraction	CKIADR
CK_{il}	Cropland interrill soil erodibility adjustment for live root biomass	Fraction	CKIALR
CK_{rc}	Cropland rill erodibility adjustment for soil consolidation	Fraction	CKRCON
CK_{rm}	Cropland rill erodibility adjustment for buried residue biomass	Fraction	CKRASR
$C\tau_{cc}$	Cropland critical shear stress adjustment for soil consolidation	Fraction	CTCCON
D_g	Depth of the soil horizon of interest	m	DG
D_i	Interrill sediment delivery rate	$kg\ s^{-1}\ m^{-2}$	Di

D_r	Rill soil detachment capacity	$kg\ s^{-1}\ m^{-2}$	Dr
F_a	Volume of entrapped air in the soil	Fraction	COCA
F_d	Coarse fragment adjustment for soil porosity	Fraction	CPM
F_{dc}	Daily soil bulk density consolidation factor	Fraction	DAYCON
F_e	Fraction of iron in the soil	Fraction	FE
FS_a	Saturated hydraulic conductivity adjustment for frozen soil	Fraction	FROF
F_e	Soil water volume at freezing/soil water volume at 0.033 MPa	Fraction	PFC
I	Rainfall intensity	$m\ s^{-1}$	I
K_i	Interrill soil erodibility parameter	$kg\ s^{-1}\ m^{-4}$	Ki
K_r	Rill soil erodibility parameter	$s\ m^{-1}$	Kr
K_s	Saturated hydraulic conductivity of the soil	$m\ s^{-1}$	SSC
M	Soil texture parameter	Fraction	M
M_b	Buried residue mass in the 0- to 0.15-m soil zone	$kg\ m^{-2}$	SMRM
M_d	Coarse fragment content by weight	Fraction	RFG
M_s	Magnesium content	$cmol\ kg^{-1}$	MG
M_r	Dead root biomass in the 0- to 0.15-m soil zone	$kg\ m^{-2}$	RTM
O_c	Organic carbon content	Fraction	ORGC
O_m	Organic matter content	Fraction	ORGMAT
ϕ_e	Effective porosity	Fraction	EPOR
ϕ_t	Total porosity	Fraction	POR
R_c	Cumulative rainfall since tillage	m	RFCUM
R_{mf}	Residue mixing factor	Fraction	RMF
R_{ho}	Ridge height immediately after tillage	m	RHo
R_h	Ridge height at time t	m	RHt
R_i	Total root mass in the 0- to 0.10-m zone of rangeland soil	$kg\ m^{-2}$	ROOT
R_r	Random roughness at time t	m	RRt
R_{ri}	Random roughness immediately after tillage	m	RRINT
R_{ro}	Random roughness of a tillage implement	m	RRo
R'	Normalized rill erodibility resistance due to consolidation	Fraction	RPRIME
ρ	Soil bulk density	$kg\ m^{-3}$	BD
ρ_c	Consolidated soil bulk density at 0.033 MPa	$kg\ m^{-3}$	BDCONS
$\Delta\rho_c$	Difference in soil bulk density between a soil that is naturally consolidated and one that has received 0.1 m of rainfall	$kg\ m^{-3}$	BDDIFF
ρ_d	Oven-dry soil bulk density	$kg\ m^{-3}$	BDDRY
$\Delta\rho_{mx}$	Maximum increase in soil bulk density with rainfall	$kg\ m^{-3}$	Ao
$\Delta\rho_{rf}$	Adjustment for increasing soil bulk density due to consolidation by rainfall	$kg\ m^{-3}$	BDIRF
$\Delta\rho_{wt}$	Daily increase in soil bulk density after 0.1 m of rainfall	$kg\ m^{-3}$	BDIWT
ρ_t	Soil bulk density after tillage	$kg\ m^{-3}$	BDTILL
$\Delta\rho_{wc}$	Change in soil bulk density with water content	$kg\ m^{-3}$	Bo
$\sum\rho_{wc}$	Cumulative bulk density change with water content from tillage until 0.1 m of rainfall	$kg\ m^{-3}$	SBDIWC
S_a	Sand content	Fraction	SAND
S_{ar}	Sodium adsorption ratio	Fraction	SAR
S_{avf}	Very fine sand content	Fraction	VFS

S_i	Silt content	Fraction	SILT
S_s	Specific surface	$mg\ g^{-1}$	SS
τ	Shear stress of the flow	Pa	TAU
τ_c	Critical shear stress of the flow necessary to initiate detachment	Pa	TAUc
θ	Soil water content by volume	Fraction	THET
θ_d	Soil water content at 1.5 MPa by volume	Fraction	THETDR
θ_f	Soil water content at freezing by volume	Fraction	SMF
θ_{fc}	Soil water content at 0.033 MPa by volume	Fraction	THETFC
θ_r	Residual soil water content by volume	Fraction	WRD
T_i	Tillage intensity	Fraction	TI
V_d	Coarse fragment content by volume	Fraction	VCF

Chapter 7. WATER BALANCE AND PERCOLATION

M. R. Savabi, A. D. Nicks, J. R. Williams, and W. J. Rawls

7.1 Introduction

The water balance and percolation component of the WEPP-hillslope model is designed to use input from the climate, infiltration, and crop growth components to estimate, soil water content in the root zone, and evapotranspiration losses throughout the simulation period. The time step in predicting evapotranspiration and percolation is 24 hours. The WEPP water balance uses many of the algorithms given in SWRRB (Simulation of Water Resources in Rural Basins) by Williams et al. (1985). Some modification has been made to improve estimation of percolation and soil evaporation parameters.

The hydrologic processes in WEPP hillslope model include infiltration, runoff routing, soil evaporation, plant transpiration, and plant growth (Fig. 7.1). The model maintains a continuous water balance on a daily basis using the equation:

$$\Theta = \Theta_{in} + P \pm S - Q - ET - D \quad [7.1.1]$$

where Θ is the soil water content in the root zone in any given day, m, Θ_{in} is the initial soil water in the root zone, m, P is the cumulative precipitation, m, S is the snow water content, m (+) for snowmelt and it equals daily snowmelt, (-) snow accumulation), Q is the cumulative amount of surface runoff, m, ET is the cumulative amount of evapotranspiration, m, and D is the cumulative amount of percolation loss below root zone, m.

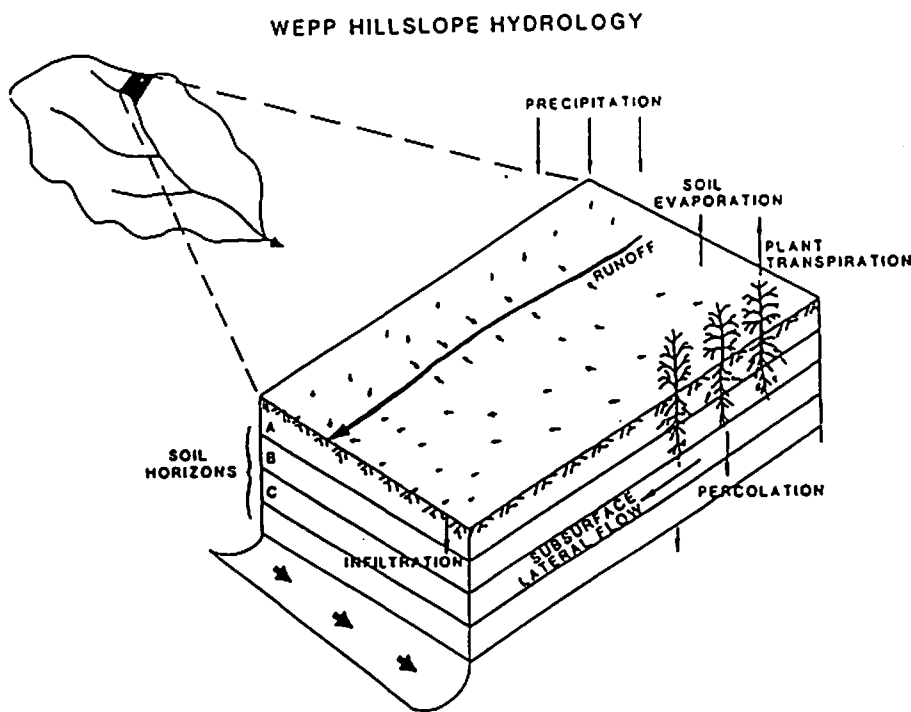


Figure 7.1.1. Processes in WEPP hillslope hydrology include precipitation (rain or snow), infiltration, runoff, plant transpiration, soil evaporation and percolation.

Precipitation is partitioned between rainfall and snowfall using average air temperature. If the average daily air temperature is zero degree Celsius or below, the precipitation is snowfall, otherwise, it is considered rain. Accumulated snowpack will be subject to evaporation and melt. Soil evaporation is considered first to come from snowpack, if present, and then from soil. Snow is melted on days when the maximum temperature exceeds zero degree Celsius. Melted snow is treated in the water balance Eq. [7.1.1] as rainfall for estimating runoff and percolation computations.

7.2 Evapotranspiration in WEPP

The evapotranspiration component of WEPP is the same as that used in EPIC (Williams et al., 1983) and SWRRB and is Ritchie's ET model (Ritchie, 1972). Potential evaporation is computed using the equation:

$$E_u = 0.00128 \frac{R(1-A)}{58.3} \frac{\delta}{\delta+0.68} \quad [7.2.1]$$

where E_u is the daily potential evapotranspiration, $m \ d^{-1}$, R is the daily solar radiation ($1y$), A is the albedo (0-1.0), and δ is the slope of the saturated vapor pressure curve at mean air temperature.

The albedo is evaluated by considering the soil, crop, and snow cover. If a snow cover exists with at least 0.005 m water content, the value of albedo is set to 0.80, otherwise the soil albedo is used. The albedo is estimated during growing season using the equation:

$$A = 0.23(1 - C_f) + (A_s) C_f \quad [7.2.2]$$

where 0.23 is the plant albedo, C_f is the soil cover index (0-1.0), and A_s is the soil albedo.

The value of C_f is calculated using the equation:

$$C_f = e^{(-0.000029 C)} \quad [7.2.3]$$

where C is the sum of above ground biomass and plant residue, $kg \ ha^{-1}$, determined in the crop growth component.

The value of δ in Eq. [7.2.1] is determined from the equation:

$$\delta = \frac{5304}{T_k^2} e^{\left[21.25 - \frac{5304}{T_k}\right]} \quad [7.2.4]$$

where T_k is the daily average air temperature, degrees Kelvin.

Potential soil evaporation, E_{sp} , is predicted (Fig. 7.2.1) with the equation:

$$E_{sp} = E_u e^{(-0.4 L)} \quad [7.2.5]$$

L is the leaf area index defined as the area of plant leaves relative to the soil surface area.

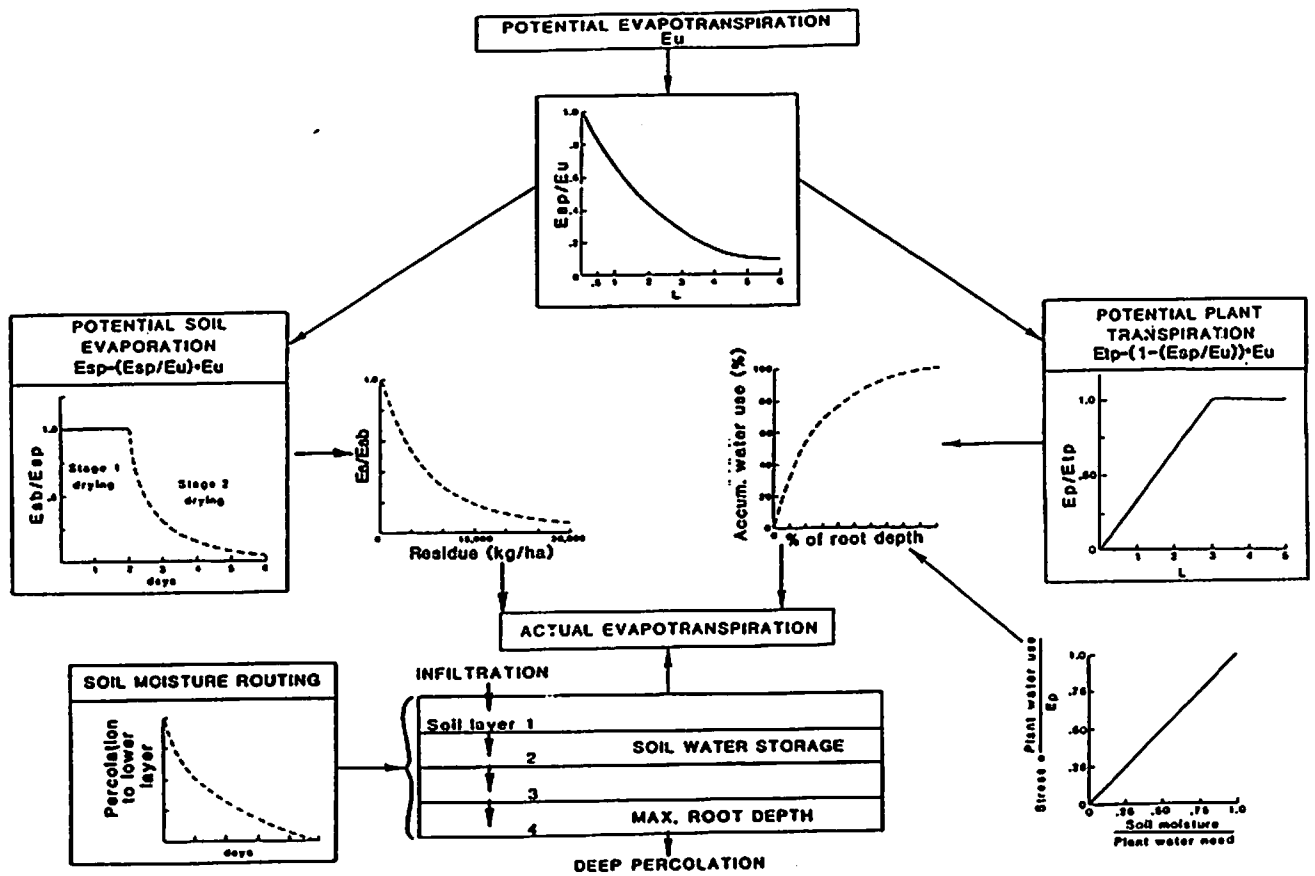


Figure 7.2.1. Schematic computational sequence of the WEPP evapotranspiration and soil water routing.

Bare soil evaporation, E_{sb} , is calculated in two stages (Fig. 7.2.1). In the first stage, soil evaporation is limited only by the energy available at soil surface and, therefore, it is equal to potential soil evaporation, E_{sp} . The upper limit for the stage one soil evaporation is calculated using equation (Ritchie, 1972):

$$E_{sm} = 0.009 (T_r - 3.0)^{0.42} \quad [7.2.6]$$

where E_{sm} is the upper limit soil evaporation of stage one, m , and T_r is the soil transmissivity ($mm \text{ day}^{-0.5}$), dependent on soil texture:

$$T_r = 4.165 + 0.02456 S_a - 0.01703 C_l - 0.0004 S_a^2 \quad [7.2.7]$$

where S_a is the percentage of sand in bare soil evaporated layer and C_l is the percentage of clay in bare soil evaporated layer.

When the accumulated soil evaporation exceeds the stage one upper limit, E_{sm} , stage two evaporation begins. Stage two soil evaporation is estimated using the equation:

$$S_2 = 0.001 T_r [d_2^{1/2} - (d_2 - 1)^{1/2}] \quad [7.2.8]$$

where S_2 is the stage two bare soil evaporation rate for a day ($m \text{ day}^{-1}$) and d_2 is the number of days since stage two soil evaporation began.

If precipitation is greater than or equal to accumulated stage two soil evaporation, the stage one soil evaporation is assumed. For more details see Ritchie (1972). During a drying cycle, evaporation from the soil continues until the soil water content is at a residual moisture content, R_{mc} , a moisture content below which no more water can be evaporated from the bare soil. R_{mc} is calculated using soil organic matter, percent clay, and soil bulk density (see chapter 6 for more detail). Computed bare soil evaporation, E_{sb} , in either stage is reduced with increased plant residue using equation

$$E_s = E_{sb} e^{(-0.000064 C_r)} \quad [7.2.9]$$

where E_s is the actual soil evaporation, $m \text{ day}^{-1}$, E_{sb} is the actual bare soil evaporation, $m \text{ day}^{-1}$, and C_r is the plant residue on soil, $kg \text{ ha}^{-1}$ (data from J. L. Steiner, personal communication).

Potential plant transpiration is computed as a linear function of L and E_u up to L of 3.

$$E_p = \frac{E_u L}{3} \quad L \leq 3 \quad [7.2.10]$$

where E_p is the daily potential plant transpiration, $m \text{ day}^{-1}$. Beyond $L = 3$, potential plant transpiration is equal to E_u .

7.3 Distribution Of Evapotranspiration In the Root Zone

The distribution of calculated soil evaporation, E_s , in the root zone is determined by considering snow cover and soil water content of the effective depth influenced by bare soil evaporation, d_x . If the water content of the snow cover is equal or greater than E_s , all the soil evaporation comes from the snow cover. If E_s exceeds the water content of the snow cover, the difference will be removed from soil water. The depth of the soil, where water is evaporated d_s is predicted with the equation:

$$d_s = d_x \frac{E_s}{\Theta} - R_{mc} d_x \quad E_s < \Theta - (R_{mc} d_x) \quad [7.3.1]$$

$$d_s = d_x \quad E_s > \Theta - (R_{mc} d_x)$$

where d_s is the soil evaporated depth at any given day, m , d_x is the maximum soil evaporated depth influenced by soil evaporation, (Lane and Stone, 1983), m , E_s is the predicted daily actual soil evaporation, m , Θ is the soil water content of the soil layers above d_x , m , and R_{mc} is the residual moisture content, percent by volume.

The maximum soil evaporation effective depth, d_x , is calculated based on soil texture with equation:

$$d_x = 0.09 - 0.00077 C_1 + 0.000006 S_2^2 \quad [7.3.2]$$

If the water content in d_x depth is not sufficient for calculated soil evaporation (E_s), soil evaporation will be reduced accordingly.

The potential plant transpiration is distributed in the root zone, RZ with the equation:

$$U_{Pi} = \frac{E_p}{1 - e^{(-V)}} \left[1 - e^{\left[-V \frac{h_i}{RZ} \right]} \right] - \sum_{j=1}^{i-1} U_j \quad [7.3.3]$$

where U_{Pi} is the potential water use rate from layer i ($m \text{ day}^{-1}$), and V is a use rate-depth parameter, 3.065 is used in WEPP, assuming about 30 percent of the total water use comes from the top 10 percent of the root zones. The details of evaluating V are given by Williams and Hann (1978). h_i is the depth of soil layer i , m , RZ is the root zone depth (m), and U is the actual water use from the soil layer above layer i (m).

The potential water use U_{Pi} is adjusted for water deficits to obtain the actual water use, U_i for each layer.

$$\begin{aligned} U_i &= U_{Pi} & \Theta_i > \Theta_c UL_i \\ U_i &= U_{Pi} \frac{\Theta_i}{\Theta_c UL_i} & \Theta_i \leq \Theta_c UL_i \end{aligned} \quad [7.3.4]$$

where Θ_i is soil water content of layer i (m), and Θ_c is a critical soil water content below which plant growth is subjected to water stress, percent by volume. Θ_c is a crop dependent parameter provided by the user. The default value is 0.25. UL_i is the upper limit soil water content for layer i , m .

Equation [7.3.4] allows roots to compensate for water deficits in certain layers by using more water in layer with adequate supplies.

7.4 Percolation In WEPP

The percolation component of WEPP uses storage routing technique to predict flow through each soil layer in the root zone. In each layer, water content exceeding the corresponding field capacity is subjected to percolation through the succeeding layer. Water moving below the root zone is considered lost and will not be traced. Saturated hydraulic conductivity is being calculated for each layer based on soil physical properties such as soil texture, organic matter and porosity. Flow through a soil layer may be reduced by coarse fragments in the layer, frozen layer, and saturated or nearly saturated lower layer.

Percolation of water in excess of field capacity from a layer is computed using the equation:

$$\begin{aligned} d_i &= (\Theta_i - FC_i) \left[1 - e^{\left[\frac{-\Delta t}{t_i} \right]} \right] & \Theta_i > FC_i \\ d_i &= 0 & \Theta_i \leq FC_i \end{aligned} \quad [7.4.1]$$

where d_i is the percolation rate through layer i ($m \text{ day}^{-1}$), FC_i is the field capacity water content (33 KPa for many soils) for layer i (m), Δt is the travel interval (s), and t_i is the travel time through layer i (s).

The travel time through a particular layer is computed with the linear storage equation:

$$t_i = \frac{\Theta_i - FC_i}{K_{sai}} \quad [7.4.2]$$

K_{sai} is the adjusted hydraulic conductivity of layer i ($m \text{ s}^{-1}$).

The hydraulic conductivity is varied from the saturated conductivity, K_s , value at saturation to near zero at field capacity.

$$K_{sai} = K_{si} \left[\frac{\Theta_i}{UL_i} \right]^{B_i} \quad [7.4.3]$$

where K_{si} is the saturated hydraulic conductivity for layer i ($m s^{-1}$) and B_i is a parameter that causes K_{sai} to approach zero as Θ_i approaches FC_i .

$$B_i = \frac{-2.655}{\log \frac{FC_i}{UL_i}} \quad [7.4.4]$$

The constant -2.655 in Eq. [7.4.4] assures K_{sai} of $0.002 * K_{si}$ at field capacity.

The computation of saturated hydraulic conductivity of each layer, K_{si} , and adjustments for rocks, frozen ground, entrapped air are presented in Chapter 6.

Flow through a soil layer may be restricted by a lower layer which is or nearly saturated. The effect of lower layer water content is given in the equation:

$$d_{ci} = d_i \sqrt{1 - \frac{\Theta_{i+1}}{UL_{i+1}}} \quad [7.4.5]$$

where d_{ci} is the percolation rate adjusted for lower layer ($i+1$) water content ($m day^{-1}$).

7.5 Linkage of Water Balance and Percolation Components With the Other WEPP Components

The infiltration component of WEPP is linked with evapotranspiration and percolation component (Fig. 7.2.1) to maintain a continuous water balance. Infiltrated water will be added to upper soil water content and routed through the soil layers. Soil water in each layer is subjected to percolation and/or evapotranspiration (Fig. 7.2.1). The upper layer soil water content is being used to establish initial moisture conditions for the infiltration component (Green and Ampt model). Percolation below the root zone is considered lost from the WEPP water balance.

Daily leaf area index, root depth, total plant biomass and residue cover are entered as input to the evapotranspiration component from the crop growth component. The plant growth water stress factor is computed by considering supply and demand in the equation:

$$W_s = \frac{\sum_{i=1}^n U_i}{E_p} \quad [7.5.1]$$

where W_s is the plant growth water stress factor (0-1.0), U_i is actual water use from layer i (m), n is number of soil layers, and E_p is the potential plant transpiration (m).

The water stress factor, W_s , is used in the WEPP plant growth component to adjust daily plant growth.

7.6 Model Validation

The Water balance component of the WEPP hillslope was evaluated using data from a tall grass prairie watershed, near Manhattan, Kansas. The model was tested independently from the WEPP hillslope model, therefore, measured infiltration (L), plant biomass, and residue cover were used in the validation. The other input data included daily maximum and minimum temperature, solar radiation, as well as watershed soil physical properties of the root zone.

7.6.1 Watershed Description and Field Measurements

Watershed 1D (37.7 ha) at the Konza prairie near Manhattan, Kansas was selected for this study (Fig. 7.6.1). The soil of the watershed is classified as Benfield-Florence Complex, which consists of Benfield silty clay and Florence cherty silt loam. The soil is well drained and has low available water capacity. Annual rainfall is about 86 cm with about 75 percent of the moisture falling during the growing season (May to August).

The native vegetation, according to Anderson and Fly (1955), are mid-grasses, such as little bluestem (*Andropogon scoparius*), side oats grama (*Bouteloua curtipendula*), and Kentucky bluegrass (*Poa Pratensis*), together with tall grasses including big bluestem (*Andropogon furcatus*), indiagrass (*Sorghastrum nutans*), and switchgrass (*Panicum virgatum*).

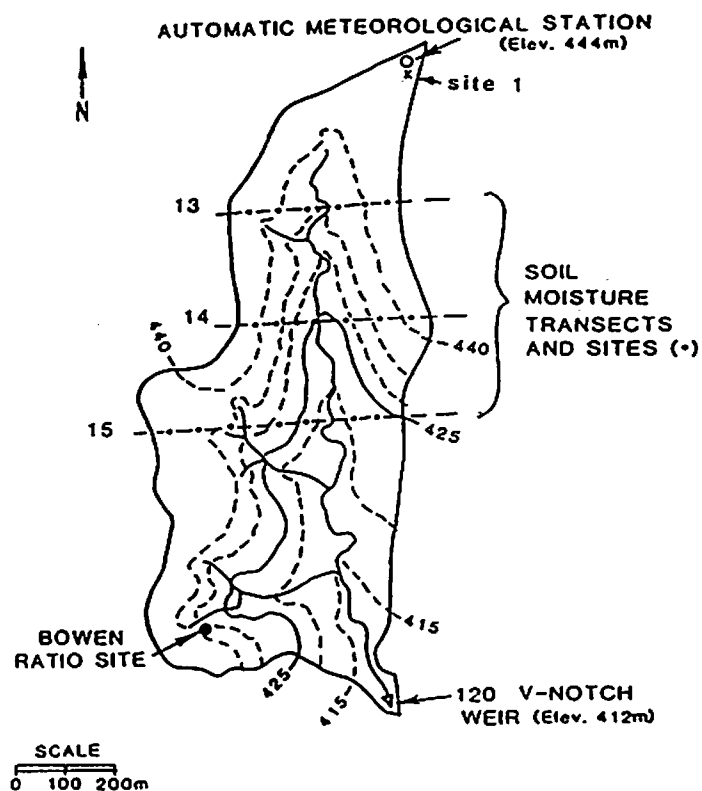


Figure 7.6.1. Watershed 1D, Konza Prairie and location of the automatic meteorological, Bowen ratio stations and soil moisture transects.

Rainfall, maximum and minimum temperature, and net radiation were measured by automatic meteorological stations (Fig. 7.6.1). Streamflow was measured with a sharp crested weir and a clock driven analog recorder. Near surface (.05 m) soil moisture was measured gravimetrically within three transects (Fig. 7.6.1). Soil moisture content was measured periodically to a depth of 2 m during the 1987 growing season via neutron meter techniques. Five neutron access tubes were installed at site 1 near the automatic meteorological station (Fig. 7.6.1).

Actual evapotranspiration was estimated using the Energy Balance Bowen Ratio (EBBR) method (Bowen, 1926; Slatyer and McIlroy, 1961). Several studies suggest that EBBR estimates of ET are in good agreement with lysimeter measurement in nonadvective conditions (Tanner, 1960; Pruitt and Lourence, 1968; and Denmead and McIlroy, 1970). The method involves determining the latent heat flux through solution of the energy balance equation,

$$LE = \frac{R_n - G}{1 + \gamma \frac{dt}{de}} \quad [7.6.1]$$

where LE is the latent heat flux ($W m^{-2}$), R_n is the net radiation ($W m^{-2}$), G is the soil heat flux ($W m^{-2}$), γ is the psychrometric constant, dt and de are the air temperature ($^{\circ}K$), and vapor pressure (Pa), differences at two heights above the canopy, respectively.

At the Bowen ratio site (Fig. 7.6.1), R_n , G , dt , and de were measured by automatic Bowen ratio system every 30 minutes during the 1987 growing season. LE was determined for every 30 minutes and integrated over 24 hours to determine daily LE . Daily LE was converted to depth of evaporated water (1 m water equals $676000 W/m^2$ at $25^{\circ}C$).

Leaf area index of live vegetation and plant residue ($kg ha^{-1}$) were among several biophysical measurements made periodically on the watershed.

The model was tested using the measured data of the 1987 growing season. No calibration was conducted. The model-simulated ET was compared with EBBR- ET . In addition, model-simulated and measured soil water contents were compared.

7.6.2 Results and Discussion

Daily model-simulated ET is compared with EBBR- ET using least square analysis (Fig. 7.6.2). The calculated coefficient of determination is 0.67 and is significant with 0.05 probability level. The intercept and the slope of the regression equation between daily model-simulated and EBBR- ET are not different from zero and unity, respectively, with 0.05 probability level which indicate statistically a good agreement between model and EBBR- ET .

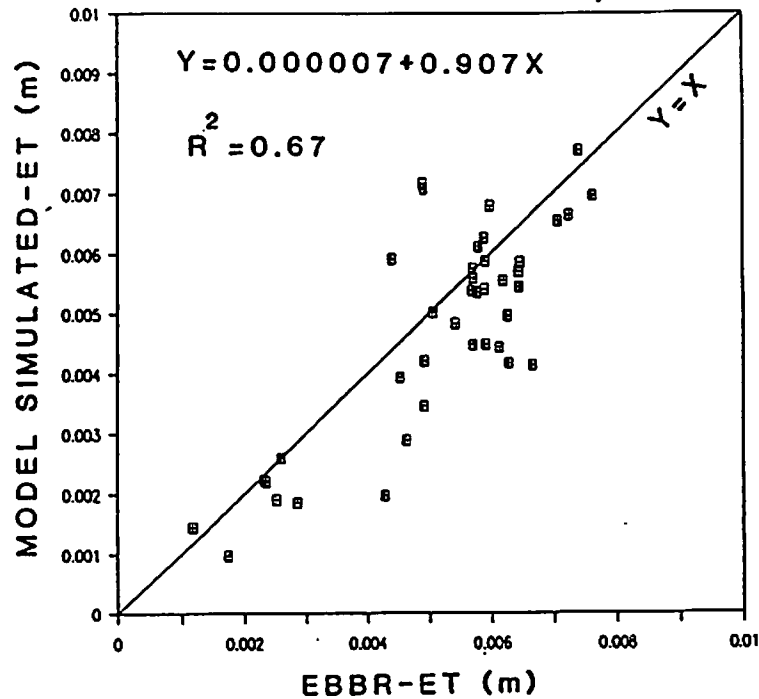


Figure 7.6.2. Least square analysis between WEPP simulation ET and estimated ET using EBBR method on watershed 1D during 1987 growing season.

Percent model-simulated and average field measured soil water content for the top .05 m of soil are shown in Fig. 7.6.3. The average field measured soil water content values are the arithmetic mean of all measurements within the three transects (13, 14, and 15, Fig. 7.6.1). The calculated standard error between model simulated and average field measured soil water content is 0.002 m. In the model, infiltrated water is added to the surface soil layer where it is subjected to percolation to lower layer, evaporation from surface layer, and transpiration from the root zone by plants. Good agreement between simulated and measured near surface soil water content indicates that the model is capable of predicting antecedent soil water content for the infiltration component of the WEPP model with reasonable accuracy.

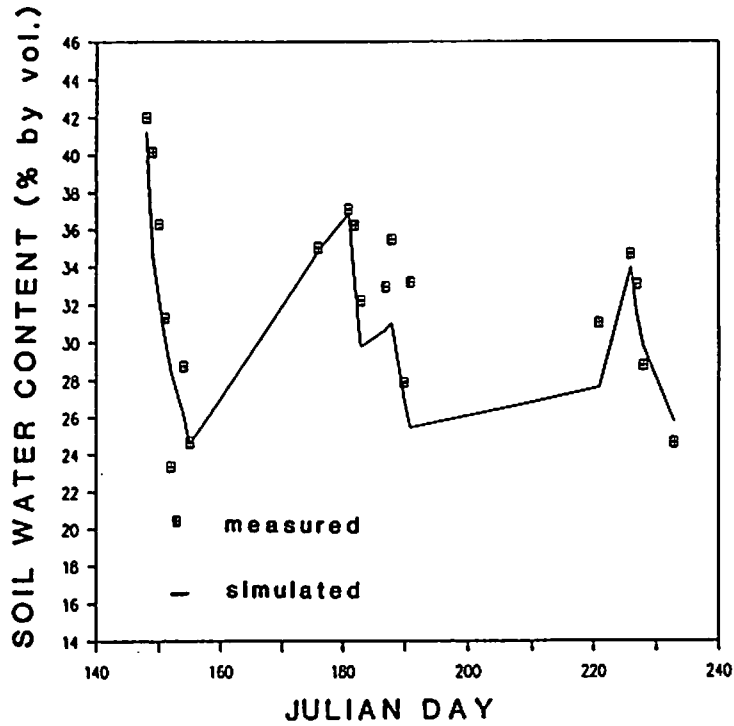


Figure 7.6.3. Comparison of model-simulated and measured soil water content of top 5 cm soil. The measured values are arithmetic mean of all measurements within the transects 13, 14, and 15.

Figure 7.6.4 shows a fair comparison between the model-simulated and average measured soil water content from the surface to 2 m depth. The average measured soil water content values are the arithmetic average of the five access tubes at site 1 (Fig. 7.6.1). Calculated standard error is 0.052 m of soil water. Except for three days, measured soil water contents lay below model-simulated water content for the 1987 growing season (Fig. 7.6.4).

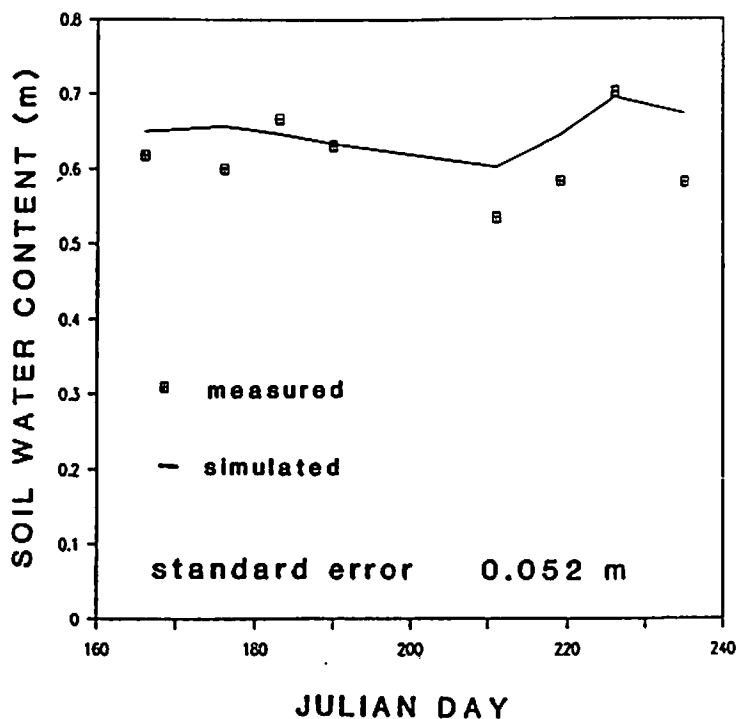


Figure 7.6.4. Comparison of model-simulated and average neutron probe measured soil water content (site 1) for the 200 cm soil depth.

The reasons for such deviations can be several including the fact that only five neutron meter access tubes are installed in the vicinity of watershed 1D and were assumed to represent the entire watershed. This assumption may not be valid because the access tubes are located at the north end of the watershed (site 1) where the elevation is greater than the entire watershed 1D (Fig. 7.6.1). The same argument can be used for the EBBR-ET measurement, however, there is a good agreement between simulated and measured water content of the top .05 m of soil which is more representative of the watershed soil water content (Fig. 7.6.1) Hence, the *ET* values given by the model are probably representative of the *ET* rate of the watershed.

7.7 Summary and Conclusions

The WEPP water balance is designed to simulate soil water evaporation, plant transpiration, and root zone soil water content. The model uses many algorithms given in EPIC model. The model was tested using measured data from the watershed 1D in the Konza natural prairie during the 1987 growing season. Comparison of model-simulated and measured *ET* and soil water content is presented. The comparison of model-simulated *ET* and EBBR-ET indicates that the model estimates are probably representative of watershed 1D. This is further supported by a good agreement between model-simulated and averaged field measured soil water content of the top .05 m of soil profile. In addition, it indicates that the model is able to simulate antecedent soil water content which is used in the infiltration model of the WEPP. The comparison of simulated and measured soil water content of surface to 2 m soil was less than desirable. Considering the size and topography of watershed 1D, soil moisture measurements at site 1 are not representing the entire watershed.

7.8 Acknowledgements

The Hydrology Laboratory, USDA-Agricultural Research Service, in cooperation with Kansas State University, provided necessary assistance for the validation study. Data collection was funded by NASA under the FIFE project.

7.9 References

- Anderson, K. L., and C. L. Fly. 1955. Vegetation-soil relationships in Flint hills bluestem pastures. *J. Range Management* 8(4):163-170.
- Bowen, I. S. 1926. The ratio of heat losses by conduction and by evaporation from any water surface. *Phys. Rev.* 27:779-787.
- Denmead, O. T., and I. C. McIlroy. 1970. Measurements of non-potential evapotranspiration from wheat. *Agric. Meteorol.* 7:285-302.
- Lane, L. J., and Stone, J. J. 1983. Water balance calculations, water use efficiency, and above ground net production. *Hydrology and Water Resources in Arizona and the Southwest. Proceedings of the 1983 meeting of the Arizona Section of AWRA* 13:27-24.
- Pruitt, W. O., and F. I. Lourence. 1968. Correlation of climatological data with water requirements of crops. Dept. of Water Sci. and Engr. Paper No. 9001, Univ. of California-Davis, 59 pp.
- Ritchie, J. T. 1972. A model for predicting evaporation from a row crop with incomplete cover. *Water Resources Research* 8(5):1204-1213.
- Slatyer, R. O., and I. C. McIlroy. 1961. Evaporation and the principle of its measurements. Slatyer, R. O., and I. C. McIlroy (eds.) In: *Practical Microclimatology*, Chapter 3, UNESCO-CSIRO Australia.
- Steiner, J. L. Personal communication, USDA-ARS Conservation and Production Research Laboratory, Bushland, Texas.
- Tanner, C. B. 1960. Energy balance approach to evapotranspiration from crops. *Soil Sci. Soc. Am. Proc.* 24:1-9.
- Williams, J. R., and Hann, R. W. 1978. Optimal operation of large agricultural watersheds with water quality constraints. *Texas Water Resources Inst., Texas A & M University, TR-96*, 152 pp.
- Williams, J. R., Dyke, P. T., and Jones, C. A. 1983. EPIC - A model for assessing the effects of erosion on soil productivity. *Proceedings Third International Conference on State-of-the-Art in Ecological Modeling, Colorado State University, May 24-28, 1982*, pp. 553-572.
- Williams, J. R., Nicks, A. D., and Arnold, J. G. 1985. Simulator for water resources in rural basins. *ASCE Hydraulics J.*, 111(6):970-987.

7.10 List of Symbols

Symbols	Definition	Unit	Variable
A	albedo	(0-1.0)	alb
A_s	soil albedo	(0-1.0)	salb
B_i	conductivity adjusted parameter for layer i	(0-1.0)	hk
C	sum of plant biomass and plant residue	kg/ha	c_v
C_f	soil cover index	(0-1.0)	eaj
C_l	percent clay content	fraction	clay
C_r	plant residue	kg/ha	resamt
D	cumulative amount of percolation loss	m	sep
d_i, d_{ci}	percolation rate through layer i	m	sep
d_s	soil evaporated depth	m	esd
$dt&de$	air temperature and vapor pressure differences at two heights above the canopy, respectively.	$^{\circ}K$ and Pa	-
d_x	maximum soil evaporated depth influenced by bare soil evaporation.	m	esb
d_2	days since stage two soil evaporation began	day	tv
E_s	actual soil evaporation	m	e_s
E_{sb}	bare soil evaporation	m	e_s
E_{sp}	potential soil evaporation	m	es
E_{su}	upper limit soil evaporation of stage one	m	tu
ET	cumulative amount of evapotranspiration	m	estep
E_{tp}	potential plant transpiration	m	ep
E_u	potential evapotranspiration	m	eo
FC	field capacity water content	-	fc
G	soil heat flux	W/m^2	-
h_i	depth of soil layer	m	solthk
i	soil layers		i
K_{sai}	adjusted hydraulic conductivity for layer i	m/s	SSC
K_{si}	saturated hydraulic conductivity for layer i	m/s	SSC
L	leaf area index	dimensionless	LAI
LE	latent heat flux	W/m^2	-
p	cumulative rainfall	m	rain
Q	cumulative amount of surface runoff	m	runoff
R	daily solar radiation	ly	rad
R_{mc}	residual moisture content	fraction	wrd
R_n	net daily solar radiation	ly	
R_z	root zone depth	m	rtd
S	snow water content	m	sno
S_a	percentage of sand	percent	sand
S_2	stage two soil evaporation	m	S2
t_i	travel time through layer i	s	xx
T_k	daily average air temperature	$^{\circ}K$	tk
T_r	soil evaporation parameter	$mm/day^{1/2}$	trans
u	actual plant water use	m	u
UL_i	upper limit soil water content for layer i	m	ul
U_{Pi}	potential water use rate for layer i	m	U
V	a use rate - depth parameter		ub

W_s	plant growth water stress factor	(0-1.0)	watstr
δ	slope of the saturated vapor pressure curve	-	d
γ	psychrometric constant	Pa/K	gma
Δt	percolation travel interval	s	84600
Θ	water content of the root zone	m	watcon
Θ_c	critical soil water content below which plants growth is subjected to water stress	(0 - 1.0)	pltol
Θ_i	soil water content in each layer	m	soilwa
Θ_{in}	initial water content	m	watcon

Chapter 8. PLANT GROWTH COMPONENT

E. E. Alberts, M. A. Weltz, and F. Ghidry

8.1 Introduction

This chapter describes the approaches used in the WEPP model to simulate plant growth and residue decomposition for cropland and rangeland conditions. The growth and decomposition of cropland and rangeland plants are simulated in separate submodels.

The plant growth models were not developed to predict grain or biomass yield. Grain or biomass yield is a user input variable, which generally sets an upper boundary for vegetative plant growth. The purpose of these models is to predict temporal changes in plant and residue variables such as canopy cover, canopy height, and residue or litter cover that influence the runoff and erosion process.

Plant and residue management options available to the user such as herbicide application, silage removal, tillage, shredding, burning, or removing residue, hay harvesting, and livestock grazing are discussed in this chapter. Separate management sections for cropland and rangeland have been developed because of differences in user input variables.

This chapter has been organized into five sections. Sections 8.2, 8.3, and 8.4 discuss plant growth, residue decomposition, and management options for cropland, respectively. Sections 8.5 and 8.6 discuss plant growth, including residue decomposition, and management options for rangeland.

8.2 Cropland Plant Growth Model

8.2.1 Crop Growth Variables

The model simulates the growth of all annual crops specified in the WEPP User Requirements including corn, soybeans, grain sorghum, cotton, winter wheat, spring wheat, and oats. In addition, the growth of peanuts, potatoes, tobacco, and annual ryegrass can be simulated. The model also simulates the growth of perennial crops, including alfalfa and brome grass. Growth functions are based on growing degree days (G_d) defined as:

$$G_d = \frac{T_{mx} + T_{mn}}{2} - T_b \quad [8.2.1]$$

where T_{mx} and T_{mn} are the daily maximum and minimum air temperatures ($^{\circ}$ C), and T_b is the base daily air temperature of a given plant ($^{\circ}$ C).

G_d initiates plant growth when the average daily air temperature exceeds the base temperature of the plant. Otherwise, G_d is set to 0 and no plant growth occurs.

Growing degree days are accumulated ($\sum G_d$) beginning at planting. Plants emerge when $\sum G_d$ reaches a critical value (CRIT) or 14 days after planting, whichever occurs first. Growth of winter wheat stops when the average daily air temperature is less than the base temperature.

Plant variables predicted include vegetative biomass (B_m), canopy cover (C_c), canopy height (H_c), total living root mass (B_{rt}), root mass within the 0- to 0.15-, 0.15- to 0.30-, and 0.30- to 0.60-m soil zones (B_{r1} , B_{r2} , B_{r3}), root depth (R_d), leaf area index (LAI), and plant basal area (A_b).

VEGETATIVE BIOMASS

The general plant growth equation taken from Ghebreyessus and Gregory (1987) is:

$$B_m = \left[\frac{\sum G_d}{G_{dm}} \right]^\omega B_{mx} \quad [8.2.2]$$

where B_m is the vegetative biomass ($kg\ m^{-2}$), $\sum G_d$ is the cumulative growing degree days from planting (C), G_{dm} is the growing degree days at physiological maturity (C), ω is a plant-dependent growth parameter, and B_{mx} is the vegetative biomass at maturity ($kg\ m^{-2}$). For annual crops, B_{mx} is calculated as a function of plant grain or biomass yield:

$$B_{mx} = Y_g Y_c \quad [8.2.3]$$

where Y_g is the plant grain or biomass yield ($kg\ m^{-2}$), and Y_c is residue mass produced per unit of grain or biomass yield.

If grain or biomass yield of an annual crop is unusually low because of poor soil or environmental conditions, and adjustment is made to increase the vegetative biomass that would be normally predicted.

The growth of a perennial crop in the Fall stops when a five-day average of minimum daily air temperatures (TMNAVG) is less than the critical growth temperature (T_{c1}). When this condition occurs, B_m is converted into standing dead residue mass. Growth is initiated in the spring when TMNAVG is greater than T_{c1} .

B_{mx} for a perennial crop is set equal to the biomass yield (YILD), which is a user input variable for all mangement options.

CANOPY COVER AND HEIGHT

Canopy cover and height for annual and perennial crops are calculated as functions of vegetative biomass:

$$C_c = 1 - e^{-\beta_c B_m} \quad [8.2.4]$$

where C_c is canopy cover (0-1). The variable β_c is defined as:

$$\beta_c = \frac{-\beta_1}{\ln \left[1 - \frac{R_w}{\beta_2} \right]} \quad [8.2.5]$$

where R_w is the row width (m), β_1 is a plant-dependent constant, and β_2 is the maximum canopy width at physiological maturity. For crops not grown in rows, R_w is set equal to the plant spacing (P_p).

$$H_c = \left[1 - e^{-\beta_h B_m} \right] H_{cm} \quad [8.2.6]$$

where H_c is the canopy height (m), H_{cm} is the maximum canopy height (m), and β_h is a plant-dependent constant.

SENESCENCE

When the fraction of growing season (F_{gs}) is equal to the fraction of the growing season when senescence begins (GSSEN), canopy cover (C_c) starts declining linearly for a given time period (S_p). The daily decline in canopy cover can be predicted with the equation:

$$\Delta C_c = C_{cm} \left[\frac{1 - C_{cs}}{S_p} \right] \quad [8.2.7]$$

where ΔC_c is the daily loss of canopy cover (0-1), C_{cm} is canopy cover at maturity (0-1), C_{cs} is the fraction of canopy cover remaining after senescence, and S_p is the number of days between the beginning and end of leaf drop.

Canopy cover is adjusted from:

$$C_{c(t)} = C_{c(t-1)} - \Delta C_c. \quad [8.2.8]$$

Because leaves are falling during the senescence period, live above ground biomass (B_m) decreases while flat residue mass (M_f) increases. B_m is updated daily during this time period from:

$$B_{m(t)} = \frac{\ln(1 - C_{c(t)})}{-\beta_c} \quad [8.2.9]$$

Flat residue mass is increased by the change in vegetative biomass:

$$M_{f(t)} = M_{f(t-1)} + (B_{m(t-1)} - B_{m(t)}) \quad [8.2.10]$$

where $M_{f(t-1)}$ is flat residue mass of the previous day, and $B_{m(t-1)}$ is vegetative biomass of the previous day. The effect of senescence on canopy cover is predicted for only the annual crops.

ROOT GROWTH

Ratios to describe partitioning between root biomass and above-ground vegetative biomass (root to shoot ratios) are used to grow plant roots for all annual and perennial crops. Total root mass on any day (B_{rt}) is predicted with the equation:

$$B_{rt} = B_m R_{rr} \quad [8.2.11]$$

where R_{rr} is the root to shoot ratio, a plant-dependent constant.

Total root mass is partitioned into the 0- to 0.15-, 0.15- to 0.30-, and 0.30- to 0.60-m soil zones (B_{r1} , B_{r2} , B_{r3}) as follows:

If root depth is < 0.15 m:

$$\begin{aligned} B_{r1(t)} &= B_{rt} \\ B_{r2(t)} &= 0.0 \\ B_{r3(t)} &= 0.0 \end{aligned}$$

If root depth is > 0.15 m and < 0.30 m:

$$\begin{aligned} B_{r1(t)} &= B_{r1(t-1)} + (0.60 * \Delta B_r) \\ B_{r2(t)} &= B_{r2(t-1)} + (0.40 * \Delta B_r) \\ B_{r3(t)} &= 0.0 \end{aligned}$$

where ΔB_r is the daily change in total root mass ($kg\ m^{-2}$).

If root depth is > 0.30 m and < 0.60 m:

$$\begin{aligned} B_{r1(t)} &= B_{r1(t-1)} + (0.45 * \Delta B_r) \\ B_{r2(t)} &= B_{r2(t-1)} + (0.30 * \Delta B_r) \\ B_{r3(t)} &= B_{r3(t-1)} + (0.25 * \Delta B_r) \end{aligned}$$

If root depth is > 0.60 m:

$$\begin{aligned} B_{r1(t)} &= B_{r1(t-1)} + (0.42 * \Delta B_r) \\ B_{r2(t)} &= B_{r2(t-1)} + (0.28 * \Delta B_r) \\ B_{r3(t)} &= B_{r3(t-1)} + (0.20 * \Delta B_r) . \end{aligned}$$

For a perennial crop, live root mass accumulates until a maximum amount of root biomass is reached (RTMMAX), which often occurs after three years of growth. After RTMMAX is reached, root growth and death are assumed equal.

The equation developed by Borg et al. (1986) is used to predict root depth:

$$R_d = R_{dx} \left[0.5 + 0.5 \sin \left[3.03 \left(\frac{D_p}{D_m} \right) - 1.47 \right] \right] \quad [8.2.12]$$

where R_{dx} is the maximum root depth (m), D_p is the number of days after planting, and D_m is the number of days to reach maturity. For a perennial crop, Eq. [8.2.12] is used to predict root depth until the first harvest. Thereafter, R_d is assumed equal to R_{dx} .

LEAF AREA INDEX

An equation described in EPIC (Williams et al., 1984) is used to predict leaf area index (LAI) for annual crops:

If $F_{gs} < F_{lai}$ then,

$$LAI = \frac{LAI_{mx} B_m}{B_m + 0.552e^{-6.8B_m}} \quad [8.2.13]$$

If $F_{gs} > F_{lai}$ then,

$$LAI = LAI_d \left[\frac{1 - F_{gs}}{1 - F_{lai}} \right]^2 \quad [8.2.14]$$

where LAI_{mx} is the maximum leaf area index potential, LAI_d is the leaf area index value when LAI starts declining, F_{gs} is the fraction of the growing season (0-1), and F_{lai} is the fraction of growing season when leaf area index starts declining.

The equation to predict leaf area index for a perennial crop is:

$$LAI = \frac{LAI_{max} B_m}{B_m + 0.276 e^{-13.6 B_m}} \quad [8.2.15]$$

PLANT BASAL AREA

Plant basal area is calculated as a function of plant population (P_m) and single stem area (A_{sp}):

$$A_{bm} = P_m A_{sp} \quad [8.2.16]$$

where A_{bm} is the plant basal area at maturity (m^2) per square meter of soil area, P_m is the plant population per square meter of soil area, and A_{sp} is the area of a single stem at maturity (m^2).

Plant population is predicted from:

$$P_m = \frac{1}{A_p} \quad [8.2.17]$$

where A_p is the area associated with one plant (m^2).

A_p is a function of plant spacing and row width:

$$A_p = P_s R_w \quad [8.2.18]$$

where P_s is the in-row plant spacing (m), and R_w is the row width (m). If R_w is zero because seed is broadcast, R_w is set equal to P_s .

The area of a single stem is:

$$A_{sp} = \pi \left(\frac{D}{2} \right)^2 \quad [8.2.19]$$

where D is the average stem diameter at maturity (m).

Plant stem diameter is assumed to increase linearly from emergence until maturity. Based on this assumption, plant basal area (A_b) is calculated from:

$$A_b = A_{bm} \frac{B_m}{B_{max}} \quad [8.2.20]$$

8.2.2 Crop Parameter Values and User Inputs

Table 8.2.1 presents constant parameter values for corn, soybeans, grain sorghum, cotton, winter wheat, spring wheat, oats, alfalfa, and brome grass required by the plant growth and decomposition models. Values for corn, soybeans, and wheat parameters were obtained from the literature or estimated using measured field data. More research data are needed to estimate some of the parameter values for

Table 8.2.1. Parameter values used in the cropland growth and decomposition submodels.†

Symbol	Variable	Corn	Soybeans	Sorghum	Cotton	Winter Wheat	Spring Wheat	Oats	Alfalfa	Brome-Grass	Peanut	Tobacco	Ryegrass
α_f	ACA	2.24	2.42	2.20	2.20	1.50	1.50	1.50	4.00	4.00	2.24	3.00	4.00
α_r	AR	2.87	2.96	2.85	2.85	2.50	2.50	2.50	4.25	4.25	2.87	3.25	4.25
α_b	AS	3.50	3.50	3.50	3.50	3.50	3.50	3.50	4.50	4.50	3.50	3.50	4.50
α_s	AST	0.22	0.24	0.22	0.22	0.15	0.15	0.15	0.40	0.40	0.22	0.30	0.40
β_h	bbb	3.00	3.00	3.00	3.50	3.00	3.00	3.00	23.00	23.00	6.92	7.00	23.00
β_1	b1	3.60	14.00	3.60	5.89	5.20	5.20	5.20	14.00	14.00	12.00	6.60	20.00
β_2	b2 (m)	1.31	0.96	1.31	1.31	0.26	0.26	0.26	0.26	0.26	1.31	1.50	0.20
T_b	BTEMP (C)	10.00	10.00	10.00	10.00	4.00	7.00	7.00	7.00	7.00	10.00	10.00	2.00
cf	CF	4.00	7.20	3.00	3.00	6.50	6.50	6.50	5.00	5.00	2.70	3.00	5.00
C_n	CN	62.00	31.00	60.00	40.00	107.00	107.00	107.00	30.00	80.00	30.00	80.00	80.00
-	CRIT (C)	60.00	60.00	60.00	90.00	60.00	60.00	60.00	30.00	30.00	60.00	60.00	30.00
-	CRITVM ($kg\ m^{-2}$)	-	-	-	-	-	-	-	0.10	0.10	-	-	-
C_{cs}	DECFACT	0.65	0.10	0.90	0.25	1.00	1.00	1.00	0.70	0.70	1.00	0.75	1.00
D	DIAM (m)	0.0508	0.0095	0.0317	0.0127	0.0064	0.0064	0.0079	0.0045	0.0022	0.0090	0.0510	0.0064
D_g	DIGEST	-	-	-	-	-	-	-	0.60	0.50	-	-	-
F_{lai}	DLAI	0.70	0.60	0.70	0.80	0.90	0.90	0.90	0.70	0.70	1.00	0.70	0.70
F_{ct}	FACT	0.99	0.99	0.99	0.99	0.99	0.99	0.99	0.99	0.99	0.99	0.99	0.99
G_{dm}	GDDMAX (C)	750.00	750.00	750.00	1750.00	750.00	750.00	750.00	600.00	600.00	1100.00	1000.00	680.00
ω	GRATE	2.60	2.60	2.60	1.60	2.60	2.60	2.60	2.60	1.50	2.60	2.60	1.75
-	GSSEN	0.75	0.70	0.85	0.85	1.00	1.00	1.00	0.85	0.85	1.00	0.75	1.00
H_{cm}	HMAX (m)	2.60	1.01	1.01	1.06	0.91	0.91	1.14	0.80	0.51	0.66	1.06	0.15
F_{pc}	PARTCF	0.40	0.00	0.75	0.85	0.65	0.65	0.50	-	-	0.00	0.00	0.00
P_s	PLTSP (m)	0.219	0.025	0.130	0.101	0.005	0.005	0.005	0.006	0.006	0.076	0.220	0.038
R_{ds}	RDMAX (m)	1.52	1.00	1.50	1.20	0.30	0.30	0.30	2.43	0.30	1.20	0.76	0.30
R_{sr}	RSR	0.25	0.25	0.25	0.25	0.25	0.25	0.25	0.33	0.33	0.33	0.33	0.50
-	RTMMAX ($kg\ m^{-2}$)	-	-	-	-	-	-	-	0.60	0.34	-	-	-
S_p	SPRIOD	30.0	14.0	40.0	30.0	14.0	14.0	14.0	14.0	14.0	14.0	14.0	14.0
T_{cu}	TMPMAX(C)	-	-	-	-	-	-	-	-	32.0	-	-	-
T_{ct}	TMPMIN(C)	-	-	-	-	-	-	-	4.0	1.1	-	-	-
Y_c	Y6	1.00	1.50	1.00	7.00	1.70	1.30	2.00	-	-	1.30	1.80	1.00
LAI_{mx}	XMXLAI	5.00	9.00	5.00	6.00	8.00	8.00	8.00	6.00	9.00	4.50	3.40	3.00

† Parameter values for potatoes are not determined. A "-" indicates not applicable.

the other crops. The flowchart in Fig. 8.2.1 presents the cropland plant management options available to the user. For cropland plant growth simulation, the user is generally required to provide the following information:

1. number of overland flow elements - (nelem)
2. number of different crops in the simulation - (ncrop)
3. cropping system (annual, perennial, or fallow) - (imngmt)
4. crop types in the simulation - (itype)
5. number of tillage sequences in the simulation - (nseq)
6. number of tillage operations within each sequence - (ntil)
7. implement code (itill), julian day of tillage (mdate), tillage depth (tildep), and tillage type (typtil)
8. initial conditions at the start of simulation, including canopy cover (C_c), interrill residue cover (C_r), rill residue cover (C_{r1}), and prior crop type (IRESD)
9. crop information including planting date (JDPLT), row width (R_w), harvesting date (JDHARV), and grain or biomass yield (Y_g)
10. weed cover information, including the date that weed canopy cover becomes important (JDWDST), the date that weed canopy cover becomes unimportant (JDWEND), and the average weed canopy cover during the period (C_w)
11. plant and residue management information for annual crops (RESMNG), including the date of herbicide application (JDHERB), the date that silage or other living biomass is removed (JDSLGE), the date of residue shredding or cutting (JDCUT), the date of residue burning (JDBURN), and the date of residue removal from a field (JDMOVE)
12. plant management information for perennial crops that are cut, including the number of cuttings (NCUT), cutting dates (CUTDAY), and biomass yields (YILD)
13. plant management information for perennial crops that are grazed, including the date that grazing begins (GDAY), the date that grazing ends (GEND), the number of animal units (N_a), average body weight (B_w), field size (A_f), digestibility of the forage (D_f), and the forage biomass produced during the grazing period (YILD).

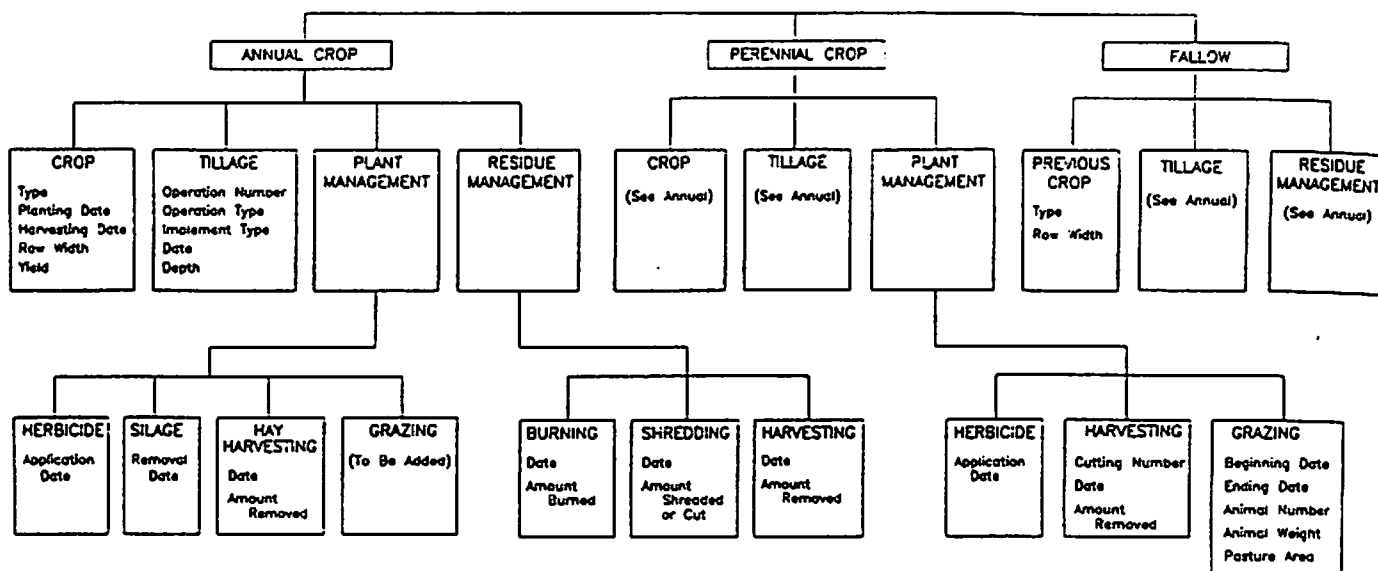


Figure 8.2.1. Flowchart of cropland options available to the user.

8.2.3 Model Summary

Procedures followed in the plant growth model are:

1. Initialize the following variables

- base daily air temperature of a plant, T_b
- growing degree days to emergence, CRIT
- parameter for plant growth equation, ω
- growing degree days at maturity, G_{dm}
- parameter for canopy cover equation, β_1
- parameter for canopy height equation, β_h
- maximum canopy height, H_{cm}
- maximum canopy width, β_2
- maximum root depth, R_{dx}
- root to shoot ratio, R_{sr}
- maximum root mass for a perennial crop, RTMMAX

- fraction of the growing season to senescence, G_{SSEN}
 - fraction of canopy cover remaining after senescence, C_{cs}
 - days from the beginning until the end of leaf drop, S_p
 - fraction of growing season when leaf area index starts declining, F_{lai}
 - maximum leaf area index potential, LAI_{mx}
 - stem diameter of a plant at maturity, D
 - in-row plant spacing, P_r
 - minimum air temperature that causes plant dormancy, T_{c1}
 - maximum air temperature that causes plant dormancy, T_{cu}
 - minimum vegetative biomass for heavy grazing, CRITVM
 - parameters to convert user input grain or biomass yield into vegetative biomass, Y1-Y6
2. Compute vegetative biomass at maturity from average grain or biomass yield, with an adjustment for low yield if necessary. For perennial crops, maximum vegetative biomass (B_{mx}) at each harvest date is input by the user.
 3. User initializes canopy cover (C_c) at the start of the simulation. If canopy cover exists, the model calculates initial vegetative biomass (B_m), canopy height (H_c), and leaf area index (LAI) values.
 4. Calculate growing degree days (G_d), and cumulative growing degree days ($\sum G_d$).
 5. Initiate plant growth when conditions for emergence are met.
 6. Compute B_m , C_c , H_c , B_{rt} , B_{r1} , B_{r2} , B_{r3} , R_d , LAI , and A_b .
 7. Continue plant growth simulation until cumulative growing degree days ($\sum G_d$) are equal to the growing degree days at maturity (G_{dm}).
 8. When G_{dm} is reached, plant growth stops with no changes until leaf drop.
 9. Starting at senescence, canopy cover decreases due to leaf drop. The variable S_p defines the number of days from the beginning until the end of leaf drop.
 10. Growth of annual and perennial crops are stopped when the average daily air temperature (T_a) is less than the base temperature of the plant (T_b).
 11. Perennial crops become dormant when a five-day average minimum temperature is less than the critical minimum temperature (T_{c1}).
 12. Perennial crops become dormant when a five-day average maximum temperature is greater than the critical maximum temperature (T_{cu}).

The model does not calculate temperature, nutrient, and aeration stress factors commonly found in more complicated plant growth models. These factors are accounted for in the grain or biomass yields specified by the user.

8.3 Cropland Residue and Root Decomposition Model

The model simulates the decomposition of standing and flat residue, buried residue, and roots within the 0- to 0.15-m soil layer for the annual and perennial crops specified in Section 8.2.1.

Total residue mass (M_r) is partitioned into standing (M_s) and flat (M_f) components at harvest before residue management occurs:

$$M_{s(t)} = M_{s(t-1)} + (M_r F_{pc}) \quad [8.3.1]$$

$$M_{f(t)} = M_{f(t-1)} + (M_r - M_{s(t)}) \quad [8.3.2]$$

where F_{pc} is the fraction of residue mass partitioned into standing residue.

The model also sets the initial stubble population at harvest equal to the plant population (P_m) calculated in the plant growth model.

8.3.1 Decomposition

The general decomposition equation taken from Ghidey et al., 1985 is:

$$\frac{M(t)}{M(t-1)} = (1 - \alpha\tau)^2 \quad [8.3.3]$$

where $M(t)$ is the present standing residue (M_s), flat residue (M_f), buried residue (M_b), or root (M_r) mass ($kg\ m^{-2}$), $M(t-1)$ is the prior day standing residue (M_s), flat residue (M_f), buried residue (M_b), or root (M_r) mass ($kg\ m^{-2}$), α is the constant used to calculate standing residue (α_s), flat residue (α_f), buried residue (α_b), or root (α_r) mass changes, and τ is the weighted-time variable calculated from air temperature, daily rainfall, and the initial C to N ratio of residue and root mass at senescence.

The variable, τ , is calculated from:

$$\tau = \frac{T_a a_m}{C_n} \quad [8.3.4]$$

where T_a is the average daily temperature (C), a_m is the antecedent moisture index (m), and C_n is the carbon to nitrogen ratio of residue and roots at senescence.

The moisture index, a_m , is calculated from (Ligeon and Johnson, 1960):

$$a_m = \sum_{i=1}^5 \frac{R(i)}{i} \quad [8.3.5]$$

where R is the depth of rainfall on a given day (m), and i is the day number with the present day being 1, previous day being 2, etc.

a_m values greater than 0.01 are set to 0.01 to reduce the rate of standing and flat residue decomposition during high rainfall periods. Another τ variable (τ_2) is calculated without the 0.01-m boundary and used to decompose buried residue and roots.

8.3.2 Stubble Population

The equation to compute stubble population is:

$$P_{(t)} = \frac{M_{s(t)}}{M_{so}} P_m F_{ct} \quad [8.3.6]$$

where $P_{(t)}$ is the stubble population at time t , $M_{s(t)}$ is the standing residue mass at time t , M_{so} is the standing residue mass at harvest, P_m is the stubble population at harvest and F_{ct} is the adjustment factor to account for the effects of wind and snow on stubble population. The default value for F_{ct} is 0.99, but it can be adjusted by the user to account for local climatic conditions.

8.3.3 Standing to Flat Residue Conversion

The equation to calculate standing residue mass from the stubble population is:

$$M_{s(t)} = \frac{P_{(t)}}{P_m} M_{so} \quad [8.3.7]$$

The equation to increase flat residue mass from the standing to flat residue conversion is:

$$M_{f(t)} = M_{f(t-1)} + (M_{s(t-1)} - M_{s(t)}) \quad [8.3.8]$$

where $M_{f(t)}$ is the flat residue mass at time t .

8.3.4 Residue Cover

Gregory's (1982) equation is used to predict residue cover from flat residue mass:

$$C_{rf} = 1 - e^{-cf M_f} \quad [8.3.9]$$

where C_{rf} is the flat residue cover (0-1), M_f is the flat residue mass ($kg\ m^{-2}$), and cf is a constant to calculate flat residue cover.

Soil cover from standing residue mass is predicted from:

$$C_{rs} = \frac{P_{(t)}}{P_m} A_{bm} \quad [8.3.10]$$

where C_{rs} is the standing residue cover (0-1), $P_{(t)}$ is the stubble population per unit area at time t , P_m is the stubble population per unit area at harvest, and A_{bm} is the plant basal area at maturity (m^2) per square meter of soil area.

Total soil cover from residue is:

$$C_{rt} = C_{rf} + C_{rs} \quad [8.3.11]$$

where C_{rt} is the total residue cover (0-1).

8.3.5 Interrill and Rill Residue Cover

The erosion model requires that interrill and rill residue cover terms be predicted (C_{ri} and C_{ri}). Interrill residue cover is the average residue cover on the soil surface and is equal to the total residue cover (C_{rt}). Rill residue cover is set equal to interrill residue cover for tillage systems that do not have well defined ridges and furrows. The model recognizes a ridge-furrow tillage system when any implement in a tillage sequence meets specific ridge height and ridge interval criteria. These criteria are that initial ridge height be equal to or greater than 0.10 m and ridge interval be equal to the row width (see Chapter 6 for more information).

Residue can be repositioned in a ridge-furrow system, either by wind blowing residue from the ridge into the furrow, by a planter with sweeps moving residue from the ridge into the furrow, or by a cultivator moving residue back to the ridge. For wind repositioning, the user must input the residue cover on the ridges at the end of the repositioning period (C_{sp}). Residue cover on the ridges is calculated from:

$$C_{rr(t)} = C_{rro} - \left[\frac{C_{rro} - C_{sp}}{60} \right] D_h \quad [8.3.12]$$

where $C_{rr(t)}$ is the residue cover on the ridges at time t , C_{rro} is the interrill residue cover immediately after harvest, C_{sp} is the residue cover on the ridges at the end of the repositioning period, and D_h is the days after harvest. All adjustments for wind moving residue from the ridge into the furrow are made within 60 days of harvest.

The daily mass of residue moved from the ridges into furrows (ΔM_w) is computed from:

$$\Delta M_w = \frac{\ln(1 - (C_{rr(t-1)} - C_{rr(t)}))}{-cf} \quad [8.3.13]$$

Total residue mass in the furrows is:

$$M_{rl(t)} = M_{rl(t-1)} + \Delta M_w \quad [8.3.14]$$

Rill cover, which is equal to the furrow cover, is then calculated from the adjusted residue mass:

$$C_{rl} = 1 - e^{-cf M_{rl}} \quad [8.3.15]$$

Residue mass on the ridges (M_{rr}) is:

$$M_{rr(t)} = M_{rr(t-1)} - \Delta M_w \quad [8.3.16]$$

Decomposition of residue on the ridges and in the furrows is accounted for separately. The partitioning coefficient (F_{pc}) is set to zero for a ridge-furrow system.

The average residue cover on the soil surface (C_n) is predicted from:

$$C_n = 0.5 C_{rr} + 0.5 C_{rl} \quad [8.3.17]$$

where ridge and furrow areas are assumed equal.

Residue repositioning at planting occurs if the user selects a planter with sweeps from the planter implement list. It is assumed that all remaining residue mass on the ridges is swept into the furrow at planting. C_{rl} is then computed from the adjusted residue mass. C_{rr} is set to zero. C_n is computed from Eq. [8.3.17].

It is assumed in a ridge-furrow system that all flat residue mass is repositioned evenly over the soil surface at cultivation ($M_{rr} = M_{rl}$). Additional cultivations do not reposition residue. Interrill and rill residue covers are recomputed and are equal until grain or biomass harvest, when the effect of wind on residue cover is again predicted.

8.3.6 Ground Cover

Total ground cover from residue and rocks is calculated from:

$$C_g = C_{cf} + C_{ri}(1 - C_{cf}) \quad [8.3.18]$$

where C_g is the total ground cover and C_{cf} is the weight fraction of coarse fragments in the soil, which is assumed equal to coarse fragment cover (0-1).

8.3.7 Cropland Residue Decomposition Model Summary

Procedures followed in the decomposition model include:

1. Initialize the following variables:

- decomposition parameter for standing residue, α_s
- decomposition parameter for flat residue, α_f
- decomposition parameter for buried residue, α_b
- decomposition parameter for roots, α_r
- parameter for flat residue cover equation, cf
- carbon to nitrogen ratio of residue and roots, C_n
- standing to flat residue adjustment factor for wind and snow, F_{ct}
- parameter to calculate standing residue mass at harvest, F_{pc}
- residue cover on ridges after wind repositioning, C_{rp} .

2. User initializes interrill and rill residue cover. The model calculates initial standing residue mass (M_s), flat residue mass (M_f), buried residue mass (M_b), root mass in the 0- to 0.15-m zone (M_r), and plant population (P).

3. Calculates (from Eq. [8.3.3] and [8.3.4]):

- weighted-time variables, τ and τ_2
- standing residue mass change, ΔM_s
- flat residue mass change, ΔM_f
- buried residue mass change, ΔM_b
- root mass change, ΔM_r .

4. Calculates residue and root mass (from Eq. [8.3.3]):

- standing residue mass (M_s)
- flat residue mass (M_f)

- buried residue mass (M_b)
 - non-living root mass (M_r).
5. Converts standing residue mass to flat residue mass. Increments flat residue mass (Eq. [8.3.7] and [8.3.8]).
 6. Computes standing, flat, total, rill, and interrill residue cover (from Eq. [8.3.10], [8.3.9], [8.3.11], [8.3.15], and [8.3.17]).
 7. Check date to see if it is a day of tillage (MDATE). If it is, use equations given in section 8.4.2 to compute standing and flat residue mass remaining after tillage. Increment buried residue mass by the mass of flat residue incorporated into the soil by tillage.
 8. Partition surface residue mass (M_s) at harvest into standing (M_s) and flat (M_f) components using F_{pc} , which depends upon harvesting equipment and techniques.

8.4 Cropland Management Options

8.4.1 Plant Management

The cropland plant growth and decomposition models can accommodate fallow, mono, double, rotation, strip, and mixed cropping practices. A mixed cropping practice is one where two or more individual cropping practices (e.g. mono and double) are used in the simulation. The models are applicable to the annual and perennial crops specified in WEPP User Requirements including corn, soybeans, grain sorghum, cotton, winter wheat, spring wheat, oats, alfalfa, and brome grass. Default parameter values required to simulate the growth and decomposition of peanuts, potatoes, tobacco, and annual ryegrass are also provided.

Herbicide Application

There are two situations where foliar contact herbicides are used to convert live vegetative biomass into standing dead residue. The first is in the defoliation of cotton. The second is killing a winter annual cover crop or perennial crop either prior to or at row-crop planting. The user must input the date of herbicide application (JDHERB). All vegetative biomass is converted into standing dead residue on JDHERB. For cotton, the fraction of the growing (F_{gs}) to JDHERB is computed and GSSSEN is set equal to this value, which initiates leaf drop. The model does not consider the effect of herbicides on broad leaf weeds or grasses.

Silage

The user must input the date that silage is removed from the field (JDSLGE), which converts live vegetative biomass into dead. The model assumes that all above ground residue is removed from the field. Standing residue cover (C_{rs}) is calculated from Eq. [8.3.10] using plant population (P_m) and basal area (A_{bm}) values. No adjustments are made to flat residue mass and cover.

8.4.2 Small Grain Harvest for Hay

If small grain is cut for hay in the dough stage, the user must input the cutting date (JDCUT), the fraction of biomass cut (F_c), the removal date (JDMOVE), and the fraction of flat biomass removed from the field at harvest (F_{rm}). Residue mass above ground after cutting is calculated from:

$$M_s(t) = M_s(t-1) + B_m(1 - F_c) \quad [8.4.1]$$

where M_s is residue mass above ground after cutting, B_m is vegetative biomass before cutting, and F_c is the fraction of biomass cut.

Flat residue mass is incremented by the change in standing residue mass on JDCUT:

$$M_{f(t)} = M_{f(t-1)} + (B_m F_c). \quad [8.4.2]$$

Flat residue mass remaining after hay removal from the field is calculated from:

$$M_{f(t)} = M_{f(t-1)}(1 - F_{rm}) \quad [8.4.3]$$

Flat and total residue cover values are updated based on changes in flat residue mass from the management operations.

8.4.3 Tillage

Effects of tillage on residue and soil properties are calculated in the model (see Chapter 6). Tillage intensity (T_i) is used as the classification variable to adjust standing and flat residue mass and cover, bulk density, random roughness, ridge height and ridge interval. T_i values are stored by implement and crop and range from 0 to 1. A residue mixing factor (R_{mf}) is calculated from:

$$R_{mf} = 1 - T_i \quad [8.4.4]$$

where R_{mf} is the ratio of flat residue cover after tillage to that before tillage. The residue mixing factor is adjusted for tillage depth by the equation:

$$R_{mf} = R_{mf} + \left(\frac{T_{dm} - T_d}{T_{dm}} \right) (1 - R_{mf}) \quad [8.4.5]$$

where T_d is the tillage depth input by the user, and T_{dm} is the mean tillage depth for that implement. Only R_{mf} 's for certain primary and secondary tillage implements are adjusted for depth.

Two adjustments are made on residue mass and cover when tillage is performed. First, standing residue is converted to flat residue using an equation from EPIC (Williams et al., 1984). Standing residue mass remaining after tillage is calculated from:

$$M_{s(t)} = M_{s(t-1)} e^{-8.535 T_i^2} \quad [8.4.6]$$

where $M_{s(t)}$ is the standing residue mass after tillage ($kg m^{-2}$), and $M_{s(t-1)}$ is the standing residue mass before tillage ($kg m^{-2}$).

Flat residue mass is incremented by the change in standing residue:

$$M_{f(t)} = M_{f(t-1)} + (M_{s(t-1)} - M_{s(t)}) \quad [8.4.7]$$

where $M_{f(t)}$ is the adjusted flat residue mass ($kg m^{-2}$), and $M_{f(t-1)}$ is the flat residue mass before tillage ($kg m^{-2}$).

Based on the adjusted residue masses, standing and flat residue covers are computed using the equations given in Section 8.3.4.

The second adjustment is the conversion of flat residue to buried residue. Flat residue cover remaining after tillage is predicted from the equation:

$$C_{rf(t)} = R_{mf} C_{rf(t-1)} \quad [8.4.8]$$

where $C_{f(t-1)}$ and $C_{f(t)}$ are flat residue covers before and after tillage, respectively.

Flat residue mass remaining after tillage is then calculated from:

$$M_{f(t)} = \frac{\ln(1 - C_{f(t)})}{-cf} \quad [8.4.9]$$

where cf is the constant used to calculate flat residue cover.

Following each tillage operation, buried residue mass (M_b) in the 0- to 0.15-m zone is increased by the mass of flat residue incorporated into the soil. Flat residue mass before tillage includes the mass of residue converted from standing to flat by the tillage operation.

8.4.4 Residue Management Options

When applicable, the user must specify a residue management option. Current options include shredding or cutting, burning, and harvesting. The date of shredding or cutting (JDCUT), burning (JDBURN), or harvesting (JDMOVE) is input by the user.

8.4.4.1 Shredding or Cutting

Standing residue (M_s) is converted into flat residue (M_f) depending upon the fraction of standing residue cut (F_c), which is a user input variable:

$$M_{f(t)} = M_{f(t-1)} + (M_{s(t)} F_c). \quad [8.4.10]$$

Flat residue cover is calculated from the adjusted flat residue mass using Eq. [8.3.9].

8.4.4.2 Burning

The effectiveness of burning on standing and flat residue mass depends upon environmental and plant conditions at the time of the burn. Therefore, the user must input the fractions of standing and flat residue that are lost by burning. Standing and flat residue masses after burning are calculated from:

$$M_{s(t)} = M_{s(t-1)} (1 - F_{bs}) \quad [8.4.11]$$

$$M_{f(t)} = M_{f(t-1)} (1 - F_{bf}) \quad [8.4.12]$$

where F_{bs} and F_{bf} are the fractions of standing and flat residue lost by burning, respectively.

8.4.4.3 Harvesting

Small grain residue is often harvested for livestock bedding. If standing residue is cut, the user must input the cutting date (JDCUT), the fraction of residue cut (F_c), the removal date (JDMOVE), and the fraction of flat residue removed (F_{rm}). Standing and flat residue masses after cutting are predicted from:

$$M_{s(t)} = M_{s(t-1)} (1 - F_c) \quad [8.4.13]$$

$$M_{f(t)} = M_{f(t-1)} + (M_{s(t-1)} - M_{s(t)}). \quad [8.4.14]$$

Flat residue mass remaining after removal from the field is calculated from:

$$M_{f(t)} = M_{f(t-1)} (1 - F_{rm}). \quad [8.4.15]$$

If standing residue is not cut and only the residue that passed through the combine is harvested, the user must input the removal date (JDMOVE) and the fraction of flat residue removed (F_{rm}). The flat residue mass remaining after removal of the residue is calculated from Eq. [8.4.15].

8.4.5 Management Options For Perennial Crops

8.4.5.1 Hay Harvesting

The user inputs the number of cuttings (NCUT) for each year, cutting dates (CUTDAY), and yield (YILD) for each cutting. At each cutting date a certain fraction (F_{rm}) of live above-ground biomass (B_m) is harvested. The remaining live biomass is calculated from:

$$B_m = B_m(1 - F_{rm}). \quad [8.4.16]$$

Equation [8.2.2] is rearranged to compute an adjusted cumulative growing degree days term ($\sum G_d$), which is based upon the vegetative biomass left after harvest:

$$\sum G_d = G_{dm} \left(\frac{B_m}{B_{mx}} \right)^{\frac{1}{\alpha}} \quad [8.4.17]$$

The adjusted $\sum G_d$ is used as the initial value at the start of the next growth period. Similar adjustments based upon B_m left after harvest are made to C_c , H_c , and LAI .

Root biomass (B_r) and root depth (R_d) continue to increase, even if the above-ground biomass is harvested, until they are equal to the maximum root biomass (RTMMAX) and maximum root depth (R_{dx}), respectively. Once maximum root mass is reached, the increment in live root biomass is assumed equal to the amount of root mass that dies daily.

After the last cutting, growth continues until a five-day average minimum temperature (TMNAV) is equal to a critical freezing temperature (T_{cf}). Then, all standing live biomass (B_m) is transferred to standing dead mass (M_d). Plant growth variables such as B_m , C_c , H_c , and LAI are set to zero. Regrowth is initiated when TMNAV is greater than T_{cf} .

8.4.5.2 Livestock Grazing

The approach taken for cropland grazing is similar to that for rangeland grazing. The user must input the date that grazing begins (GDAY) and ends (GEND). The number of animals (N_a), their average body weight (B_w), and the size of the pasture being grazed (A_f) are also user input variables. The daily total vegetative uptake (F_i) is predicted from:

$$F_i = 0.1 \left[\frac{B_w^{0.75}}{D_g} \right] \left[\frac{N_a}{A_f} \right] \quad [8.4.18]$$

where D_g refers to the digestibility of the vegetation and is a plant-dependent constant for perennial crops. Vegetative biomass can not decrease below a critical value (CRITVM) under heavy grazing, which is also a user input variable.

8.5 Rangeland Plant Growth Model

Initiation and growth of above and below ground biomass for range plant communities is estimated by using a potential growth curve. The potential growth curve can be defined with either a unimodal or a bimodal distribution (Fig. 8.5.1 and 8.5.2). The potential growth curve (Eq. [8.5.1]) is described by a modification of the generalized Poisson density function (Parton and Innis 1972, and Wight 1987). The potential growth curve should be defined to represent the aggregate total production for the plant community. The flexibility of the potential growth curve allows for description of either a warm or cool season plant community or for a combination of the two communities.

For a unimodal potential growth curve:

$$g_i = G_1 \left[\alpha e^{\frac{c}{d}(1-\beta)} \right] \quad [8.5.1]$$

where

$$\alpha = \left[\frac{t_i - G_b}{P_d - G_b} \right]^c \quad [8.5.2]$$

$$\beta = \left[\frac{t_i - G_b}{P_d - G_b} \right]^d \quad [8.5.3]$$

g_i is the increment of growth expressed as a fraction of 1.0, G_1 is the fraction of maximum live biomass at

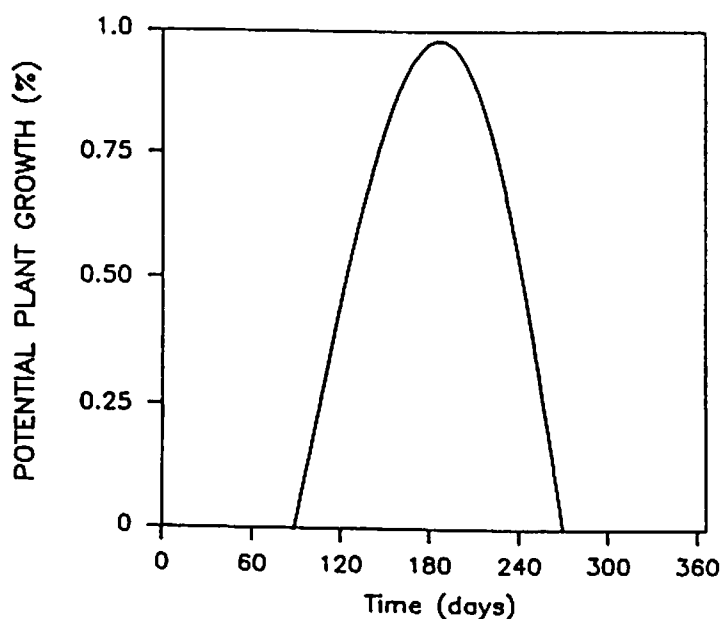


Figure 8.5.1. Unimodal potential plant growth.

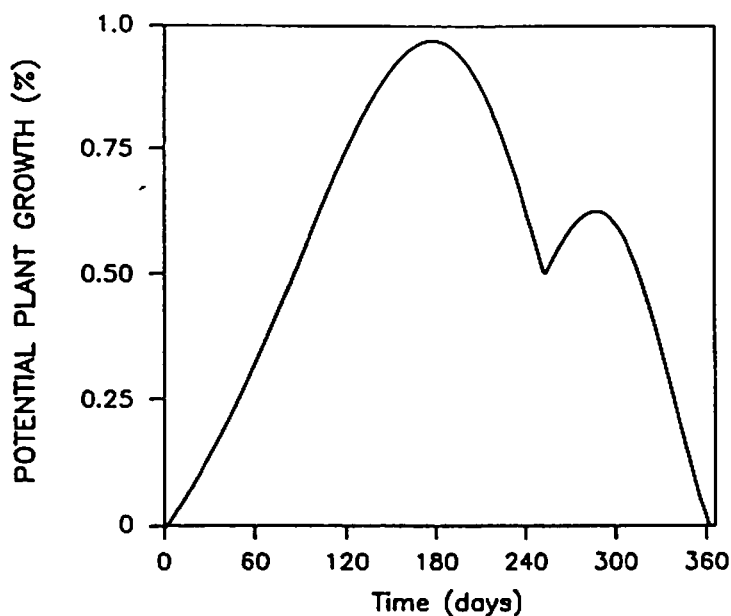


Figure 8.5.2. Bimodal potential plant growth.

the first peak, P_d is the Julian day peak live biomass occurs, G_b is the Julian day the growth curve begins, c is the shape parameter for the ascending side of the curve, d is the shape parameter for the descending side of the curve, and t_i is the current Julian day.

An optimization routine was developed to predict the shaping parameters c and d based on G_b , f_p , and P_d . Where f_p is the frost free period in Julian days.

$$c = 8.515 - 22.279 a + 16.734 a^2 \quad [8.5.4]$$

$$d = 12.065 - 63.229 a + 87.34 a^2 \quad [8.5.5]$$

where

$$a = \frac{P_d - G_b}{\left[\frac{G_1 f_p}{G_1 + G_2} \right]}$$

The user may either enter the potential maximum live above ground biomass (P_{mx}) or the model can estimate this value as a function of growing season precipitation (P_g) for grasslands (Sims and Singh, 1978). The equations have not been validated for shrub and tree dominated landscapes and should be used with caution on these landscapes. To have the model estimate P_{mx} for grazed and ungrazed grasslands, P_{mx} must be initialized to 0.0.

For grazed areas:

$$P_{mx} = \frac{35.69 + 0.36P_g}{100} \quad [8.5.6]$$

For non-grazed areas:

$$P_{mx} = \frac{77.23 + 0.30P_g}{100} \quad [8.5.7]$$

The initiation of growth and senescence for the plant community for the growth curve are predicted based on air temperature. The physiological information necessary to define the growth curve is the minimum temperature necessary for initiation of growth in the spring (GTEMP) and a critical sustained minimum temperature which will induce dormancy (TEMPMN). Where the average daily temperature (T_a) is calculated as $T_a = \frac{T_{mx} + T_{mn}}{2}$. T_{mx} and T_{mn} are defined as the maximum and minimum daily temperature (C), respectively.

Plant growth is initiated when g_i is greater than 0.001. Once g_i has reached 1.0 plant growth stops for that growth period. Change from standing live biomass (L_i) to standing dead biomass (R_a) is a function of the decay rate of the growth curve, a minimum temperature which induces dormancy, and drought stress. Once a 5 day average minimum temperature is equal to a minimum temperature (TEMPMN) all standing live biomass is transferred to standing dead.

The drought stress (D_s) transfers old standing live to standing dead biomass as a function of actual evapotranspiration, potential evapotranspiration, and a plant specific available soil water variable (PLTOL) (see chapter 7.2). D_s has been defined such that the maximum single day reduction in old standing live biomass is 3%. The daily water stress (W_a) is calculated as a running four day average of the calculated water stress (WST; see chapter 7.2).

$$D_s = 1 - e^{-3.5W_a} \quad [8.5.8]$$

Increments of new growth are calculated as:

$$L_i = g_i P_{mx} \quad [8.5.9]$$

where L_i is the new plant growth on day of simulation, g_i is the positive increment between today's and yesterday's g_i , and P_{mx} is the potential maximum live biomass ($kg\ m^{-2}$).

Water stress is calculated as the ratio of actual transpiration to potential transpiration. If available soil water is limiting then W_a is utilized to kill standing live biomass and transfer the recently killed biomass to standing dead biomass. W_a is only calculated when the actual soil water content is below a plant specific critical soil water content (PLTOL). If PLTOL is not known for a specific plant community then set PLTOL to 0.0 and the model will use a default value of 25% of the soil water content at field capacity. After 20 consecutive days of water stress development of new phytomass ceases. Initiation of growth is reactivated after 80 mm of precipitation.

For plant communities with an evergreen component the RGCMIN parameter can be initialized to maintain the live biomass at a given fraction of maximum live biomass for the entire year. When the calculated value of g_i is less than RGCMIN, g_i is set to RGCMIN. This modification allows for a daily leaf area index value for evergreen communities like sagebrush, and creosote bush which may actively transpire water throughout the entire year (Fig. 8.5.3).

For a bimodal potential growth curve two potential growth curves are calculated and then spliced together. To describe the second peak in potential live biomass, the user must define two additional parameters, G_2 and P_2 . G_2 is the fraction of maximum live biomass at the second peak. P_2 is the Julian day the second peak in live biomass occurs. The shaping coefficients d and e for the second growth curve

are calculated in a similar manner as c and d for the first growth curve. For the second growth curve the coefficient, a , is calculated as:

$$a = \frac{P_2 - \left(\frac{G_1 f_p}{G_1 G_2} + G_b \right)}{f_p - \frac{G_1 f_p}{G_1 + G_2}} \quad [8.5.10]$$

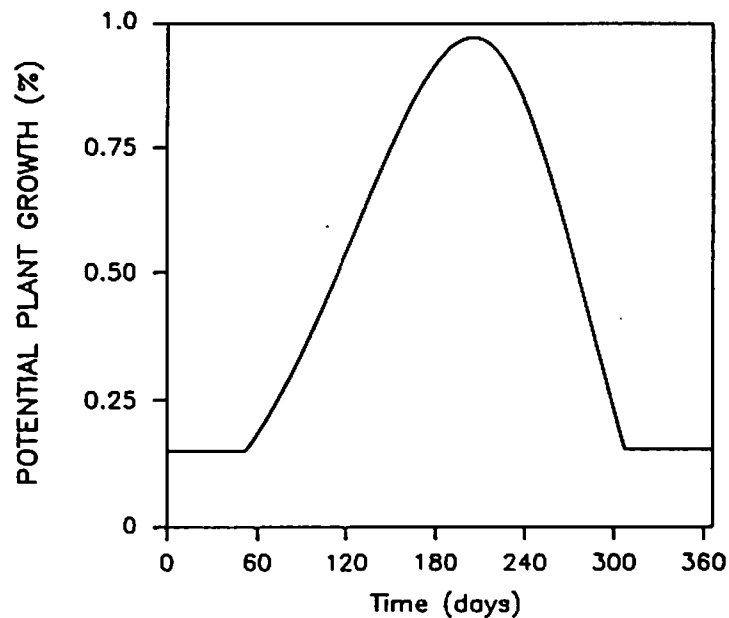


Figure 8.5.3. Bimodal potential plant growth with a minimum live component.

The user must initialize both above ground standing dead biomass and litter and organic residue on the soil surface. The transfer of standing live biomass (L_s) to R_a is calculated as a function of the rate of decline in the potential growth curve. The transfer (δ) of R_a to R_s is a function of daily rainfall. R is the daily rainfall (m). δ has been defined such that the maximum single day reduction in old standing dead is 5%.

$$\delta = e^{-3.5 R} \quad [8.5.11]$$

The decomposition of litter and organic residue on the soil surface is a function of antecedent rainfall, average daily temperature, and the carbon nitrogen ratio of the residue and was based on the work of Ghidry et al. (1985).

$$R_s = (R_s \omega_L) - B_c \quad [8.5.12]$$

$$\omega_L = 1 - (\alpha_f \tau)^2$$

$$\tau = \frac{S_{mi} T_a}{C_n}$$

where ω_L is the fraction of litter after decay, α_f is the litter decay coefficient, and B_c is a daily disappearance of litter as a function of insects and rodents. τ is a function of the antecedent moisture index, average daily temperature, and the carbon nitrogen ratio of dead leaves and roots (C_n). S_{mi} is the amount of rainfall recorded in the last 5 days. S_{mi} values > 100 mm are set to 100 mm to reduce the decomposition rate of litter and organic residue during high rainfall periods.

For woody plant communities the trunks, stems, branches, and twigs (W_n) of the plants are considered to be non-decomposable but are important components in the calculation of foliar cover and ground surface cover. W_n is estimated on day one of the simulation as the product of N_a and R_a . W_n is held constant until management changes.

Plant characteristics that the model currently calculates are plant height (H_c), projected plant area (P_a), litter and organic residue cover on the soil surface (C_r), foliar canopy cover (C_c), ground surface cover (C_g), and leaf area index (LAI). The height of the plant canopy is calculated on the weighted average of coverage between the woody and the herbaceous plant components. The canopy height for the woody component (H_t and H_s) are input by the user and are held constant for duration of the simulation or until management changes.

$$H_c = \frac{(H_t E_t) + (H_s E_s) + (H_g E_g)}{\eta} \quad [8.5.13]$$

where $\eta = \frac{A}{P_a}$. A is the representative total vertical surface area of the overland flow plane. P_a is the effective projected plant area. H_t , H_s , and H_g are canopy heights for the tree, shrub, and herbaceous plant components, respectively. E_t , E_s , and E_g are the vertical area of the tree, shrub, and herbaceous components, respectively.

The canopy height for the herbaceous community (H_g) is estimated with an exponential function and is updated daily. The parameters necessary to estimate herbaceous plant height are the live standing biomass (L_t), dead standing biomass (R_a), maximum herbaceous plant height (H_{cm}), and a shaping coefficient (B_h). Plant canopy height is defined not as the uppermost extension of the canopy, but where the maximum amount of rainfall interception occurs.

$$H_g = H_{cm} (1 - e^{-B_h L_t R_a}) \quad [8.5.14]$$

The effective project plant area is calculated as a function of the plant height (m), average canopy diameters (m), number of plants along a 100m transect, and a geometric shape coefficient for the various plant components (Eq. [8.5.15]) and is based on work done by Hagen and Lyles (1988). The effective projected plant area is defined as the percent vertical cover and is used in calculating the distribution and depth of the snow pack.

$$P_a = \frac{E_a}{A} \quad [8.5.15]$$

The total projected area of the vegetation for the overland flow plane is computed as:

$$E_a = E_g + E_s + E_t \quad [8.5.16]$$

E_t , E_s , and E_g are computed in a similar manner and are a function of plant height, plant diameter, plant

density, and the geometric shape coefficient for each plant component, respectively. Equation [8.5.17] shows the calculation for the herbaceous plant component.

$$E_g = H_g G_{di} G_c G_p \quad [8.5.17]$$

The geometric shape coefficients G_c , S_c and T_c vary between 0.0 and 1.0. Where the geometric shape of a square has been defined as 1.0, a cylinder as 0.78, a trapezoid 0.75 (the bottom diameter is one-half of the top diameter), a parabola as 0.67, and an equilateral triangle as 0.43. The total vertical surface area is calculated from the taller of the two plant components as:

$$A = LH_t \quad [8.5.18]$$

where L is a some distance perpendicular to a slope. L has been set to 100m.

The WEPP model partitions the erosion process into rill and interrill erosion areas. The potential rill and interrill areas and the fraction of ground surface cover for both rill and interrill areas must be estimated. The area between plant canopies is defined as the potential rill area. A tentative relationship has been developed to estimate the distance between the center of the potential rills based on plant density (R_s). The lower and upper boundary constraints are 0.5 and 5m, respectively, and L has been defined as 100m.

$$R_s = \frac{L}{G_p + S_p + T_p + 1} \quad [8.5.19]$$

The fraction of the soil surface covered with litter is estimated with an exponential function. Where C_f is a shaping coefficient and R_s is litter and organic residue mass on the soil surface. Rill ground surface cover (RILCOV) has been defined as equal to C_{ri} .

$$C_{ri} = 1 - e^{-C_f R_s} \quad [8.5.20]$$

$$C_f = 10^{1.085 (1.0 + 1.69 e^{-12.61 R_s}) - 0.583}$$

Ground surface cover is calculated with a multiple regression equation (developed from WEPP field data) and is equal to interrill ground cover (INRCOV).

$$C_g = 1.28C_{ri} + 0.947C_f + 1.24C_{cr} \quad [8.5.21]$$

C_f is the fraction of soil surface covered by impervious material greater than 2 mm and is a user input. C_{cr} is the fraction of the soil surface covered by a cryptogamic crust, and is a user input. Cryptogams are defined here as all mosses, lichens, and algae that occur on the soil surface. The rock and cryptogamic crust are fixed variables and do not change as a function of plant growth. The rock and cryptogamic crust will change as a result of some management options when that subroutine is implemented. Exposed bare soil is calculated by difference from the other components of ground surface cover.

The relationship between standing biomass and canopy cover (C_c) is difficult to estimate for complex plant communities. The relationship between standing biomass and canopy cover is a function of specie, plant height, density, and architecture. No continuous function was found that would describe the relationship across all lifeforms. Canopy cover is estimated using an exponential function, where f_c is

a shaping coefficient based on plant community and B_t is total standing biomass. The shaping coefficient f_c is calculated as a function of the parameter C_o . C_o is defined as the standing biomass ($kg\ m^{-2}$) where canopy cover is 100% (Fig. 8.5.4).

$$C_c = 1 - e^{f_c B_t} \quad [8.5.22]$$

$$F_c = 21.39 - 54.91 C_o + 61.11 C_o^2 - 30.44 C_o^3 + 5.56 C_o^4$$

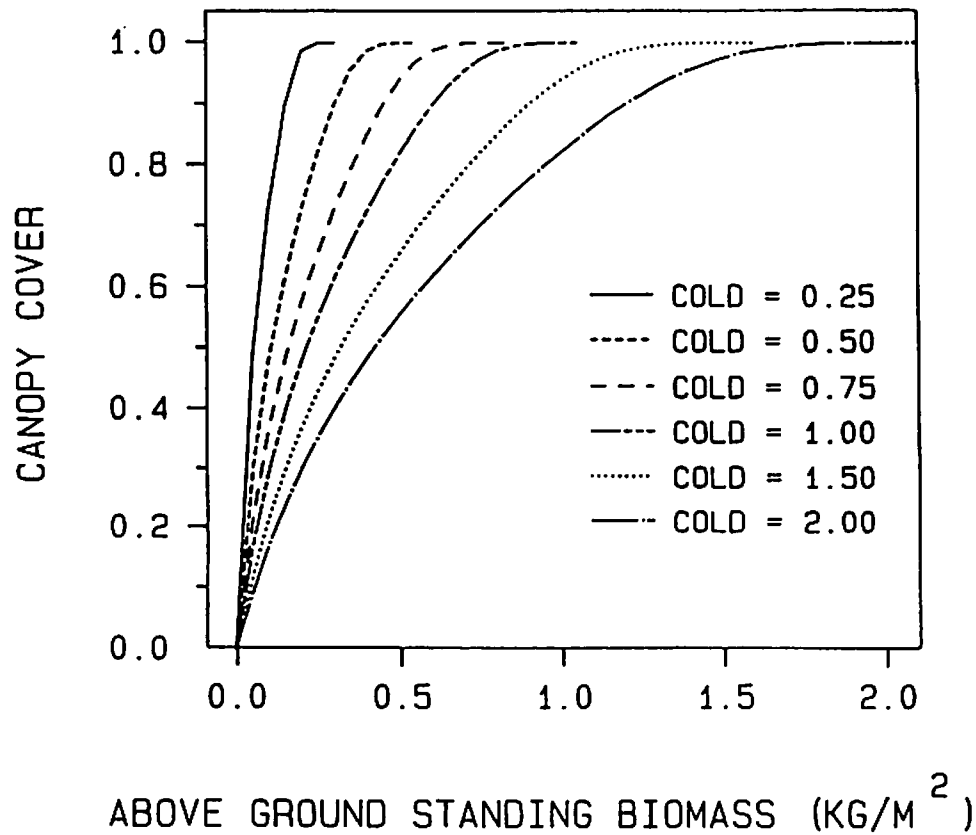


Figure 8.5.4. Relationship of above ground standing biomass to canopy cover as a function of COLD.

Leaf area index is difficult to estimate for complex plant communities. Wertz (1987) has shown that leaf area index can be computed as a function of dry leaf weight to leaf (single side) area divided by the area of the canopy. Leaf weight per unit area is not constant over the growing season. Leaf weight per unit area increases with time during the growing season and reaches a maximum value after the leaf reaches maturity. At this time no functional equation has been developed to account for this change in leaf weight to leaf area term. At the present the model uses a weighted mean average leaf weight to leaf area coefficient (L_c) for all plants across the growing season.

$$LAI = L_t L_c \quad [8.5.23]$$

The range plant growth model estimates root mass by soil layer. For perennial ecosystems the roots are assumed to have reached a maximum rooting depth (RTD). RTD has been defined as equal to depth of the soil profile. The initial distribution of root mass by depth is calculated by soil horizon using an exponential function.

$$R_i = R_t R_o (100 S_d^{R_f}) \quad [8.5.24]$$

where R_i is the total mass of roots ($kg\ m^{-2}$) in the soil horizon, R_t is the fraction of maximum roots on January 1 (estimated from root turnover studies and ranges from 0.50-0.80), S_d is the ending depth of soil layer (m). R_f is a root depth coefficient and has been set at 0.43. R_o is a root biomass coefficient and is estimated from the root mass (R_{10}) in the top 0.1 m of the soil surface.

$$R_o = \frac{R_{10}}{10^{R_f}} \quad [8.5.25]$$

From the initial root mass distribution the percentage of roots in each soil horizon is calculated (R_p). B_r is the total root mass in the soil profile.

$$R_p = \frac{R_i}{B_r} \quad [8.5.26]$$

The daily increment of root growth is calculated in a similar manner as above ground plant growth using the potential growth curve function. The range plant model does not separate roots into live and dead components within the soil profile. Roots are grown and decayed as a single unit.

$$B_r = B_{r-1} + (R_i g_i W_a B_{r-1}) \quad [8.5.27]$$

The decomposition of roots is calculated in a similar manner as is litter and organic residue.

$$B_r = B_r \chi \quad [8.5.28]$$

where $\chi = 1 - (\alpha_r v)^2$, χ is the fraction of roots after decay, α_r is the root decay coefficient, and $v = \frac{S_r T_a}{C_r}$. v is carbon-nitrogen ratio of dead leaves and roots. S_r is the amount of rainfall recorded in the last 5 days.

8.6 Rangeland Management Options

The range plant growth subroutine contains default parameters for 7 plant communities. The following section contains the management options currently available to the user and the parameters necessary for running the range plant growth model. The management options currently supported by the WEPP model are no plant growth, plant growth, grazing by livestock, burning, and herbicide application. The model currently does not support mechanical practices on rangeland.

8.6.1 No Plant Growth

The rangeland plant growth subroutine can be initialized for no above and below ground biomass production. Additionally the model can be parameterized to simulate a wide range of user-defined initial above and below ground biomass conditions (Table 8.6.1).

Table 8.6.1. Options for initial above ground standing dead biomass, litter, root biomass conditions, and model parameters for rangeland plant communities with no plant growth during simulation.

Standing dead biomass (kg m)	Litter (kg m)	Root biomass (kg m)	Variable	Model Parameters
Yes	Yes	Yes	P R_{10} R_a R_g R_t	PLIVE = 0 ROOT10 > 0 RMOGT > 0 RMAGT > 0 ROOTF > 0
Yes	None	Yes	P R_{10} R_a R_g R_t	PLIVE = 0 ROOT10 > 0 RMOGT = 0 RMAGT > 0 ROOTF > 0
None	Yes	Yes	P R_{10} R_a R_g R_t	PLIVE = 0 ROOT10 > 0 RMOGT > 0 RMAGT = 0 ROOTF > 0
None	None	None	P R_{10} R_a R_g R_t	PLIVE = 0 ROOT10 = 0 RMOGT = 0 RMAGT = 0 ROOTF = 0

8.6.2 Plant Growth

The rangeland plant growth subroutine can be initialized for either a unimodal or bimodal growth sequences. The user may choose to define the plant growth parameters for the plant community or utilize the default parameters. To initialize the unimodal growth sequence the parameters P_2 and G_2 must be initialized to 0. The user must initialize the fraction of the soil surface covered by cryptogamic crust (C_{cr}), and rocks, gravel and other impervious substances (C_g). The initial standing dead biomass and the initial residue mass on the soil surface must also be initialized by the user before the start of every simulation. To simulate a bimodal growing season parameters P_2 and G_2 must be initialized to > 0. In addition, the user must also initialize the same parameters as for a unimodal growth sequence.

8.6.3 Grazing Management Option

The grazing subroutine allows for multiple grazing periods and multiple herbs. The model currently allows for 10 grazing periods per year within each of the 10 pastures. Pastures are equivalent to overland planes. The grazing animals, number of animals, and accessibility of forage within each pasture can be defined uniquely for each pasture. Currently, the model does not allow for the change in the attributes of the grazing animals within a year. However, the model does allow for changes in the grazing animals characteristics and grazing sequences across years.

The grazing period is initialized by the user by entering the Julian day for the start of the grazing period (GDAY) and the last day of the grazing period (GEND). The grazing routine estimates the daily amount of forage required for the average grazing animal. The total daily forage requirement is calculated as the daily forage intake times the number of grazing animals. The daily forage requirement is a function of body size (kg) and digestibility of the forage.

Digestibility (D) of forage changes with time (Eq. [8.6.1]). Currently, the mean average digestibility of standing live leaves (D_{mx}) and old standing dead leaves (D_r) of the plant community are user inputs. Digestibility (Eq. [8.6.2]) is calculated as a function of the live-dead leaf ratio (D_l). Where D_l is calculated as $\frac{L_i}{R_a}$. If $D_l < 0.1$ then digestibility is equal to the minimum digestibility. If $D_l > 1.0$ then digestibility is equal to the maximum digestibility.

$$D = (D_r D_{mx}) + [(1 - D_r) D_{mx}] \quad [8.6.1]$$

$$D_r = 1 - e^{-5D_l} \quad [8.6.2]$$

The physiological limit on forage intake is estimated (Eq. [8.6.3]) as a function of body weight (B_w) based on the work of Brody (1945). Animal weight gains and animal performance are not modeled in the grazing subroutine. The total forage demand (F_i) by a single grazing animal is estimated as:

$$F_i = 0.1 \left[\frac{B_w^{0.75}}{D} \right] \quad [8.6.3]$$

Supplemental feed (SUPPMT) can be given to the grazing animals between user defined Julian days (SSDAY and SEND). The grazing animals consume all of the supplemental feed first, before consuming any of the available forage. The grazing animal consumes forage as a homogeneous unit since no individual species are grown.

The availability of forage (B_a) is a function of two parameters N_d and A_c . N_d is the parameter used to define the fraction of standing biomass that is woody. This fraction of biomass is considered to be unavailable for consumption, can not be broken down by trampling and will not decompose (Eq. [8.6.4]). A_c is the parameter used to determine the fraction of standing biomass available for consumption.

$$W_a = N_d R_a \quad [8.6.4]$$

The available forage is composed of two fractions: live (L_i) and dead (R_a). If the parameter N_d has been used then only a fraction of the standing dead is available. If a portion of the forage is unavailable for consumption due either to height, palatability, or location in the grazing area that fraction can be removed from the available forage with the parameter A_c . If available forage is less than a equal to a ten day supply of forage then the model automatically supplies supplemental feed to the animals.

$$B_a = [A_c(R_a + L_i)] + (R_a - W_a) \quad [8.6.5]$$

The utilization (U) of available forage is calculated as:

$$U = \frac{F_i}{Y + 0} \quad [8.6.6]$$

where F_t is the total forage consumed, Y is total standing biomass produced that year, and O is the initial standing biomass on January 1.

The model allows the grazing animals to consume the evergreen fraction of the standing biomass (X). In subsequent growing periods the evergreen component is replaced. Unavailable forage (U_b) is calculated as:

$$U_b = (1 - A_c)(R_a + L_t) \quad [8.6.7]$$

Trampling by cattle accelerates the transfer of standing dead material to litter. The trampling effect (t_r) by cattle is limited to 5% of the standing dead material on any given day. The trampling effect is estimated with an exponential function. The rate of transfer of standing material is a function of the stocking density. Stock density, (S), is defined as the number of animals divided by the pasture area (ha).

$$t_r = 0.05R_a(1 - e^{-0.015S}) \quad [8.6.8]$$

8.6.4 Burning

The user must define the Julian date that the pasture is burned. A minimum fuel load of 800 kg ha^{-1} is required for the model to allow burning of the area (Wink and Wright 1973; Beardall and Sylvester 1976). If rainfall is greater than 7.5 mm or if the 5 day antecedent rainfall is greater than 25 mm then the model will delay burning until moisture conditions are favorable. The entire pasture will be burned on that date. The user can control the effects of the fire with the parameters: A_f , B , C , H , and R .

Wildfires and prescribed burning can result in changes to accessibility of forage for grazing animals. To reflect the change in accessibility as a result of burning a pasture the parameter C should be initialized greater than 0.0. If C is initialized to 0.0 then all forage will be inaccessible to the grazing animals and the grazing animals should be removed from the pasture. The product of C and A_c can not exceed 1.0.

$$A_c = A_c C \quad [8.6.9]$$

The effectiveness of burning on removal of standing woody biomass depends upon environmental and plant conditions at the time of the burn. Therefore, the user must input the percent reduction in standing woody biomass. The remaining standing woody biomass is calculated as:

$$W_n = W_n B \quad [8.6.10]$$

The potential growth rate of above ground biomass (Eq. [8.6.11]) and root biomass (Eq. [8.6.12]) maybe affected by both prescribed and wild fires. The percent change in growth rate depends on the time of year, the intensity of the burn and the plant species involved. Therefore, the user must input the percent increase or decrease in growth rate. The new growth rates are calculated as:

$$P = PC \quad [8.6.11]$$

$$R_o = R_o C \quad [8.6.12]$$

The quantity of live above ground herbaceous biomass that is consumed as a result of burning depends on environmental conditions and the spatial arrangement of the plants in the pasture. The dynamics of burning are not simulated in WEPP. Therefore, the user must input the percent reduction (H) in above ground herbaceous biomass as a result of burning. The standing herbaceous biomass after burning is computed from:

$$L_t = L_i H \quad [8.6.13]$$

The percent reduction in the live evergreen leaf biomass (Eq. [8.6.14]) and the herbaceous standing dead biomass (Eq. [8.6.15]) is a function of R_l . R_l also reduces the litter and the organic residue mass on the soil surface (Eq. [8.6.16]).

$$L_t = [R_l(L_t - X)] + X R_l \quad [8.6.14]$$

$$R_a = R_l R_a \quad [8.6.15]$$

$$R_t = R_l R_t \quad [8.6.16]$$

8.6.5 Herbicides

The user must define the Julian date the herbicide is applied. The herbicide management option is only operational if live aboveground biomass is greater than 0.0 kg ha^{-1} . If rainfall is greater than 10 mm on day of application then the application date is delayed one day. The user can choose between two methods of herbicide activity: 1) A foliar herbicide which kills on contact; 2) A soil applied herbicide which is activated when sufficient rainfall has occurred to dissolve the herbicide and transport it into the root zone. The user can control the effect of the herbicide with the parameters: ACTIVE, WOODY, L_k , H_k , R_e , and U_l .

ACTIVE is a flag to determine which type of herbicide activity will be used. If ACTIVE is equal to 0 then a foliar contact herbicide is applied and death is instantaneous. If ACTIVE is equal to 1, then a pelleted soil herbicide is applied. The effect of the pelleted herbicide will be delayed until 12.5 mm of rainfall has occurred. Once the rainfall limit has been achieved death is instantaneous.

The effectiveness of herbicides in killing herbaceous vegetation depends upon the type of herbicide, time of year, and the plant species involved. The WEPP model does not simulate the processes involved in plant growth and death from herbicide application. Therefore, the user must input the percent reduction (L_k) in above ground live herbaceous biomass as a result of herbicide application. The reduction in live herbaceous biomass is computed differently for herbaceous plant communities and plant communities with both herbaceous and evergreen components. The reductions in herbaceous biomass are computed as:

For herbaceous species only:

$$D_r = L_t - (L_t L_k) \quad [8.6.17]$$

For herbaceous species within evergreen plant communities:

$$H_o = (L_t - x) - \{L_k (L_t - X)\} \quad [8.6.18]$$

The percent reduction in the live evergreen biomass from herbicide application is a user input (H_k). The remaining evergreen leaf biomass after herbicide application is computed as:

$$A_d = X - (XH_k) \quad [8.6.19]$$

The application of herbicides may affect the percent increase or decrease in the potential growth rate of above ground herbaceous biomass (Eq. [8.6.20]) and root mass (Eq. [8.6.21]). The effect of the herbicide on individual plant species is not being modeled. However, the user can increase or decrease the potential growth rate for the plant community. The new potential growth rate after herbicide application is calculated as:

$$P = PR_e \quad [8.6.20]$$

$$R_o = R_o R_e \quad [8.6.21]$$

The application of herbicides can affect plant distribution, plant height, and accessibility of forage. The application of herbicides can result in either a increase or decrease in forage accessibility. The change in accessibility of forage is a user input (U_d) and is calculated as:

$$A_c = U_d A_c \quad [8.6.22]$$

If U_d is initialized as 0.0, then all forage is inaccessible and grazing should not be allowed. Accessibility of forage should not exceed 1.0.

WOODY is a flag which allows the user to determine if defoliation is instantaneous or if defoliation will occur over several months. If WOODY is initialized to 0, then defoliation will be instantaneous. The increase in litter and organic residue mass from herbicide application is computed separately for herbaceous plant communities and plant communities with both herbaceous and evergreen components as:

For herbaceous plants:

$$R_t = R_t + D_t \quad [8.6.23]$$

For evergreen plants:

$$R_t = R_t + A_d + H_o \quad [8.6.24]$$

If WOODY is initialized to 1, then the dead leaves, branches, and stems of the evergreen plants will be retained on the plant.

$$D_d = H_o + A_d \quad [8.6.25]$$

The rate of decomposition and transfer of the dead leaves retained on the trees and shrubs to litter is computed at the same rate as decomposition of litter on the soil surface (Eq. [8.6.26]). The dead stems, branches, and twigs of shrubs and trees decompose at a slower rate than do the dead leaves. The rate of

transfer of dead stems has been estimated at 25% of the transfer of leaves (Eq. [8.6.27]). The rate of decomposition is computed as a function of the average air temperature, rainfall, and the carbon-nitrogen ratio of the material in a similar manner as the decomposition of litter.

$$R_t = R_g + [D_d - (D_d \omega_L)] \quad [8.6.26]$$

$$R_t = R_g + \left\{ W_n - \left[W_n \left(\frac{1 - \omega_L}{4} \right) \right] \right\} \quad [8.6.27]$$

8.7 References

- Beardall, L. E., and V. E. Sylvester. 1976. Spring burning for removal of sagebrush competition in Nevada. Proc. Tall Timbers Fire Ecol. Conf. 8:202-218.
- Borg, H., and D. W. Williams. 1986. Depth development of roots with time: An empirical description. Trans. ASAE 29(1):194-197.
- Brody, S. 1945. Bioenergetics and Growth. Reinhold Publishing Corp. New York.
- Ghebreiyessus, Y., and J. M. Gregory. 1987. Crop canopy functions for soil erosion prediction. Trans. ASAE 30(3):676-682.
- Ghidey, F., J. M. Gregory, T. R. McCarty, and E. E. Alberts. 1985. Residue decay evaluation and prediction. Trans. of the ASAE 28(1):102-105.
- Gregory, J., M. 1982. Soil cover prediction with various amounts and types of crop residue. Trans. ASAE 25(5): 1333-1337.
- Hagen, L. J., and L. Lylcs. 1988. Estimating small equivalents of shrub-dominated rangelands for wind erosion control. Trans. ASAE 31(3):769-775.
- Ligeon, J. T., and H. P. Johnson. 1960. Infiltration capacities of fayette silt loam from analysis of hydrologic data. Trans. ASAE 3(1): 36-37.
- Parton, W. J., and G. S. Innis. 1972. Some graphs and their functional forms. U.S. International Biological Program Grassland Biome. Colorado State University Technical Report No. 153, Fort Collins, 41 p.
- Sims, P. L., and J. S. Singh. 1978. The structure and function of ten western North American grasslands. III. Net primary production, turnover and efficiencies of energy capture and water use. J. Ecology 66, 573-597.
- Weltz, M. A. 1987. Observed and estimated (ERHYM-II Model) water budgets for south Texas rangelands. PhD. Diss., Texas A&M Univ., College Station, TX. 173 p.
- Wight, J. Ross. 1987. ERHYM-II: Model description and user guide for the basic version. U.S. Department of Agriculture, Agriculture Research Service, ARS-59, 24 p.
- Williams, J. R., C. A. Jones, and P. T. Dyke. 1984. A modeling approach to determining the relationship between erosion and soil productivity. Trans. ASAE 27(1):129-142

Wink, R. L., and H. A. Wright. 1973. Effects of fire on an Ashe juniper community. *J. Range Manage.* 26, 326-329.

8.8 List of Symbols

Symbols	Description	Unit	Variable	Land Use*
A	Total vertical projected area	m	TAREA	R
A_b	Plant basal area in one square meter	m^2	BASAL	C
A_{bm}	Plant basal area at maturity in one square meter	m^2	BASMAT	C
A_c	Forage available for consumption	NOD	ACCESS	R
-	Flag for soil or foliar applied herbicide	-	ACTIVE	R
A_d	Evergreen phytomass after herbicide application	$kg\ m^{-2}$	ADHERE	R
A_f	Pasture size being grazed	m^2	AREA	R,C
A_p	Soil area associated with one plant	m^2	AREACV	C
A_{sp}	Single plant stem area	m^2	STEMAR	C
A_1	Change in forage accessibility from burning	NOD	ALTER	R
a_m	Antecedent moisture index for standing and flat residue decomposition	m	AM	R,C
a_{m2}	Antecedent moisture index for buried residue and root decomposition	m	AM2	R,C
α_b	Decomposition constant to calculate mass change of buried residue	NOD	AS	C
α_f	Decomposition constant to calculate mass change of flat residue	NOD	ACA	R,C
α_r	Decomposition constant to calculate mass change of roots	NOD	AR	R,C
α_s	Decomposition constant to calculate mass change of standing residue	NOD	AST	C
B	Reduction in standing dead biomass from burning	NOD	BURNED	R
B_a	Available standing biomass for grazing animals	$kg\ m^{-2}$	AVABIO	R
B_c	Daily removal of surface organic material by insects	$kg\ m^{-2}$	BUGS	R
B_m	Vegetative biomass	$kg\ m^{-2}$	VDM	C
B_{mx}	Vegetative biomass at maturity	$kg\ m^{-2}$	VDMMAX	C
ΔB_r	Daily change in total root biomass	$kg\ m^{-2}$	DELT	C
B_{rp}	Live root biomass of a perennial crop	$kg\ m^{-2}$	TRTMASS	C
B_{rt}	Total root biomass of an annual crop	$kg\ m^{-2}$	RTMASS	R,C
-	Maximum root biomass of a perennial crop	$kg\ m^{-2}$	RTMMAX	C
B_{r1}	Root biomass in the 0- to 0.15-m soil zone	$kg\ m^{-2}$	RTM15	C
B_{r2}	Root biomass in the 0.15- to 0.30-m soil zone	$kg\ m^{-2}$	RTM30	C
B_{r3}	Root biomass in the 0.30- to 0.60-m soil zone	$kg\ m^{-2}$	RTM60	C
B_t	Total above ground standing biomass	$kg\ m^{-2}$	VDMT	R
B_w	Average body weight of a grazing animal	kg	BODYWT	R,C
β_c	Parameter for canopy cover equation	NOD	bb	C
β_h	Parameter for canopy height equation	NOD	bbb	R,C
β_1	Plant-dependent constant to compute canopy cover	NOD	b1	C
β_2	Maximum canopy width at maturity	NOD	b2	C
C	Change in potential above and below ground biomass production from burning	NOD	CHANGE	R

C_c	Canopy cover	NOD	CANCOV	R,C
ΔC_c	Daily loss of canopy cover	NOD	DEC	C
C_{cf}	Soil surface cover by coarse fragments	NOD	WCF	R,C
C_{cr}	Soil surface covered by cryptogams	NOD	CRYPTO	R
C_{cs}	Fraction of canopy cover remaining after senescence	NOD	DECFACT	C
cf	Parameter for flat residue cover equation	NOD	CF	R,C
C_g	Total soil cover including residue and rocks	NOD	GCOVER	R,C
C_{cm}	Canopy cover at maturity	NOD	CCMAT	C
C_n	Carbon to nitrogen ratio of residue and roots	NOD	CN	R,C
C_{ri}	Interrill residue cover	NOD	INRCOV	R,C
C_{rf}	Flat residue cover	NOD	FLRCOV	C
C_{ri}	Rill residue cover	NOD	RILCOV	R,C
C_{rr}	Residue cover on ridges	NOD	RIGCOV	C
C_{rs}	Standing residue cover	NOD	STRCOV	C
C_{rt}	Total residue cover	NOD	RESCOV	R,C
C_{sp}	Residue cover on ridges after wind repositioning	NOD	SPRCOV	C
C_w	Average weed canopy cover during the nongrowing season	NOD	WDCOV	C
c	Shaping coefficient for ascending side of first growth curve	NOD	CSHAPE	R
C_o	Standing biomass where canopy cover is 100%	$kg\ m^{-2}$	COLD	R
-	Growing degree days to plant emergence	C	CRIT	C
-	Critical biomass for a perennial crop below which grazing animals no longer consume vegetation	$kg\ m^{-2}$	CRITVM	C
-	Integer that represents whether a cultivator is front or rear mounted	NOD	CULPOS	C
-	Cutting or harvesting day for a perennial crop	Julian date	CUTDAY	C
D	Plant stem diameter at maturity	m	DIAM	C
D_d	Decomposable standing dead biomass after herbicide application	$kg\ m^{-2}$	SDEAD	R
D_g	Digestibility of a perennial crop being grazed	NOD	DIGEST	R,C
D_h	Number of days after harvest	NOD	DAH	C
D_l	Dead/live ratio of leaves	NOD	DL	R
D_{mx}	Maximum digestibility of forage	NOD	DIGMAX	R
D_m	Number of days to physiological maturity	NOD	DTM	C
D_n	Minimum digestibility of forage	NOD	DIGMIN	R
D_p	Number of days after planting	NOD	DAP	C
D_r	Digestibility coefficient	NOD	DLR	R
D_s	Reduction in live above ground biomass from drought stress	NOD	DEATH	R
d	Shaping coefficient for descending side of first growth curve	NOD	DSHAPE	R
E_a	Total plant project area	m	TOTPAI	R
E_g	Herbaceous project plant area	m	GPAI	R
E_s	Shrub projected plant area	m	SPAI	R
E_t	Tree projected plant area	m	TPAI	R
e	Shaping coefficient for ascending side of second growth curve	NOD	ESHAPE	R
F_{bs}	Fraction of standing residue mass	NOD	FBRNAG	C

	lost by burning			
F_{bf}	Fraction of flat residue mass lost by burning	NOD	FBRNOG	C
F_c	Fraction of standing residue mass mechanically shredded or cut	NOD	FRCUT	C
F_{ct}	Standing to flat residue adjustment factor for wind and snow	NOD	FACT	C
F_{gs}	Current fraction of the growing season	NOD	FGS	C
F_i	Quantity for forage consumed by grazing animals	$kg\ day^{-1}$	FEED	R,C
F_{lai}	Fraction of growing season when leaf area index starts declining	NOD	DLAI	C
F_{pc}	Portion of vegetative biomass partitioned into standing residue mass at harvest	NOD	PARTCF	C
F_{rm}	Fraction of vegetative or flat residue mass removed from a field	NOD	FRMOVE	C
F_t	Daily total vegetative uptake by livestock	$kg\ m^{-2}$	TFOOD	R,C
f	Shaping coefficient for descending side of second growth curve	NOD	FSHAPE	R
f_c	Coefficient for canopy cover	NOD	FFK	R
f_p	Frost free period	Julian date	FFP	R,C
-	Date that grazing begins	Julian date	GDAY	R
G_b	Day on which first growth period begins	Julian date	STRRGC	R
G_c	Projected plant area coefficient for herbaceous plants	NOD	GCOEFF	R
$\sum G_d$	Cumulative growing degree days	C	SUMGDD	C
G_d	Growing degree days	C	GDD	C
G_{di}	Average diameter for herbaceous plants	m	GDIAM	R
G_{dm}	Growing degree days at maturity	C	GDDMAX	C
-	End of a grazing period	Julian date	GEND	R,C
G_p	Average number of herbaceous plants along a 100 m transect	NOD	GPOP	R
G_1	Proportion of biomass produced during the first growing season	NOD	CF1	R
G_2	Proportion of biomass produced during the second growing season	NOD	CF2	R
g_i	Daily increment of relative growth curve	NOD	RGC	R
-	Number of days from planting to harvest	NOD	GS	C
-	Fraction of growing season to reach senescence	NOD	GSEN	C
-	Minimum temperature to initiate growth	C	GTEMP	R
-	Flag for grazing rangelands	NOD	GRAZIG	R
H	Reduction in above ground standing biomass from after burning	NOD	HURT	R
H_c	Canopy height	m	CANHGT	R,C
H_{cm}	Maximum canopy height	m	HMAX	R,C
H_g	Initial canopy height for herbaceous plants	m	GHGT	R
H_k	Decrease in evergreen phytomass from herbicide application	NOD	HERB	R
H_o	Live evergreen phytomass retained after herbicide application	$kg\ m^{-2}$	HOLD	R
H_s	Average shrub height	m	SHGHT	R
H_t	Average tree height	m	THGT	R
η	Ratio of total vertical area to prospected area	NOD	--	R

- Integer that represents a certain crop type	NOD	ITYPE	R,C
- Integer that represents a double-cropping system	NOD	IDBCRP	C
- Integer that indicates whether a critical freezing temperature has occurred	NOD	IFREEZ	C
- Julian date of herbicide application rangelands	Julian date	IHDATE	R
- Integer that represents annual, perennial, or fallow cropping	NOD	IMNGMT	C
- Integer used to identify the simulation year for a perennial crop	NOD	IPRNYR	C
- Integer that indicates a well-defined ridge-furrow system	NOD	IRDG	C
- Integer that represents the crop grown prior to the start of simulation	NOD	IRESD	C
- Integer that indicates the first cutting of a perennial crop has occurred	NOD	ISTART	C
- Integer that represents a certain primary, secondary, planting, or cultivating implement used in one tillage sequence	NOD	ITILL	R,C
- Integer that represents the number of crops grown in the simulation	NOD	NCROP	R,C
- Number of landscape segments that have uniform cropping, management, soil, and topography	NOD	NELEM	R,C
- Integer that indicates that weed canopy cover is important during the non growing season	NOD	IWEED	C
- Julian day of burning residue	Julian date	JDBURN	C
- Julian day of burning rangeland	Julian date	JFDATE	R
- Julian day of residue shredding or cutting	Julian date	JDCUT	C
- Julian day of grain or biomass harvest	Julian date	JDHARV	C
- Julian day of herbicide application	Julian date	JDHERB	C
- Julian day of residue removal from a field	Julian date	JDMOVE	C
- Julian day of planting	Julian date	JDPLT	C
- Julian day of silage removal from a field	Julian date	JDSLGE	C
- Julian day to permanently stop the growth of a perennial crop	Julian date	JDSTOP	C
- Julian day that weed canopy cover becomes important	Julian date	JDWDST	C
- Julian day that weed canopy cover becomes unimportant	Julian date	JDWEND	C
<i>LAI</i> Leaf area index	NOD	LAI	R,C
<i>LAI_d</i> Leaf area index value when leaf area index starts declining	NOD	XLAIMX	C
<i>LAI_{mx}</i> Maximum leaf area index potential	NOD	XMXLAI	C
<i>L_c</i> Leaf weight to leaf area coefficient	$m^2 kg^{-1}$	ALEAF	R
<i>L_i</i> Live phytomass produced today	$kg m^{-2}$	SLIVE	R
<i>L_t</i> Reduction in live above ground biomass from herbicide application	NOD	DLEAF	R
<i>L_n</i> Minimum amount of live biomass	NOD	RGCMIN	R
<i>L_t</i> Total live phytomass	$kg m^{-2}$	TLIVE	R
- Julian day of tillage in one tillage sequence	Julian date	MDATE	C
- Integer that represents a management option for a perennial crop	NOD	MGTOPT	C
- Number of annual cuttings of a perennial crop	NOD	NCUT	C
- Number of annual grazing cycles	NOD	NCYCLE	C

-	Number of tillage sequences used during the simulation	NOD	NSEQ	C
-	Number of tillage operations within one tillage sequence	NOD	NTILL	C
-	Integer that represents the number of crops growth annually	NOD	NYCROP	C
ΔM_b	Buried residue mass change	NOD	SMRATIO	R,C
M_b	Buried residue mass	$kg\ m^{-2}$	SMRM	C
ΔM_f	Flat residue mass change	NOD	FRATIO	C
M_f	Plant residue mass lying on the ground	$kg\ m^{-2}$	RMOG	C
M_r	Non-living root mass	$kg\ m^{-2}$	RTM	C
$\Delta M_r, \chi$	Root mass change	NOD	RRATIO	R,C
M_{rl}	Rill residue mass	$kg\ m^{-2}$	RILRM	C
M_{rr}	Residue mass on ridges	$kg\ m^{-2}$	RIGRM	C
M_{rt}	Total residue mass at harvest	$kg\ m^{-2}$	RESAMT	C
ΔM_s	Standing residue mass change	NOD	SRATIO	C
M_s	Plant residue mass standing above ground	$kg\ m^{-2}$	RMAG	C
M_{s0}	Standing residue mass at grain or biomass harvest	$kg\ m^{-2}$	SRMHAV	C
ΔM_w	Residue mass moved from ridges to furrows by wind	$kg\ m^{-2}$	DELTRM	C
N_a	Number of grazing animals	NOD	ANIMAL	R,C
N_d	Initial standing non-decomposable woody biomass	NOD	WOOD	R
o	Initial standing above ground biomass	$kg\ m^{-2}$	OLDPLT	R
ω	Plant-dependent growth parameter	NOD	GRATE	C
ω_L	Litter after decay	NOD	SMRATI	R
P	Maximum potential standing live above ground biomass	$kg\ m^{-2}$	PLIVE	R
P_a	Projected plant area	NOD	BASDEN	R
-	Plant drought tolerance factor	NOD	PLTOL	R
P_d	Day of peak standing crop, 1st peak	Julian date	PSCDAY	R
P_s	Annual growing season precipitation	m	PPTG	R
P_m	Plant population at maturity	NOD	POPMAT	C
P	Plant population	NOD	POP	C
P_s	In-row plant spacing	m	PLTSP	C
P_2	Day of peak standing crop, 2nd peak	Julian date	SCDAY2	R
R	Daily rainfall amount	m	RAIN	R,C
R_a	Standing above ground dead biomass	$kg\ m^{-2}$	RMAGT	R
R_d	Root depth	m	RTD	R,C
R_{dx}	Maximum root depth	m	RDMAX	C
R_e	Change in potential above and below ground potential biomass production from herbicides	NOD	REGROW	R
R_f	Root distribution coefficient for mass by depth	NOD	RDF	R
-	Integer to indicate a plant or residue management option	NOD	RESMNG	C
R_g	Litter and organic residue mass	$kg\ m^{-2}$	RMOGT	R
R_i	Root mass in a soil horizon	$kg\ m^{-2}$	ROOT	R
R_l	Reduction in litter and organic residue from burning	NOD	REDUCE	R
R_{mf}	Residue mixing factor	NOD	RMF	C
R_o	Root mass coefficient	$kg\ m^{-2}$	PROOT	R
R_p	Proportion of within soil horizon to total root mass root mass in soil profile	NOD	DROOT	R
R_{sr}	Root to shoot ratio	NOD	RSR	C
R_s	Potential rill spacing	m	RSPACE	R

R_r	Root turn-over coefficient	NOD	ROOTF	R
R_w	Row width	m	RW	C
R_{10}	Root mass in top 0.10 m of soil profile	$kg\ m^{-2}$	ROOT10	R
S	Stock density	animal ha^{-1}	SD	R
S_c	Projected plant area coefficient for shrubs	NOD	SCOEFF	R
S_d	Depth of soil layer	m	SOLTHK	R
S_m	Average canopy diameter for shrubs	m	SDIAM	R
S_{mi}	Antecedent moisture index for litter decomposition	m	AMC	R
-	Day supplemental feeding ends	Julian date	SEND	R
S_p	Average number of shrubs along a 100m transect	NOD	SPOP	R
S_p	Number of days between the beginning and end of leaf drop	NOD	SPRIOD	C
S_r	Antecedent moisture index for root decomposition	m	AMC2	R
-	Day supplemental feeding begins	Julian date	SSDAY	R
-	Day on which second growth period begins	Julian date	STRGC2	R
-	Average amount of supplement feed per day	$kg\ animal^{-2}$	SUPPMT	R
τ	Weighted-time variable for standing and flat residue	NOD	TAU	R,C
τ_2	Weighted-time variable for buried residue and roots	NOD	TAU2	R,C
T_a	Average daily temperature	$^{\circ}C$	TEMP	R
T_a	Average daily air temperature	$^{\circ}C$	TAVE	C
T_b	Base daily air temperature of a growing plant	$^{\circ}C$	BTEMP	C
T_c	Project plant area coefficient for trees	NOD	TCOEFF	R
T_d	Average canopy diameter for trees	m	TDIAM	R
T_d	Tillage depth	m	TILDEP	C
T_{dm}	Mean tillage depth	m	TDMEAN	C
-	Minimum temperature to induce dormancy	$^{\circ}C$	TEMPMN	R,C
T_i	Tillage intensity	NOD	MFO	C
T_{cl}	Critical freezing temperature of a perennial crop	$^{\circ}C$	TMPMIN	C
T_{cu}	Critical upper temperature of a perennial crop that induces dormancy	$^{\circ}C$	TMPMAX	C
T_{mx}	Maximum daily air temperature	$^{\circ}C$	TMAX	R,C
T_{mn}	Minimum daily air temperature	$^{\circ}C$	TMIN	R,C
-	5-day average daily minimum air temperature	$^{\circ}C$	TMNAVG	C
-	5-day average daily maximum air temperature	$^{\circ}C$	TMXAVG	C
-	Vegetative dry matter of a perennial crop not harvested or grazed	$kg\ m^{-2}$	TOTHAV	C
-	Integer that represents whether tillage is primary or secondary	NOD	TYPTILL	C
T_p	Average number of trees along a 100m transect	NOD	TPOP	R
t_i	Current Julian date	Julian date	SDATE	R,C
t_r	Amount of standing dead biomass transferred to litter as a result of grazing animals	$kg\ m^{-2}\ day^{-1}$	TR	R
-	Amount of standing dead biomass transferred to litter as a result of precipitation	$kg\ m^{-2}\ day^{-1}$	TRANS	R
U	Utilization of available forage by grazing animals	NOD	UTILIZ	R
U_b	Unavailable standing biomass for grazing animals	$kg\ m^{-2}$	UNBIO	R
U_d	Change in forage accessibility from herbicide application	NOD	UPDATE	R
W_a	Four day average water stress	NOD	STRESS	R
-	Flag for decomposition of woody biomass as a	-	WOODY	R

	of herbicide application			
W_n	Standing woody biomass	$kg\ m^{-2}$	DECOMP	R
W_s	Daily water stress index starts declining	NOD	WST	R
X	Evergreen phytomass	$kg\ m^{-2}$	XLIVE	R
-	Grain yield boundary below which an adjustment to residue biomass is made	$bu\ ac^{-1}$	Y1	C
-	Residue mass when grain yield is zero	$kg\ ha^{-1}$	Y2	C
-	Change in residue mass per unit change in grain yield between grain yield limits (0 and Y1)	$kg\ ha^{-1}/bu\ ac^{-1}$	Y3	C
-	Pounds of grain per bushel of grain	$lb\ bu^{-1}$	Y4	C
-	Pounds per acre to kilogram per hectare conversion	$kg\ ha^{-1} / lb\ ac^{-1}$	Y5	C
Y	Total above ground biomass produced	$kg\ m^{-2}\ year^{-1}$	YIELD	R
Y_c	Residue to grain weight ratio	NOD	Y6	C
-	Yield at each cutting date for a perennial crop	$kg\ m^{-2}$	YILD	C
Y_t	Grain or biomass yield	$kg\ m^{-2}$	YLD	C

- C and R refer to cropland and rangeland.

Chapter 9. HYDRAULICS OF OVERLAND FLOW

J. E. Gilley, S. C. Finkner, M. A. Nearing, and L. J. Lane

9.1 Introduction

Procedures used for overland flow routing and hydrograph development are outlined in Chapter 5. In Chapter 11, equations for estimating erosion, deposition and sediment transport are presented. To accurately route runoff and sediment, proper identification of hydraulic parameters is essential.

The Chezy equation has been widely used to describe flow characteristics. Under uniform flow conditions, the Chezy friction coefficient, C , is given as (Chow, 1959)

$$C = \left(\frac{8g}{f} \right)^{1/2} \quad [9.1.1]$$

where f is the Darcy-Weisbach friction factor. Units for the Chezy friction coefficient used in this chapter are exclusively $m^{1/2} s^{-1}$. Equations used to predict hydraulic roughness coefficients in the WEPP model are presented below.

9.2 Roughness Coefficients for Overland Flow Routing

Separate estimates of the Darcy hydraulic roughness coefficient are made for the rill and interrill areas. A total equivalent Darcy friction factor, f_e , is then computed as an area weighted average of the rill and interrill areas using the relationship

$$f_e = f_r A_r + f_i (1 - A_r) \quad [9.2.1]$$

where f_e is the total friction factor in the rill, f_i is the total friction factor for the interrill area, and A_r is the fraction of the total area in rills. The fraction of the total area in rills is determined from the computed rill width as described in Chapter 10.

9.3 Roughness Coefficients for Rills

Shear stress in rills is partitioned into two parts, one part that acts on the soil to cause detachment and another portion that acts on exposed residue or other surface cover and is thus not active in terms of soil detachment. The portion of the shear stress which acts on the soil and causes erosion is proportional to the ratio of the hydraulic friction factor for the soil to the total friction factor (soil plus cover). If cover exists in the rill, the portion of total shear which acts on the soil will be only a fraction of the total shear stress in the rill. The total friction factor for rill areas, f_r , is given as

$$f_r = f_{sr} + f_{cr} \quad [9.3.1]$$

where f_{sr} is friction coefficient for rill soil roughness, and f_{cr} is the friction coefficient for rill surface cover.

The friction coefficient for surface roughness was determined from WEPP cropland field experimental data (Chapter 11). For the five soils tested, the friction coefficient increased with greater clay content. The variations in friction coefficients are due to differences in cloddiness of the soils; the soils with a high clay content are more cloddy than the sandy soils. The friction coefficient for rill soil roughness, f_{sr} , is calculated as

$$f_{sr} = 1.62 \left(3.42^{clay} \right) / 12.42^{(sand)} \quad [9.3.2]$$

where *sand* and *clay* are the fraction of these respective components.

The equation used to estimate the friction coefficient for rill surface cover f_{cr} , is given as

$$f_{cr} = f_c r_c^{1.267} \quad [9.3.3]$$

where f_c is a coefficient which is a function of residue type and r_c is the fraction of the rill covered by nonmovable material such as ground residue, stems, or stones.

9.4 Roughness Coefficients for Interrill Areas

The friction coefficient for interrill areas is influenced by surface roughness, surface cover, and hydraulic roughness for a smooth, bare soil. Total friction factor for interrill areas, f_i , is given as

$$f_i = f_{si} + f_{ci} + f_{bi} \quad [9.4.1]$$

where f_{si} is the friction coefficient for interrill surface roughness, f_{ci} is the friction coefficient for interrill surface cover, and f_{bi} is the friction coefficient for a smooth, bare soil.

Interrill form roughness elements are primarily affected by the type of tillage operation which is performed and the cumulative rainfall occurring since tillage (Zobeck and Onstad, 1987). Form roughness elements may be quite large compared to flow depth on interrill areas. Finkner (1988) related form roughness elements to friction coefficients using the relationship for Chezy C of

$$C_{si} = \frac{12.5}{[f_o^{1.128} e^{(-3.088(1.0-r_i))}]^{1/2} - C_{bi}} \quad [9.4.2]$$

where

$$f_o = \frac{8.85}{[\exp(3.024 - 5.042 e^{(-161.0 r_o)})]^{1/2}} \quad [9.4.3]$$

and r_o is the initial random roughness of a freshly tilled soil (m), r_i is the ratio of random roughness at some later time to r_o , and f_o is the friction factor for a freshly tilled surface in the absence of cover. The basis for the relationships describing C_{si} is given in Chapter 11, Section 2.

The value of the friction coefficient for interrill surface cover, f_{ci} , is given by

$$f_{ci} = 18.52 i_c^{1.267} \quad [9.4.4]$$

where i_c is the fraction of the interrill area covered with nonmovable material. Finally, the friction coefficient for a smooth, bare soil can be calculated from the equation

$$f_{bi} = 4.0 \left[\frac{3.42^{clay}}{12.42^{sand}} \right] \quad [9.4.5]$$

where *sand* and *clay* represent the respective fractions of each of these components.

9.5 Temporal Variations in Friction Coefficients

Temporal variations in the friction coefficients are determined indirectly through the parameters used in the prediction equations. These parameters include r_i , the ratio of random roughness at some later time to initial random roughness, and the fraction of rill and interrill area covered with nonmovable material, r_c , and i_c respectively. Details of temporal variations in these parameters are given in Chapters 6 and 8.

Two components of the interrill friction coefficient are affected by temporal variations. The values of the friction coefficients for interrill surface roughness, C_{si} , as determined from Eq. [9.4.1] and [9.4.2] will decrease as r_o is reduced by rainfall. Changes in surface cover due to decomposition of residue, tillage or harvesting will affect the fraction of the rill or interrill area covered with nonmovable material, r_c and i_c respectively. These variations in turn will affect the friction coefficients. The friction coefficient for a smooth, bare soil, f_{bi} , is unaffected by temporal variations. f_{sr} , the friction coefficient for rill surface roughness, is also assumed to be invariant with time.

9.6 References

- Chow, V.T. 1959. *Open Channel Hydraulics*, Mcgraw-Hill Book Co., New York, NY. 680 pp.
- Finkner, S. C. 1988. Hydraulic roughness coefficients as affected by random roughness. M.S. Thesis, Univ. of Nebraska. 89 pp.
- Zobeck, T. M., and Onstad, C. A. 1987. Tillage and rainfall effects on random roughness: A review. *Tillage Res.* 9:1-20.

9.7 List of Symbols

Symbol	Definition	Units	Variable
A_r	fraction of the total area in rills	-	rilave
C	Chezy friction coefficient	$m^{1/2}/s$	chezyc
C_{si}	Chezy friction coefficient for interrill surface roughness	$m^{1/2}/s$	-
<i>clay</i>	fraction of the clay component	-	clay
f_{bi}	Darcy friction coefficient for a smooth, bare soil	-	inrfco
f_c	coefficient	-	fcoef
f_{ci}	Darcy friction coefficient for interrill surface cover	-	inrfco
f_{cr}	Darcy friction coefficient for rill surface cover	-	frccov
f_e	total equivalent Darcy friction factor	-	frcteq
f_i	total Darcy friction factor for the interrill area	-	inrfto
f_o	Darcy friction factor for a freshly tilled surface in the absence of cover	-	foinr
f_r	total Darcy friction factor in the rill	-	frctrl
f_{si}	Darcy friction coefficient for interrill surface roughness	-	inrfro
f_{sr}	Darcy friction factor for rill surface roughness	-	frcsol
i_c	fraction of the interrill area covered by nonmovable material	-	inrcov
R	hydraulic radius	m	R
r_c	fraction of the rill covered by nonmovable material	-	rilcov
r_i	the ratio of random roughness at some later time to initial random roughness	-	rrinr

r_o	initial random roughness of a freshly tilled surface	m	rroinr
S	average slope	-	avgslp
<i>sand</i>	fraction of the sand component	-	sand
V	flow velocity	m/s	V

Chapter 10. EROSION COMPONENT

G.R. Foster, L.J. Lane, M.A. Nearing
S.C. Finkner, D.C. Flanagan

10.1 Introduction

The purpose of this chapter is to describe the erosion model used in the WEPP technology. The governing equations for sediment continuity, detachment, deposition, shear stress in rills, and transport capacity are presented. Relationships describing temporal modifications to baseline erodibility parameters (i.e., those measured for a standard condition) as a function of above and below ground residue, plant canopy, and soil consolidation are also presented. The normalized forms of the equations and parameters, the means for characterizing downslope spatial variability, and solution methods are discussed.

10.2 Governing Equations

10.2.1 Sediment Continuity Equation

The WEPP erosion model uses a steady-state sediment continuity equation to describe the movement of suspended sediment in a rill:

$$\frac{dG}{dx} = D_f + D_i \quad [10.2.1]$$

where x represents distance downslope (m), G is sediment load ($kg\ s^{-1}\ m^{-1}$), D_i is interrill erosion rate ($kg\ s^{-1}\ m^{-2}$), and D_f is rill erosion rate ($kg\ s^{-1}\ m^{-2}$). Interrill erosion, D_i , is considered to be independent of x . Rill erosion, D_f , is positive for detachment and negative for deposition. For purposes of calculations, both D_f and D_i are computed on a per rill area basis, thus G is solved on a per unit rill width basis. After computations are complete, soil loss is expressed in terms of loss per unit area.

Interrill erosion is conceptualized as a process of sediment delivery to concentrated flow channels, or rills, whereby the interrill sediment is then either carried off the hillslope by the flow in the rill or deposited in the rill. Sediment delivery from the interrill areas is considered to be proportional to the square of rainfall intensity, with the constant of proportionality being the interrill erodibility parameter. The function for interrill sediment delivery also includes terms to account for ground and canopy cover effects. The interrill functions are discussed in detail below.

Net soil detachment in rills is calculated for the case when hydraulic shear stress exceeds the critical shear stress of the soil and when sediment load is less than sediment transport capacity. For the case of rill detachment

$$D_f = D_c \left(1 - \frac{G}{T_c}\right) \quad [10.2.2]$$

where D_c is detachment capacity by rill flow ($kg\ s^{-1}\ m^{-2}$), and T_c is sediment transport capacity in the rill ($kg\ s^{-1}\ m^{-1}$). When hydraulic shear stress exceeds critical shear stress for the soil, detachment capacity, D_c , is expressed as

$$D_c = K_r(\tau_f - \tau_c) \quad [10.2.3]$$

where K_r ($s\ m^{-1}$) is a rill erodibility parameter, τ_f is flow shear stress acting on the soil particles (Pa), and τ_c is the rill detachment threshold parameter, or critical shear stress, of the soil (Pa). Rill detachment is considered to be zero when shear is less than critical shear of the soil.

Net deposition is computed when sediment load, G , is greater than sediment transport capacity, T_c . For the case of deposition

$$D_f = \left(\frac{\beta V_f}{q} \right) (T_c - G) \quad [10.2.4]$$

where V_f is effective fall velocity for the sediment ($m s^{-1}$), q is flow discharge per unit width ($m^2 s^{-1}$), and β ($= 0.5$) is a raindrop-induced turbulence coefficient.

10.2.2 Hydrologic Inputs

The three hydrologic variables required to drive the erosion model are peak runoff, P_r ($m s^{-1}$), effective runoff duration, t_r (s), and effective rainfall intensity, I_e ($m s^{-1}$). These variables are calculated by the hydrology component of the WEPP model which generates breakpoint precipitation information and runoff hydrographs. To transpose the dynamic hydrologic information into steady state terms for the erosion equations, the value of steady-state runoff, P_r , is assigned the value equal to that of the peak runoff on the hydrograph. The effective duration of runoff, t_r , is then calculated to be the time required to produce a total runoff volume equal to that given by the hydrograph with a constant runoff rate of P_r . Thus, t_r is calculated as

$$t_r = \frac{V_t}{P_r} \quad [10.2.5]$$

where V_t is the total runoff volume for the rainfall event (m). Effective rainfall intensity, I_e , which is used to estimate interrill soil loss, was calculated from the equation

$$I_e = \left[\frac{(\int I^2 dt)}{t_e} \right]^{1/2} \quad [10.2.6]$$

where I is rainfall intensity, t is time, t_e is the total time during which the rainfall rate exceeds infiltration rate, and the integral is evaluated over the time t_e .

10.2.3 Flow Shear Stress

Shear stress of rill flow is computed at the end of an average uniform profile length by assuming a rectangular rill geometry. The uniform profile is defined as a profile of constant or uniform gradient, \bar{S} , that passes through the endpoints of the profile. The shear stress from the uniform profile is used as the normalization term for hydraulic shear along the profile as discussed below. Width, w , of the channel at the end of the rill (m) is calculated using the relationship

$$w = c Q_e^d \quad [10.2.7]$$

where Q_e is flow discharge at the end of the slope ($m^3 s^{-1}$), and c and d are coefficients derived from data from the study of Lafien et al. (1987). Discharge rate is given by

$$Q_e = P_r L R_s \quad [10.2.8]$$

where P_r is peak runoff rate ($m s^{-1}$), L is slope length (m), and R_s is the distance between rills (m).

Depth of flow in the rill is computed with an iterative technique using the Darcy-Weisbach friction factor of the rill, the rill width, and the average slope gradient. Hydraulic radius, R (m), is then computed from the flow width and depth of the rectangular rill. Shear stress acting on the soil at the end of the uniform slope, τ_e (Pa), is calculated using the equation

$$\tau_{fe} = \gamma \bar{S} R \left(\frac{f_s}{f_t} \right) \quad [10.2.9]$$

where γ is the specific weight of water ($kg\ m^{-2}\ s^{-2}$), \bar{S} is average slope gradient, f_s is friction factor for the soil, and f_t is total rill friction factor. The ratio of f_s/f_t represents the partitioning of the shear stress between that acting on the soil and the total hydraulic shear stress, which includes the shear stress acting on surface cover (Foster, 1982).

10.2.4 Sediment Transport Capacity

Sediment transport capacity, as well as sediment load, is calculated on a unit rill width basis. Sediment load is converted to a unit field width basis when the calculations are completed. The transport capacity, T_c , as a function of flow shear stress is calculated using a simplified transport equation of the form

$$T_c = k_t \tau_f^{3/2} \quad [10.2.10]$$

where τ_f is hydraulic shear acting on the soil (Pa), and k_t is a transport coefficient ($m^{1/2}\ s^2\ kg^{-1/2}$). Transport capacity at the end of the slope is computed using the Yalin equation. The coefficient, k_t , is calibrated from the transport capacity at the end of the slope, T_{ce} , using the method outlined by Finkner et al. (1989). A representative shear stress is determined as the average of the shear stress at the end of the representative uniform average slope profile and the shear stress at the end of the actual profile. The representative shear stress is used to compute T_{ce} using the Yalin equation and k_t is then determined from the relationship given in Eq. [10.2.10]. Differences between the simplified equation and the Yalin equation, using the calibration technique, are minimal (Finkner et al., 1989).

10.3 Normalizations

10.3.1 Normalized Parameters

The erosion computations are made by solving non-dimensional equations and then redimensionalizing the final solution. By non-dimensionalizing, shear stress and transport capacity can be written as polynomials of x . Thus, the solutions to the detachment and deposition equations are more readily obtained and require less computational time. Conditions at the end of a uniform slope through the endpoints of the given profile are used to normalize the erosion equations. Distance downslope is normalized to the slope length, i.e., $x_* = x/L$. The slope at a point is normalized to the average uniform slope gradient and is expressed as

$$s_* = a x_* + b \quad [10.3.1]$$

where a and b are calculated from slope input data describing the hillslope. Note that a and b need not be, and usually will not be, constant over an entire slope length. Equation [10.3.1] for a given set of a , b values describes a simple slope shape, either convex, concave, or uniform, depending on whether the value of a is positive, negative, or zero. The profile input to the model is processed in such a way as to describe the hillslope in sections of simple slope shapes, and to calculate a , b values for each section.

Shear stress as a function of downslope distance is normalized to shear stress at the end of the uniform slope, τ_{fe} . The function for shear stress vs. downslope distance is derived using the Darcy-Weisbach uniform flow equation and the assumption that discharge varies linearly with x , hence,

$$\tau_f = \gamma \left[\left(\frac{P_f}{C} \right) x s \right]^{2/3} \quad [10.3.2]$$

where C is the Chezy discharge coefficient ($C = (8g/f_t)^{1/2}$). Thus the normalized shear stress acting on the

soil, τ . (where $\tau = \tau_r/\tau_{fc}$), using Eq. [10.3.1] and [10.3.2] and assuming that γ , P_r , and C are constant on the hillslope, is

$$\tau = (a x^2 + b x)^{2/3} \quad [10.3.3]$$

Sediment load normalized to transport capacity at the end of the uniform slope is

$$G_s = \frac{G}{T_{ce}} \quad [10.3.4]$$

Transport capacity normalized to transport capacity at the end of the uniform slope is

$$T_{cs} = \frac{T_c}{T_{ce}} \quad [10.3.5]$$

Since T_{ce} is equal to $k_{t1} \tau_{fc}^{3/2}$, using Eq. [10.2.10] and [10.3.3], then

$$T_{cs} = k_{tr} \tau^{3/2} = k_{tr} (a x^2 + b x) \quad [10.3.6]$$

where k_{tr} is the ratio of k_t (from Eq. [10.2.10]), as calibrated by Finkner et al. (1989), to k_{t1} , the value of the transport coefficient for the uniform representative profile.

The model has four erosion parameters; one for interrill erosion, two for rill erosion, and one for deposition.

10.3.2 Rill Detachment Parameters

The parameters for rill detachment are η and τ_{cn} given by

$$\eta = \frac{L K_r K_{rc} K_{rbr} \tau_{fc}}{T_{ce}} \quad [10.3.7]$$

and

$$\tau_{cn} = \frac{\tau_c \tau_{cc}}{\tau_{fc}} \quad [10.3.8]$$

In these equations K_r and τ_c are the baseline rill erodibility and critical hydraulic shear of the soil as determined under standard conditions as defined by Laflen et al. (1987). Standard conditions for cropland are for unconsolidated bare soil immediately after tillage. Relationships for K_r and τ_c as a function of soil properties were given in Chapter 6. The parameters K_{rc} and τ_{cc} (non-dimensional) are adjustments to erodibility and critical shear to account for soil consolidation with time after tillage, and also for freeze-thaw effects if present. Methods for calculating the consolidation parameters, K_{rc} and τ_{cc} , were developed and presented by Nearing et al. (1988). The parameter K_{rbr} (non-dimensional) represents the effect of below ground residue on sediment generation. Relationships for calculating K_{rbr} were presented by Brown et al. (1989).

10.3.3 Interrill Detachment Parameters

The interrill detachment parameter, θ , is given by

$$\theta = \frac{L D_i}{T_{ce}} \quad [10.3.9]$$

where

$$D_i = K_i I_e^2 C_e G_e \left(\frac{R_e}{w}\right) \quad [10.3.10]$$

in which: K_i is baseline-interrill erodibility, I_e is effective rainfall intensity, C_e is the effect of canopy on interrill erosion, G_e is the effect of ground cover on interrill erosion, R_e is the spacing of rills, and w is the computed rill width (Eq. [10.2.7]). Relationships between baseline interrill erodibility parameters and soil properties are presented in Chapter 6. The canopy effect is estimated by

$$C_e = 1 - F_c e^{-0.34H_c} \quad [10.3.11]$$

where F_c is fraction of the soil protected by canopy cover and H_c is effective canopy height (m) (Lafren et al., 1985). The equation for the ground cover effect on interrill sediment delivery is

$$G_e = e^{-2.5 g_i} \quad [10.3.12]$$

where g_i is fraction of interrill covered by ground cover.

10.3.4 Deposition Parameters

The non-dimensional deposition parameter, ϕ , is given by

$$\phi = \frac{\beta V_f}{P_r} \quad [10.3.13]$$

The equations derived by Foster et al. (1985) are used to compute the diameter, specific gravity, and fractions of the particle classes primary clay, silt and sand, and large and small aggregates as a function of primary sand, silt, and clay fractions and organic matter content of the surface soil horizon. The effective diameter is computed from

$$d_e = e^{\frac{3}{\sum_{i=1}^3 \log(d_i)/3}} \quad [10.3.14]$$

summed over the smallest three size classes where d_e is the effective particle diameter and d_i is the diameter of the particle class. Effective specific gravity is calculated similarly. Fall velocity is computed for a particle class having the effective diameter and effective specific gravity assuming spherical particles and standard drag relationships. A value of $\beta = 0.5$ is assumed for overland flow (Foster et al., 1981).

10.3.5 Normalized Erosion Equations

The model solves the normalized sediment continuity equations. For the case of detachment the normalized equation is

$$\frac{dG_o}{dx_o} = \eta (\tau_o - \tau_{cn}) \left(1 - \left(\frac{G_o}{T_{c_o}}\right)\right) + \theta \quad [10.3.15]$$

where η , τ_{cn} , and θ are the normalized detachment parameters given by Eq. [10.3.7], [10.3.8], and [10.3.9], and G_o , T_{c_o} , and τ_o are the normalized functions of x_o given by Eq. [10.3.3], [10.3.4], and [10.3.6]. Equation [10.3.15] is solved using a Runge-Kutta numerical method.

The normalized deposition equation is

$$\frac{dG_o}{dx_o} = \left(\frac{\phi}{x_o}\right) (T_{c_o} - G_o) + \theta \quad [10.3.16]$$

where ϕ and θ are normalized erosion parameters and G_o and T_{c_o} are functions of x_o presented in the above section. Equation [10.3.16], with substitutions for the normalized terms, has a closed-form solution.

10.3.6 Sediment Yield

Normalized sediment load, G_o , is converted to actual load on a per unit width basis by the formula

$$G = G_o T_{c_o} \left[\frac{w}{R_s} \right] \quad [10.3.17]$$

where G is in terms of $kg\ s^{-1}$ per unit width. Total load for the entire storm event is obtained by multiplying the load per unit time by the effective storm runoff duration, t_r .

10.4 Downslope Variability

The WEPP erosion model calculates soil loss for cases involving downslope variability such as surface roughness cover and canopy differences, soil type, and surface runoff rates. The model does this by dividing the hillslope into homogeneous overland flow elements and treating each element as an independent hillslope with added inflow of water and sediment equal to that coming from the upslope overland flow element. The flow elements may have complex topography, but within each element all other properties are considered homogeneous.

Finkner et al. (1989) presented the method for calculating non-dimensional shear stress and transport capacity for the case of added inflow of water onto an overland flow element. Non-dimensional shear stress becomes

$$\tau_o = (A x_o^2 + B x_o + C)^{2/3} \quad [10.4.1]$$

where

$$A = \frac{a}{(q_{o_o} + 1)} \quad [10.4.2]$$

$$B = \frac{(a q_{o_o} + b)}{(q_{o_o} + 1)} \quad [10.4.3]$$

and

$$C = \frac{b q_{o_o}}{(q_{o_o} + 1)} \quad [10.4.4]$$

In the above equations, q_{o_o} is non-dimensional influx of water onto the overland flow element given by

$$q_{o_o} = \frac{q_o}{P_r L} \quad [10.4.5]$$

where q_o ($m^2\ s^{-1}$) is the inflow of water at the top of the element. Non-dimensional transport capacity for

the case of added inflow of water becomes

$$T_{c^*} = k_{tr} (A x^2 + B x + C) \quad [10.4.6]$$

Solutions of the detachment and deposition equations for the case of strips remain similar as for the case of no inflow except that the boundary conditions for inflow of sediment change to account for sediment influx at the top of the strip. The form of the deposition equation and its analytic solution also changes slightly. The denominator of the first term on the right side of Eq. [10.4.4] becomes $x^* + q_{o^*}$. Calculation of water and sediment from the strip act as boundary conditions for the next strip downslope.

10.5 Sediment Enrichment

Sediment enrichment refers to the mass fraction increase of the more chemically-active fine sediment particles (silt, clay, and organic matter) due to selective deposition of coarser sediment. The WEPP model predicts the particle size distribution and composition of detached sediment based on the primary sand, silt, clay, and organic matter content of the *in situ* soil (Foster et al., 1985). When flow is routed through a deposition region, a new particle size distribution must be computed.

Equation [10.3.16] was solved for G_* for the case of added inflow, since the solution had to be general enough to perform with the downslope variability possible in the model. The solution is:

$$G_* = (x_* + q_{o^*})^{-\phi} \left[\frac{\phi k_{tr} A}{\phi + 2} (x_* + q_{o^*})^{\phi+2} + \frac{(\phi k_{tr} B + \theta - 2k_{tr} A \phi q_{o^*})}{\phi + 1} (x_* + q_{o^*})^{\phi+1} + k_{tr} (A q_{o^*}^2 - B q_{o^*} + C) (x_* + q_{o^*})^{\phi} \right] + K (x_* + q_{o^*})^{-\phi} \quad [10.5.1]$$

The constant of integration, K , was obtained by imposing the boundary condition at the upper edge of a deposition region. At this point, $x_* = x_{u^*}$ and $G_* = G_{u^*}$, and K is:

$$K = (x_{u^*} + q_{o^*})^{\phi} \left[G_{u^*} - \frac{\phi k_{tr} A}{\phi + 2} (x_{u^*} + q_{o^*})^2 - \frac{\phi k_{tr} B + \theta - 2k_{tr} A \phi q_{o^*}}{\phi + 1} (x_{u^*} + q_{o^*}) - k_{tr} (A q_{o^*}^2 - B q_{o^*} + C) \right] \quad [10.5.2]$$

Equations [10.5.1] and [10.5.2] are solved for the 5 individual particle size classes at $x_* = x_{u^*}$, the end of the deposition region. A total exiting load is computed, and fractions exiting the region are calculated. A check is performed to insure that mass is conserved within each size class, so that the amount of a particle type predicted to be leaving a region cannot exceed that entering plus the interrill contribution in the region. If exiting load in a class is too high, the excess load is distributed among the other classes.

Several of the equation variables have to be partitioned among the particle classes. The deposition parameter, ϕ , is computed for each class using Eq. [10.3.13] with a fall velocity for the class found using the class diameter and specific gravity. The interrill detachment parameter, θ , is multiplied by the fraction of each class in detached sediment. The transport coefficients A , B , and C are proportioned for each particle class based on the fractions of transport capacity computed using the Yalin equation when the shear stress at the end of the slope is the average of the shear stresses calculated using the actual end slope and the average slope.

G_{u^*} is multiplied by the current sediment fractions in the flow at the point on the profile where deposition is predicted to begin. As sediment is routed downslope through detachment and deposition regions, the fraction of each particle size class is updated. At the top of the first deposition region on a

hillslope the incoming sediment fractions are the same as those for the detached sediment. At a subsequent deposition region, the fractions of sediment exiting the detachment region above are computed using:

$$f_{out}(i) = \frac{f_{in}(i) G_{in} + f_{det}(i) (G_{out} - G_{in})}{G_{out}} \quad [10.5.3]$$

where $f_{out}(i)$ is the fraction of a size class leaving the detachment region (entering the next deposition region or exiting an overland flow element), $f_{in}(i)$ is the fraction in the flow determined at the end of the previous deposition region, $f_{det}(i)$ is the fraction of detached sediment for a size class, G_{in} is non-dimensional sediment load at the end of the previous deposition region, and G_{out} is non-dimensional sediment load at the end of the current detachment region or overland flow element.

At the end of each overland flow element an updated sediment size distribution is computed using Eq. [10.5.3], and then an enrichment ratio of the specific surface area is also calculated using:

$$ER = \frac{SSA_{sed}}{SSA_{soil}} \quad [10.5.4]$$

where ER is enrichment ratio, SSA_{sed} is the specific surface area of the sediment (m^2g^{-1}), and SSA_{soil} is the specific surface area of the *in situ* soil (m^2g^{-1}) (USDA, 1980). The specific surface area of the sediment is computed using:

$$SSA_{sed} = \sum_{i=1}^5 f_{out}(i) \left[\frac{frsnd(i) * ssasnd + frslt(i) * ssaslt + frcly(i) * ssacly}{1 + frorg(i)} + \frac{frorg(i) * ssaorg}{1.73} \right] \quad [10.5.5]$$

where $frsnd(i)$, $frslt(i)$, $frcly(i)$, and $frorg(i)$ are the fractions of sand, silt, clay, and organic matter comprising each particle class, respectively, and $ssasnd$, $ssaslt$, $ssacly$, and $ssaorg$ are the specific surface area for sand, silt, clay, and organic carbon, respectively. Values for the specific surface area used in the model computations were 0.05, 4.0, 20.0, and 1000.0 m^2/g of sand, silt, clay, and organic carbon, respectively, as used in the CREAMS model (Foster et al., 1980).

The specific surface area of the surface soil is computed using:

$$SSA_{soil} = \frac{orgmat * ssaorg}{1.73} + \frac{sand * ssasnd + silt * ssaslt + clay * ssacly}{1 + orgmat} \quad [10.5.6]$$

where $sand$, $silt$, $clay$, and $orgmat$ are the fractions of sand, silt, clay, and organic matter in the surface soil, respectively.

Typical values for enrichment ratios are between 1.0 and 3.0, though the range can be from 0 to greater than 8. Some high silt soils have ratios less than 1.0 due to deposition of aggregates containing large amounts of clay and organic matter which increases the less chemically-active primary silt fraction. The procedure described here does not address the problems that occur when multiple overland flow elements composed of different soil types are input. Each element will possibly have aggregates of different sizes and composition, which will mix with the incoming sediment from the previous element. This could affect enrichment ratio values since the specific surface area of the soil is for the current flow element, and the actual sediment may have arrived from somewhere upslope and have an entirely different composition. In practice this may not be a serious problem if the various soil types present are not greatly different in composition, or if there is a region of significant detachment in each flow element.

10.6 Summary

The WEPP erosion model uses a steady state sediment continuity equation as the basis for describing the movement of suspended sediment in a rill. Like other recent erosion models, such as the one used in CREAMS (Foster et al., 1981), the WEPP erosion model calculates erosion from rill and interrill areas and uses the concept that detachment and deposition rates in rills are a function of the portion of the transport capacity which is filled by sediment. Unlike other recent models, the WEPP erosion model partitions runoff between rill and interrill areas and calculates shear stresses based on rill flow and rill hydraulics rather than sheetflow (Page, 1988).

The model presented here does not rely on USLE relationships for parameter estimation. Erodibility parameters are based on the extensive field studies of Laflen et al. (1987) and Simanton et al. (1987) which were specifically designed and interpreted for the erosion model. Temporal variations of erodibility are based on the consolidation model of Nearing et al. (1988). Adjustments due to cropping-management effects are directly represented in the model in terms of plant canopy, surface cover, and buried residue effects on soil detachment and transport. These adjustments are made possible with the plant growth and residue decomposition routines in the WEPP model. Finally, because the WEPP erosion routines make use of daily water balance and infiltration routines which are spatially varied, the model can calculate erosion for the case of non-uniform hydrology on hillslopes.

10.7 References

1. Brown, L.C., G.R. Foster, and D.B. Beasley. 1989. Rill erosion as affected by incorporated crop residue. TRANS ASAE (in press).
2. Finkner, S.C., M.A. Nearing, G.R. Foster, and J.E. Gilley. 1989. Calibrating a simplified equation for modeling sediment transport capacity. TRANS ASAE (in press).
3. Foster, G.R. 1982. Modeling the erosion process. p. 297- 360. In: C.T. Haan (ed.), Hydrologic Modeling of Small Watersheds. ASAE Monograph No. 5. Am. Soc. Agric. Eng., St. Joseph, MI.
4. Foster, G.R., L.J. Lane, and J.D. Nowlin. 1980. A model to estimate sediment yield from field sized areas: Selection of parameter values: In: CREAMS - A Field Scale Model for Chemicals, Runoff, and Erosion from Agricultural Management Systems. Vol. II: User Manual. Conservation Research Report No. 26. USDA, Sci. and Educ. Admin. Chap. 2. pp 193-195.
5. Foster, G.R., L.J. Lane, J.D. Nowlin, J.M. Laflen, and R.A. Young. 1981. Estimating erosion and sediment yield on field-sized areas. TRANS ASAE 24:1253-1262.
6. Foster, G.R., R.A. Young, and W.H. Neibling. 1985. Sediment composition for nonpoint source pollution analyses. Trans. ASAE 28:133-139.
7. Laflen, J.M., G.R. Foster, and C. Onstad. 1985. Simulation of individual storm soil losses for modeling the impact of soil erosion on cropland productivity. In: El-Swaify, Moldenhauer, and Lo (Eds.) Soil Erosion and Conservation, pp. 285-295. SCSA, Anakey, IA.
8. Laflen, J.M., A. Thomas, and R. Welch. 1987. Cropland experiments for the WEPP project. ASAE paper no. 87- 2544, Am. Soc. Ag. Engrs., St. Joseph, MI.
9. Nearing, M.A., L.T. West, and L.C. Brown. 1988. A consolidation model for estimating changes in rill erodibility. TRANS ASAE. 31:696-700.
10. Page, D.I. 1988. Overland flow partitioning for rill and interrill erosion modeling. M.S. Thesis, Univ. of Arizona, Tucson, AZ. 112pp.
11. Simanton, J.R., L.T. West, M.A. Weltz, and G.D. Wingate. 1987. Rangeland experiments for water erosion prediction project. ASAE paper no. 87-2545.

12. U.S. Department of Agriculture (USDA), 1980. CREAMS - A Field Scale Model for Chemicals, Runoff, and Erosion from Agricultural Management Systems. Conservation Research Report No. 26. USDA, Sci. and Educ. Admin. 643 pp.

10.8 List of Symbols

Symbol	Definition	Units	Variable
A	coefficient for shear stress	NOD	ainf
B	"	NOD	binf
C	"	NOD	cinf
C	Chezy discharge coef.	$m^{1/2}s^{-1}$	chezch
C_e	canopy effect coefficient	na	caneff
D_c	detachment capacity		
	by flow	$kg/s \cdot m^2$	na
D_f	rill erosion rate	$kg/s \cdot m^2$	na
D_i	interrill erosion	$kg/s \cdot m^2$	detinr
ER	enrichment ratio of		
	specific surface area	NOD	enrato
F_c	fraction of soil protected		
	by canopy cover	NOD	cancov
G	sediment load	$kg/s \cdot m$	na
G_e	effect of ground cover		
	on interrill erosion	NOD	grdeff
G_n	sediment load normalized		
	to transport capacity	NOD	load
G_{n^*}	normalized sediment load		
	at top of deposition region	NOD	ldtop
G_{in^*}	normalized sediment load		
	at top of detachment region	NOD	lddend
G_{out^*}	normalized sediment load		
	at end of deposition region		
	or end of flow element	NOD	ldtop
H_c	effective canopy height	m	canhgt
I_e	effective rainfall rate	m/s	effint
K_i	interrill soil erodibility		
	parameter	$kg \ s / m^4$	ki
K_r	rill erodibility		
	parameter	s/m	kr
L	slope length	m	slplen
P_r	peak runoff rate	m/s	peakro
Q_e	flow discharge at end of slope	m^3/s	qshear
R	hydraulic radius	m	hydrad
R_s	distance between rill	m	rspace
\bar{S}	average slope gradient	NOD	avgslp
SSA_{sed}	specific surface area		
	of exiting sediment	m^2/g	sumssa
SSA_{soil}	specific surface area		
	of surface soil	m^2/g	ssasol
T_c	sediment transport		
	capacity in rill	$kg/s \cdot m$	na

T_c	transport capacity normalized to transport capacity at end of uniform slope.	NOD	tcap
V_f	effective fall velocity of particles	m/s	veleff
V_t	total runoff volume	m	runoff
c	coefficient	NOD	wcoef
d	coefficient (= 0.3)	na	nd
d_e	effective particle diameter	m	diaeff
d_i	diameter of particle class	m	dia
$f_{da}(i)$	mass fraction of detached sediment	NOD	frac
$f_{ia}(i)$	sediment mass fraction at top of detachment region	NOD	frclw
$f_{oa}(i)$	sediment mass fraction at end of detachment region or end of flow element	NOD	frclw
f_s	friction factor for soil	NOD	frcsol
g_i	fraction of interrill area with surface cover	NOD	inrcov
k_i	transport coefficient	$m^{1/2} s^2 kg^{-1/2}$	kt
q	flow discharge per unit width	m^2/s	
q_o	inflow of water at top	NOD	m^2/s
q_o^*	non-dimensional influx of water onto strip	NOD	qostar
t_c	total time during which the rainfall rate exceeds infiltration rate	s	durrun
t_r	effective runoff duration	s	effdm
w	width of channel at end of the rill	m	width
x	distance down slope	m	na
x_o	normalized downslope distance	NOD	xinput
$clay$	fraction of clay		
$frcl(i)$	fraction of clay in particle class i	NOD	frcly
$frorg(i)$	fraction of organic matter in class i	NOD	frorg
$frslt(i)$	fraction of silt in particle class i	NOD	frslt
$frsnd(i)$	fraction of sand in particle class i	NOD	frsnd
$orgmat$	fraction of organic matter in surface soil	NOD	orgmat
$sand$	fraction of sand in surface soil	NOD	sand
$silt$	fraction of silt in surface soil	NOD	silt

<i>ssacly</i>	specific surface area of clay		
<i>ssaorg</i>	specific surface area of organic carbon	m^2/g	<i>ssacly</i>
<i>ssaslt</i>	specific surface area of silt	m^2/g	<i>ssaorg</i>
<i>ssasnd</i>	specific surface area of sand	m^2/g	<i>ssaslt</i>
β	coefficient reflecting raindrop-induced turbulence	m^2/g	<i>ssasnd</i>
γ	specific weight of water	NOD	beta
η	non-dimensional rill parameter	$kg/m^2 \cdot s^2$	gamma
ϕ	non-dimensional deposition parameter	NOD	cata
θ	interrill parameter	NOD	phi
τ_0	normalized shear stress	NOD	theta
τ_c	rill detachment threshold parameter (critical shear stress)	NOD	shear
τ_f	flow shear stress	Pa	shcrit
τ_{fc}	shear stress acting on soil at end of uniform slope.	Pa	na
		Pa	shrsol

Chapter 11. PARAMETER IDENTIFICATION FROM PLOT DATA

M. A. Nearing, M. A. Weltz, S. C. Finkner,
J. J. Stone, and L. T. West

11.1 Introduction

An extensive field research program was initiated for the purpose of developing relationships to estimate parameter values for the WEPP profile erosion model. Three major projects were identified in terms of the parameterization efforts, those being one for cropland, one for rangeland, and one for forestland. Test site locations for these three efforts are shown in Fig. 11.1.1. Numerous other experimental efforts were completed to complement the three major efforts and to address some of the needs that were not accounted for in the three projects mentioned above.

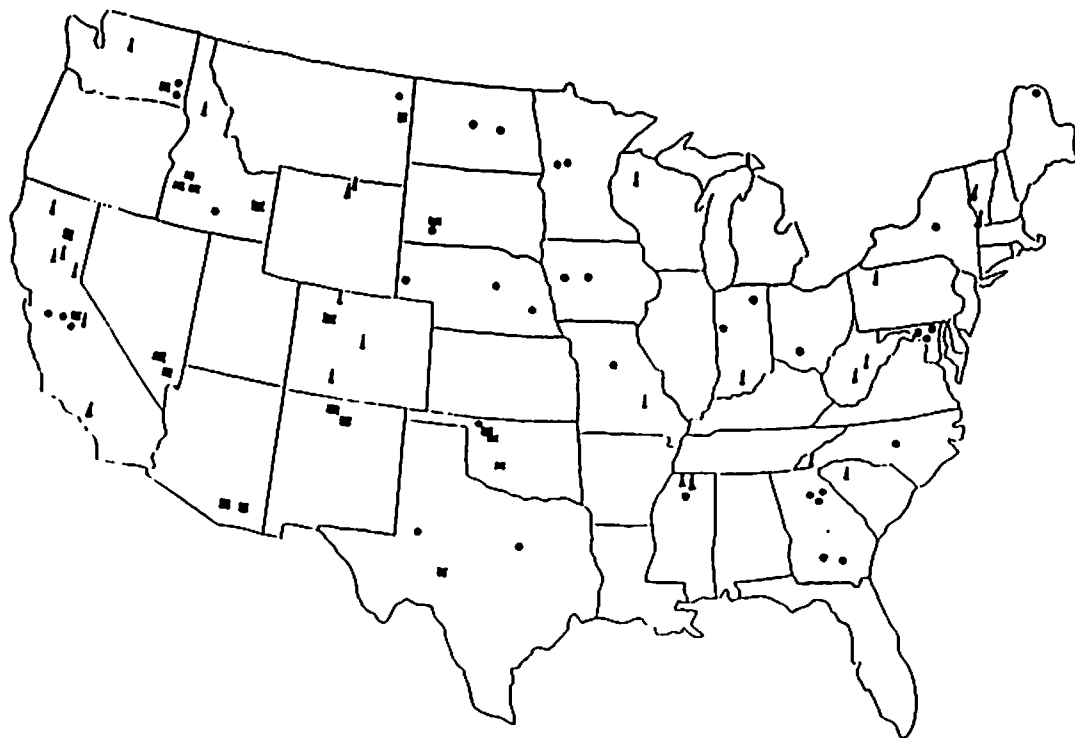


Fig. 11.1.1. Baseline erodibility test locations.

The cropland experiments for the WEPP consisted of using rainfall simulation techniques to develop relationships for infiltration, rill erodibility, and interrill erodibility parameters as a function of soil properties on "baseline" soil conditions. Baseline conditions for cropland were defined as those for bare soil immediately after complete disturbance by tillage with no buried or surface residue present. For the case of rangelands, no clear definitions of a baseline condition were delineated at the start of the experiments. Rainfall simulation experiments on rangelands began with the stated objectives of defining a baseline condition on rangeland sites and determining infiltration and erosion parameter relationships as a function of soil, living plant, and plant residue cover factors. Forestland experiments focused on conditions most susceptible to erosion, those being primarily forest roads and recently harvested areas.

Other experiments were designed and carried out to study specific elements of erosion mechanics to develop relationships necessary to the model. Experiments in Lafayette, IN; Columbia, MO; and Temple, TX; were conducted to derive parameter values related to temporal changes in soil erodibility on cropland. Studies in Lincoln, NE; Tombstone, AZ; and Lafayette, IN; were conducted to derive relationships for rill and interrill hydraulic friction factors. Studies in Columbia, MO, and Watkinsville, GA, were designed to evaluate the effects of root biomass on erosion parameters. A study in Lafayette, IN, was carried out to relate buried residue amounts to reductions in rill erodibility.

This chapter reports some of the techniques that were used to evaluate the field experimental data to derive parameter values for the WEPP model.

11.2 Erodibility Parameters

Erosion in the WEPP model is divided between rill and interrill processes, with separate and different erodibility parameters for each process. Interrill erodibility is defined as the proportionality constant between sediment delivery from interrill areas and rainfall intensity squared. Sediment transport on the interrill areas is considered implicitly in the interrill slope function (Chapter 10); the interrill erosion functions do not use runoff, flow shear stress, or sediment transport terms to differentiate between interrill soil detachment, deposition, transport, and sediment delivery to rills.

Rill erosion is represented in the model as a linear function of flow shear stress in the concentrated flow areas on the soil surface. The rill erodibility parameters represent the linear coefficients which relate soil detachment in rills (by clear water) to flow shear stress. Thus rill erosion is a function of hydraulic parameters (i.e., shear stress) which depend on runoff volume, infiltration, etc..., but the rill erodibility parameters for a given soil are independent of any hydraulic parameters. Thus, rill erodibility is independent of soil permeability or infiltration.

Interrill erodibility parameters for cropland and rangeland experimental sites are calculated from the sediment delivery from small (0.5 by 0.75 m) plots and the rainfall intensity applied to the plots. Interrill erodibility parameters were related to soil properties (Chapter 6) using data from the baseline (disturbed) experiments on croplands.

Rill erodibility on the cropland sites was determined using preformed rills and measuring the hydraulic parameters in the rills necessary to calculate flow shear stresses and the sediment delivery from the rills. Varying levels of added inflow to the upper ends of the rills were used to provide multiple levels of shear stress in the rills. For rangeland sites large (10.7 by 3.05 m) plots were used with varying levels of inflow added to the upper ends of the plots. Shear stresses and sediment discharge in individual rills on the rangeland plots could not be determined, so that a direct relationship between flow shear and sediment yield could not be determined for the range sites. Rill erodibility parameters for the range sites were determined using an optimization technique that finds the erodibility parameters giving the best fit between measured soil loss and soil loss as calculated by the model (Nearing et al., 1989).

11.3 Infiltration parameters

The two parameters of the Green and Ampt infiltration equation, K_s (saturated conductivity) and P_{si} (matric potential across the wetting front) were developed from the WEPP rainfall simulator field data. K_s was estimated using the very wet run data, P_{si} was estimated using the dry run data, and the values of the parameters were tested using the wet run data.

Saturated conductivity: K_s was estimated as

$$K_s = i_e - q_e \quad [11.3.1]$$

where i_e is rainfall application rate at equilibrium (L/T), and q_e is runoff rate at equilibrium (L/T).

The equilibrium rates above are those for the very wet run at 5 inch per hour rainfall application rate. This method assumes that the soil is saturated enough and the application rate is high enough so that the final infiltration is reached.

Matric potential: P_{si} was estimated as

$$P_{si} = \frac{N_s}{(1 - sat) por} \quad [11.3.2]$$

where N_s is effective matric potential (L), sat is soil saturation before the run (L/L), and por is soil porosity (L/L).

N_s was estimated by solving the Green and Ampt equation for N_s as

$$N_s = \frac{F(f - K_s)}{K_s} \quad [11.3.3]$$

where F is total cumulative infiltration amount (L), f is final infiltration rate (L/T), and K_s is saturated conductivity as estimated from the very wet run (L/T).

When Eq. [11.3.3] is used with data from the dry run, it can be written as

$$N_s = \frac{(P - Q) [(i_f - q_f) - K_s]}{K_s} \quad [11.3.4]$$

where P is total rainfall volume (L), Q is total runoff volume (L), i_f is rainfall rate at the end of the run (L/T), and q_f is runoff rate at the end of the run (L/T).

The above method of estimating P_{si} and N_s is extremely sensitive to the value of K_s obtained from the very wet run (Eq. [11.3.1]). If the equilibrium runoff rate is very close to the application rate during the very wet run, then the denominator in Eq. [11.3.4] approaches zero which yields unrealistic values for N_s .

The values for K_s and P_{si} obtained by the methods outlined above were tested with the data from the wet run. The effective matric potential was calculated by rearranging Eq. [11.3.2] and solving for N_s using P_{si} obtained from the dry run, soil porosity and soil saturation before the wet run.

11.4 Hydraulic Roughness Coefficients

11.4.1 Introduction

Total hydraulic roughness on a site may be influenced by both soil surface conditions and ground cover (crop residue, vegetative materials, stones, etc.). Soil roughness may be a combination of hydraulic roughness for a smooth, bare soil plus depressional roughness. Field and laboratory experiments were conducted to allow estimates of hydraulic roughness for a wide range of cropping and management conditions.

11.4.2 Soil Surface Induced Roughness

Soil micro-relief may affect flow hydraulics. Random roughness measurements have been used to identify relative differences in micro-relief. A considerable amount of information exists in the literature on random roughness values induced by various tillage implements. However, procedures were not available for using random roughness values to estimate soil surface induced hydraulic roughness.

A field study was therefore initiated to measure hydraulic roughness coefficients for a wide range of random roughness conditions, and to develop regression equations which relate hydraulic roughness

coefficients to random roughness parameters. Six tillage implements were used to produce surfaces having widely varying roughness characteristics. Sixty plots, on which varying amounts of simulated rainfall was applied, were established. From information collected on the plots, regression equations were developed that related friction factors to the random roughness of the surfaces, and to reductions in random roughness caused by rainfall. Input variables for the regression equations include type of tillage implement, and total cumulative rainfall since the last tillage operation. Information collected at the field site was also used to identify hydraulic roughness for a smooth, bare soil on interrill areas. Details of the experimental procedures, and development and testing of the predictive equations are given by Finkner (1988).

Information collected from the cropland rainfall simulation program was used to determine soil surface induced friction factors for rills (Chapter 9). The friction coefficient was evaluated for Amarillo, Heiden, Sharpsburg, Sverdrup, and Wala Wala soils. Soil texture was found to significantly influence rill friction factors. A regression equation was developed which related hydraulic roughness to sand and clay fractions.

11.4.3 Ground Cover Induced Roughness

The effect of residue cover on hydraulic roughness coefficients is assumed to be the same for both rill and interrill areas. A laboratory study was conducted to measure hydraulic roughness coefficients for selected types and rates of crop residue, and develop regression equations relating residue induced friction factors to residue rates over a broad range of flow conditions.

Laboratory tests have been completed on corn, cotton, grain sorghum, peanut, soybean, sunflower, and wheat residue. Input variables for the regression equations include either percent residue cover or residue weight. A series of field experiments are planned to further test the laboratory derived relationships.

Runoff plot data obtained from the WEPP rangeland simulation program will be used to identify vegetative induced hydraulic roughness coefficients. Optimization techniques will be employed to fit calculated hydrographs to the observed hydrographs. The hydraulic roughness coefficients obtained from hydrograph fitting will then be related to vegetative characteristics identified at each of the rangeland sites. Generalized regression relationships will then be developed which related hydraulic roughness coefficients to selected vegetative characteristics.

11.5 Soil Parameters

11.5.1 Introduction

The objectives of the WEPP experimental program were to measure erodibility and infiltration parameters of cropland and rangeland sites and to soil properties to develop relationships that can be used to predict the erodibility and infiltration parameters for other soils. This section describes the samples that were collected from each of the WEPP rainfall simulation sites, the protocol for collecting the samples, and the field and laboratory measurements that were used to characterize the physical, chemical, biological, and mineralogical properties of the soils.

11.5.2 Field Measurements

At each rainfall simulation site, bulk density and soil strength indices were measured in the field at the time of rainfall simulation. These properties are potentially important for estimation of soil erodibility parameters and can easily be measured in the field as part of the site evaluation for application of the erosion prediction methodology.

For the cropland sites, field measurements taken were bulk density from 0 to 2 cm and 2 to 5 cm by the compliant cavity method, unconfined compressive strength index with the pocket penetrometer, and

shear strength indices with the torr vane, Pilcon hand vane, and Swedish fall cone. The locations of the measurements within the plot are shown in Fig. 11.5.1. Bulk density was measured immediately prior to initiation and after completion of the rainfall simulation sequence (Lafren et al., 1987). Strength indices were measured after rainfall, after rainfall plus added inflow, and after added inflow without rainfall. Pocket penetrometer, torr vane, and Pilcon hand vane measurements were made on both the rill side slope and the rill bottom at each location. Fall-cone measurements were made only of the rill bottom.

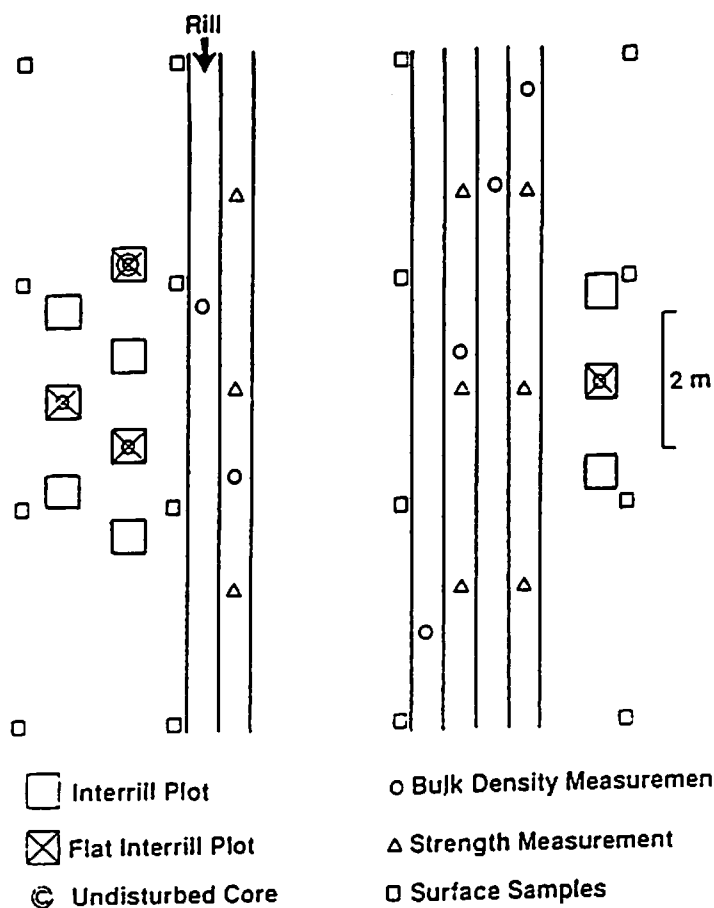


Fig. 11.5.1. Location of soil measurements and soil surface samples for rainfall simulator plots.

Field measurements for the rangeland sites were similar to those on cropland. However, because of coarse fragments in the soils, Pilcon hand vane measurements are impractical and were omitted. Also, the strength of the surface crust on these undisturbed sites was not penetrable with the fall cone, and this strength measurement was also omitted. The other measurements; bulk density, torr vane, and pocket penetrometer, were made on each of the two bare plots at each site (Simanton et al., 1987). Locations of the measurements within the plot are illustrated in Fig. 11.5.2. The locations of the strength index measurements correspond to the locations of point counts of vegetation and soil surface cover previously made on the plot (Simanton et al., 1987). Strength index measurements were made immediately after the dry run and the very wet run (Simanton et al., 1987).

Three bulk density measurements were made in an area adjacent to the interrill plots before rainfall. After completion of the rainfall sequence, three bulk density measurements were made in the covered interrill plots, in the uncovered interrill plots, in unrilled areas of the large plots, and in rilled areas of the

large plots if rills were present. At rangeland sites that have a vegetative community that includes shrubs, bulk density was measured under shrubs and in intershrub areas to evaluate vegetation effects on bulk density.

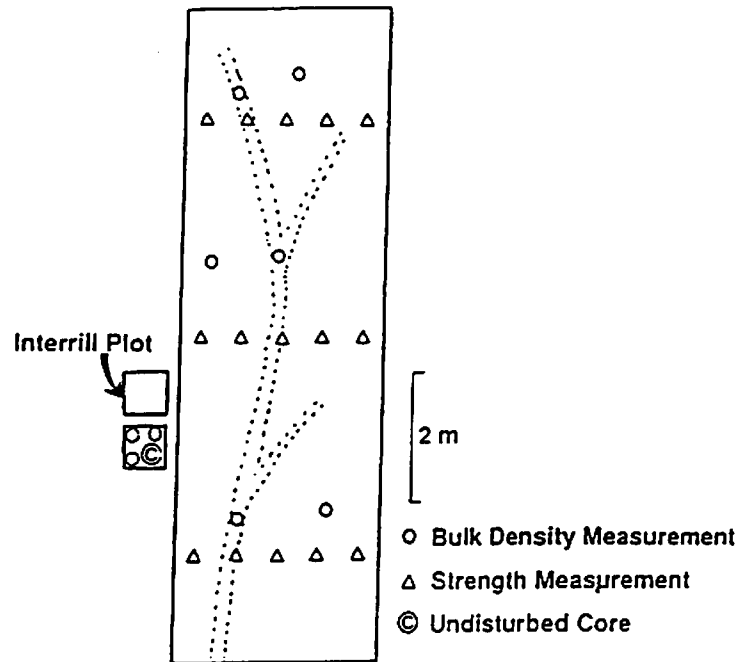


Fig. 11.5.2. Location of soil measurements for rangeland rainfall simulator plots.

11.5.3 Soil Samples and Analyses

Two types of soil samples were collected from each of the WEPP rainfall simulator sites tested in 1987 and 1988, and each were used for different types of soil measurements that were thought potentially useful for predicting soil erodibility parameters. Sample types were: 1) pedon samples from each soil horizon for characterization by the Soil Conservation Service National Soil Survey Laboratory (SCS NSSL); and 2) bulk samples of the surface horizon in the aggregation state at the time of rainfall simulation that were used for analyses of the soils and for current and future laboratory studies of erosion processes.

11.5.3.1 Pedon Samples

Site Selection and Sampling Protocol

Cropland sites: Because soils are not spatially uniform, one of the major tasks in selecting and sampling a site for field experiments is insuring that the soil within the plot area is uniform and that the soil sampled represents soil conditions over all or at least a major portion of the plot. Thus, a detailed plan was developed to evaluate soil variability within potential sites before final selection and sampling. The evaluation of potential sites consisted of brief morphological examination to a depth of 0.5 m of 22 pedons around the perimeter of the site (Fig. 11.5.3). From these observations, one pedon representative of each side of the plot area was described in detail to a depth of 1 m. If these four pedons were similar in terms of expected erosion related behavior, the site was used for the rainfall simulation experiments.

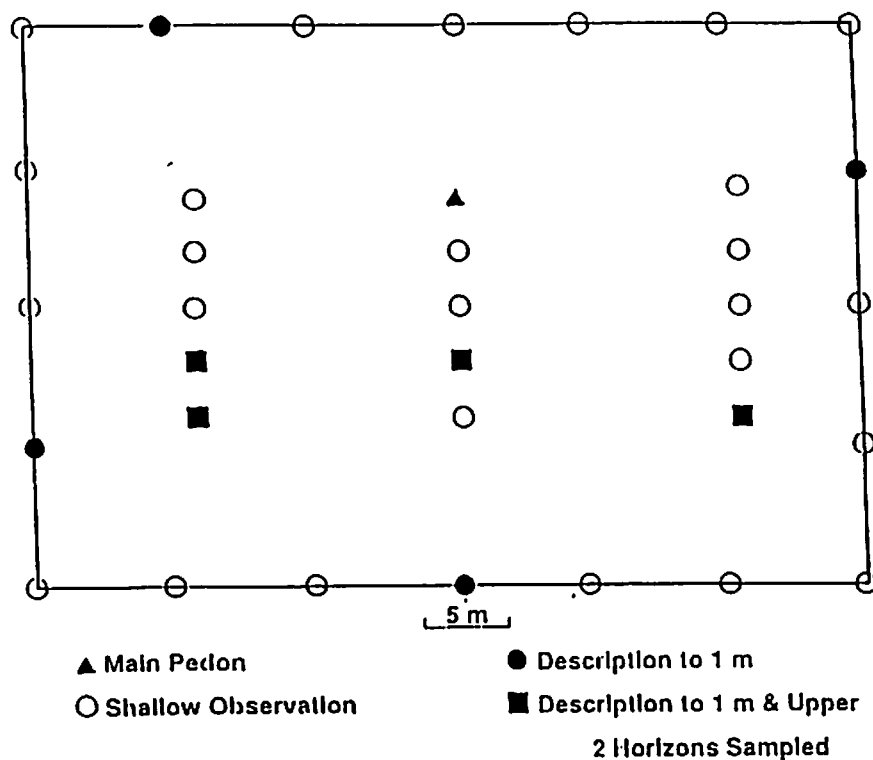


Fig. 11.5.3. Location of soil observations, descriptions, and pedon samples for rainfall simulator sites.

To insure that the pedon sampled within the plot area was representative and that any changes in properties within the plot were well documented, 15 additional pedons within the plot area were examined to a 0.5 m depth (Fig. 11.5.3). From these observations, the pedon for complete description and sampling was selected to represent the dominant soil condition. This pedon was described using standard terminology (Soil Survey Staff, 1981), and bulk samples and Saran-coated clods were collected from each horizon. In addition to this "mother pedon," four satellite pedons selected to represent both the dominant and minor soil conditions within the plot were described in detail to a depth of 1 m and the upper two horizons sampled. In the descriptions of the soils, emphasis was placed on properties of the upper horizons, especially the presence of traffic pans or other features that may impact runoff and erosion.

Rangeland sites: For rangeland sites with uniform surface condition, the procedure used to evaluate potential sites was identical to that used for cropland sites. However, in some semi-arid and arid rangeland areas, surface soil characteristics are related to the vegetation and may vary over short distances. This type of variability further complicates selecting a site with uniform soil characteristics and sampling a representative pedon. For potential rainfall simulation sites where this short-range variability occurred, detailed observations were made outside the plot area to determine the vegetation and surface condition relationships, and the 22 perimeter observations were made in areas with the dominant surface condition rather than at preselected distances. As with the cropland sites, one representative pedon on each side of the plot area was described to 1 m, and these pedons were used to determine the suitability of a site.

In areas without short-range surface condition variation, the sampling procedures were the same as those used for cropland. In areas with short-range variability, six pedons within large areas of the

dominant surface condition were briefly examined to a depth of 0.5 m. From these observations, one pedon was chosen for complete characterization, and an additional pedon was chosen for description to 1 m and sampling of the two upper horizons. In addition to the dominant surface condition, six pedons in minor components that comprised more than 20% of the plot area were briefly examined to 0.5 m. From these six pedons, two were described and sampled to and including the first horizon that was similar to the dominant component.

In addition to samples from each horizon of the main pedon at each cropland and rangeland site, about 80 kg of the upper part of the subsoil was collected at the time that the pedon samples are taken. These samples will not be analyzed immediately. They were stored for future reference and possible erosion studies of subsoil material.

Laboratory Analyses

The various laboratory analyses that were performed on the pedon samples are listed in Table 11.5.1. The procedures used for the analyses are outlined in Soil Survey Investigations Report No. 1 (Soil Survey Staff, 1972; 1984). Most of the measurements were made on air-dried soil material that was crushed to pass a 2 mm sieve. Bulk density and low-tension water contents were measured on Saran-coated clods (Brasher et al., 1966). Data from the particle size and fabric related analyses were used with infiltration data collected during rainfall simulation to verify infiltration relationships in the model.

Table 11.5.1. Soil measurements for pedon samples.

Particle-size analyses
Coarse fragments 20-5 mm and 5-2 mm
Sand, 5 fractions; 2-1 mm, 1-0.5 mm, 0.5-0.25 mm, 0.25-0.10 mm, 0.10-0.05 mm
Silt, 2 fractions and total; 0.05-0.02 mm, 0.02-0.002 mm, 0.05-0.002 mm
Clay, 2 fractions and total; coarse, 0.002-0.0002 mm; fine, < 0.0002 mm; total, < 0.002 mm
Water dispersible total clay
Carbonate clay (calcareous samples only)
Fabric-related analyses
Moist and oven-dry bulk density from clods
Coefficient of linear extensibility (COLE)
Water retention differences (WRD)
Water release curve with tension of 1/10 or 1/3 bar (1/10 bar for sandy textures, 1/3 bar for other textures), 2-bar, 15 bar, and total porosity with Baumer model
Reconstituted bulk density and test for crusting propensity (experimental)
Cation exchange analyses
Bases extractable with ammonium acetate
Extractable acidity at pH 8.2
Al extractable by KCl (only when pH < 5.2)
Cation exchange capacity by ammonium acetate method
Cation exchange capacity by summing base and acidity
Effective cation exchange capacity by summing bases and Al
Exchange Na percent (where applicable only)

Table 11.5.1. Soil measurements for pedon samples. (Cont.)

Soluble salts
"Quick" electrical conductivity where salts suspected and the following analyses made if salt detected.
Electrical conductivity of saturation extract
Cations and anions of saturation extract
Computed total salts
Sodium adsorption ratio
Other chemical analyses
Organic C
Total C
Total N
Dithionite-citrate extractable Fe and Al
pH (1:1 in water)
pH (1:2 in CaCl ₂)
Calcium carbonate equivalent (where applicable)
Gypsum (where applicable)
Mineralogical analyses (total clay fraction)
X-ray diffraction analysis and interpretation (qualitative to semi-quantitative)
Differential scanning calorimetry
Total chemical analysis (K, Fe, Si, Al)
CEC/Clay
General interpretation of mineralogy

The complete set of analyses (Table 11.5.1) was not made on every sample. For horizons below the uppermost two horizons (third horizon and below), crusting tests and measurement of fine clay, water dispersible clay, reconstituted bulk density, and total carbon were omitted. Mineralogical analyses were made only for the A horizon and one or two major horizons below the A horizon. Additionally, for the rangeland and forestland rainfall simulation sites that were selected for reasons other than to represent a range of soil properties (Alberts et al., 1987), only the major horizons to and including the first horizon strongly limiting to water movement within the soil were analyzed. These sites are considered to be of less future interest from a soil's aspect than the other sites selected solely for the soils represented.

11.5.3.2 Soil Surface Samples

Sampling Protocol

Disturbed samples collected from the soil surface horizon of each rainfall simulation site immediately prior to rainfall application were used for a variety of purposes. The first was to have samples of the surface horizon as it existed in the field immediately prior to rainfall simulation for laboratory measurements of aggregate and mechanical properties. In addition to these measurements, these samples were used in several planned laboratory experiments at various locations. The remaining samples were stored and made available for future erosion studies.

Because the tilled condition of the cropland sites can be more easily approximated in the laboratory than the undisturbed condition of the rangeland sites, most of the laboratory-based erosion studies

currently planned will use samples from the cropland sites only. To meet the needs of these experiments and to have sample remaining for future studies, about 360 kg of the tilled surface of the cropland sites will be collected. A smaller quantity, about 40 kg, was collected from the undisturbed rangeland and forestland simulator sites.

Again, because of soil variability, a sampling scheme was designed to insure that the sample collected was representative of the conditions present in the plot. Cropland samples were collected as 16 subsamples of 20 kg each arrayed in a grid of four rows and four columns. At the laboratory, each subsample was dried, and the four subsamples from each column were mixed. A sample from each of these four subsamples was retained for analysis and variability documentation. The remaining soil in each of these four subsamples was mixed into one composite sample from each site. Portions of this sample were sent to scientists requesting samples from the rainfall simulation sites, and the remainder stored at the USDA-ARS National Soil Erosion Research Laboratory in West Lafayette, Indiana for future use. From the cropland sites, a separate 3-4 kg sample of the tilled surface soil was collected and maintained at its field water content for analysis of selected mechanical properties by the SCS Soil Mechanics Laboratory.

For rangeland sites, a 20 kg sample was collected from an area adjacent to each of the two bare plots (Simanton et al., 1987). These areas were prepared in a manner similar to the "bare" plots so that they approximated conditions inside the plot. Samples from the forestland sites were collected in a similar fashion. These samples were not mixed for storage.

Laboratory Analyses

The analyses for the soil surface samples were primarily related to their aggregate, mechanical, and related properties (Table 11.5.2). Most of these analyses were made by the SCS Soil Mechanics Laboratory on the surface sample collected and maintained at its field water content (Table 11.5.2). Some of these analyses as well as additional measurements were made on the four variability subsamples by the ARS Watershed Research Unit at Columbia, MO (Table 11.5.2). Other analyses were made on the composite sample at the ARS National Soil Erosion Research Laboratory (Table 11.5.2).

Table 11.5.2 Measurements of mechanical and related properties of tilled surface horizons.

Atterberg limits ^{*#} (ASTM, 1984)
Modulus of rupture [#] (Reeve, 1965)
Unconfined compressive <i>strength</i> [*] (ASTM, 1984)
Direct shear strength at low confining pressure [*] (ASTM, 1984)
Pin-hole test for dispersion/erodibility (test ran with distilled water and the water used for the field rainfall simulation) [*] (USDA-SCS, 1984)
Middleton dispersion ratio ^{*#} (modification of ASTM, 1984)
Volume change under variable 1-dimension applied load of saturated and unsaturated conditions

Table 11.5.2 Measurements of mechanical and related properties of tilled surface horizons (Cont.).

Tensile strength test ⁺

Soil detachment by flow (flume studies)⁺

Aggregate stability by sieving [#] (Kemper et al., 1986)

Aggregate stability rainfall and sieving [#] (Young et al., 1984)

Various simplified tests of aggregation and crusting propensity[#] (experimental)

* Analyses by SCS Soil Mechanics Laboratory, Lincoln, NE on samples maintained at their field moisture content.

Analyses by ARS Watershed Research Unit, Columbia, MO on variability subsamples.

+ Analyses by ARS National Soil Erosion Research Laboratory, West Lafayette, IN on composite samples.

11.6 Plant Parameters on Rangelands

11.6.1 Introduction

Erosion on western rangelands is a function of many factors including precipitation, vegetation community, soil type, topographic position, and land use. Vegetation influences the rate of erosion on rangelands through several processes. Aboveground biomass reduces the kinetic energy of precipitation, increases surface roughness, time to ponding, time to runoff, physically covers the soil surface, and alters the water balance of the soil. Belowground biomass (roots) influences erosion by physically binding the soil in place, adding organic matter which increases aggregate stability and reduces particle detachment, decreases bulk density, and increases the number of macropores.

Plant parameters were measured on the WEPP rangeland sites. Three treatments, each replicated twice within a soil type and/or a given grazing intensity, were evaluated for a total of six plots per site. The treatments were natural vegetation, vegetation clipped to a 2 cm stubble height, and bare soil. The natural vegetation treatment was maintained in a undisturbed state for the duration of the project. The clipped treatments had all vegetation removed from the plot by hand to a 2 cm stubble height. Litter was removed and rock cover of the soil surface was undisturbed. The bare soil had all aboveground plant material and root crowns removed by hand. Furthermore, all rocks > 5mm that were not embedded in the soil were removed.

Developing and instituting sampling techniques for quantification of below and aboveground biomass on WEPP study sites locations was difficult. With the broad range in ecosystems and past site history, no rigid sampling procedure could be developed that would optimize precision, accuracy and the time necessary to collect data. Therefore, some aspects of the procedures were specified on-site based on site specific conditions.

Biomass ($kg\ ha^{-1}$) sampling on WEPP study sites was separated into three categories, aboveground herbaceous biomass, aboveground woody biomass, and belowground biomass. Determination of biomass involved the use of several different vegetation sampling methods. Sampling methods used to quantify vegetative canopy cover, ground surface cover, and biomass during the two field seasons are discussed here by type of biomass.

11.6.2 Aboveground Herbaceous Biomass

Vegetative canopy cover and ground surface cover (%) were estimated by the point-frame method. Ten transect lines evenly spaced over each plot were read with a 49 point (each point spaced 6 cm apart) vertical point frame for a total of 490 points (Fig. 11.6.1). The point-frame base was attached to the plot boundaries of the rainfall simulation plot at permanently marked locations. The legs of the point-frame were adjustable to allow the point-frame to be located directly over the vegetation (maximum height 150 cm). The first foliar hit of herbaceous vegetation and cover of the ground surface was recorded by species and type of cover (e.g. rock, litter, bare ground, and plant base). Points intersecting cryptogams were considered as basal hits, and were included in ground surface cover.

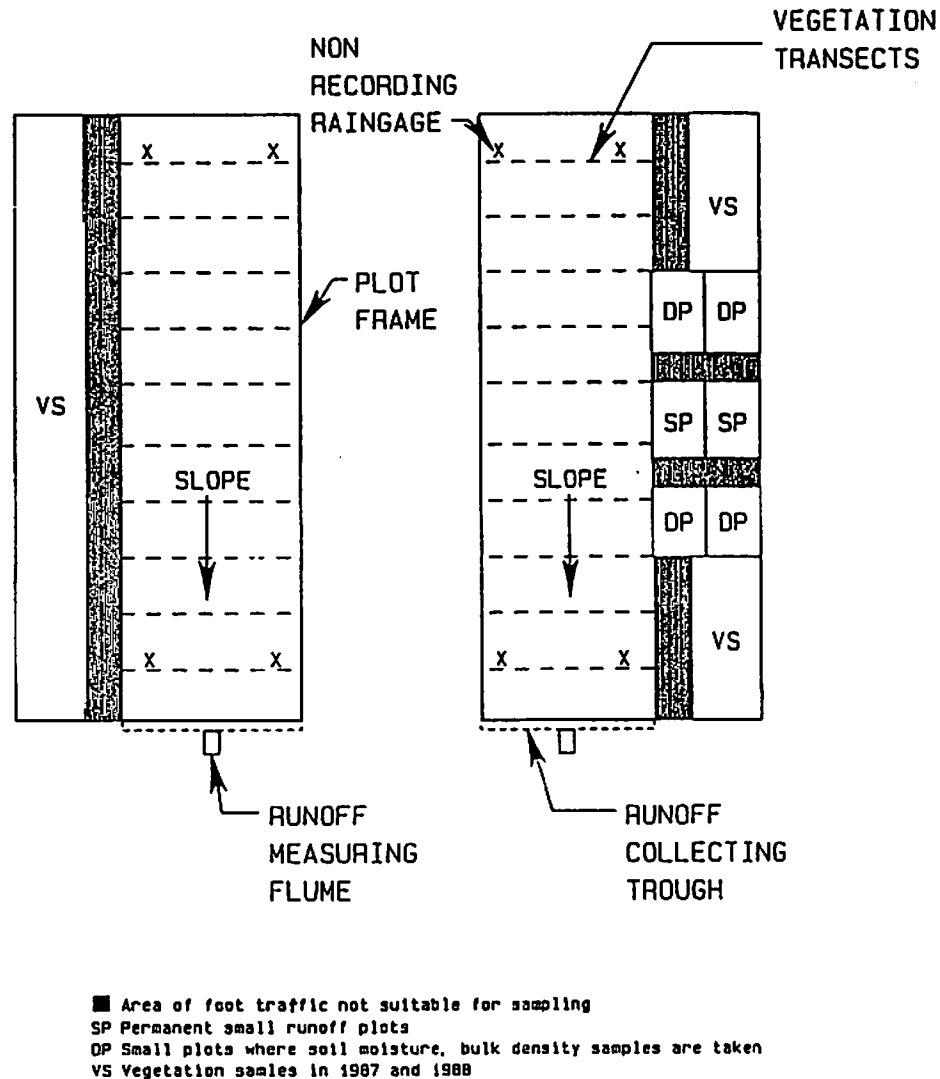


Fig. 11.6.1. Location of vegetation and soil samples on WEPP rangeland sites.

Aboveground standing herbaceous vegetation ($kg\ ha^{-1}$) was determined by clipping six $0.5\ m^2$ micro-plots ($50 \times 100\ cm$) from areas near the rainfall simulation plots. Foliar canopy cover was determined for each of the micro-plots with a 20-pin point-frame. Three transect lines were read from each micro-plot for a total of 60 points. Once foliar cover had been determined the plots were clipped to a 2 cm stubble height by life form and partitioned into live and dead biomass. Cryptogam biomass was determined by scalping the soil surface with a sharp knife to separate the plant material from the soil

surface. To remove soil contamination cryptogam samples were ashed. Litter was collected by hand once the standing vegetation was removed.

Leaf area (cm^2) of the grasses was determined with a Li-Cor 3100 leaf area meter. Once leaf area to weight ($cm^2 g^{-1}$) relationships had been estimated, all plant material was dried at $60^\circ C$ for 72 hours, and weighed. Regression relationships relating leaf area to leaf weight, biomass to canopy cover (%), and leaf area to canopy cover were determined. The regression relationships developed on the micro-plots were used to estimate standing herbaceous biomass and LAI of the rainfall simulation plots for all three treatments.

11.6.3 Aboveground Woody Biomass

Stem diameter, tree height, canopy volume and dimensional analysis have been used successfully to predict shrub biomass and leaf area (Murray and Jacobson, 1982; Scifres et al., 1974; Ludwig et al. 1975; and Weltz, 1987). Dimensional and multiple regression analyses of shrub attributes (e.g. height, canopy diameter, and canopy volume) were used to estimate aboveground woody biomass from shrubs sampled in the clipped and bare plots. Individuals of each species were selected such that the range of sizes on the study area was represented for the major species. The following attributes were measured for every shrub on the sample plots, (1) longest diameter of the canopy, (2) diameter of canopy at a right angle to the first measurement, (3) maximum height of shrub, (4) average height of plant canopy, (5) canopy depth (distance between the upper and lower most extension of foliage), and (6) basal stem diameter at 10 cm.

An estimate of leaf area and leaf biomass was determined by subsampling the canopy. A standard volume ($3375 cm^3$), from an area that was visually judged to be representative of the canopy, was clipped from the plant and a volume ratio (dry leaf weight / volume) was established. This volume ratio was then multiplied by the estimated canopy volume to estimate total leaf weight.

After the sample of leaves was removed by hand from the shrub, it was placed in a plastic bag and packed on ice to prevent dehydration of the leaves. The leaf samples were used to develop leaf area to leaf weight relationships similar to the procedure for grasses. After the leaf samples were removed, shrubs were cut to ground level and weighed. Relationships were determined for the different shrub species relating leaf area to leaf weight, canopy volume to biomass, and canopy volume to leaf area index. These regression relationships were then used to estimate leaf area index and standing biomass of shrubs.

11.6.4 Belowground Biomass

Belowground biomass (roots) impact erosion rates through two processes. Roots alter soil water content and physical properties of the soil. Thus, roots affect the infiltration rate, infiltration capacity, water balance, aggregate stability, and particle detachment and movement of soils.

Estimation of root distribution and biomass is time consuming, expensive, and difficult. Root studies in general indicate a non-linear decrease in root biomass with depth (Price and Heitschmidt, 1987; Foxx et al., 1984; Sims et al., 1978; Davis and Pase, 1977). Phillips (1963) reported that mesquite (*Prosopis* spp.) roots were found at > 58 m in an open pit mine in Arizona. Davis and Pase (1977) and Hellmers et al. (1955) reported that roots of many shrubs in the chaparral region of Arizona and California exceeded 7 m. The distribution of root biomass with depth is complicated by the type and lateral extent of woody roots. Cable (1977) and Young et al. (1984) reported that mesquite and western juniper (*Juniperus occidentalis*) roots extended laterally to 15 and 6 m, respectively, from the tree base.

To help reduce the variability that would occur if soil cores were collected from random locations, the soil cores were stratified by vegetation community. Soil cores were collected from the grass areas, beneath shrub canopies, and from within the interspace areas. The center of the soil cores, collected

beneath the shrub canopies, was located 15 cm from the base of the shrub. Furthermore, samples within the interspace were taken from bare areas and through the center of the dominant grass species. Soil cores were taken in 10 cm increments, with a 7 cm diameter hand auger, to a depth of 50 cm. Root biomass was determined by washing the soil cores through a 0.5 mm² mesh sieve. All roots, root crowns, and rhizomes remaining in the sieve were collected, dried in a microwave, and weighed. Roots were ashed in a muffle furnace for 4 hours at 500° C. Weight of the ash was subtracted from the dry matter weight yielding organic matter weight (Bohm, 1979). No attempt was made to separate live and dead roots or to separate woody and herbaceous roots.

Depth of maximum root penetration was determined from the four soil profiles described at each location by Soil Conservation Service personnel and from the literature where values exist. Non-linear regression relationships were developed from the root distribution and biomass data collected by depth and were used to estimate root biomass below 50 cm.

11.7 References

- Alberts, E. E., Holzhey, C. S., West, L. T., and Nordin, J. O. 1987. Soil selection: USDA-water erosion prediction project. Paper No. 87- 2542. American Society of Agricultural Engineers. St. Joseph, MI.
- Bohm, W. 1979. *Methods of Studying Root Systems*. Springer-Verlag. Berlin, New York. 188 p.
- Brasher, B. R., Franzmeier, D. P., Valassis, V. T., and Davidson, S. E. 1966. Use of Saran resin to coat natural soil clods for bulk density and water retention measurements. *Soil Sci.* 101:108.
- Cable, D. R. 1977. Seasonal use of soil water by mature velvet mesquite. *J. Range Manage.* 30:4-11.
- Davis, E. A., and Pase, C. P. 1977. Root systems of shrub live oak: Implications of water yield in Arizona chaparral. *J. Soil and Water Cons.* 32:174-180.
- Finkner, S. C. 1988. Hydraulic roughness coefficients as effected by random roughness. M. S. Thesis, University of Nebraska. 89 pp.
- Foxx, T. S., Tierney, G. D., and Williams, J. M. 1984. Rooting depths of plants on low-level waste disposal sites. Los Alamos Sci. Lab Rept. LA-10253-MS, Los Alamos, NM. 23 p.
- Hellmers, H., Horton, J. S., Juhren, G., and O'Keefe, J. 1955. Root systems of some chaparral plants in Southern California. *Ecology.* 36: 667-678.
- Laflen, J. M., Thomas, A., and Welch, R. 1987. Cropland experiments for WEPP project. Paper No. 87-2544. American Society of Agricultural Engineers, St. Joseph, MI.
- Ludwig, J. A., Reynolds, J. F., and Whitson, P. D. 1975. Size-biomass relationship of several Chihuahuan Desert shrubs. *Amer. Midl. Nat.* 94:451-461.
- Murray, R. B., and Jacobson, M. Q. 1982. An evaluation of dimensional analysis of predicting shrub biomass. *J. Range Manage.* 35:451-454.
- Nearing, M.A., D.I. Page, J.R. Simanton, and L.J. Lane. 1989. Determining erodibility parameters from rangeland field data for a process-based erosion model. *Transactions ASAE.*
- Phillips, W. E. 1963. Depth of roots in soil. *Ecology.* 44:424.
- Price, D. L., and Heitschmidt, R. K. 1987. Root biomass and distribution of roots for three major grasses at the Texas Experimental Ranch. pp. 81-86. In: W. H. Blackburn (ed.) *Water Yield Improvement From Rangeland Watersheds*. Annual Progress Rept., Texas Agr. Exp. St. Expanded Res. Rept. No. 15570 6190-2140. College Station. 151 p.

Scifres, C. J., Kothmann, M. M., and Mathis, G. W. 1974. Range site and grazing systems influence regrowth after spraying honey mesquite. *J. Range Manage.* 35:451-454.

Simanton, J. R., West, L. T., and Weltz, M. A. 1987. Rangeland experiments for water erosion prediction project. Paper No. 87-2545. American Society of Agricultural Engineers, St. Joseph, MI.

Sims, P. L., Singh, J. S., and Launerth, W. K. 1978. The structure and function of ten western North American grasslands. I. Abiotic and vegetational characteristics. *J. Ecology* 66:251-285.

Soil Survey Staff. 1972. Soil survey laboratory methods and procedures for collecting soil samples. Soil Survey Investigations Report No. 1. USDA-SCS. U.S. Government Printing Office, Washington, D.C.

Soil Survey Staff. 1981. Soil Survey Manual (Chapter 4). USDA-SCS. U.S. Government Printing Office, Washington, D.C.

Soil Survey Staff. 1984. Procedures for collecting soil samples and methods of analysis for soil survey. Soil Survey Investigations Report No. 1. USDA-SCS. U.S. Government Printing Office, Washington, D.C.

Weltz, M. A. 1987. Observed and estimated (ERHYM-II model) water budgets for South Texas rangelands. PhD. Thesis, Texas A&M Univ., College Station. 200 p.

Young, J. A., Evans, R. A., and Eash, D. A. 1984. Stemflow on western juniper (*Juniperus occidentalis*) trees. *Weed Sci.* 32:320-327.

6.17 List of Symbols

Symbol	Definition	Unit	Variable
f	final infiltration rate	L/T	f
F	total cumulative infiltration amount	L	ff
i_e	rainfall application rate at equilibrium	L/T	-
i_f	rainfall rate at end of run	L/T	-
K_s	saturated conductivity	L/T	ks
N_s	effective matric potential	L	avens
P	total rainfall volume	L	rain
por	soil porosity	fraction	por
P_{si}	matric potential across wetting front	L	sf
Q	total runoff volume	L	runoff
q_e	runoff rate at equilibrium	L/T	-
q_f	runoff rate at end of run	L/T	-
sat	soil saturation before run	fraction	sat

Chapter 12. IRRIGATION COMPONENT

G. Kottwitz and J.E. Gilley

12.1 Introduction

Erosion from areas irrigated using solid-set, side-roll, or hand-move irrigation systems can be estimated using a modified version of the WEPP profile model. Each of these systems irrigates a large area simultaneously and thus simulates natural rainfall of uniform intensity. Either natural precipitation or irrigation events may cause erosion. The relative contribution of each of these processes to total soil loss from an irrigated area can be identified using the profile model.

12.2 Description of Irrigation Component

Each of the components found in the profile model (i.e. climate generation, frozen soil, infiltration, surface runoff, water balance, plant growth, and erosion) are utilized by the irrigation component. Since the solid-set, side-roll and hand-move irrigation systems all provide uniform rainfall input, substantial alterations to the model were unnecessary. The principal changes made to the profile model to accommodate irrigation include: a) addition of rainfall provided by irrigation; b) updating water balance; c) timing of irrigation events; d) irrigation scheduling options; e) model output from irrigation events; and f) irrigation system configuration.

12.3 Addition of Rainfall Provided by Irrigation

The model is able to accommodate rainfall input from both natural precipitation and irrigation. Once an irrigation has been specified, it is treated internally by the model in the same fashion as natural rainfall. Since the irrigation events are of uniform intensity, the ratio of time to rainfall peak to rainfall duration, and the ratio of maximum rainfall intensity to average rainfall intensity are equal to 1.0.

12.4 Updating Water Balance

As was true with the surface runoff component, input from both natural precipitation and irrigation are treated identically for purposes of water balance. No special irrigation efficiency factor is required by the model. Existing model parameters are used to partition rainfall input into that portion which infiltrates and that which is removed by runoff.

12.5 Timing of Irrigation Events

Irrigation events, like rainfall occurrences, are assumed to occur prior to any daily soil water depletion. Several assumptions are made regarding the timing of irrigation relative to the rainfall event for days both rainfall and irrigation occur.

1. The rainfall event is assumed to take place before the irrigation event.
2. Any runoff from the rainfall event is assumed to have ceased prior to the start of irrigation.
3. The irrigation application does not begin until rainfall induced surface ponding has disappeared.

If a rainfall and irrigation event occur on the same day, the soil properties that are affected by the rainfall event are not adjusted prior to irrigation. Following irrigation, the soil properties affected by both the rainfall and irrigation events are updated.

12.6 Irrigation Scheduling Options

A variety of procedures can be used for scheduling irrigation. Four scheduling options were incorporated into the model to provide the user considerable flexibility. These scheduling alternatives are described below.

12.6.1 No Irrigation

The no irrigation option was included so that the profile version of the model with the added irrigation routine could also be used for non-irrigated conditions. After completion of all irrigation events, the model will move to the no irrigation option.

12.6.2 Depletion Level Scheduling

Depletion level scheduling results when soil water depletion exceeds some critical, predetermined quantity. If a rainfall event occurs on a day on which irrigation may be required, the amount of precipitation which infiltrates is added to the existing available soil water to provide an adjusted value. This adjustment serves to decrease that amount of irrigation which is required.

If an irrigation is to be simulated, the quantity of water to be applied must be determined. The amount of water necessary to fill the soil profile to field capacity for the appropriate rooting depth will define the irrigation requirement. If desired, the user may specify application of only a percentage of the total irrigation requirement. The soil water depletion level at which irrigation is necessary is also provided as a user specified input.

The user also identifies the minimum irrigation amount required to reasonably justify irrigation. This information is necessary to prevent the frequent application of small quantities of water. This factor is of principal concern at the beginning of an irrigation season when a very shallow rooting depth may be present. The beginning and end of the irrigation season must also be provided as a user input. If the simulation date is prior to the specified irrigation period, no irrigation will occur. If the simulation date corresponds with the end of the irrigation period, the model checks for additional irrigation periods. When no additional irrigation events are identified, the model then operates under a no irrigation condition.

12.6.3 Fixed Date Scheduling

The fixed date scheduling option uses known irrigation dates and amounts. This alternative is especially useful in situations where irrigation water is provided at predetermined dates during the growing season. This option may also be used for irrigation systems employed for frost protection. An irrigation will occur when the date of simulation is equal to the date specified for the fixed date irrigation. If no additional fixed date irrigation events are identified, the model then moves into a no irrigation mode.

12.6.4 Combination of Fixed Date and Depletion Level Scheduling

A combination of depletion level and fixed date scheduling is included in the model primarily to allow for pre-planting irrigation. When this scheduling alternative is used, the model checks on a daily basis for a fixed date irrigation. If a fixed date irrigation is indicated, the effects of the irrigation application are identified. If a fixed date irrigation is not indicated, then the need for irrigation using depletion level scheduling is evaluated.

After completion of a cropping season, irrigation scheduling alternatives must be reevaluated. If no additional irrigation periods are identified, the model then moves into a fixed date irrigation mode. The model will use depletion level scheduling alternatives if no additional fixed date irrigations are specified.

12.7 Model Output From Irrigation Events

The output information provided for non-irrigated conditions is also furnished for irrigated situations. However, in addition, the percentage of total (natural precipitation plus irrigation) runoff and erosion occurring during the irrigation events is also provided. This information furnishes a relative estimate of the effect of irrigation on total erosion and runoff.

Irrigation serves to replenish water depleted in the root zone through evapotranspiration. Thus, more runoff and erosion would be expected from a natural precipitation event on a recently irrigated area. This increased erosion potential caused by irrigation is not incorporated into the irrigation induced runoff and erosion percentage output by the model.

12.8 Irrigation System Configuration

The profile model performs calculations on an overland flow element basis. An overland flow element is a region over which management parameters are constant. Physically, the irrigation system area might be divided into two or more sub-areas.

These irrigation system based sub-areas must be continuous and may contain plant, soil or other management practice boundaries requiring additional division of the profile into overland flow elements. As a result, the irrigation system based sub-area boundaries must correspond to overland flow element boundaries, but overland flow element boundaries may exist where the irrigation based sub-area boundaries are not present. If a plant, soil, or other management practice boundary lies within the irrigation sub-area, more than one overland flow element will be irrigated on a given day.

Irrigation of more than one sub-area per day is not allowed in the model. The fixed date irrigation data file should be constructed to reflect the requirement of continuous sub-areas and irrigation of only one sub-area per day. However, the user may specify irrigation on any combination of overland flow elements on any day.

CHAPTER 13. IMPLICATIONS OF THE WEPP HILLSLOPE MODEL FOR SOIL CONSERVATION PLANNING

P.B. Hairsine, G.A. Weesies and M.A. Nearing

13.1 Introduction

The WEPP model provides a physically based description of the erosion phenomenon and as such, it is an improvement on the statistically based USLE approach. A further improvement that the WEPP hillslope model provides is the description of the spatial distribution of the processes on a given hillslope. This information is described to the user and may be useful in interpretation, guiding the user in planning soil conservation strategies.

The aim of this chapter is to discuss the implications of more spatial and temporal information of the movement of soil particles on a hillslope to soil conservation planning. In this chapter effects of on-site and off-site erosion are delineated. Use of the detailed information provided by WEPP enables the user to identify the expected areas of net soil loss and net deposition over a long period of time. Thus the model may serve as a design tool in which soil conservation measures may be spatially and temporally arranged to meet conservation objectives.

13.2 The Erosion Output of the Model

The format of the erosion output of the WEPP hillslope model is given in Fig. 13.2.1. The output is clearly divided (on separate screens) between "on site effects" and "off-site effects." On-site effects describe the predicted net soil loss and net deposition on the hillslope. Thus the on-site effects are of prime importance to decisions made on the basis of erosion/productivity. The off-site effects describe the sediment delivered from the hillslope and are of prime importance to decisions made on the basis of water quality, that is, chemicals and sediment leaving a hillslope.

Screen I of the output gives details of the on-site effects. This screen is divided into three sections: area(s) of net soil loss, area(s) of net deposition, and detailed soil loss/net deposition on the hillslope. The user is first given the average rate of soil loss. This is the key output parameter used for many soil conservation decisions based on erosion productivity. The maximum rate of soil loss and the point at which this occurs is then predicted. The area(s) of net soil loss are also given, together with the average loss in each of these areas. These parameters will be useful in the design of conservation systems (see section 13.5).

The average rate of soil loss on Screen I is directly equivalent to the soil loss per unit area in the Universal Soil Loss Equation (USLE) (Wischmeier and Smith, 1978). The USLE was developed by statistically summarizing results from plot studies that did not include areas of net deposition. By calculating the location and amount of net deposition which occurs on a hillslope, WEPP does not share this limitation of the USLE.

The user is then provided with a summary of the rates and areas of net deposition on the hillslope. Such information may be useful in assessing the impact of sediment accumulation; for instance in evaluating the accumulation of deposited sediment behind a contour terrace.

Finally a detailed output of the soil loss/net deposition on the hillslope is given, in which the soil loss or gain is given for each increment down the slope. This information is the basis of the soil loss/gain diagrams given in Fig. 13.3.1, 13.4.2, and 13.5.1. It is anticipated that such graphical output will be available in subsequent versions of WEPP and will replace the table of loss versus distance downslope in the current version.

Screen II of the output shows the off-site effects which describe the sediment delivered off the hillslope. The characteristics of the sediment leaving the hillslope are given on the basis of five classes: primary clay, primary silt, primary sand, small aggregates and large aggregates. The following detail is

given for each of those classes: the mass fraction detached from the original soil, the mass fraction in the sediment leaving the hillslope, the composition in terms of primary particles, the percent organic matter, the assumed diameter and the assumed specific gravity. The enrichment ratio provides a summarizing measure of the ability of the sediment leaving the hillslope to carry sorbed chemicals compared with that of the originally detached soil.

13.3 Slope Length: Inputs and Output

The slope length, slope shape and the slope steepness are user inputs to the WEPP model. The lower boundary of the hillslope under consideration is usually defined by a concentrated flow area (such as an ephemeral gully, a terrace channel, or diversion bank) or by the property boundary. The WEPP model requires no judgement on the part of the user as to where an area of net deposition will occur. The location of areas of net soil loss and net deposition are predictions of the WEPP model. By using slope length inputs which are based on hillslope boundaries, the WEPP model avoids the uncertainties associated with user estimates of the slope length for net soil loss used in the USLE methodology.

Figure 13.3.1 illustrates the importance of separating the on-site and off-site effects. The two hillslopes shown in Fig. 13.3.1a and 13.3.1b are identical except the profile in Fig. 13.3.1a has been truncated at point B. For a given sequence of runoff events on these identical slopes the soil and deposition is plotted in the lower portion of the figure. In the area of net soil loss the soil loss in Fig. 13.3.1a and 13.3.1b, the soil loss is identical as expected. On the lower, flatter portion of the hillslope, net deposition is predicted and the sediment load reduced as a result. The sediment delivered to point B in each of these cases is identical for the segment A to B. WEPP predicts that the soil loss per unit area (in the area of net soil loss) is identical. The off-site effects are, however, clearly a function of the position of the lower, user-defined, boundary.

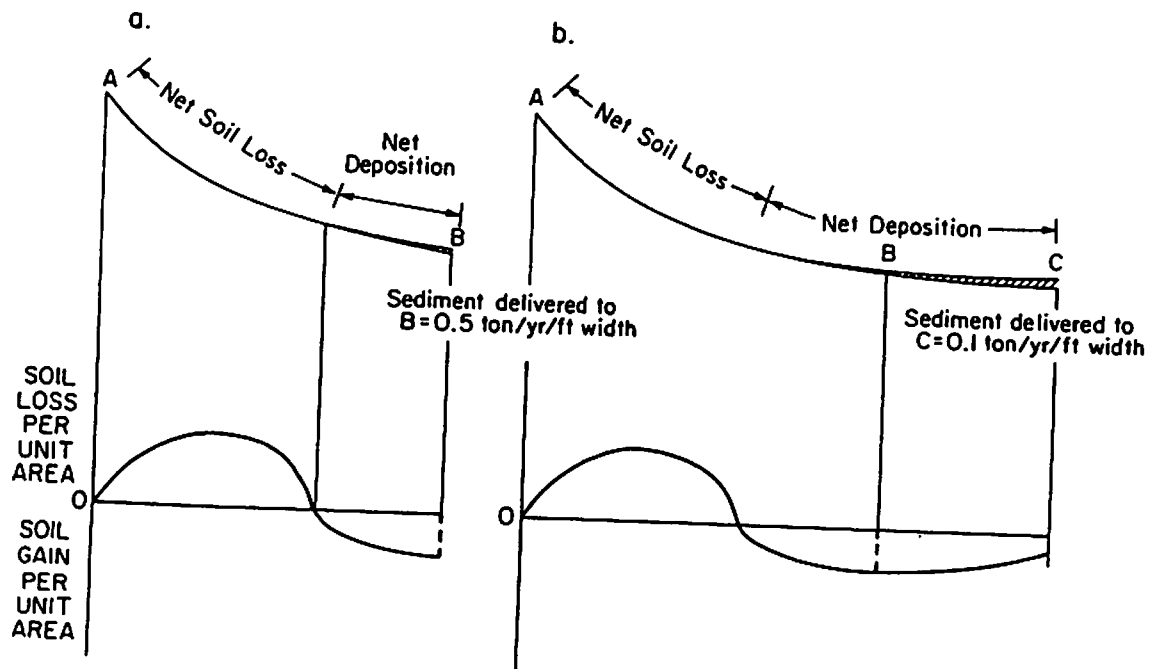


Fig. 13.3.1.

13.4 Implications of a Continuous Simulation

WEPP is a continuous simulation model which predicts erosion for a series of generated precipitation events in the presence of management and soil conditions which vary with time. Identical storms do not necessarily result in identical soil movement as crop cover, residue, soil moisture, and surface roughness may differ for the two events. On a hillslope with rotating strips of vegetation, a location that has soil loss in one event may have net soil gain (deposition) in another. Over the period of the simulation the effects of the series of storms are integrated to give the output shown in Fig. 13.2.1 and 13.4.1.

The effect of integration of soil loss and deposition over the period of the simulation is illustrated in Fig. 13.4.2. The erosion output of WEPP for a simple crop rotation for a two strip system may be summarized by two net soil loss/gain diagrams which summed give Fig. 13.4.2e. Clearly some of the soil deposited in the vegetative strips in one rotation is eroded in the following rotation. The WEPP model permits the net soil loss/gain over the period of simulation to be integrated in the presence of crop rotations.

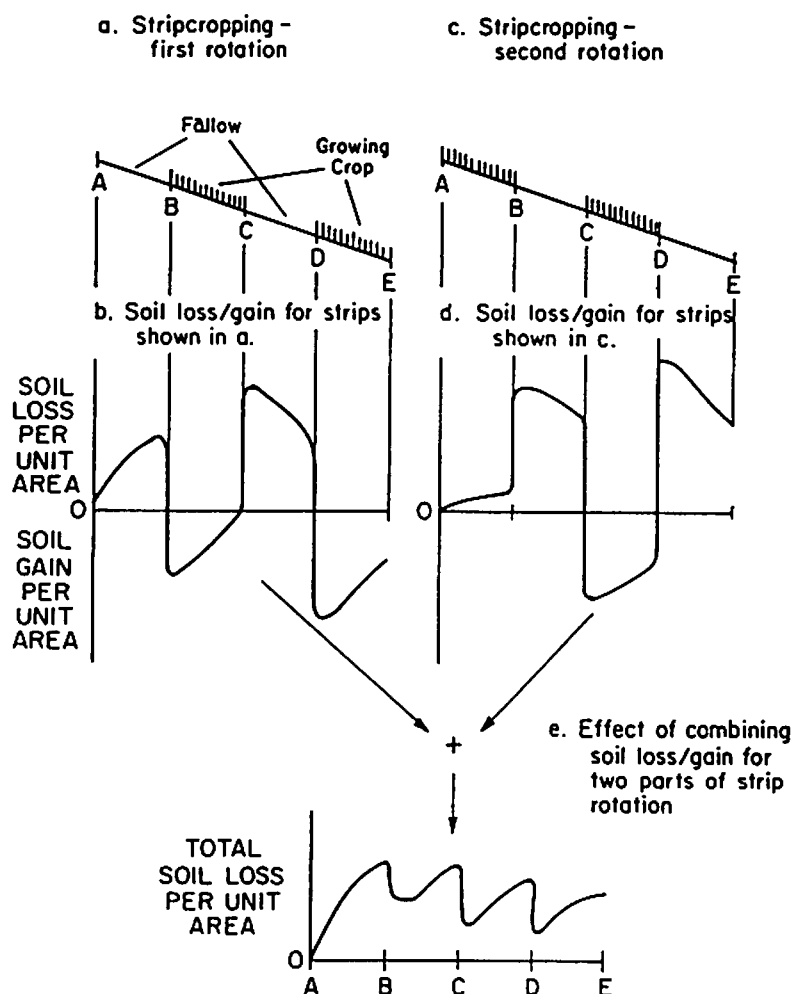


Fig. 13.4.2.

13.5 Design of Conservation Systems

A major role of the WEPP hillslope model is to aid the land user in the design of conservation systems. The model compliments the user's practical knowledge of the land management options by quantifying erosion consequences of an existing or proposed soil conservation strategy. The spatial detail provided by simulations will assist the user in identifying areas of prime net soil loss for the existing, or proposed, land use and thus provide a guide to the location of measures such as contour terraces and strips of vegetation.

Consider the hillslope shown in Fig. 13.5.1a. The erosion output for the existing land use system (eg., mono-cropping with a long winter fallow) is shown in Fig. 13.5.1b. Based on this output, the user can decide to run a second simulation with a contour terrace at location A resulting in output as plotted in Fig. 13.5.1c. If the user decides the net soil loss in the area immediately downslope of location A is still unacceptable, then another soil conservation technique may be tested. For example, a narrow sod strip immediately below the terrace might be considered. This strip on area between location A and B will then reduce the soil loss on this area resulting in the output shown in Fig. 13.5.1d.

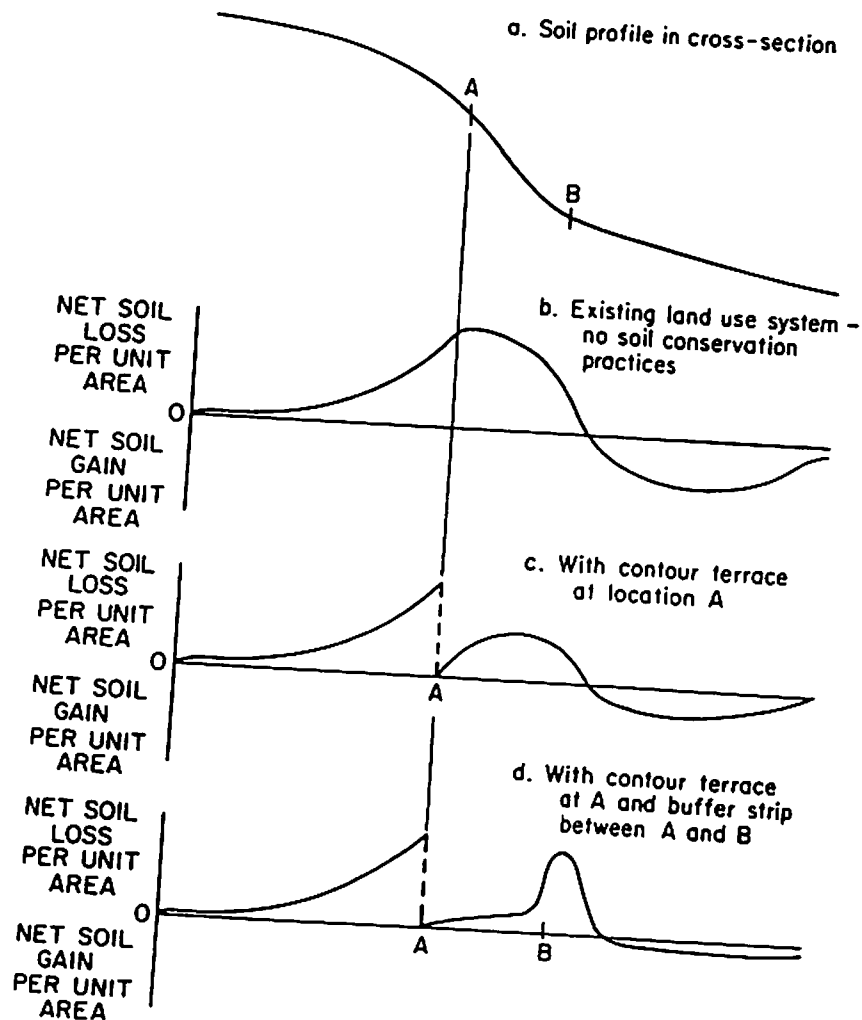


Fig. 13.5.1.

The short area of relatively high net soil loss immediately downslope of point B in Fig. 13.5.1d results from flow containing a low sediment concentration leaving the grass strip and entering an area of soil with low residue/crop cover levels. This "clear water effect" is characterized by scour immediately downslope of vegetative strips. The WEPP model predicts this effect so that it is identified to the user. However such an effect will require careful design to ensure that the use of vegetative strips does not just move the area of maximum soil loss on the slope.

The "clear water effect" is particularly important in assessing the use of buffer strips or filter strips. Such strips are permanent vegetative strips that induce deposition of sediment carried from upslope. The runoff leaving these strips is capable of detaching large amounts of sediment on exiting the strip. In the erosion model of WEPP this effect is described by the term $[1-G/T_c]$ in the expression for rill erosion rate, D_f :

$$D_f = D_c \left[1 - \frac{G}{T_c} \right] \quad [13.5.1]$$

where D_c is the rill detachment capacity expressed in Eq. [10.2.1.3]. When the sediment load, G , is low relative to the transport capacity, T_c , as it is coming out of the buffer strip, then the rill erosion rate approaches the rill detachment capacity, D_c , so that the sediment load rapidly increases. Thus, the output of the WEPP model clearly illustrates the potential for rapid scouring immediately below buffer strips. The spatial detail of the WEPP model allows the user to assess the importance of this effect and thus appraise whether a buffer strip has the desired soil conserving effect.

13.6 Summary

The WEPP model provides spatial detail of soil movement that will assist the land manager in soil conservation planning. It predicts erosion at every point on the hillslope. It identifies precise locations on the slope of erosion problem areas. This spatial detail separates on-site and off-site effects to aid in the interpretation of the output of the model. Slope length inputs to the model are defined by hillslope boundaries and the areas of net soil loss and net deposition are calculated internally. As a continuous simulation model, WEPP integrates soil movement over the period of the simulation within which management inputs and soil conditions vary with time.

13.7 Reference

Wischmeier, W.H., and D.D. Smith, 1978. Predicting rainfall erosion losses. U.S. Department of Agriculture, Agriculture Handbook No. 537, 58pp.

13.8 List of Symbols

Symbol	Definition	Units	Variable
D_c	detachment capacity by flow	$kg / s \cdot m^2$	NA
D_f	rill erosion rate	$kg / s \cdot m^2$	NA
G	sediment load	$kg / s \cdot m$	NA
T_c	sediment transport capacity in the rill	$kg / s \cdot m$	NA

Fig. 13.2.1 (Screen I).

1. *****ON-SITE EFFECTS *****

A. Area of Net Soil Loss.

Average rate of soil loss = _____ ton/ac/yr

Maximum rate of soil loss = _____ ton/ac/yr at _____ ft

Areas of net soil loss:

_____ ft to _____ ft with average loss _____ ton/ac/yr

_____ ft to _____ ft with average loss _____ ton/ac/yr

B. Area of Net Deposition.

Average rate of net deposition = _____ ton/ac/yr

Maximum rate of net deposition = _____ ton/ac/yr

Areas of net deposition:

_____ ft to _____ ft with average deposit _____ ton/ac/yr

_____ ft to _____ ft with average deposit _____ ton/ac/yr

C. Detailed soil loss/net deposition on the profile

Distance downslope ft.	Soil loss/Gain* ton/ac/yr	Element No.
(for example)		
10	20.3	1
20	-1.5	1
30	-11.7	1
...

* Negative value means soil gain, that is net deposition.

Fig. 13.4.1 (Screen II).

2. ***** OFF-SITE EFFECTS *****

Sediment Delivery:

Sediment delivered from profile = _____ ton/yr/ft width

Sediment Characteristics leaving profile

Size Class	Mass Fraction		Composition by primary particles				Diameter (mm)	Specific gravity
	% soil detached	% leaves profile	% sand	% silt	% clay	% o.m.		
(for example) clay	5	20	0	0	100	0.1	0.002	2.6
silt	15	23	0	100	0	0.5	0.010	2.6
sand	15	8	100	0	0	0.0	0.200	2.6
small aggs.	28	38	40	20	40	5.0	0.046	1.8
large aggs.	37	11	50	20	30	7.8	0.660	1.6

Sediment enrichment ratio = _____

APPENDIX A

USDA - WATER EROSION PREDICTION PROJECT (WEPP)
WEPP HILLSLOPE COMPUTER MODEL

PROGRAM DOCUMENTATION
(Revised in July 1989)

V. L. Lopes, E. Perry, J. J. Stone, J. Ascough, and J. Ferris

I. PROGRAM SUMMARY

1. Title (temporary) of program: VERS89
2. Computers for which the program has been designed:

VAX 11/780 running under VAX/VMS 4.3 or UNIX 4.3
IBM PC and compatibles running under MS-DOS 3.2 or later

3. Programming language: ANSI FORTRAN 77
4. Peripherals used: input/output devices, mass storage, line printer
5. Separate documentation available:

Foster, G.R. (Compiler), 1987. User Requirements: USDA-Water Erosion Prediction Project (WEPP). NSERL Report No. 1, Nat. Soil Erosion Res. Lab., USDA-ARS, W. Lafayette, IN, 43p.

Lane, L.J., and Nearing, M.A. (editors), 1989. WEPP profile model documentation (Draft 2.0). February 1989. (Available by request from editors)

WEPP Hillslope Data Definition Table, available from L. Lane and V. Lopes

6. Keywords: sediment generation (erosion), sediment transport, deposition, mathematical modeling, soil physics, erosion prediction on hillslopes, computer simulation, water balance, overland and concentrated flow hydraulics, climate generator, storm disaggregation.
7. Nature of problem:

The Universal Soil Loss Equation (USLE) is the current method for predicting average, long-term sheet and rill erosion. However, the USLE does not define separate factor relationships for the fundamental hydrologic processes of rainfall, infiltration, runoff, and the fundamental erosion processes of detachment by raindrop impact, detachment by overland and concentrated flow, transport by rain splash, transport by flow, and deposition by flow. These aspects limit the potential for increased accuracy and major improvement of the USLE as a predicting tool for conservation planning and resource conservation.
8. Method of solution:

The USDA/WEPP hillslope computer model is an improved erosion prediction technology

based on fundamentals of hydrology, soil physics, runoff hydraulics, and erosion mechanics. The model includes components for climate, snow accumulation and melt, infiltration, surface runoff, hillslope erosion, water balance, plant growth, plant residue, tillage, and other practices disturbing the plant canopy and soil surface.

9. Further information on WEPP computer models is available from M. A. Nearing, National Soil Erosion Laboratory, Purdue University, West Lafayette, IN 47907.

II. PROGRAM DESCRIPTION

This section covers the individual subroutines and their functions, the variables and parameters used, and the model input and output files. The WEPP Hillslope program structure is shown in Figure 1.5.1. The interactions between the subroutines within the WEPP model are shown in Fig. A.1.

1. Subroutines and functions:

MAIN It prints out the program's headings and calls SR CONTIN, the master program that coordinates the initialization and simulation runs for WEPP.

SR CONTIN It is the master program in WEPP. It coordinates the initialization and the reading of the input data through calls to SR INFILE, SR OUTFIL, SR INPUT, SR TILAGE, SR INIT1, SR RNGINT, SR PRTCMP, SR SCON, SR SOIL, and SR WATBAL. It controls the simulation runs and the writing of the program's output through calls to SR STMGET, SR IRS, SR FRCFAC, SR TFAIL, SR XINFLO, SR PARAM, SR WATBAL, SR ROUTE, SR SUMRUN, SR SLOSS, SR PRINT, SR SEDOUT, SR TILAGE. It is called from MAIN.

a. Initialization calls:

SR INFILE INFILE gets the filenames for the slope, climate, soil, and management files from the user. INFILE calls SR OPEN to open these files and checks the file structures to make sure that each one includes information for the same number of strips down the hillslope. This subroutine is called from SR CONTIN.

SR OUTFIL This subroutine calls SR OPEN to open output files (if requested) for water balance, plant growth, soil parameters, and detailed hydrology output. It is called from SR CONTIN.

SR OPEN This subroutine is called from SR INFILE and SR OUTFIL to open the WEPP control and output files.

SR INPUT INPUT reads in WEPP input data files for slope, soil, and a management option. This subroutine is called from SR CONTIN. It calls SR PROFILE.

SR PROFIL This subroutine is called from SR INPUT to compute dimensionless elevations, horizontal distances, and slopes (assumed linear between points).

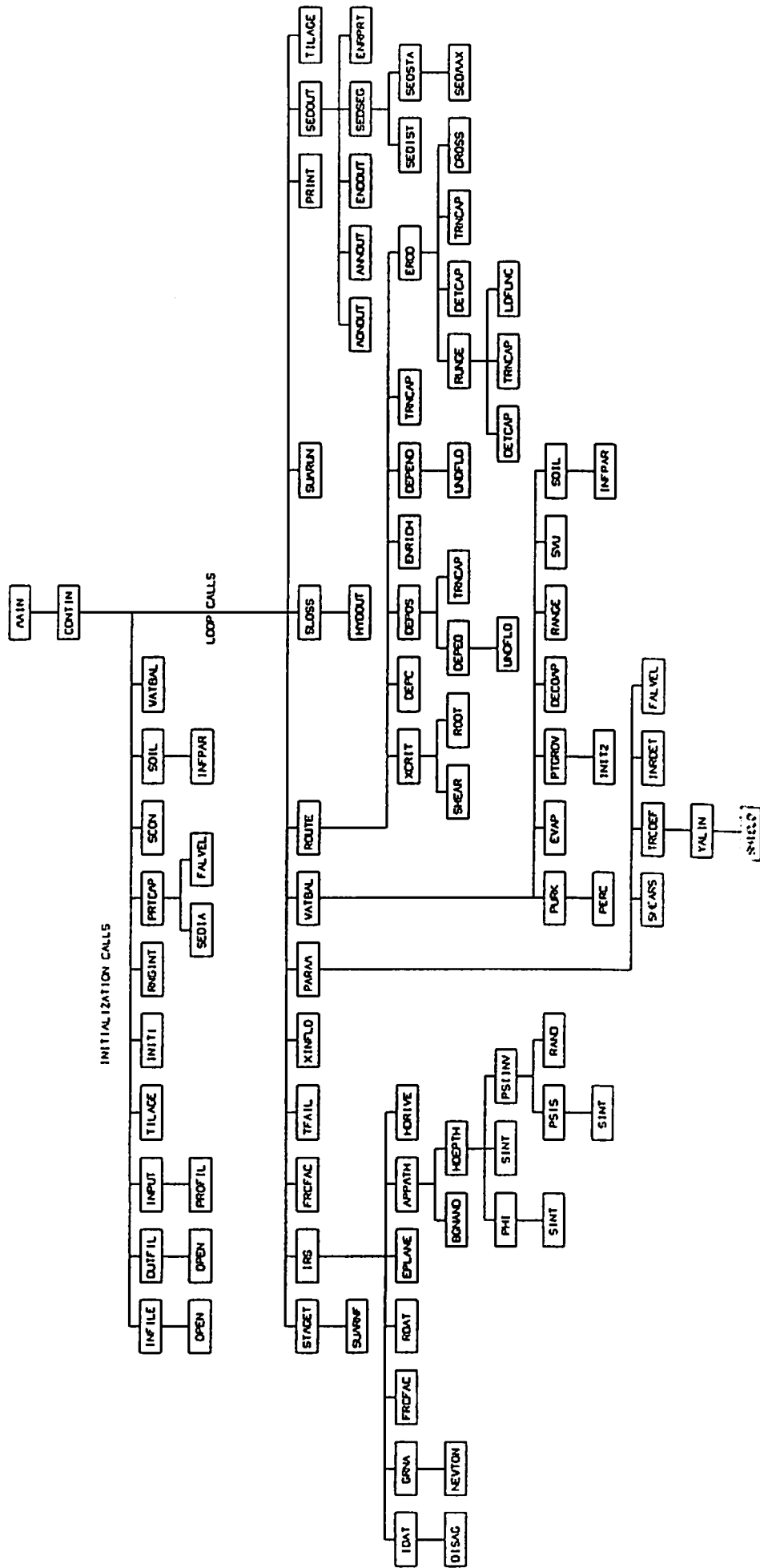


Fig.A.1. Information Flow in Program VERS86.

- SR TILAGE TILAGE is called from SR CONTIN to read crop, tillage, and management options for the first year of the simulation.
- SR INIT1 This subroutine is called from SR CONTIN (when land use is cropland) to initialize variables used in SR PTGROW.
- SR RNGINT This subroutine is called from SR CONTIN (when land use is rangeland) to initialize variables used in SR RANGE.
- SR PRTCMP This subroutine is called from SR CONTIN to generate a default set of particles for the program using the soil characteristics read in with the initial parameters. It calls FN SEDIA and FALVEL.
- FN SEDIA This function calculates the equivalent sand diameter of a particle class. It is called by SR SEDIA.
- FN FALVEL This function calculates the fall velocity of a particle class. It is called by SR SEDIA.
- SR SCON This subroutine is called from SR CONTIN to initialize some soil parameters which remain constant throughout the simulation, i.e., parameters which are independent of changes in bulk density.
- SR SOIL SOIL is called from SR CONTIN to initialize soil parameters such as bulk density, porosity, etc. It calls SR INFPAR.
- SR INFPAR It is called from SR SOIL to calculate saturated hydraulic conductivity and effective matric potential from (1) bare soil saturated hydraulic conductivity, (2) average potential across the wetting front, (3) effective porosity, (4) percent ground cover, (5) percent canopy cover, and (6) relative effective saturation.
- SR WATBAL This subroutine is called from SR CONTIN to initialize some variables for the water balance (evaporation, infiltration, percolation, plant transpiration, etc.) Later it is called from SR CONTIN to perform the continuous water balance calculations.
- b. Loop calls:
- SR STMGET This subroutine is called from SR CONTIN to read in storm data on a storm-by-storm basis. It calls SR SUMRNF.
- SR SUMRNF This subroutine is called from SR STMGET to sum up the number of rainfall producing events and rainfall amounts during the simulation period.
- SR IRS This subroutine is called from SR CONTIN (if there is precipitation) to develop the hyetograph (through rainfall disaggregation techniques), calculate rainfall excess rates, adjust time variant hydraulic friction factors, generate runoff hydrographs, print out (if requested) the detailed hydrology

- output, compute shear stress, sediment transport coefficients, and particle fall velocity. To perform all these tasks it calls SR IDAT, SR GRNA, SR FRCFAC, SR RDAT, SR EPLANE, SR APPMTH, SR HDRIVE.
- SR IDAT** This subroutine (called from SR IRS) brings in storm rainfall amount, rainfall duration, and rainfall pattern, expressed in terms of the ratios time to peak intensity to rainfall duration, and maximum rainfall intensity to average rainfall intensity (reads in the climate input file by SR STMGET and passed through a common block). To generate the hyetographs (through calls to SR DISAG) and to calculate the time step for infiltration and insert this time step into the rainfall data.
- SR DISAG** This subroutine (called from SR IDAT) disaggregates storms into a double exponential intensity pattern with relative time to peak intensity, T_p , and relative maximum intensity, $I_p = \text{Max INT/AVE intensity}$, satisfying $0 < T_p < 1$ and $I_p \geq 1$ through calls to SR CONST and SR DBLEX.
- SR CONST** It is called from SR DISAG to calculate step functions to represent nint, delta T, and intensity = 1.0 intervals for constant intensity.
- SR DBLEX** It is called from SR DISAG to solve a double exponential distribution function. It calls FN EQROOT.
- FN EQROOT** It is called from SR DBLEX to solve the following equation for u , using the Newton's method: $1 - e^{-u} = a u$, with a positive, u positive (unless $a = 1$).
- SR GRNA** This subroutine is called from SR IRS to calculate infiltration rates and depths for unsteady rain using the Green and Ampt infiltration equation as modified by Mein and Larson. It calls SR NEWTON to solve the infiltration equation iteratively using the Newton's method.
- SR NEWTON** This subroutine is called from SR GRNA to calculate cumulative infiltration via Newton's method.
- SR FRCFAC** This subroutine is called from SR IRS to compute the time-variant roughness coefficients for overland flow routing.
- SR RDAT** This subroutine is called from SR IRS to set up the input to SR HDRIVE. It gets the distance and time locations for depth calculations; converts alpha and rainfall excess rates to internal length and time; and computes $si(n)$ as the integral of s with respect to t from 0 to $t(n)$ for n between 1 and $ns+1$.

- SR EPLANE This subroutine calculates the equivalent Chezy roughness coefficient for using the equivalent plane method. This is for handling multiple strips down the hillslope. SR EPLANE is called from SR IRS.
- SR APPMTH This subroutine is called from SR IRS (unless runoff routing is required by user) to compute peak runoff and runoff duration based on regression equations related to rainfall pattern and soil characteristics.
- SR HDRIVE This subroutine is called from SR IRS (if runoff routing is requested) to compute kinematic flow depths on a plane at selected distances down the plane and at selected time spacing. The lateral inflow (rainfall excess) is presented as a positive step function up to a given time and is zero thereafter. (If step value is given as zero, it is set to 1.E-8). It calls SR BGNRND and FN HDEPTH.
- SR BGNRND This subroutine is called from SR HDRIVE to initialize the seed for the random number generator (SR RAND).
- FN HDEPTH This function is called from SR HDRIVE to find depth h on an overland flow plane by solving the partial differential equation: $S = h1 + \alpha * m * h^{(m-1)} * h2$. It calls FN PHI, FN SINT, and FN PSIINV.
- FN PHI This function is called from FN HDEPTH to compute ϕ (time) values for function ψ (see Chapter 5 for details). It calls FN SINT.
- FN SINT This function is called from FN HDEPTH, FN PHI, and SR PSIS to compute accumulated rainfall to time t .
- FN PSIINV This function is called from FN HDEPTH to compute the inverse of function ψ . It calls SR PSIS and SR RAND.
- SR PSIS This subroutine is called from FN PSIINV to compute function ψ , and its derivative $d\psi$. The results are returned in COMMON /psis/. It calls FN SINT.
- SR RAND This subroutine generates random numbers between 0 and 1 using the multiplicative congruential method. It is called from FN PSIINV to restart at a random value for variable u when function ψ is zero.
- SR FRCFAC This subroutine is called from SR CONTIN and generates the interrill and rill friction factors for the erosion component.
- SR TFAIL This subroutine is called from SR CONTIN and determines if the contours for a flow element and storm fail or not.
- SR PARAM This subroutine is called from SR IRS to calculate the dimensionless rill and interrill erosion parameters: one for

- interrill erosion (θ), two for rill rill erosion (ϵ and τ), and one for deposition (ϕ). It calls FN SHEARS, FN TRCOEF, FN INRDET, and FN FALVEL.
- FN SHEARS** This function is called from SR PARAM to compute rill width adjustments, Chezy's coefficient for rill flow, rill flow depth, wetted area, wetted perimeter, hydraulic radius, and shear stress at the end of the slope.
- FN TRCOEF** This function is called from SR PARAM to compute a sediment transport coefficient for rill flow. It calls SR YALIN.
- SR YALIN** This routine is called from FN TRCOEF to compute sediment transport capacity using the Yalin equation. It calls FN SHIELD.
- FN SHIELD** This function is called from SR YALIN to generate parameters (Shield parameters) by interpolating values from a table (Shields diagram) for given Reynolds numbers.
- FN INRDET** This function is called from SR PARAM to compute ground cover and canopy effects on interrill erosion.
- FN FALVEL** This function is called from SR PARAM to compute particle fall velocity for a specific particle size, given its specific gravity, diameter, the kinematic viscosity of water, and the acceleration of gravity.
- SR WATBAL** The water balance subroutine is called from SR CONTIN in the loop calls to update the water balance during the simulation period. It calls SR PURK, SR EVAP, SR PTGROW (if land use is cropland), SR DECOMP, SR RANGE (if land use is rangeland), SR SWU, and SR SOIL.
- SR PURK** This subroutine is called from SR WATBAL to drive the percolation process. It divides each flow layer into 4 mm slugs and manages the routing process. It calls SR PERC.
- SR PERC** This subroutine is called from SR PURK to compute percolation for a soil layer when the soil layer field capacity is exceeded.
- SR EVAP** This routine is called from SR WATBAL to compute the amount of soil evaporation and the potential plant evaporation using Ritchie's model.
- SR PTGROW** This is the plant growth subroutine. It is called from SR WATBAL to predict canopy cover, canopy height, root depth, root mass, and leaf area index at different soil depths on croplands. It calls SR INIT2.
- SR INIT2** This subroutine is called from SR PTGROW (if the Julian date is a planting date) to calculate initial surface and submerged

- residue masses and root mass by crop type.
- SR DECOMP This routine is called from SR WATBAL (if the land use is cropland) to estimate changes in residue and root masses, compute the remaining flat, standing, and submerged residue and root masses, compute residue cover, and make adjustments for tillage operations.
- SR RANGE This is the range plant growth subroutine. It is called from SR WATBAL to predict plant growth (canopy cover, canopy height, root depth, root mass, and leaf area index) on rangelands.
- SR SWU This subroutine is called from SR WATBAL to calculate actual plant water use based on soil water availability.
- SR SOIL This subroutine is called daily from SR WATBAL to calculate time-variant soil parameters such as bulk density, porosity, saturated hydraulic conductivity, etc. It calls SR INFPAR.
- SR INFPAR It is called from SR SOIL (in the simulation loop) to calculate saturated hydraulic conductivity and effective matric potential from (1) bare soil saturated hydraulic conductivity, (2) average potential across the wetting front, (3) effective porosity, (4) percent ground cover, (5) percent canopy cover, and (6) relative effective saturation.
- SR ROUTE This subroutine is called from SR CONTIN to calculate detachment (when shear stress exceeds critical shear stress) or deposition at the upper end of the slope segment and route sediment through the hillslope profile. It calls SR XCRIT, FN DEPC, SR DEPOS, SR ENRICH, FN DEPEND, FN TRNCAP and SR EROD.
- SR XCRIT This subroutine is called from SR ROUTE to determine whether or not shear stress exceeds critical shear stress for a certain segment and returns a flag. It calls FN SHEAR and SR ROOT.
- FN SHEAR This routine is called from SR XCRIT to calculate non-dimensional shear stress.
- SR ROOT This subroutine is called from SR XCRIT to find roots for equation $y = a*x**2+b*x+c$
- FN DEPC This routine is called from SR ROUTE to compute a portion of the deposition equation.
- SR DEPOS This subroutine is called from SR ROUTE to calculate deposition in each segment of the hillslope. It calls FN DEPEQ and FN TRNCAP.

FN DEPEQ	This function is called from SR DEPOS to solve the deposition equation. It calls SR UNDFLO.
SR UNDFLO	This subroutine is called from FN DEPEQ and FN DEPEND to compute the other portion of the deposition equation (see FN DEPC).
FN TRNCAP	This function is called from SR DEPOS, SR EROD, and SR ROUTE to calculate dimensionless sediment transport capacity.
SR ENRICH	This subroutine is called from SR ROUTE and computes the new particle size distribution of sediment in runoff following routing through a deposition region.
FN DEPEND	This function is called from SR ROUTE to calculate where deposition ends in a segment on the hillslope. It calls SR UNDFLO.
SR EROD	This subroutine is called from SR ROUTE to calculate detachment in each segment of the hillslope. It calls SR RUNGE, FN DETCAP, FN TRNCAP, and FN CROSS.
SR RUNGE	This subroutine is called from SR EROD to perform the Runge-Kutta iteration. It calls FN DETCAP, FN TRNCAP, and FN LDFUNC.
FN DETCAP	This function is called from SR RUNGE and SR EROD to calculate detachment capacity at a point.
FN LDFUNC	This function is called from SR RUNGE to calculate the non-dimensional load function for a rill segment.
FN CROSS	This function is called from SR EROD to determine a point where two lines cross each other.
SR SLOSS	This subroutine is called from SR CONTIN calculates sediment concentration and sediment yield on a storm-by-storm basis, and prints out soil loss and sediment load information by input segment and by erosion/deposition section. It also prints out an abbreviated hydrology output for the event under consideration, by calling SR HYDOUT.
SR HYDOUT	This subroutine is called from SR SLOSS to print out an abbreviated hydrology output.
SR SUMRUN	This subroutine is called from SR CONTIN to generate a summary of the number of runoff events and total runoff volume generated during the simulation period.
SR PRINT	This subroutine is called from SR CONTIN to print out (when requested by user) a detailed hydrology output for every storm that is routed (i.e, runoff > 0).

SR SEDOUT	This subroutine is called from SR CONTIN and controls the printing of the output. It calls SR MONOUT, SR ANNOUT, SR ENDOUT, SR SEDSEG, and SR ENRPRT.
SR MONOUT	This subroutine is called from SR SEDOUT to generate monthly summaries of soil loss information from the model.
SR ANNOUT	This subroutine is called from SR SEDOUT to generate annual summaries of soil loss information from the model.
SR ENDOUT	This subroutine is called from SR SEDOUT to summarize soil loss information for the entire simulation period.
SR SEDSEG	This subroutine is called from SR SEDOUT and breaks the hillslope profile into detachment or deposition segments. It calls SR SEDIST and SR SEDSTA.
SR SEDIST	This subroutine is called from SR SEDSEG and creates a representative hillslope profile (sediment load, x-distance, delta x) from overland flow elements.
SR SEDSTA	This subroutine is called from SR SEDSEG and finds the mean and standard deviation of detachment or deposition points within a segment. It calls SR SEDMAX.
SR SEDMAX	This subroutine is called from SR SEDSTA. It finds the maximum and minimum detachment and deposition from segments.
SR ENRPRT	This subroutine is called from SR SEDOUT to print out the particle size distributions of the sediment in the runoff and the enrichment ratios for the overland flow elements.
SR TILAGE	This subroutine reads in the crop, tillage, and management options for each year of the simulation. It is called by SR CONTIN.

2. Information flow in the program: See Fig. 1.5.1

3. Block data:

This section lists those variables which are initialized at the beginning of a model run in a BLOCK DATA form. For more information on any of these variables, please refer to the COMMON BLOCK name which is given after the variable. This COMMON BLOCK name can be used to look up information about a variable in Section 6 below.

- a. DATA kiadjf, kradjf, tcadjf, prestr, ntill (/COVER/).
- b. DATA ft (/WATER/), cdre, cdre2, cddre (/FALL/).
- c. DATA npart (/PART/), accgav, wtdens, kinvis, msdens (/CONSTA/).
- d. DATA nrainf, nrainy, nrainm, traint, trainy, trainm, nrunot, nrunoy, nrunom, trunot, trunoy, trunom, avlost, avlosy, avlosm (/SUMOUT/).

e. DATA frmm1, frmm2, frcy1, frcy2, frff1, frff2 (/ENRPAS/).

f. DATA tmnavg, tmxavg (/CLIM/), rtmass (/CRPOUT/).

4. Parameters:

The following parameters are used in the model:

integer*4 ntype, mxnsl, tiltyp, mxtime, mxpond, mxgraz, mxplan, mxcrop, mxtlsq, mxtil, mxcut, mxelem, mxchan, mxpnd, mxseq, mxpts.

ntype = 10 : maximum number of crops represented down a hillslope.

mxnsl = 10 : maximum number of soil layers.

tiltyp = 30 : number of tillage type options.

mxtime = 1000 : maximum number of time points for hydrology.

mxpond = 20 : maximum number of occurrences of ponding conditions during an event.

mxgraz = 10 : maximum number of grazing cycles per pasture.

mxplan = 10 : maximum number of overland flow areas, (i.e., strips of different soils and /or crops)

mxcrop = 3 : maximum number of crops during one year

mxtlsq = 10 : maximum number of tillage sequences per simulation.

mxtil = 10 : maximum number of tillage operations per tillage sequence.

mxcut = 5 : maximum number of cuttings for a perennial crop.

mxelem = 10 : maximum number of elements.

mxchan = 10 : maximum number of channels.

mxpnd = 10 : maximum number of impoundments.

mxseq = 50 : maximum number of detachment or deposition segments.

mxpts = 1000 : maximum number of slope points per total number of elements.

5. Input/Output files

INPUT FILES:

Unit #	File type	Description
10	I	input file containing slope data
11	I	input file containing soil data
12	I	input file containing management data
13	I	input file containing climate data
20	I	input file containing irrigation schedule data

OUTPUT FILES:

Unit #	File type	Description
14	O	output file containing soil loss data and hydrology summaries
15	O	output file containing single storm output
16	O	output file containing water balance information
17	O	output file containing plant growth information
18	O	output file containing soil parameters information
19	O	output file containing winter (snow melt, snow depth, frost depth, thaw depth, etc.) information.

6. Variables in common blocks:

Common block	Variable name	Type	Description
/avloss/	ioutpt	I*4	output flag for continuous overall soil loss options
	ioutss	I*4	output flag for continuous storm by storm options
	ioutas	I*4	output flag for continuous annual storm options
	iroute	I*4	overland flow routing flag for printing enrichment output
	avsols	R*4	storm sediment loss (kg/m**2)
	avsole	R*4	storm sediment loss (kg/m)
	avsolm	R*4	monthly sediment loss (kg/m)
	avsoly	R*4	annual sediment loss (kg/m)
	avsoif	R*4	total sediment loss (kg/m)
	dsmon(mxplan,100)	R*4	monthly sediment loss at each point for each overland flow element (kg/m**2)
	dsyear(mxplan,100)	R*4	annual sediment loss at each point for each overland flow element (kg/m**2)
	dsavg(mxplan,100)	R*4	total sediment loss at each point for each overland flow element (kg/m**2)
/chan/	nelem	I*4	number of elements
/chng/	nfile(3)	I*4	a flag for optional program's output
/clim/	tmin	R*4	minimum daily temp. (°C)
	tmax	R*4	maximum daily temp. (°C)
	tave	R*4	average daily temp. (°C)
	rad	R*4	daily solar radiation
	am	R*4	five day antecedent moisture for surface residue (m)
	am2	R*4	five day antecedent moisture for submerged residue (m)
	tmnavg	R*4	five day minimum temperature average

	tmxavg	R*4	five day maximum temperature average
/cliyr/	ibyear	I*4	beginning year of simulation
	numyr	I*4	maximum number of years in climate file
	nyear	I*4	number of years of simulation
/cntour/	cntslp(mxplan)	R*4	contour slope (m/m)
	rowspc(mxplan)	R*4	contour row spacing (m)
	rowlen(mxplan)	R*4	contour row length (m)
	rdghgt(mxplan)	R*4	contour ridge height (m)
	cnfail(mxplan)	R*4	flag for contour failure: 0 = contour holds 1 = contour fails
	cntlen(mxplan)	R*4	contour length
	cnslp(mxplan)	R*4	contour slope
	conseq(mxplan)	R*4	contour sequence from management input
/cons/	ck1(mxnsi,mxplan)	R*4	coefficient used to calculate rawls coefficient
	ck2(mxnsi,mxplan)	R*4	coefficient used to calculate rawls coefficient
	rre(mxplan)	R*4	random roughness parameter
	bddry(mxnsi,mxplan)	R*4	dry bulk density at 15 bars of tension (kg/m**3)
	bdcons(mxnsi,mxplan)	R*4	consolidated bulk density (kg/m**3)
	cpm(mxnsi,mxplan)	R*4	rock fragment correction factor
	coca(mxnsi,mxplan)	R*4	entrapped air correction factor
	avpor	R*4	average porosity for infiltration zone
	thtdk1(mxnsi,mxplan)	R*4	coefficient to calculate 15 bar water content
	thtdk2(mxnsi,mxplan)	R*4	coefficient to calculate 15 bar water content
	thetfk(mxnsi,mxplan)	R*4	1/3 bar water content (m**3/m**3)
	wrdk(mxnsi,mxplan)	R*4	residual water content (m**3/m**3)
/consta/	accgav	R*4	acceleration of gravity (m/s**2)
	wtdens	R*4	specific weight of water (kg/m**2/s**2)
	kinvis	R*4	kinematic viscosity of water (m**2/s)
	msdens	R*4	specific mass of water (kg/m**3)
/consts/	a1	R*4	coefficient = m*alpha
	a2	R*4	coefficient = m-1
/contcv/	mindxy(mxplan)	I*4	index to update mgnt. operation
	tilseq(mxplan)	I*4	tillage sequence from management input
/cover/	canhgt(mxplan)	R*4	canopy height (m)
	cancov(mxplan)	R*4	canopy cover (0-1, unitless)
	inrcov(mxplan)	R*4	interrill cover (0-1, unitless)
	rilcov(mxplan)	R*4	rill cover (0-1, unitless)
	gcover(mxplan)	R*4	ground cover (0-1, unitless)

	kiadjf(mxplan)	R*4	Ki adjustment factor
	kradjf(mxplan)	R*4	Kr adjustment factor
	daydis(mxplan)	R*4	days since previous disturbance
	rilare(mxplan)	R*4	rill area (m**2)
	landuse(mxplan)	I*4	flag for land use
	tcadjf(mxplan)	R*4	consolidation adjustment factor for critical shear stress
	prestr(mxplan)	R*4	maximum previous consolidation stress since last tillage (Pascals)
	ntill(mxplan)	I*4	number of tillage operations during a simulation year
<hr/>			
/crpout/	rescov(mxplan)	R*4	residue cover (0-1)
	rd	R*4	root depth (m)
	rtmass	R*4	total root mass (kg/m**3)
	rtm15	R*4	root mass at 15 cm
	rtm30	R*4	root mass at 30 cm
	rtm60	R*4	root mass at 60 cm
	bd(mxnsi, mxplan)	R*4	bulk density per soil layer
	lai(mxplan)	R*4	leaf area index
	rrc(mxplan)	R*4	random roughness coefficient
<hr/>			
/crpprm/	itype(mxcrop, mxplan)	I*4	plant type
	jdplt(mxcrop, mxplan)	I*4	planting date in Julian day (1-366)
	jdharv(mxcrop, mxplan)	I*4	harvesting date in Julian day (1-366)
	rw(mxcrop, mxplan)	R*4	row width (m)
	yld(mxcrop, mxplan)	R*4	crop yield (kg/m**2)
	itill(mxtilsq, mxtil)	I*4	type of tillage for current day
	iresd(mxplan)	I*4	residue type
	grazig(mxplan)	I*4	a flag for grazing occurrence
	resmgt(mxcrop, mxplan)	I*4	residue management option 1 = herbicide application 2 = burning 3 = silage 4 = shredding 5 = residue removal 6 = none
	dap(mxplan)	I*4	current day after planting (julian)
	dtm(mxcrop, mxplan)	I*4	number of days to maturity (julian)
	sumgdy(mxplan)	R*4	cumulative growing degree days (julian)
	btemp(10)	R*4	base daily air temperature (°C)
	gs(mxcrop, mxplan)	I*4	growing season (days julian)
	nycrop (mxplan)	I*4	number of crops per year
<hr/>			
/crpvr1/	rmogt(mxplan)	R*4	surface residue mass on the ground today (kg/m**2)
	rmogy(mxplan)	R*4	surface residue mass on the ground yesterday (kg/m**2)

	rmagt(mxplan)	R*4	surface residue mass above ground today (kg/m**2)
	rmagy(mxplan)	R*4	surface residue mass above ground (kg/m**2)
	rtm	R*4	non living root mass today (kg/m**2)
	rtmy(mxplan)	R*4	non living root mass yesterday (kg/m**2)
	srm	R*4	submerged residue mass today (kg/m**2)
	srmmy(mxplan)	R*4	submerged residue mass yesterday (kg/m**2)
	sratio	R*4	surface residue mass change (kg/m**2)
	smrati	R*4	submerged residue mass change (kg/m**2)
	rratio	R*4	dead residue mass change (kg/m**2)
	tau	R*4	weighted time variable for surface residue (°C-m)
	tau2	R*4	weighted time variable for submerged residue (°C-m)
	ctaut	R*4	cumulative weighted time variable for surface residue today (°C-m)
	ctauy(mxplan)	R*4	cumulative weighted time variable for surface residue yesterday
	mfo(tiltyp,ntype)	R*4	fraction of initial surface residue remaining after tillage (0-1, unitless)
	ptol(ntype)	R*4	plant drought resistance factor (0 to 1), no units
/crpvr2/	resamt	R*4	initial surface residue mass (kg/m**2)
	cn(ntype)	R*4	carbon-nitrogen ratio of residue and roots (unitless)
	aca(ntype)	R*4	decomposition constant for flat residue
	as(ntype)	R*4	decomposition constant for buried residue
	cf(ntype)	R*4	flat residue cover coefficient (ha/kg)
	ar(ntype)	R*4	decomposition constant for roots
	y7(ntype)	R*4	residue coefficient
	aminit	R*4	residue mass at beginning of simulation (kg/m**2)
	sminit	R*4	submerged residue mass at beginning of simulation (kg/m**2)
	rminit	R*4	non-living root mass at beginning of simulation (kg/m**2)
	fct1(mxplan)	R*4	adjustment factor for above and on ground residue mass
	fct2(mxplan)	R*4	"
	vdmt	R*4	vegetative dry matter today (kg/m**2)
	vdmy(mxplan)	R*4	vegetative dry matter yesterday (kg/m**2)
/crpvr3/	gdd	R*4	growing degree days - the number of heat units necessary to reach peak standing biomass (°C)
	fgs(mxplan)	R*4	current fraction of the growing season (0-1)
	sumgdd	R*4	cumulative growing degree days (°C)
	hmax(ntype)	R*4	maximum plant height (m)
	crit(ntype)	R*4	growing degree days to emergence (°C)
	gddmax(ntype)	R*4	growing degree days at maturity (°C)
	bb(ntype)	R*4	parameter value for canopy cover equation (unitless)

	bbb(nstype)	R*4	parameter value for canopy height equation (unitless)
	rdmax(nstype)	R*4	maximum root depth (m)
	rsr(nstype)	R*4	root to shoot ratio, (unitless)
	decfct(nstype)	R*4	fraction by which canopy cover decays after reaching senescence (0-1, unitless)
	fct	R*4	crop yield coefficient
	dlai(nstype)	R*4	fraction of growing season when leaf area index starts to decline (0-1), unitless
	gssen(nstype)	R*4	fraction of growing season to reach senescence (0-1, unitless)
	xmxlai(nstype)	R*4	maximum leaf area index (unitless)
	vdmmax(mxplan)	R*4	vegetative dry matter at maturity (kg/m**2)
	gddsen(nstype)	R*4	growing degree days at senescence (°C)
/crpvr4/	y1(nstype)	R*4	upper grain yield boundary for which an adjustment to biomass is made (bu/ac)
	y2(nstype)	R*4	residue biomass when grain yield is zero (kg/ha)
	y3(nstype)	R*4	change in residue mass per unit change in grain yield between grain yield limits (0 to y1)
	y4(nstype)	R*4	pounds of grain per bushel of grain
	y5(nstype)	R*4	pound/ac to kg/ha conversion
	y6(nstype)	R*4	residue to grain yield ratio
	b1(nstype)	R*4	canopy cover coefficient
	b2(nstype)	R*4	"
/crpvr5/	pltsp(nstype)	R*4	plant spacing (m)
	diam(nstype)	R*4	plant stem diameter at maturity (m)
	basmat(mxplan)	R*4	plant basal area at maturity (m**2/ha)
	basal(mxplan)	R*4	plant basal area (m**2)
	isimyr	I*4	simulation year (1 for 1st year, etc.)
	ncount(mxplan)	I*4	a counter for number of days after senescences when canopy cover starts to decay
/data/	tr(mxtime)	R*4	array with time increments for rainfall
	tf(mxtime)	R*4	array with time increments for infiltration
	r(mxtime)	R*4	rainfall rate (m/s)
	rcum(mxtime)	R*4	accumulated rainfall depth (m)
	f(mxtime)	R*4	infiltration rate (m/s)
	ff(mxtime)	R*4	accumulated infiltration depth (m)
	re(mxtime)	R*4	rainfall excess rate (m/s)
	recum(mxtime)	R*4	accumulated rainfall excess depth (m)
	rr(mxtime)	R*4	rainfall depths (m)
	dt	R*4	infiltration time step (s)
	nr	I*4	number of rainfall intervals
	nf	I*4	number of infiltration intervals

	nm	I*4	maximum rainfall excess index
	nqt	I*4	number of runoff intervals
/diss1/	int(20)	R*4	rainfall intensity (m/s)
	timem(20)	R*4	elapsed time (s)
	isqint	R*4	rainfall intensity squared
	dur	R*4	storm duration (s)
	nint	I*4	number of rainfall intensity values
/diss2/	intdl(20)	R*4	unitless rainfall intensity
	timedl(20)	R*4	unitless elapsed time
/diss3/	p	R*4	total rainfall depth (m)
	fq	R*4	cumulative normalized rainfall depth (m)
	deltfq	R*4	incremental normalized rainfall depth (m)
	timep	R*4	ratio time to rainfall peak to rainfall duration
	ip	R*4	relative peak intensity: ratio maximum rainfall intensity to average rainfall intensity
/dist/	xinput(101,mxplan)	R*4	unitless distances (points) down the slope
	slplen(mxplan)	R*4	slope length (m)
/ends/	tcend	R*4	sediment transport capacity at end of slope (kg/m.s)
	rspace(mxplan)	R*4	distance between rills (m)
	width(mxplan)	R*4	rill width (m)
	ktrato	R*4	sediment transport coefficient ratio
	qshear	R*4	discharge used to calculate shear stress (m**3/s)
	qin	R*4	water discharge in/out of strip
	qout	R*4	water discharge in/out of strip
	qsout	R*4	sediment discharge in/out of strip
	strldn	R*4	non-dimensional form of qsout
/enrps/	frclw(10,mxplan)	R*4	fraction of each particle type
	enrato(mxplan)	R*4	storm by storm enrichment ration
	enrmm1	R*4	used to calculate monthly weighted enrichment ratio
	enrmm2	R*4	used to calculate monthly weighted enrichment ratio
	enryy1	R*4	used to calculate annual weighted enrichment ratio
	enryy2	R*4	used to calculate annual weighted enrichment ratio
	enrff1	R*4	used to calculate total weighted enrichment ratio
	enrff2	R*4	used to calculate total weighted enrichment ratio
	enrmon	R*4	enrmm1/enrmm2 used for monthly weighted enrichment ratio
	enryr	R*4	enryy1/enryy2 used for annual weighted enrichment ratio
	enravg	R*4	enrff1/enrff2 used for total weighted enrichment ratio
	frmm1(10)	R*4	used to calculated monthly weighted particle size fractions exiting

	frmm2(10)	R*4	used to calculated monthly weighted particle size fractions exiting
	frcy1(10)	R*4	used to calculated annual weighted particle size fractions exiting
	frcy2(10)	R*4	used to calculated annual weighted particle size fractions exiting
	frcff1(10)	R*4	used to calculated total weighted particle size fractions exiting
	frcff2(10)	R*4	used to calculated total weighted particle size fractions exiting
	frmon(10)	R*4	frmm1/frmm2 used for monthly weighted fraction of particle size classes exiting
	frcyr(10)	R*4	frcy1/frcy2 used for annual weighted fraction of particle size classes exiting
	frcavg(10)	R*4	frcff1/frcff2 used for total weighted fraction of particle size classes exiting
/erdval/	detach(101)	R*4	unitless detachment for each point down the slope
	dtot(101)	R*4	total detachment for each point down the slope
	load(101)	R*4	unitless sediment load for each point down the slope
	tc(101)	R*4	sediment transport capacity for each point down the slope (kg/s/m)
	ldseg(10)	R*4	sediment load from each segment
	ldsec(10)	R*4	sediment load from each section
/fall/	cdre(9)	R*4	coefficient for particle size calculations
	cdre2(9)	R*4	"
	cddre(9)	R*4	"
/ffact/	frcsol	R*4	soil grain friction factor
	frctrl	R*4	total rill friction factor
	frcteq	R*4	equivalent weighting friction factor for rill
/flags/	iflag	I*4	a flag for initialization calls
/hydrol/	rain	R*4	daily rainfall amount (m)
	stmdur	R*4	storm duration (s)
	avrint	R*4	average rainfall intensity (m/s)
	runoff(mxplan)	R*4	daily runoff amount (m)
	extrain	R*4	cumulative amount of rainfall excess (m)
	durexr	R*4	duration of rainfall excess (s)
	peakro(mxplan)	R*4	peak runoff rate (m/s)
	durrun	R*4	duration of runoff (s)
	effdm	R*4	effective duration
	effint(mxplan)	R*4	effective rainfall intensity (m/s)
	remax	R*4	maximum rainfall excess (m/s)

<i>/infcof/</i>	ainf(10)	R*4	adjustment slope profile coefficients for flow unto strips
	binf(10)	R*4	"
	cinf(10)	R*4	"
	qostar	R*4	non-dimensional discharge out of strips
<i>/intgrl/</i>	si(mxtime+1)	R*4	integral of rainfall excess
	ii	I*4	index for time array (current time is between t(ii) and t(ii+1))
<i>/new1/</i>	wdcode(mxplan)	I*4	flag for weed cover
	jdwdst	I*4	date weed cover becomes important (julian)
	jdwend	I*4	date weed cover becomes unimportant (julian)
	wdcover	R*4	average week cover
	sprcov(nstype)	R*4	residue cover on ridges in spring (0-1)
	critvm(nstype)	R*4	critical live biomass value below which
<i>/parame/</i>	ks(mxplan)	R*4	saturated hydraulic conductivity (m/s)
	sm(mxplan)	R*4	effective matric potential (m)
	ksm	R*4	product Ks*sm
	tt	R*4	real infiltration time
	tp(mxpond)	R*4	time to ponding (s)
	ts	R*4	pseudo time to adjust the real time for infiltration (s)
	cu	R*4	ponding indicator when no ponding at the beginning of interval (cu < 0 implies no ponding, cu > 0 implies ponding)
	cp	R*4	ponding indicator when ponded at the beginning of interval (cp < 0 implies ponding stops during interval, cp > 0 implies ponding)
	pt(mxpond)	R*4	accumulated rainfall at time of ponding (m)
	por(mxplan,mxsl)	R*4	porosity for each soil
	sat(mxplan)	R*4	soil saturation index
<i>/part/</i>	npart	I*4	number of particle classes
	dia(10,mxplan)	R*4	diameter of each particle class (m)
	spg(10)	R*4	specific gravity of each particle class
	eqsand(10,mxplan)	R*4	equivalent sand diameter of each particle class
	frac(10,mxplan)	R*4	fraction of each particle class (0-1)
	fall(10,mxplan)	R*4	fall velocity of each particle class (m/s)
	frcly(10,mxplan)	R*4	fraction of clay (0-1)
	frslt(10,mxplan)	R*4	fraction of silt (0-1)
	frsnd(10,mxplan)	R*4	fraction of sand (0-1)
	frorg(10,mxplan)	R*4	fraction of organic matter (0-1)

<i>/parval/</i>	eata	R*4	unitless parameter for rill erosion
	tauc	R*4	unitless parameter for rill critical shear stress
	theta	R*4	unitless parameter for interrill erosion
	phi	R*4	unitless parameter for deposition
	shcrit(mxplan)	R*4	rill detachment threshold parameter, or critical shear stress (kg/m/s**2)
<i>/pass/</i>	s(mxtime)	R*4	rainfall excess rate (m/s)
	t(mxtime)	R*4	real rainfall excess time (s) = tr(i)-tp+ts
	q(mxtime)	R*4	runoff rate (s)
	tq(mxtime)	R*4	runoff time (s)
	len	R*4	length of plane (m)
	nq	I*4	number of runoff points
	ns	I*4	number of rainfall excess points
	trf(mxtime)	R*4	times for disaggregated rainfall (s)
	rf(mxtime)	D*4	rainfall rates from disaggregation (m/s)
	qtot(mxtime)	R*4	cumulative runoff (m)
	tq1(mxtime)	R*4	time counter for excess rainfall and runoff
<i>/peren/</i>	imngmt(itype)	I*4	cropping system 1) annual 2) perennial 3) fallow
	yild(mxcut,mxplan)	R*4	yield (tons/ac)
	cutday(mxcut,mxplan)	I*4	cutting date (Julian)
	mgtopt(mxplan)	I*4	crop management option 1) cutting 2) grazing 3) not harvested or grazed
	ncut(mxplan)	I*4	number of cuttings
	popmat(mxplan)	R*4	plant population at maturity
	grate(ntype)	R*4	growth rate parameter
	spriod(ntype)	R*4	number of days between beginning & end of leaf drop
	jdherb(mxcrop,mxplan)	I*4	herbicide application date (Julian)
	jdbum(mxcrop,mxplan)	I*4	residue burning date (Julian)
	jdslge(mxcrop,mxplan)	I*4	silage date (Julian)
	fbmag(mxcrop,mxplan)	R*4	fraction of flat residue burned (0-1)
	fbmog(mxcrop,mxplan)	R*4	fraction of standing residue burned (0-1)
	partcf(ntype)	R*4	portion of vegetative biomass partitioned into standing residue mass at harvest
	pop(mxplan)	R*4	plant population on day of simulation
	srmhav(mxplan)	R*4	flat residue mass at harvest (kg/m**2)
	ncycle(mxplan)	I*4	number of grazing cycles
	jdcut(mxcrop,mxplan)	I*4	standing residue shredding or cutting date (Julian)

	jdmove(mxcrop,mxplan)	I*4	residue removal date (Julian)
	frmove(mxcrop,mxplan)	R*4	fraction of flat residue removed (0-1)
	digest(mxplan)	R*4	digestibility
	fact(ntype)	R*4	standing to flat residue adjustment factor (wind, snow, etc.)
	jdstop(mxplan)	I*4	perennial crop growth stop date (Julian)
	tothave(mxplan)	R*4	maximum above ground biomass produced (tons/acre)
	nnc(mxplan)	I*4	perennial crop index for the number of cuttings and grazings
	ipmyr(mxplan)	I*4	flag for year of simulation 1) first year of perennial growth 2) otherwise
	tmpmin(ntype)	R*4	minimum daily temperature (°C)
	tmpmax(ntype)	R*4	maximum daily temperature (°C)
	istart(mxplan)	I*4	flag for first cutting date for perennial crops
	ifreez(mxplan)	I*4	flag for freezing temperature
	rtmas(mxplan)	R*4	total root mass for perennial crops
	rtmmax(ntype)	R*4	maximum root mass for a perennial crop (tons/acre)
	frcut(mxcrop,mxplan)	R*4	fraction of flat residue shredded
<hr/>			
/prams/	alpha(mxplan)	R*4	Chezy depth-discharge coefficient
	m	R*4	Chezy depth-discharge exponent
	tstar	R*4	time when rainfall excess stops (s)
	nroute	I*4	flag for runoff routing
	norun(mxplan)	I*4	flag for runoff occurrence
<hr/>			
/psis1/	psi	R*8	the position on the characteristics, starting at "u", at time "time"
	dpsi	R*8	the derivation on the characteristics, starting at "u", at time "time"
<hr/>			
/rinpt1/	flk(ntype)	R*4	coefficient used to calculate foliar cover
	aleaf(ntype)	R*4	coefficient for leaf area (m**2/kg)
	plive (ntype)	R*4	maximum standing live plant biomass (kg/m**2)
	proot(ntype)	R*4	maximum peak root biomass (kg/m**2)
	wcf(mxplan)	R*4	fraction of ground surface covered with rocks and gravel (0-1)
	crypto(mxplan)	R*4	fraction of ground surface covered with cryptograms (0-1)
	animal(mxplan)	R*4	animal units grazing each npast pastures (animal units per year)
	bodywt(mxplan)	R*4	average body weight of an animal (kg)
	suppmt(mxplan)	R*4	average amount of supplement feed per day (kg/day)
	digmin(ntype)	R*4	minimum digestibility of forage index (0-1)
	digmax(ntype)	R*4	maximum digestibility of forage index (0-1)
	gday(mxgraz,mxplan)	I*4	Julian day grazing starts

	gend(mxgraz,mxplan)	I*4	Julian day grazing stops
	ssday(mxgraz,mxplan)	I*4	Julian day supplementary feeding begins
	send(mxgraz,mxplan)	I*4	Julian day supplementary feeding ends
	area(mxplan)	R*4	pasture area
	jgraz(mxplan)	R*4	grazing cycle per pasture per simulation
	access(mxplan)	R*4	fraction of forage available for consumption (0-1)
	cold(ntype)	R*4	a flag for plant defoliation
	bugs(ntype)	R*4	daily disappearance of surface organic residue (kg/m**2)
	wood(ntype)	R*4	fraction of standing biomass which is woody
	woody(ntype)	R*4	a flag for user to specify whether defoliation is instantaneous or occurs over several months
	yield(ntype)	R*4	total above ground plant production for a simulation year (kg/m**2)
	pyield(ntype)	R*4	daily net primary plant production (kg/m**2)
/rinpt2/	pptg(ntype)	R*4	precipitation during the growing season (m)
	rootf(ntype)	R*4	fraction of roots from maximum (both live and dead) at start of year (day 1)
	rdf(ntype)	R*4	root distribution coefficient for mass by depth (unitless)
	pscday(ntype)	R*4	day peak standing crop is reached for first peak on the relative growth curve (1-366)
	strgc(ntype)	R*4	Julian day growth begins (1-366)
	cshape(ntype)	R*4	shaping parameter for the left side of growth curve
	dshape(ntype)	R*4	shaping parameter for the right side of growth curve for the first peak
	sday2(ntype)	R*4	day peak standing crop is reached for second peak on the relative growth curve
	strgc2(ntype)	R*4	Julian day second growth period begins (1-366)
	eshape(ntype)	R*4	shaping parameter for the left side of growth curve for the second peak
	fshape(ntype)	R*4	shaping parameter for the right side of growth curve for the second peak
	rgcmin(ntype)	R*4	minimum fraction of live biomass at any point of a year (0-1)
	cf1(ntype)	R*4	fraction of maximum live standing forage for the first peak (0-1)
	cf2(ntype)	R*4	fraction of maximum live standing forage for the second peak (0-1)
	gtemp(ntype)	R*4	minimum temperature to start growth in the spring (°C)
	tempmn(ntype)	R*4	minimum temperature for plant to stop growth in fall (°C)
	root10(ntype)	R*4	root biomass in top 10 cm
	ffp(ntype)	R*4	frost free period
/rinpt3/	alter(mxplan)	R*4	coefficient of increase in accessibility (0-1)

	burned(mxplan)	R*4	fraction of reduction or increase in standing dead wood after burning
	change(mxplan)	R*4	fraction increase or decrease in potential above and below ground biomass
	hurt(mxplan)	R*4	fraction increase or decrease of evergreen biomass
	jfdate(mxplan)	I*4	Julian day of burning
	reduce(mxplan)	R*4	fraction reduction in standing herbaceous and organic residue as a function of burning
	shgt(ntype)	R*4	average plant height (m) of shrub plant component
	spop(ntype)	R*4	average number of plants along a 100 m transect, shrub plant component
	sdiam(ntype)	R*4	average canopy diameter for shrub plant component
	ghgt(ntype)	R*4	average plant height (m) of shrub plant component
	scoeff(ntype)	R*4	projected plant area coefficient, for shrub plant component
	gpop(ntype)	R*4	average number of plants along a 100 m transect, herb. plant component
	gdiam(ntype)	R*4	average canopy diameter for herb. plant component
	gcoeff(ntype)	R*4	projected plant area coefficient, for herb. plant component
	basden	R*4	effective plant basal density
/rinpt4/	ihdate(mxplan)	I*4	Julian day of herbicide application
	active(mxplan)	I*4	flag if herbicide used (0=no, 1=yes)
	herb(mxplan)	R*4	fraction representing change in the evergreen biomass (above ground)
	update(mxplan)	R*4	fraction of change in accessibility after herbicide, 0 to 1
	regrow(mxplan)	R*4	fraction of change in PTLIVE and PROOT that is expected after applying the herbicide
	dleaf(mxplan)	R*4	fraction of change in standing live biomass
	ptlive(mxplan)	R*4	previous total live leaf biomass (kg/m**2)
	first(ntype)	R*4	previous years initiation of growth date (julian)
	decomp(mxplan)	R*4	standing dead biomass left after burning or herbicide (kg/m**2)
	xlive(mxplan)	R*4	evergreen leafy component (kg/m**2)
/rinpt5/	thgt(ntype)	R*4	average tree height, meters
	tpop(ntype)	R*4	average number of plants along a 100 m transect, shorter plant component
	tdiam(ntype)	R*4	canopy diameter, meters tree plant component
	tcoeff(ntype)	R*4	projected plant area, plant coefficient

/mdm/	x	R*4	updated "seed" for SR RAND (It is called initially from SR BGNRND)
	aa	R*4	a multiplier for the MCM used for random number generation
	mmd	R*4	a multiplier for the MCM used for random number generation
/rout/	feed	R*4	daily forage requirement for grazing animals (kg/day)
	unbio	R*4	forage unavailable for consumption (kg/m**2)
	utiliz	R*4	fraction of forage consumed during the grazing season (0-1)
	tfood	R*4	total forage consumed by grazing animals (kg/year)
	tlive(mxplan)	R*4	total live plant material on day of simulation (kg/m**2)
	slive	R*4	new plant growth on day on simulation (kg/m**2)
	root(mxns1)	R*4	roots for each soil layer today (kg/m**2)
	lroot(mxns1)	R*4	new roots added for each soil layer on day of simulation (kg/m**2)
	droot(mxns1)	R*4	fraction of total roots in a soil layer (0-1)
	rooty(mxns1)	R*4	total root mass in a soil layer on day of simulation
/sedld/	dstot(mxpts)	R*4	sediment loss for all points down hillslope (all overland flow elements) (kg/m**2)
	stdist(mxpts)	R*4	distance down hillslope at each point (m)
	delxx(mxpts)	R*4	delta x increments between each point down hillslope (m)
	ibegin	I*4	beginning of deposition/detachment segment
	iend	I*4	ending of deposition/detachment segment
	jflag(mxseg)	R*4	flag for whether deposition/detachment is occurring
	lseg	I*4	flag for number of deposition/detachment segments on hillslope
	dstotl(mxpts)	R*4	sediment loss down hillslope for only overland flow elements routed
	spdist(mxpts)	R*4	sediment loss down hillslope for only overland flow elements routed
	deltax(mxpts)	R*4	sediment loss down hillslope for only overland flow elements routed
/slinit/	rrinit(mxplan)	R*4	initial ridge roughness (m)
	rhinit(mxplan)	R*4	initial ridge height (m)
	rfcum(mxplan)	R*4	cumulative rainfall since last tillage (mm)
	bdtill(mxplan)	R*4	bulk density after last tillage (g/cc)
	ao(mxplan)	R*4	coefficient for change in bulk density due to rainfall
/slope/	xu(10,mxplan)	R*4	unitless upper end of section
	xl(10,mxplan)	R*4	unitless lower end of section

	slinp(10,mxplan)	R*4	slope points
	a(10,mxplan)	R*4	profile coefficient for curvature
	b(10,mxplan)	R*4	profile coefficient for slope gradient
	nslpts	I*4	number of slope input points
	nsec(mxplan)	I*4	number of slope input sections
	xsec(10,mxplan)	R*4	length of each input section (m)
	typsec(10,mxplan)	I*4	type of section (detachment or deposition section)
	avgslp(mxplan)	R*4	average slope gradient
	slpend(mxplan)	R*4	gradient at end of slope
<hr/>			
/slpopt/	ninpts	I*4	number of slope length pairs
	xdel(100)	R*4	segment length (m)
	xslp(100)	R*4	slope of segment
	itop	I*4	flag for slope at top of field 0 - slope equal to zero 1 - slope not equal to zero
	aspect	R*4	aspect of field
	width	R*4	width of field (m)
<hr/>			
/solvar/	soltex(mxplan)	I*4	flag for soil texture
	sand(mxns1,mxplan)	R*4	fraction sand (0-1)
	silt(mxns1,mxplan)	R*4	fraction silt (0-1)
	clay(mxns1,mxplan)	R*4	fraction clay (0-1)
	orgmat(mxns1,mxplan)	R*4	fraction organic matter (0-1)
	intsat	I*4	flag for saturation
	cec(mxns1,mxplan)	R*4	cation exchange capacity
	solcon(mxns1,mxplan)	R*4	soil constant
	rfg(mxns1,mxplan)	R*4	amount of rocks in soil (0-1)
	ki(mxplan)	R*4	initial interrill detachment parameter (baseline interrill erodibility, kg s m ⁻⁴)
	kr(mxplan)	R*4	initial rill detachment rate parameter (s/m)
	kt	R*4	sediment transport capacity coefficient = (kt1+kt2)/2
<hr/>			
/stmflg/	norain	I*4	flag for no rain
	nmon	I*4	flag for month
	jyear	I*4	flag for simulation year
<hr/>			
/struct/	iplane	I*4	current overland flow segment (strip)
<hr/>			
/sumout/	nrain	I*4	number of total rainfall events during the simulation period
	nrainy	I*4	number of rainfall events per year during simulation
	nrainm(13)	I*4	number of rainfall events per month during simulation

	traint	R*4	total rainfall amount during the simulation period (m)
	trainy	R*4	total rainfall amount per year during simulation (m)
	trainm(13)	R*4	total rainfall amount per year during simulation (m)
	nrunot(mxplan)	I*4	number of total runoff events during the simulation period
	nrunoy(mxplan)	I*4	number of total runoff events per year during simulation
	nrunom(13,mxplan)	I*4	number of total runoff events month during simulation
	trunot(mxplan)	R*4	total runoff amount during the simulation period (m)
	trunoy(mxplan)	R*4	total runoff amount per year during simulation (m)
	trunom(13,mxplan)	R*4	total runoff amount per month during simulation (m)
	avlost(mxplan)	R*4	total sediment yield during the simulation period (kg/m**2)
	avlosy(mxplan)	R*4	total sediment yield per year during simulation (kg/m**2)
	avlosm(13,mxplan)	R*4	total sediment yield per month during simulation (kg/m**2)
<hr/>			
/tfrac/	tcf1(10,mxplan)	R*4	transport capacity for each size class
<hr/>			
/temp/	sand1(mxns1,mxplan)	R*4	% sand
	clay1(mxns1,mxplan)	R*4	% clay
	orgma1(mxns1,mxplan)	R*4	% organic matter
	rfg1(mxns1,mxplan)	R*4	% rock fragments
	cec1(mxns1,mxplan)	R*4	cation exchange capacity
	nslogr(mxplan)	I*4	number of soil layers
	ssc1(mxns1,mxplan)	R*4	initial saturated hydraulic conductivity (mm/h)
	bd1(mxns1,mxplan)	R*4	initial bulk density (g/cc)
	thetd1(mxns1,mxplan)	R*4	initial 15-bar soil water content (mm/mm)
	thetf1(mxns1,mxplan)	R*4	initial 1/3 bar soil water content (mm/mm)
	solth1(mxns1,mxplan)	R*4	cumulative thickness of soil layer (mm)
	avclay(mxplan)	R*4	average % clay based on primary and i secondary tillage layers
	avsand(mxplan)	R*4	average % sand based on primary and i secondary tillage layers
<hr/>			
/tillage/	tildep(10,mxplan)	R*4	tillage depth (m)
	nrplt	I*4	planter row number
	nrcul	I*4	cultivator row number
	tillay(2,mxplan)	R*4	depth of secondary (tillay (1)) and primary (tillay (2))
	typtil(10,mxplan)	R*4	tillage type 1) primary 2) secondary

	ro(tiltyp)	R*4	random roughness value after tillage (m)
	rho(tiltyp)	R*4	ridge height value after tillage (m)
	rint(tiltyp)	R*4	ridge interval (m)
	tdmean(tiltyp)	R*4	mean tillage depth (m)
	nrdril	I*4	drill row number
	cltpos	I*4	cultivator position
<hr/>			
/update/	day	I*4	day of year
	mon	I*4	month of year
	year	I*4	year of simulation
	sdate	I*4	date of year in Julian date
	mdate(mxntill,mxntlsq)	I*4	Julian date on which tillage occurs
	indy(mxplan)	I*4	management operation index
<hr/>			
/water/	salb(mxplan)	R*4	soil albedo (0-1)
	ep	R*4	plant transpiration (m/day)
	es	R*4	soil evaporation (m)
	fin	R*4	infiltrated water amount
	st(mxns1,mxplan)	R*4	current available water content per soil layer
	ul(mxns1)	R*4	upper limit of water content per soil layer
	ssc(mxns1,mxplan)	R*4	saturated hydraulic conductivity
	hk(mxns1)	R*4	a parameter that causes SC approach zero as soil water approaches FC
	fc(mxns1)	R*4	soil field capacity
	ft(mxns1)	R*4	soil temperature C
	ub	R*4	a plant water use rate-depth parameter = 3.065
	sep(mxplan)	R*4	seepage
	su	R*4	soil water available for evaporation
	j1	I*4	soil layers subjected to soil evaporation
	j2	I*4	soil layers
	s1(mxplan)	R*4	stage 1, soil evap.
	s2(mxplan)	R*4	stage 2, " "
	cv	R*4	residue amount
	tu(mxplan)	R*4	upper limit sol evap., stage 1
	thetadr(mxns1,mxplan)	R*4	15-bar soil water content (wilting point)
	thetafc(mxns1,mxplan)	R*4	1/3-bar soil water content (field capacity)
	nsl(mxplan)	I*4	number of soil layers
	soilw(mxns1)	R*4	soil water content per layer
	solthk(mxns1,mxplan)	R*4	cumulative thickness of soil layer
	ul4	R*4	parameter to adjust potential water use by plants
	watstr(mxplan)	R*4	water stress parameter for plant growth
	dg(mxns1,mxplan)	R*4	depth of each soil layer, meters

APPENDIX B

STATUS OF COMPUTER CODE AS OF AUGUST, 1989

M.A. Nearing

The computer code delivered to user agencies represented on the WEPP core team in August of 1989 was hillslope profile version 89. Version 89 does not entirely reflect the completed hillslope profile model as described in this document. Differences between the model as documented herein and version 89 are described below.

1. **NON-UNIFORM HYDROLOGY:** Version 89 of the computer code does not include non-uniform hydrology as described in Chapter 5. The method of section 4.2.2 is used to calculate an average rainfall excess for the entire hillslope which is then distributed evenly over the entire hillslope.
2. **WINTER ROUTINES:** The winter routines described in Chapter 3 including snowmelt, snowdrift, and frozen soils is not in version 89.
3. **IRRIGATION:** The irrigation routines described in the user summary and Chapter 12 are not included in version 89.
4. **SURFACE COVER MOVEMENT:** Differences between rill and interrill surface residue cover as described in Chapter 8 are not in version 89 of the model.
5. **WIND SPEED AND DIRECTION:** The model version 89 does not read dew point temperature, wind speed, and wind direction as described in Chapter 2. The model will accept files which contain that information as generated by CLIGEN, however.